THE ROLE OF CELL SURFACE HEPARAN SULFATE IN ENTEROVIRUS A71 INFECTIONS AND THE DEVELOPMENT OF ANTIVIRAL AGENTS TARGETING VIRAL ATTACHMENT AND RNA TRANSLATION INITIATION

TAN CHEE WAH

THESIS SUBMITTED IN FULFILLMENT
OF THE REQUIREMENTS
FOR THE DEGREE OF DOCTOR OF PHILOSOPHY

FACULTY OF MEDICINE
UNIVERSITY OF MALAYA
KUALA LUMPUR

2014

UNIVERSITI MALAYA

ORIGINAL LITERARY WORK DECLARATION

Name of candidate: Tan Chee Wah (I.C/Passport No: 860902-56-5845)

Registration/Matric No: MHA110001

Name of Degree: Doctor of Philosophy

Title of Project Paper/Research Report/Dissertation/Thesis ("this Work"):
The role of cell surface heparan sulfate in enterovirus A71 infections and the development of antiviral agents targeting viral attachment and RNA translation initiation

Field of Study: Molecular Virology

I do solemnly and sincerely declare that:
(1) I am the sole author/writer of this Work;
(2) This Work is original;
(3) Any use of any work in which copyright exists was done by way of fair dealing and for permitted purposes and any excerpt or extract from, or reference to or reproduction of any copyright work has been disclosed expressly and sufficiently and the title of the Work and its authorship have been acknowledged in this Work;
(4) I do not have any actual knowledge nor do I ought reasonably to know that the making of this work constitutes an infringement of any copyright work;
(5) I hereby assign all and every rights in the copyright to this Work to the University of Malaya ("UM"), who henceforth shall be owner of the copyright in this Work and that any reproduction or use in any form or by any means whatsoever is prohibited without the written consent of UM having been first had and obtained;
(6) I am fully aware that if in the course of making this Work I have infringed any copyright whether intentionally or otherwise, I may be subject to legal action or any other action as may be determined by UM.

Candidate's signature Date

Subscribed and solemnly declared before,

Witness's Signature Date
Name:
Designation:

ABSTRACT

Enterovirus A71 (EV-A71) is the main causative agent of hand, foot and mouth disease (HFMD). Recent EV-A71 outbreaks in Asia-Pacific were not limited to mild HFMD, but were associated with neurological complications including aseptic meningitis, brainstem encephalitis and deaths. The absence of licensed therapeutics for clinical use has intensified research into anti-EV-A71 development. Since virus-host receptor interaction is the first essential event during virus infection, inhibitors that block this event could act as potential therapeutics. EV-A71 VP1 capsid protein is involved in viral-host receptor interactions and carries multiple receptor binding sites. Screening of 95 overlapping peptides covering the entire EV-A71 VP1 capsid protein was hypothesized to identify potential viral attachment inhibitors, as well as unknown receptors. Out of 95 overlapping peptides, a peptide designated as SP40 peptide significantly inhibited EV-A71-induced cytopathic effect, plaque formation, RNA synthesis and viral protein synthesis. Mechanism of action analysis revealed that SP40 peptide is not virucidal, but blocked EV-A71 attachment to the cell surface. Alanine scanning analysis showed that positively charged amino acids were critical for the antiviral activities. Sequence analysis revealed that SP40 peptide carried a heparan sulfate-specific binding domain (-RRKV-), which led to the hypothesis that EV-A71 could use cell surface heparan sulfate as an attachment receptor. Highly sulfated heparin, dextran sulfate and suramin significantly inhibited EV-A71 infections in a dose-dependent manner. Interference with heparan sulfate biosynthesis either by sodium chlorate treatment or through transient knockdown of N-deacetylase/N-sulfotransferase-1 and exostosin-1 expression reduced EV-A71 infection. Enzymatic removal of cell surface heparan sulfate by heparinase I/II/III inhibited EV-A71 infection. Biochemistry analysis revealed that EV-A71 interacts with heparan sulfate through electrostatic interactions. These findings support the hypothesis and confirmed that EV-A71 uses

cell surface heparan sulfate as an attachment receptor. Other than the attachment inhibitor, this study also tested DNA-like antisense-mediated morpholino oligomers as anti-EV-A71 agents. Two octaguanidinium-conjugated morpholino oligomers (vivo-MOs) targeting EV-A71 internal ribosome entry site (IRES) significantly inhibited EV-A71 infections at multiple time points, in a dose-dependent manner. EV-A71 resistance to vivo-MO-1 arose after 8 blind passages in the presence of increased concentrations of vivo-MO-1, but not vivo-MO-2. A single nucleotide mutation at the extreme 3' end (T to C substitution at position 533) was sufficient to confer vivo-MO-1 resistance. In mismatch tolerance analysis, results demonstrated that the positions and the number of mismatches affect vivo-MO-1 efficacy. A single mismatch at the center of the targeted region was more tolerable compared to a mismatch at the end of the targeted region. In conclusion, this study has identified an antiviral peptide that potentially blocks viral attachment to heparan sulfate, and led to the discovery of a novel EV-A71 attachment receptor. This study also identified two antisense-mediated vivo-MOs targeted sites for antiviral intervention. This study suggests that blocking of viral attachment and viral RNA translation are good strategies for antiviral intervention.

ABSTRAK

Enterovirus A71 (EV-A71) adalah agen utama penyebab penyakit kaki, tangan dan mulut (HFMD). Tanda-tanda klinikal HFMD adalah demam, ruam di tapak tangan dan kaki dan juga ulser di dalam mulut. Walau bagaimanapun, wabak EV-A71 di Asia Pasifik tidak terhad kepada HFMD yang ringan, tetapi dihubungkait dengan komplikasi neurologi seperti meningitis aseptik, ensefalitis, paralisis dan kematian. Pilihan rawatan untuk jangkitan EV-A71 adalah terhad kepada melegakan gejala jangkitan dan tiada agen antivirus yang berkesan untuk penggunaan klinikal. Oleh itu, pembangunan agen antivirus yang berkesan terhadap jangkitan EV-A71 adalah amat diperlukan dengan segera. Protein kapsid EV-A71 VP1 merupakan tapak pengikatan reseptor. Pemeriksaan 95 peptida bertindih meliputi seluruh EV-A71 VP1 protein kapsid dapat mengenalpasti inhibitor reseptor penyikat yang berpotensi serta mengenalpasti reseptor yang tidak diketahui. Daripada 95 peptida bertindih, peptida bernama SP40, didapati menghalang EV-A71 jangkitan dalam bentuk kesan sitopati (CPE), pembentukan plak, sintesis RNA dan sintesis protein di dalam kultur tisu. Analisis mekanisme tindakan membuktikan bahawa SP40 tidak menyahaktif virus, tetapi menyekat pengikatan reseptor EV-A71. Imbasan alanine mendedahkan bahawa asid amino yang bercas positif adalah penting untuk aktiviti-aktiviti antiviral. Analisis urutan peptida mendedahkan bahawa SP40 mempunyai domain pengikatan heparan sulfat (-RRKV-) yang spesifik. Ini telah menuju hipotesis penyelidikan bahawa EV-A71 menggunakan heparan sulfat sebagai tapak pengikatan reseptor. Heparin, dextran sulfat dan suramin didapati menghalang jangkitan EV-A71 dengan ketara. Dengan menggunakan varian heparin yang kekurangan kumpulan O-sulfat atau kedua-dua kumpulan O-sulfat and N-sulfat serta natrium klorat, kajian ini telah mengenalpastikan bahawa kumpulan sulfat dalam heparin adalah kritikal untuk kesan antivirus. Penyingkiran sel permukaan heparan sulfat dengan enzim heparinase atau halangan biosistensis heparan sulfat dengan siRNA

telah mengurangkan jangkitan EV-A71 dengan ketara. Analisis biokimia mendedahkan bahawa EV-A71berinteraksi dengan heparan sulfat melalui interaksi elektrostatik. Selain daripada inhibitor adhesi, kajian ini telah mengenal pasti dua perantara-antierti morpholino oligonukleotida berkonjugasi dengan octaguanidinium dendrimer (vivo-MO) yang menyasarkan tapak kemasukan internal ribosom (IRES) mempunyai aktiviti antivirus yang berkesan terhadap jangkitan EV-A71. Penyelidikan masa rawatan telah mengenalpastikan bahawa vivo-MO mengekalkan aktiviti-aktiviti antivirus apabila rawatan diberikan 4 jam sebelum atau 6 jam selepas jangkitan EV-A71. EV-A71 yang mempunyai rintangan terhadap vivo-MO-1 didapati mempunyai mutasi daripada T kepada C, dalam kedudukan 533 selepas lapan kali sub-kultur. Dengan menggunakan mutasi berarahan-tapak spesifik untuk analisi toleransi sepadan, kajian ini telah mengenalpastikan bahawa kedudukan mutasi dan juga bilangan mutasi adalah penting untuk aktiviti-aktiviti antivirus oleh vivo-MO. Mutasi di tengah-tengah rantau yang disasarkan adalah lebih ditoleransi berbanding dengan mutasi di hujung rantau yang disasarkan. Dalam kajian ini, saya telah mengenalpasti peptida antivirus yang berpotensi menyekat EV-A71 adhesi kepada heparan sulfat dan telah membawa kepada penemuan peranan heparan sulfat sebagai reseptor adhesi untuk EV-A71. Kajian ini juga mengenalpasti dua perantara-antierti vivo-MO tapak sasaran untuk pembangunan antivirus yang berkesan.

ACKNOWLEDGEMENTS

I would like to express my sincere thanks and utmost gratitude to:

GOD for HIS limitless guidance, love, spiritual courage and strength to face the challenges and overcome the obstacles. Amen.

Dr. Chan Yoke Fun for her unwavering guidance, sound advice and most importantly, for her support and the opportunity to continue my postgraduate studies under her close supervision in University of Malaya. I am indebted to you for providing me with the motivation to develop a passion towards science and sharing your research experiences with me.

Professor Poh Chit Laa for the opportunity to pursue my postgraduate studies under her supervision. Thank you for your invaluable guidance and encouragement throughout the course of this study.

Professor Jamal I-Ching Sam for his co-supervision, advice and guidance throughout the course of this study.

Chun Wei, Shie Yien, Chong Long, Chee Sieng, Shih Keng, Kam Leng, Jeffrey, Hui Vern, Nadia and interns for their friendship, guidance, and help in all the laboratory matters.

Yee Chin for her patience and understanding throughout my postgraduate study. Thank you for your endless encouragement and support. Your love and sincerity has indeed changed me into a better person.

My parents for their unconditional love, concern and understanding in every possible ways.

MyBrain 15 for the sponsorship throughout my PhD candidature.

Department of Medical Microbiology and Faculty of Medicine for the PhD opportunity and the facilities provided.

TABLE OF CONTENTS

LIST OF FIGURES

LIST OF TABLES

LIST OF SYMBOLS AND ABBREVIATIONS

Å	Angstrom
℃	Degree Celsius
µg	Microgram
µL	Microliter
µM	Micromolar
x g	Gravitational acceleration
AIDS	Autoimmune disease symptom
ATA	Aurintricarboxylic acid
ATCC	American Type Culture Collection
BHK	Baby hamster kidney
BSA	Bovine serum albumin
bp	Base pair
cDNA	Complementary deoxyribonucleic acid
CHIKV	Chikungunya virus
CHO	Chinese hamster ovary
CO_2	Carbon dioxide
COP	Coat protein complex
CoV	Coronavirus
CPE	Cytopathic effect
CV	Coxsackievirus
DAPI	4’,6-diamidino-2-phenylindole
DENV	Dengue virus
DIDS	4,4’-diisothiocyano-2,2’-stilbenedisulfonic acid
DMEM	Dulbecco’s modified Eagle’s medium
DMSO	Dimethyl sulfoxide
DNA	Deoxyribonucleic acid
dNTP	Deoxynucleotide
DTriP-22	4-1-phenyl-1*H*-pyr-azolo (3,4-d) pyrimidine
DTT	Dithiothreitol
EDTA	Ethylenediaminetetraacetic acid
EEEV	Eastern equine encephalitis virus
EGFP	Enhanced green fluorescence protein
eIF4G	Eukaryotic initiation factor 4G
EMEM	Eagle minimum essential medium
EV-A71	Enterovirus A71
EXT	Exostosin glycosyltransferase
F-12K	Kaighn’s modification of Ham’s F-12
FBP	Far upstream element binding protein
FBS	Fetal bovine serum
FDA	Food and Drug Administration
FMDV	Foot-and-mouth disease virus
g	Gram
GAG	Glycosaminoglycan
Gal	Galactosamine
GlcA	Glucuronic acid
GlcNAc	N-acetyl glucosamine
gp	Glycoprotein
HBV	Hepatitis B virus
HCV	Hepatitis C virus

HeLa	Human cervical adenocarcinoma epithelial cell
HFMD	Hand, foot and mouth disease
HIV	Human immunodeficiency virus
hnRNP	Heterogeneous nuclear ribonucleoprotein
HPV	Human papillomavirus
HRP	Horseradish peroxidase
HSV	Herpes simplex virus
HT-29	Human colon adenocarcinoma cell
IC_{50}	Inhibition concentration 50%
IdoA	Iduronic acid
IFN-γ	Interferon gamma
Ig	Immunoglobulin
IRES	Internal ribosome entry site
ITAF	IRES-specific transacting factor
kbp	Kilobase pair
KCl	Potassium chloride
kDa	Kilodalton
LC3	Light chain 3
$MgCl_2$	Magnesium chloride
$MgSO_4$	Magnesium sulfate
ml	Mililiter
mM	Milimolar
MO	Morpholino oligonucleotide
MOI	Multiplicity of infection
mRNA	Messenger ribonucleic acid
NaCl	Sodium chloride
NDST	N-deacetylase/N-sulfotransferase
NEAA	Non-essential amino acids
nM	Nanomolar
ORF	Open reading frame
PAGE	Polyacrylamide gel electrophoresis
PBS	Phosphate buffer saline
PCR	Polymerase chain reaction
PFU	Plaque forming unit
PI4KIIIβ	Phosphatidylinositol 4-kinase IIIβ
PMO	Phosphorodiamidate morpholino oligonucleotide
PPMO	Peptide-conjugated phosphorodiamidate morpholio oligomer
PSGL-1	P-selectin glycoprotein 1
PTO	Phosphorothioate oligonucleotide
PV	Poliovirus
RISC	RNA induced silencing complex
RD	Rhabdomyosarcoma
RdRP	RNA-dependent RNA polymerase
RNA	Ribonucleic acid
RNAi	Ribonucleic acid interference
RT-PCR	Reverse transcription polymerase chain reaction
S	Sedimentation coefficient
SARS	Severe acute respiratory syndrome
SCARB2	Scavenger receptor class B2
SDS	Sodium dodecyl sulfate
shRNA	Small hairpin ribonucleic acid
siRNA	Small interfering ribonucleic acid

TAE	Tris-acetate-EDTA buffer
TMEV	Theiler's murine encephalitis virus
UTR	Untranslated region
Vero	African green monkey kidney cell
Vivo-MO	Octaguanidinium-conjugated morpholino oligomer
VP	Virus protein
VPg	Viral protein genome linked
v/v	Volume per volume
w/v	Weight per volume
WIN	Winthrop
WNV	West Nile virus

LIST OF APPENDICES

CHAPTER 1

INTRODUCTION

Human enterovirus A71 (EV-A71) is the main causative agent of hand, foot and mouth disease (HFMD). EV-A71 was first described in 1969 during an outbreak of HFMD with central nervous system complications in California, USA. Since then, the virus has been subsequently associated with many other outbreaks including Bulgaria (Chumakov *et al.*, 1979), Hungary (Nagy *et al*., 1982; Kapusinszky *et al.*, 2010), Japan (Hagiwara *et al.*, 1978), Singapore (Chan *et al.*, 2003), Taiwan (Chen *et al.*, 2007), Malaysia (AbuBakar *et al.*, 2000), China (Tan *et al.*, 2011) and Vietnam (Thoa Le *et al.*, 2013). The clinical symptoms of HFMD are mild febrile illness, rashes on palms and feet, and oral ulcers (Ooi *et al.*, 2010). Unlike other enteroviruses that cause HFMD, EV-A71 is associated with neurological complications such as aseptic meningitis, brainstem encephalitis and poliomyelitis-like acute flaccid paralysis with deaths among infants and children aged below 6 years old (Ooi *et al.*, 2010). Considering the impact of fatality and long-term neurological sequelae in severely infected children, EV-A71 should be regarded as the most feared neurotropic enterovirus after the eradication of poliovirus (PV) (Chang *et al.*, 2007). To date, no effective antiviral agent is available for treatment of EV-A71 infection. Therefore, there is an urgent need to develop effective antiviral agents against EV-A71 infection.

Virus-host receptor interaction is the first essential event during virus infection. Viruses fail to enter cells to initiate infection when susceptible receptors are not available. Therefore, receptor availability is one the factors that determine virus tissue tropism and virulence. Receptor antagonists are often used as antiviral intervention. To date, five EV-A71 receptors have been identified, which are scavenger receptor class B2 (SCARB2) (Yamayoshi *et al.*, 2009), P-selectin glycoprotein ligand-1 (PSGL-1)

(Nishimura *et al.*, 2009), sialylated glycan (Yang *et al.*, 2009), annexin II (Yang *et al.*, 2011) and vimentin (Du *et al.*, 2014). Antibodies targeting SCARB2 and PSGL-1 significantly inhibited EV-A71 infection, but were insufficient to completely abrogate it (Yamayoshi *et al.*, 2009; Nishimura *et al.*, 2009). Thus, there are likely to be multiple receptors involved during EV-A71 infection.

Peptides that can block viral attachment or entry into the cells have therapeutic potential. A successful example of an antiviral peptide is the human immunodeficiency virus (HIV) fusion inhibitor, enfuvirtide, which obtained US Food and Drug Administration (FDA) approval in March 2003 for treatment of patients infected with HIV resistant to other antiretroviral drugs. Enfuvirtide is a 36 amino acid peptide derived from the heptad repeat region-2 sequence of the HIV transmembrane protein gp41. Enfuvirtide interacts with the host $CD4^+$ T cell receptor and thus blocks the HIV fusion step (Wild *et al.*, 1994; Kilby *et al.*, 1998). Screening of 441 overlapping peptides covering the entire hepatitis C virus (HCV) led to discovery of an 18-mer amphipathic α-helical peptide, designated as C5A. C5A exhibited significant antiviral activity against HCV, and other flaviviruses, paramyxoviruses and HIV through destabilizing the viral membranes (Cheng *et al.*, 2008). A peptide derived from the pre-S1 surface protein of hepatitis B virus (HBV) also inhibited HBV infection (Kim *et al.*, 2008).

Capsid protein VP1 of enteroviruses are known to interact with cellular receptors to initiate infection. Site-directed mutagenesis studies on EV-A71 VP1 capsid protein revealed that EV-A71 interacts with SCARB2 through the cleft around EV-A71 VP1 Q172 (Chen *et al.*, 2012). The molecular determinant of PSGL-1 binding was also identified at the VP1 Q145 and K244 (Nishimura *et al.*, 2013). Peptides targeting these functional receptors could potentially act as receptor antagonists and lead to new antiviral intervention. This study hypothesizes that screening of overlapping synthetic

peptides covering the entire EV-A71 VP1 capsid protein will enable identification of attachment or entry receptor(s) inhibitors, as well as to identify unknown receptors.

Cell surface carbohydrates such as glycosaminoglycans (GAGs) and sialic acid are often targeted by pathogens as attachment factors or co-receptors (Bergstrom *et al.*, 1997; Liu and Thorp, 2002; Oh *et al.*, 2010). These cell surface carbohydrates are abundantly expressed in most cell types. GAGs such as heparin, heparan sulfate, and chondroitin sulfate are negatively-charged linear polysaccharides composed of hexosamine/hexuronic acid repeats (Kjellen *et al.*, 1980; Kjellen and Lindahl, 1991). Viruses like herpes simplex virus (HSV) (WuDunn and Spear, 1989; Spear *et al.*, 1992), dengue virus (DENV) (Chen *et al.*, 1997), HIV (Vives *et al.*, 2005), human papillomavirus (HPV) (Giroglou *et al.*, 2001), echovirus (Goodfellow *et al.*, 2001), coxsackievirus B3 (CV-B3) (Zautner *et al.*, 2006) and foot-and-mouth disease virus (FMDV) (Jackson *et al.*, 1996; O'Donnell *et al.*, 2008) are known to utilize cell surface heparan sulfate as an attachment receptor. As EV-A71 has been shown to be inhibited by heparin mimetics (Pourianfar *et al.*, 2012) and an antiviral peptide with a heparan sulfate binding domain (Tan *et al.*, 2012), this study further hypothesized that EV-A71 could utilize cell surface heparan sulfate as an attachment receptor.

Other than receptor antagonists, antisense-mediated mechanism antiviral agents have been under investigation and promising outcomes have been demonstrated (Kole *et al.*, 2012). The first and only antisense-mediated antiviral agent that has received US FDA approval is a 21-mer phosphorothioate oligonucleotide (PTO) known as fomivirsen. Fomivirsen is approved for intravitreal treatment of cytomegalovirus retinitis in patients with acquired immunodeficiency syndrome (AIDS) (Perry and Balfour, 1999). The use of antisense-mediated short interfering RNA (siRNA) or short hairpin RNA (shRNA) targeting various regions of the EV-A71 genome have also shown promising outcomes (Sim *et al.*, 2005; Tan *et al.*, 2007a; Tan *et al.*, 2007b; Wu *et al.*, 2009; Yang *et al.*,

2012). However, the major limitations of these antisense molecules are that they require a delivery agent which may be toxic to the cells, as well as having a very short half-life in plasma. To overcome these limitations, this study involved the use of phosphorodiamidate morpholino oligomers (PMOs) which are highly resistant to nuclease degradation and coupled with a non-peptide cell-penetrating moiety known as octaguanidinium dendrimer (Moulton and Jiang, 2009). The use of peptide-conjugated PMOs (PPMOs) targeting multiple picornaviruses, including PV, CVB3, rhinovirus and FMDV, showed significant antiviral effects (Yuan *et al.*, 2006; Vagnozzi *et al.*, 2007; Stone *et al.*, 2008). This study further hypothesized that the use of translational suppressing vivo-morpholino oligomers (vivo-MOs) targeting EV-A71 internal ribosome entry site (IRES) stem-loop structures in the 5' untranslated region (UTR) and EV-A71 RNA-dependent RNA polymerase (RdRP) gene could efficiently inhibit EV-A71 infection in a tissue culture system.

With the advancement in recombinant DNA technology which allows modification of genomic DNA through mutagenesis, understanding of virus pathogenesis and virulence can be achieved through infectious cDNA clones construction. This allows genetic manipulation of viral RNA genomes which facilitates the investigation of viral virulence determinants and characterization of antiviral drug resistance mechanisms (Wimmer *et al.*, 2009; Hall *et al.*, 2012). Infectious cDNA clones of multiple enteroviruses have been constructed (Racaniello and Baltimore, 1981; Kraus *et al.*, 1995; Martino *et al.*, 1999; Harvala *et al.*, 2002; Liu *et al.*, 2011). Several infectious cDNA clones of EV-A71 have been previously constructed using different EV-A71 genotypes (Arita *et al.*, 2005; Chua *et al.*, 2008; Han *et al.*, 2010; Phuektes *et al.*, 2011; Yeh *et al.*, 2011; Zaini *et al.*, 2012). Multiple EV-A71 infectious clones have been constructed to study the virulence determinants of EV-A71 either *in vitro* or *in vivo* through site-directed mutagenesis (Arita *et al.*, 2007; Phuektes *et al.*, 2011; Yeh *et al.*,

2011; Kok *et al.*, 2012). Infectious cDNA clones tagged with reporter genes offer a rapid platform for drug screening and detailed study of the mechanistic action of the drug. This study involved construction of EV-A71 strain 41 (genotype B4) clones with and without the reporter gene, enhanced green fluorescence protein (EGFP). The EV-A71 infectious cDNA clone constructed in this study allowed detailed analysis of the drug mechanistic action using a reporter assay, and drug resistance through site-directed mutagenesis.

CHAPTER 2

LITERATURE REVIEW

2.1 The virology of enterovirus A71

2.1.1 Classification of enteroviruses

Human enteroviruses are members of the Enterovirus genus in the *Picornaviridae* family. *Picornaviridae* family is divided into 26 genera which consist of *Aphthovirus*, *Aquamavirus*, *Avihepatovirus*, *Avisivirus*, *Cardiovirus*, *Cosavirus*, *Dicipivirus*, *Enterovirus*, *Erbovirus*, *Gallivirus*, *Hepatovirus*, *Hunnivirus*, *Kobuvirus*, *Megrivirus*, *Mischivirus*, *Mosavirus*, *Oscivirus*, *Parechovirus*, *Pasivirus*, *Passerivirus*, *Rosavirus*, *Salivirus*, *Sapelovirus*, *Senecavirus*, *Teschovirus* and *Tremovirus* (Adams *et al.*, 2013) (http://www.picornaviridae.com).

Initially, the human enteroviruses were classified into four main groups based on pathogenicity in man and suckling mice, which were polioviruses (types 1-3), coxsackieviruses group A (types 1-22, 24), coxsackieviruses group B (types 1-6) and echoviruses (types 1-7, 11-27, 29-34) (Nasri *et al.*, 2007). As sequence data increases, these subgroups did not match the observed phylogenetic relationships. Furthermore, each observed type was associated with a wide spectrum of disease, and therefore classification on the basis of clinical terms was impossible.

As a result of this limitation, human enteroviruses have been classified into four species (A-D) on the basis of sequence identity and phylogenetic relationships. However, classification based on the phylogenetic relationships and sequence identity has led to the recognition that many animal viruses fall within the genus of *Enterovirus*, such as simian enteroviruses in enterovirus A, B and D. This resulted in the recent proposal to remove the host species from the enterovirus nomenclature. To date, the genus of

Enterovirus consists of 12 species, which are enterovirus A-H, enterovirus J and rhinovirus A-C (Table 2.1). Human rhinoviruses were classified under the *Enterovirus* genus on the basis of the similarities in genome organization, life cycle and phylogenetic relationships (Laine et al., 2005). EV-A71 is classified as a member of the species of enterovirus A (Brown and Pallansch, 1995; Pallansch and Roos, 2007; Racaniello, 2007).

Table 2.1: Current genetic classifications of enteroviruses

Species	Serotypes	Name of members
Enterovirus A	24	Coxsackieviruses A2-A8, A10, A12, A14, A16, enteroviruses A71, A76, A89-92, A114, A119, A120, simian enteroviruses SV19, SV43, SV46, baboon enterovirus BA13
Enterovirus B	61	Coxsackieviruses A9, B1-B6, echoviruses 1-7, 11-21, 24-27, 29-33, enteroviruses B69, B73-75, B77-88, B93, B97, B98, B100, B101, B106, B107, B110, B111, simian enterovirus SA5
Enterovirus C	23	Polioviruses 1-3, coxsackieviruses A1, A11, A13, A17, A19-22, A24, enteroviruses C95, C96, C99, C102, C104, C105, C109, C113, C116, C117,C118.
Enterovirus D	5	Enteroviruses D68, D70, D94, D111, D120
Enterovirus E	4	Enteroviruses E1-4
Enterovirus F	6	Enteroviruses F1-6
Enterovirus G	11	Enteroviruses G1-11
Enterovirus H	1	Enterovirus H1
Enterovirus J	6	Simian enterovirus SV6, enteroviruses J103, J108, J112, J115, J121
Rhinovirus A	80	Rhinoviruses A1-2, A7-13, A15-16, A18-25, A28-34, A36, A38-41, A43, A45-51, A53-68, A71, A73-78, A80-82, A85, A88-90, A94, A96, A100-109
Rhinovirus B	32	Rhinoviruses B3-6, B14, B17, B26-27, B35, B37, B42, B48, B52, B69, B70, B79, B83-84, B86, B91, B93, B97, B99-106
Rhinovirus C	54	Rhinoviruses C1-54

Information included in this table is adapted from information available on the Picornavirus Study Group website (www.picornaviridae.com; www.picornastudygroup.com).

2.1.2 Genomic and structural components of enterovirus A71

EV-A71 consists of a single-stranded, positive-sense ribonucleic acid (RNA) genome of approximately 7411 nucleotides (Brown and Pallansch, 1995). EV-A71 is a small, non-enveloped virus with a diameter of approximately 30 nm. The genome is enclosed within the icosahedral viral capsid (Plevka *et al.*, 2012; Wang *et al.*, 2012b). The EV-A71 genome has a single open reading frame (ORF) encoding a polyprotein, flanked by 5' and 3' untranslated regions (UTRs). As shown in Figure 2.1, the polyprotein is cleaved into four structural proteins (VP1, VP2, VP3 and VP4) and seven non-structural proteins (2A, 2B, 2C, 3A, 3B, 3C and 3D) (Brown and Pallansch, 1995). The 5' UTR of EV-A71 contains six putative stem-loop structures. The stem-loop I (cloverleaf) is involved in viral RNA synthesis and stem-loops II-VI make up the EV-A71 internal ribosome entry site (IRES) involved in cap-independent viral RNA translation (Thompson and Sarnow, 2003). The 3'UTR of picornavirus RNA contains three putative stem-loop structures followed by a poly(A) tail which is required for genome replication (Rohll *et al.*, 1995).

With the recent availability of the crystal structure of EV-A71 at 3.8 Å resolution, EV-A71 capsid has been shown to have quasi-T=3 symmetry with 60 identical units each consisting of four structural proteins VP1, VP2, VP3 and VP4 arranged in an icosahedral shape (Figure 2.2). VP1-VP3 capsid proteins are the main structural components of the virion, whereas VP4 is located internally. The surface loops of VP1 are located around the icosahedral 5-fold axis and the canyon of EV-A71 was found to be shallower than most of the other enteroviruses. Thus, it cannot provide immunological seclusion for the residues located at the bottom of the canyon and hence it is not likely to serve as a binding site for receptors (Plevka *et al.*, 2012).

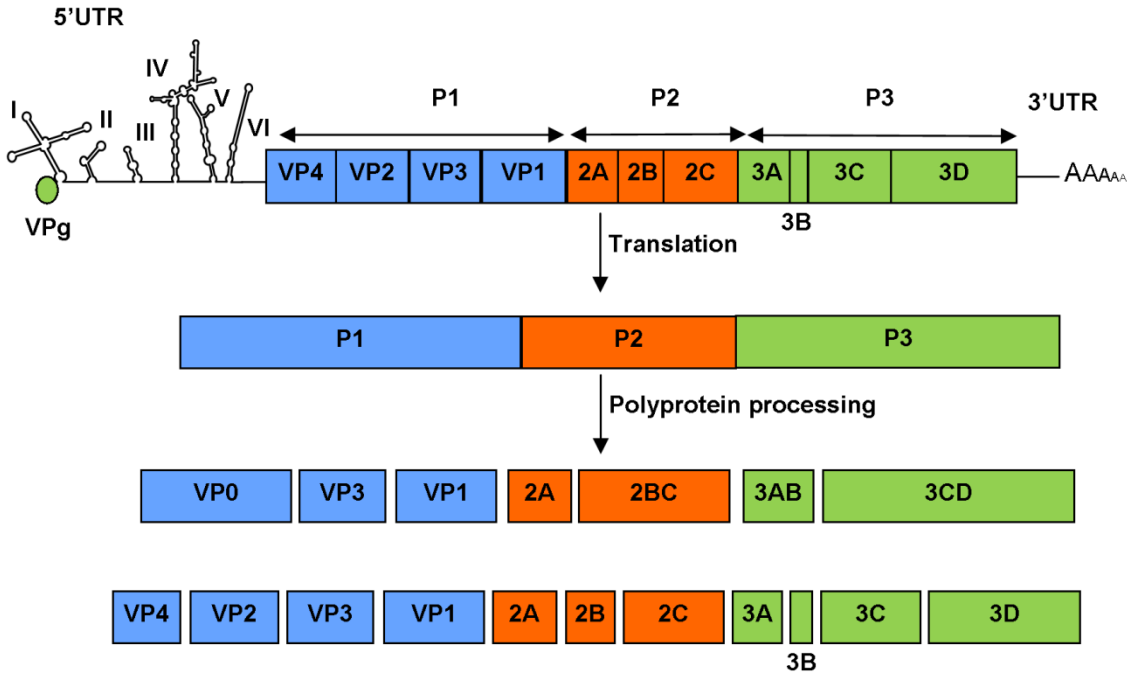

Figure 2.1: Schematic illustration of EV-A71 genomic RNA, translation and polyprotein processing. The EV-A71 genome consists of a single ORF flanked by 5' UTR and 3' UTR. The roman numerals (I-VI) refer to the six putative IRES stem-loop structures. The IRES-dependent translation of EV-A71 positive-sense RNA produces a polyprotein, which is then cleaved into individual products by EV-A71 2A and 3C proteases. VP1-VP4 are structural proteins, while 2A-2C and 3A-3D are non-structural proteins. The figure was adapted with modifications from Brown and Pallansch (1995) and Solomon *et al.* (2010).

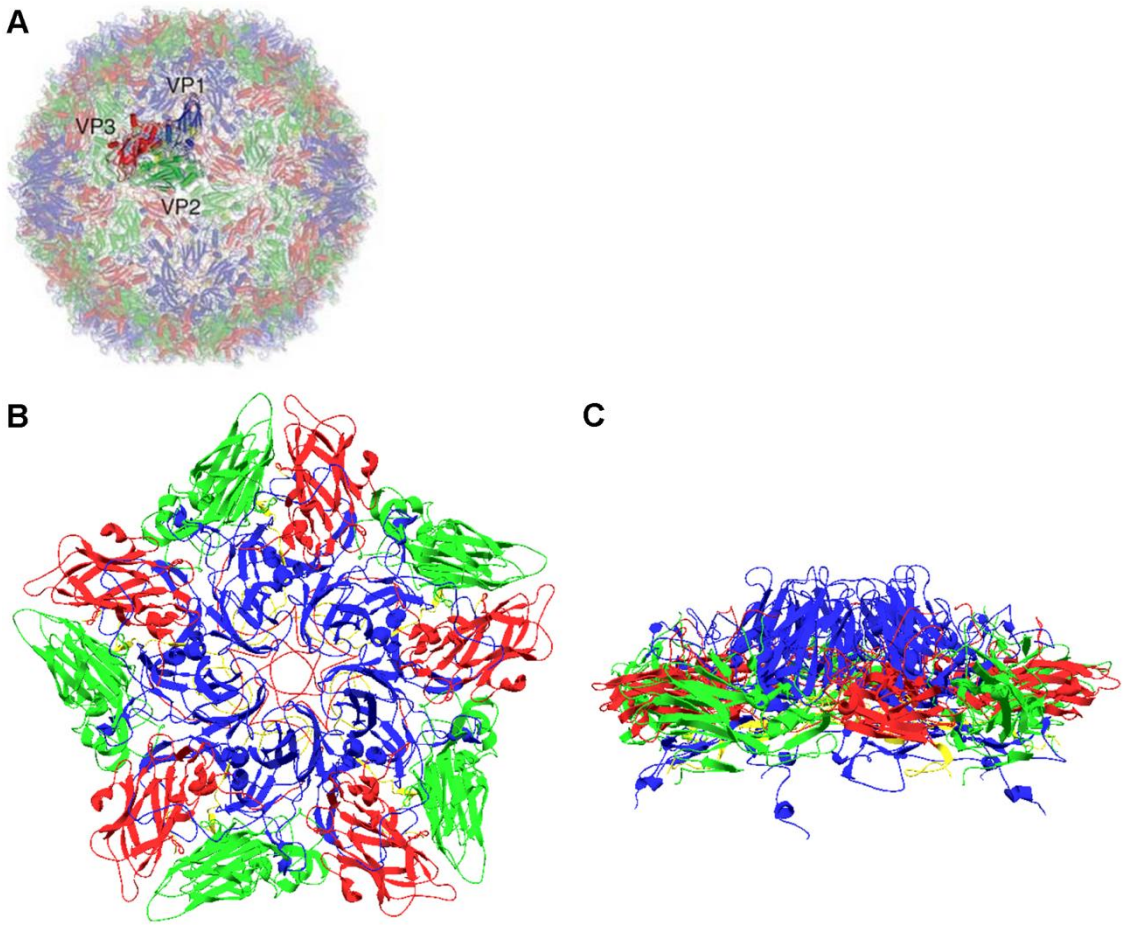

Figure 2.2: Crystal structure of EV-A71. (A) The mature EV-A71 virion, looking down an icosahedral two-fold axis, with VP1, VP2, VP3 and VP4 drawn in blue, green, red and yellow, respectively. The 5-fold axis of the EV-A71 virion in top view (B) and side view (C). This figure was adapted with modification from Wang *et al.* (2012b).

2.1.3 Life cycle of enterovirus A71

The EV-A71 life cycle involves viral attachment, entry, uncoating, IRES-dependent translation, polyprotein processing, genomic RNA replication, and finally maturation and release (Figure 2.3). Details on the EV-A71 life cycle are explained in the sub-sections below.

2.1.3.1 Enterovirus A71 attachment, entry and uncoating

Virus infection is initiated by attachment of the virus to a cellular receptor at the surface of a susceptible cell which then initiates a chain of dynamic events to enable viral internalization and uncoating. Multiple attachment receptors may be used sequentially, or in a cell-specific manner, and co-receptors may be involved (Tuthill *et al.*, 2010; Bergelson and Coyne, 2013). Cellular receptors determine tissue tropism and pathogenicity of the viruses (Haywood, 1994). To date, five EV-A71 receptors have been discovered, including PSGL-1 (Nishimura *et al.*, 2009), SCARB2 (Yamayoshi *et al.*, 2009), sialic acid (Yang *et al.*, 2009), annexin II (Yang *et al.*, 2011) and vimentin (Du *et al.*, 2014). However, none of the receptors reported are members of the immunoglobulin superfamily, unlike other reported enteroviruses receptors, such as poliovirus receptor, intracellular adhesion molecule-1 and coxsackievirus-adenovirus receptor (Tuthill *et al.*, 2010).

Human P-selectin glycoprotein ligand-1 (PSGL-1) is a sialomucin leukocyte membrane protein that is expressed as a homodimer of disulfide-linked subunits. It is expressed as a dimeric mucin-like glycoprotein that is N-glycosylated and contains both sialylated and fucosylated O-linked oligosaccharides (Laszik *et al.*, 1996; Somers *et al.*, 2000). PSGL-1 is involved in the entering and rolling of leukocytes on vascular endothelium. PSGL-1 is a type I transmembrane receptor found on the surface of neutrophils, monocytes and most lymphocytes. However, PSGL-1 receptor is not expressed in

neuroepithelial (SK-N-MC) and rhabdomyosarcoma (RD) cells which support the production of EV-A71 infection. PSGL-1 is only expressed on the dendritic cells of lymph nodes and on macrophages in the intestinal mucosa, which could be the primary site of EV-A71 replication after viral ingestion. PSGL-1 is proposed to be involved in the viremic phase of EV-A71 infection in which induction of apoptosis in the infected leukocytes results in the depletion of T cells, and changes in cytokine levels observed in severe encephalitis cases with pulmonary edema (Nishimura *et al.*, 2009). In another recent study, transgenic mice expressing human PSGL-1 alone did not enhance EV-A71 infection (Liu *et al.*, 2012). Therefore, PSGL-1 is not considered a major EV-A71 receptor. A study using the EV-A71 strain 1095 revealed that VP1-145Q regulates the molecular switch of PSGL-1 binding, and VP1-244K interacts with PSGL-1 (Nishimura *et al.*, 2013). The tyrosine sulfation sites at the amino terminus of PSGL-1 interact with EV-A71 (Nishimura *et al.*, 2010).

Besides PSGL-1, human scavenger receptor class B, member 2 (SCARB2) (also known as lysosomal integral membrane protein II, LGP85 and CD36b like-2) was identified as an EV-A71 functional receptor. SCARB2 is a heavily N-glycosylated type III transmembrane protein with a large extracellular domain (with ~ 400 amino acids) and short cytoplasmic domain at the amino and carboxyl-terminus (Fujita *et al.*, 1992). SCARB2 is the most abundant protein in the lysosomal membrane, and is involved in enlargement of early endosomes and late endosomes or lysosomes, and impairs endocytic membrane traffic out from the enlarged compartments (Kuronita *et al.*, 2002). SCARB2 was previously implicated in the endocytosis of high-density lipoprotein and the internalization of pathogenic bacteria. SCARB2-deficient mice have ureteropelvic junction obstruction, deafness and peripheral neuropathy (Gamp *et al.*, 2003). Although SCARB2 is primarily located in endosomes, surface expression of SCARB2 has also been demonstrated. SCARB2 is ubiquitously expressed in various cell types (Eskelinen

et al., 2003) and has been suggested to be the major receptor of EV-A71 (Yamayoshi *et al.*, 2009). Recent study has demonstrated that SCARB2, but not PSGL-1 is required for EV-A71 entry and uncoating (Lin *et al.*, 2012b; Yamayoshi *et al.*, 2013). Other enteroviruses including coxsackievirus A7, coxsackievirus A14 and coxsackievirus A16 (CV-A16) also use SCARB2 as a receptor (Yamayoshi *et al.*, 2012). Comparison of human SCARB2 and mouse SCARB2 revealed that amino acid residues 142-204 of the human SCARB2 are critical for EV-A71-SCARB2 interaction (Yamayoshi and Koike, 2011). The cleft around Q172 of the EV-A71 VP1 capsid protein was further deduced to interact with the variable region of the SCARB2 amino acid residues 144-151 (Chen *et al.*, 2012).

The third receptor reported for EV-A71 is cell surface sialylated glycan (Yang *et al.*, 2009). Glycans make up the major part of the cell surface and extra-cellular matrix of epithelial cells. A number of microbial pathogens utilize glycans on the host cell surface as attachment sites to invade host epithelial cells (Olofsson and Bergstrom, 2005). Sialic acids are found as terminal monosaccharides on the glycan chains of glycoproteins (Varki and Varki, 2007). Several viruses, including EV-A70 (Alexander and Dimock, 2002) and CV-A24 (Nilsson *et al.*, 2008) utilize cell surface sialylated glycan as an attachment receptor. Removal of cell surface sialic acid residues by neuraminidase was able to protect DLD-1, RD and SK-N-SH cells from EV-A71 infection (Yang *et al.*, 2009, Su *et al.*, 2012). Furthermore, pre-treatment of RD and SK-N-SH cells with α2-3 or α2-6 sialic acid binding lectin was found to inhibit EV-A71 infection. A recent study revealed that sialic acid present on SCARB2 is critical for EV-A71 infection. EV-A71 binding to SCARB2 was abolished after removal of the sialic acids present on SCARB2 (Su *et al.*, 2012).

Annexin II is also another functional receptor for EV-A71. Annexin II is a member of the annexin family, which are multifunctional phospholipid binding proteins. Annexin

II on the endothelial cells acts as a pro-fibrinolytic co-receptor for both plasminogen and tissue plasminogen activator facilitating the generation of plasmin (Kim and Hajjar, 2002). Previous work has found that annexin II could be the receptor of respiratory syncytial virus on epithelial cells (Malhotra *et al.*, 2003). Pre-incubation of EV-A71 viral particles with annexin II or pre-incubation of RD cells with anti-annexin II antibody resulted in reduced viral attachment. The authors suggested that binding of EV-A71 to annexin II could enhance viral entry and infectivity (Yang *et al.*, 2011).

Recently, vimentin has been reported as EV-A71 attachment receptor (Du *et al*., 2014). Vimentin is a 53 kDa polypeptide comprised of 466 amino acids, with a α-helical rod domain that is flanked by non-α-helical N- and C-terminal. Vimentin is widely expressed and a highly conserved protein of type III microfilament (Satelli and Li, 2011). Vimentin and other cytoskeletal filaments have been reported to play critical roles in attachment, entry and infection for many viruses including cowpea mosaic virus (Koudelka *et al*., 2009), HIV (Shoeman *et al.*, 1990), Japanese encephalitis virus (Das et al., 2011) and FMDV (Gladue *et al.*, 2013). Soluble vimentin and anti-vimentin antibodies could inhibit EV-A71 binding to host cells. Knockdown of vimentin expression on the cell surface remarkably reduced EV-A71 binding (Du *et al.*, 2014).

EV-A71 infection is initiated by attachment to the EV-A71 functional receptors and internalization through the clathrin-mediated endocytosis pathway (Hussain *et al.*, 2011). A few EV-A71 VP1 capsid protein domains such as Q172 were critical for SCARB2 interactions (Chen *et al.*, 2012). EV-A71-SCARB2 complexes are internalized through clathrin-mediated endocytosis and viral uncoating occurs within the acidified endosome (Lin *et al.*, 2012b). Eight amino acid residues from positions 144-151 on SCARB2 are critical for interaction with EV-A71. However, seven out of the eight residues are different from murine SCARB2, which explains why EV-A71 infects human cell lines but not murine cell lines (Chen *et al.*, 2012). Interestingly, the caveolar-mediated

endocytosis pathway is utilized when EV-A71 interacts with PSGL-1 receptor (Lin *et al.*, 2013a). The involvement of annexin II and sialylated glycan in viral entry are not well defined.

Upon attachment to the entry receptor, a series of conformations are triggered, resulting in formation of an "A-particle" that is primed for genome release. Formation of the "A-particle" is the first essential event during picornavirus uncoating. Both VP4 capsid protein and the lipid moiety (pocket factor) resides in the hydrophobic pocket within the VP1 may be expelled out. The second uncoating event occurs after endocytosis; an unknown trigger causes RNA expulsion from the "A-particle", leaving behind an empty capsid (Rossmann, 1989; Rossmann *et al.*, 2002; Shingler *et al.*, 2013). The formation of the 135S "A-particle" results in the presence of both SCARB2 entry receptor and an acidic pH environment, implying that "A-particle" formation happens after endocytosis in the early endosomes (Chen *et al.*, 2012b).

2.1.3.2 Enterovirus A71 translation and polyprotein processing

EV-A71 protein synthesis commences in a cap-independent manner which depends on the IRES element at the 5' UTR of the EV-A71 genome (Thompson and Sarnow, 2003). The IRES is a *cis*-acting element that forms secondary and tertiary RNA structures with the assistance of IRES-specific *trans*-acting factors (ITAFs). This recruits cellular translation machinery such as ribosomes to the viral RNA for initiation of translation. EV-A71 type I IRES requires eIF4A, eIF2, eIF3 and ATP to assemble the 48S complex for translation initiation (Thompson and Sarnow, 2003). Heterogeneous nuclear ribonucleoprotein (hnRNP) A1 interacts with the IRES; and either hnRNP A1 or hnRNP A2, but not both, are essential for IRES-directed translation (Lin *et al.*, 2009c). Far upstream element binding proteins (FBPs) are also involved in EV-A71 translation. FBP-1 enhances the IRES activity of EV-A71 RNA, while FBP-2 down-regulates IRES

activity. FBPs are well-known to interact with certain mRNA and participate at various steps in transcription, RNA processing, RNA transport and RNA catabolism. However, involvement of FBPs in viral translation remains largely unexplored (Lin *et al.*, 2009b).

The EV-A71 ORF is translated into a single polyprotein, which is subsequently processed by virus-encoded proteases 2A and 3C into the structural capsid proteins and the nonstructural proteins involved mainly in the replication of viral RNA (Lin *et al.*, 2009a). Picornavirus 2A protease cleavage sites were found at the C-terminus of capsid protein precursor P1 and within the 3CD fragment which generates 3C protease and RdRP (Yu and Lloyd, 1991). The 2A protease also cleaves eukaryotic initiation factor 4G (eIF4G) and therefore shuts off host cap-dependent translation to permit IRES-dependent translation of viral RNA (Thompson and Sarnow, 2003). The picornavirus 3C protease cleaves Gln-Gly pairs in the P2-P3 regions during proteolytic maturation of the viral proteins (Kitamura *et al.*, 1981).

2.1.3.3 Enterovirus A71 genome replication

The positive-sense RNA genome must be first transcribed into negative-sense RNA which is then used as a template for synthesis of new genomic positive-sense RNA. Enterovirus genome replication occurs in the cytoplasm. Two cellular pathways contribute to viral RNA replication, are membranous vesicles derived from membranes of endoplasmic reticulum (ER) and/or Golgi complex and autophagosome-like vesicles (Belov and Ehrenfeld, 2007). Coat protein complex 1 (COPI) and COPII vesicles are essential components of the trafficking machinery cycling between ER and the Golgi complex. COPI and COPII are involved in the formation of picornavirus-induced vesicles for several enteroviruses including PV and echovirus 11. Recently, Wang *et al.* (2012a) demonstrated that COPI, but not COPII is required for EV-A71 replication. EV-A71 replication is inhibited when brefeldin A and golgicide A inhibits COPI

activity. Co-localization of viral non-structural protein 2C with COPI subunits was demonstrated. Like other picornaviruses, EV-A71 infection also induces membranous vesicles derived from ER and Golgi complex for replication (Wang *et al.*, 2012a).

Co-localization of viral proteins and microtubule-associated protein 1 light chain 3 (LC3) has been reported in PV (Jackson *et al.*, 2005). Like PV, Huang *et al.* (2009) has established that EV-A71 infection of RD and SK-N-SH cells induces autophagy. Co-localization of autophagosome-like vesicles with EV-A71 VP1 or LC3 protein in neurons of the cervical spinal cord of ICR mice was shown. EV-A71 replication was also inhibited by the autophagic inhibitor 3-methyladenine, suggesting that autophagy induced by EV-A71 is crucial for virus replication.

Viral replication requires both cellular and viral factors which include viral non-structural proteins (2B, 3A and 3D), cellular RNA binding proteins and *cis*-acting RNA secondary structures (Lin *et al.*, 2008). The viral RdRP plays a key role in synthesis of both negative and positive strands (Neufeld *et al.*, 1994). Destabilization of the 3' UTR stem-loop structures interaction by site-directed mutagenesis severely suppressed viral RNA synthesis (van Ooij *et al.*, 2006).

2.1.3.4 Enterovirus A71 packaging and release from cells

The assembly and virion secretion of enteroviruses is a multi-step process (Racaniello, 2007). Recently, the structure of the procapsid of EV-A71 was resolved by cryo-electron microscopy (cryo-EM) and the virion assembly has been postulated (Cifuente *et al.*, 2013). Similar to other picornaviruses, the protomer (5S) is first assembled from VP1, VP3 and VP0 proteins and subsequently five promoters are self-assembled into a pentamer (14S). The newly synthesized RNA is packaged into the empty capsid by unknown mechanism, with 12 pentamers assembling into a procapsid (Jacobson and Baltimore, 1968; Jacobson *et al.*, 1970). Alternatively, the RNA may recruit the

pentamers which are subsequently packed into a capsid around the genome (Ghendon *et al.*, 1972; Marongiu *et al.*, 1981). These events produce the provirion (150S) and maturation occurs when VP0 is cleaved into VP2 and VP4, and the virions finally develop into infectious viruses (160S). Viruses are released from the cytoplasm when the cells lyse.

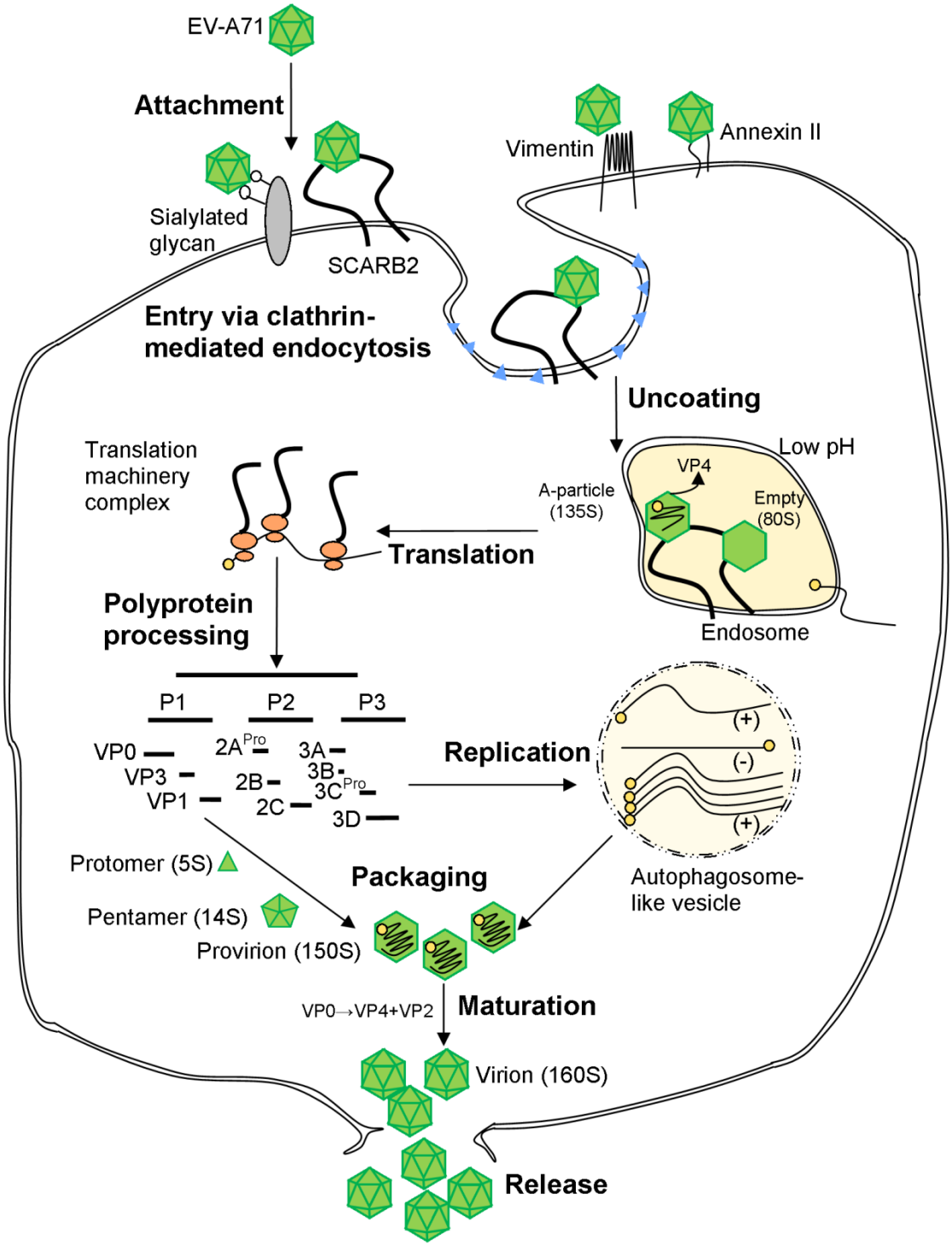

Figure 2.3: Intracellular replication of EV-A71. The EV-A71 replication life cycle involves nine critical steps: (1) attachment, (2) entry, (3) uncoating, (4) translation, (5) polyprotein processing, (6) replication, (7) packaging, (8) maturation and (9) release.

2.1.4 Epidemiology of enterovirus A71

2.1.4.1 Outbreaks of enterovirus A71

EV-A71 was first isolated from the stool of a 9-month-old child with encephalitis in 1969, in California (Schmidt *et al.*, 1974). In the 1970s, two large EV-A71 epidemics occurred in Europe. In Bulgaria in 1975, the neurovirulence of EV-A71 was manifested during a large EV-A71 outbreak and resulted in 44 fatalities among 451 children (Chumakov *et al.*, 1979). The second epidemic happened in Hungary in 1978 with 1550 cases (826 aseptic meningitis, 724 encephalitis) and 47 fatalities reported (Nagy *et al.*, 1982). Epidemics of HFMD and EV-A71 were also reported in Sweden and Japan in 1973 (Blomberg *et al.*, 1974; Hagiwara *et al.*, 1978).

In Sarawak, Malaysia in 1997, a large outbreak of EV-A71 with 2618 HFMD cases and 34 deaths was reported. In Peninsular Malaysia, 4 fatalities were reported in 1997 (Cardosa *et al.*, 1999; Chan *et al.*, 2000). In 1998, 129,106 estimated cases with 78 fatalities were reported in Taiwan. In 1999, 6,000 HFMD cases were reported and 29 infected patients died from the disease in Taiwan (Ho *et al.*, 1999). Small sporadic outbreaks occurring every 2 to 3 years were also reported in Australia, Korea, Japan, Vietnam and Singapore (Bible *et al.*, 2007). Large outbreaks of HFMD were reported in 2006 in Sarawak, Malaysia with 13 deaths (Chua and Kasri, 2011). The largest EV-A71 epidemics occurred in China and the number of cases grew from 489,000 cases and 126 deaths in 2008 to 1,775,000 cases and 905 deaths in 2010 (Tan *et al.*, 2011; Mao *et al.*, 2012). In addition, more than 137 fatal cases have been reported in Vietnam during 2011(Khanh *et al.*, 2012). The emergence of EV-A71 in recent years in Asia showed that EV-A71 will continue to be a global threat.

2.1.4.2 Molecular epidemiology of enterovirus A71

EV-A71 is further classified into 11 subgenotypes within 3 genotypes, A, B (B1-B5) and C (C1-C5), based on sequence comparison of VP1 genes, and each group has at least 15% nucleotide divergence from the others (Brown *et al.*, 1999; Cardosa *et al.*, 2003; Bible *et al.*, 2007; Chan *et al.*, 2010; Tee *et al.*, 2010) (Figure 2.4). Genotype A consists of the prototype BrCr strain which was first identified in California, USA in 1969 (Schmidt *et al.*, 1974). Since then, no circulation has been reported, till recently, when genotype A was isolated in five out of 22 children with HFMD in Anhui province of China in 2008 (Yu *et al.*, 2010).

The molecular epidemiology of EV-A71 in the Asia-Pacific region between 1973 and 2010 is summarized in Table 2.2. Genotype B was predominant in Malaysia and Singapore. Subgenotypes B1 and B2 were predominantly circulating in 1970s and 1980s in Japan, Taiwan and United States (Brown *et al.*, 1999; Chu *et al.*, 2001). EV-A71 subgenotypes B3 and B4 have been circulating since 1997 in Singapore, Malaysia and Japan; and subgenotype B5 has been circulating since 1999 in Malaysia, 2001 in Thailand and Singapore, 2003 in Japan and Taiwan, and 2006 in Brunei (Cardosa *et al.*, 1999; Shimizu *et al.*, 1999; Cardosa *et al.*, 2003; AbuBakar *et al.*, 2009; Chan *et al.*, 2012; Zaini and McMinn, 2013; Linsuwanon *et al.*, 2014).

Genotype C is predominant in East Asia including China (Ooi *et al.*, 2010). Subgenotypes C1 and C2 were initially reported in 1980s and subgenotype C3 was reported in Korea in 2003 (Cardosa *et al.*, 2003). Subgenotype C4 has caused major outbreaks in China since 2000, and has also been reported in Japan, Vietnam, Thailand and Taiwan in recent years (Lin *et al.*, 2006; Tu *et al.*, 2007; Zhang *et al.*, 2010b). Subgenotype C5 has been reported in southern Vietnam and Taiwan (Tu *et al.*, 2007; Huang *et al.*, 2008b).

Molecular epidemiology studies have improved the understanding of the evolution of EV-A71. Genetic diversity of the virus can influence its pathogenic properties and circulation. As a result of a lack of proof-reading ability in the RdRP, EV-A71 is genetically diverse with an estimated evolution rate of 4.5×10^{-3} substitutions per nucleotide per year (Tee *et al.*, 2010). Molecular epidemiological analysis revealed that each genotype either circulates predominantly or co-circulates with other genotypes within the same epidemic region. Co-circulation of four distinct subgenotypes has been reported in Malaysia between 1997 and 2000 (Herrero *et al.*, 2003). Currently, only subgenotype B5 circulates in Malaysia (Chan *et al.*, 2012).

Other than a high error rate in replication, recombination contributes to genetic diversity and evolution of EV-A71. Intertypic recombination between EV-A71 and other Enterovirus A including CV-A16 has been demonstrated. Multiple recombination breakpoints were reported in EV-A71 non-structural genes (Yoke-Fun and AbuBakar, 2006). Intratypic recombination between EV-A71 genotype B and genotype C has also been demonstrated and the recombinant breakpoints were located at the 3' end of the 2A and 3D non-structural protein genes (Huang *et al.*, 2008a).

Table 2.2: EV-A71 subgenotypes circulating in the Asia-Pacific region between 1973 and 2013*

	1973	1980	1986	1990	1993	1996	1997	1998	1999	2000	2001	2002	2003	2004	2005	2006	2007	2008	2009	2010	2011	2012	2013
Singapore							B4	B3, B4	B3	B4, B5	B4	C1, B4						B5, C2					
Malaysia							B3, B4, C1, C3	C1	B4, B5, C1	B4, B5, C1	B4, C1	C1	B5, C1		B5	B5	B5	B5	B5				
Australia			C1			C1, C2		C2	B3, C2	B4, C1	B4												
Japan	B1			B2, C1	B2		B3, B4, C2	C2	C2	B4	C2	B4, C2	C4, B5	C4		C4	C4						
Taiwan		B1	B1					C2, B4	B4	B4	B4	B4, C4	B4, B5	C4	C4, C5	C5	C5, B5	B5	B5	C4	B5, C4	B5	
Korea									C3	C3			C4				C4		C1, C4, C5				
Brunei																B5							
Vietnam															C1, C4, C5								
Thailand											B5, C1	C1	C1	C1		C1, C5	B5, C1, C2, C4, C5	C1, C2, C4, C5	B5, C4	B5	B5	B5, C4	B5
China								C4		C4	C4	C4	C4	C4			C4	A, C4	B5, C4	C4	C4	C4	

*Table adapted from Solomon *et al.* (2010) and Chan *et al.* (2012)

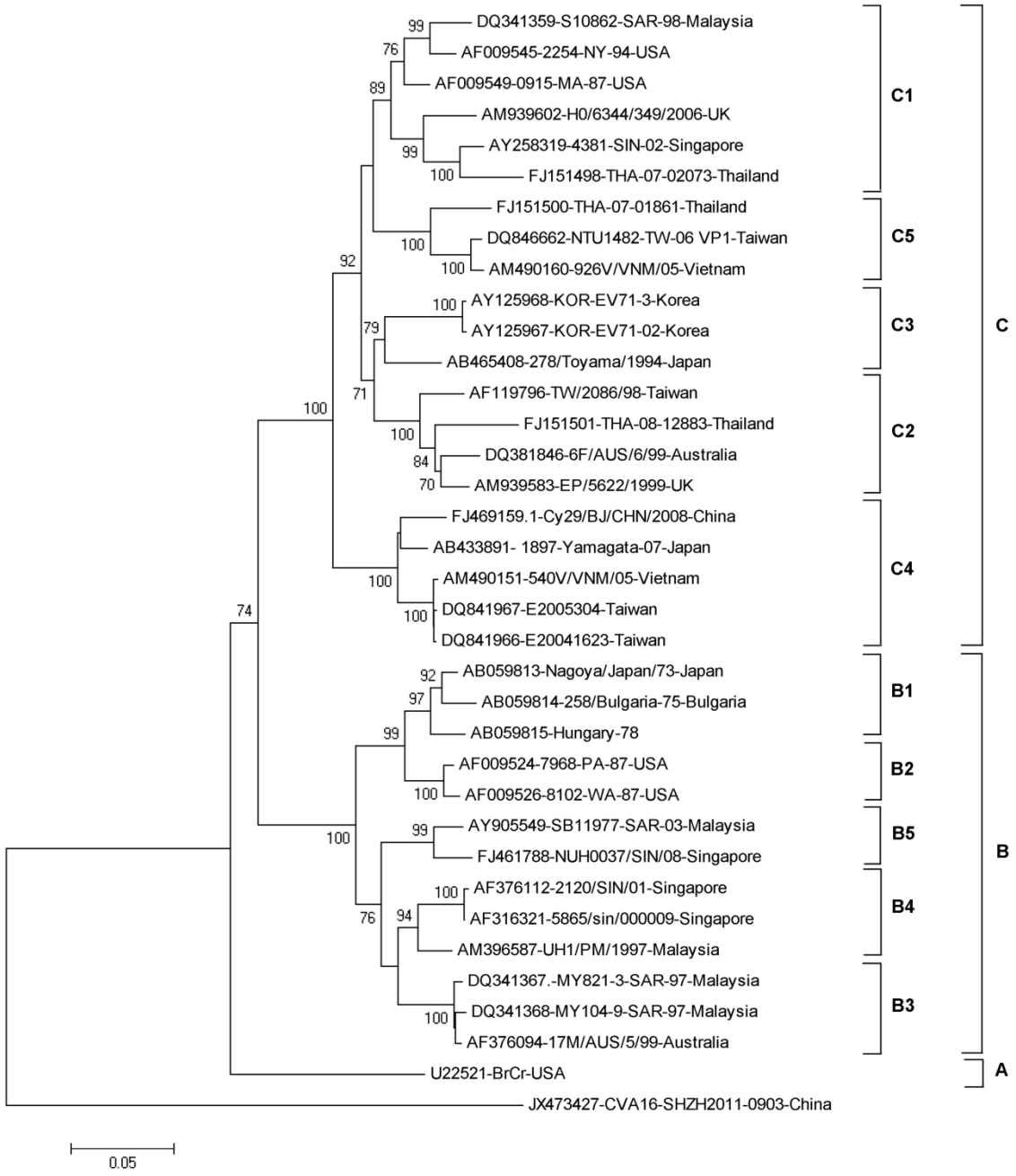

Figure 2.4: Phylogenetic analysis of EV-A71 VP1 gene sequences. The neighbor-joining tree was constructed with the Kimura-2 parameter as a model for nucleotide substitution using MEGA 5 software. The robustness of the tree was determined by bootstrapping with 1000 pseudoreplicates.

2.1.5 Clinical manifestations of enterovirus A71 infections

EV-A71 first appeared in 1969 and since then has caused outbreaks with clinical manifestations ranging from hand, foot and mouth disease (HFMD), herpangina, aseptic meningitis and encephalitis (Schmidt *et al.*, 1974; Liu *et al.*, 2000). HFMD is a common childhood exanthema characterized by a mild febrile illness with papulovesicular rash on the palms and soles, and multiple oral ulcers (Liu *et al.*, 2000). Other frequently encountered symptoms include poor appetite, vomiting and lethargy. EV-A71 also causes herpangina, an illness characterized by an abrupt onset of fever and sore throat, associated with development of raised papular lesions on the mucosa of the anterior pharyngeal folds, tonsils and soft palate. HFMD and herpangina are common clinical syndromes of EV-A71 infection, but they are usually mild and self-limiting. HFMD can be caused by other enteroviruses such as coxsackievirus (CV) A5, A10, A16 and echovirus 7. However, unlike these enteroviruses, EV-A71 infections are more commonly associated with neurological complications such as aseptic meningitis, acute flaccid paralysis and brainstem encephalitis (McMinn, 2002). Table 2.3 summarizes various neurological syndromes associated with EV-A71 infection. Similar to poliomyelitis EV-A71 infection can also present as severe cardiorespiratory symptoms, due to neurogenic cardiac failure and pulmonary edema (Chang *et al.*, 1999). Several epidemics have occurred in Sarawak, and approximately 10-30% of children hospitalized with EV-A71-related HFMD also developed central nervous system complications, which were not present in children with CV-A16 infections (Ooi *et al.*, 2007).

EV-A71-infected patients with aseptic meningitis generally have a complete recovery. However, patients with acute flaccid paralysis frequently have permanent weakness or paralysis (McMinn *et al.*, 1999). Radiological and histopathological evidence suggests that acute flaccid paralysis occurs when EV-A71 establishes a lytic infection in anterior

horn motor neurons of the spinal cord, similar to the pathogenesis of poliomyelitis (Shen *et al.*, 2000; Wong *et al.*, 2008; Li *et al.*, 2012). Brainstem encephalitis is the most severe neurological complications of EV-A71 infections. Extensive inflammation develops in the hypothalamus, brainstem, spinal cord and cerebellar dentate nucleus (Lum *et al.*, 1998b; Huang *et al.*, 1999; Wang *et al.*, 1999). The onset of brainstem encephalitis is characterized by rapidly progressive cardio-respiratory failure, which leads to shock and pulmonary edema or hemorrhage with death (Lum *et al.*, 1998a). Children occasionally recover fully from brainstem encephalitis, but may have permanent neurological sequelae with delayed neurodevelopment and reduced cognitive function (Huang *et al.*, 2006; Chang *et al.*, 2007).

Table 2.3: Neurological syndromes associated with EV-A71 infection

Neurological manifestations
Encephalitis Acute flaccid paralysis Encephalomyelitis Aseptic meningitis Cerebellar ataxia Transverse myelitis
Neurological and systemic manifestations
Brainstem encephalitis with cardiorespiratory failure
Manifestations indicative of immune-mediated mechanisms
Guillain-Barr ésyndrome Opsoclonus-myoclonus syndrome Benign intracranial hypertension

Modified from Ooi *et al.* (2010).

2.1.6 Development of therapeutics against enterovirus A71 infection

To date, no antiviral agents are currently licensed for clinical use. The only treatment option for EV-A71-infected patients is symptomatic relief. A number of antiviral agents have been developed to target different EV-A71 life cycles, including viral attachment, entry, uncoating, RNA translation, polyprotein processing, RNA replication and virus maturation. However, only a few of these antiviral agents are currently in clinical trials. Figure 2.5 summarizes all the antiviral agents discussed in this section.

2.1.6.1 Therapeutics targeting viral attachment and entry

Virus-host receptor interaction is the first essential event during virus infection. The ability to recognize and bind to specific receptors determines host range and tissue tropism (Haywood, 1994). Since virus-host receptor interactions are the first event during infection, inhibitors that block this event could act as potential therapeutics. The soluble form of cellular receptors could act as molecular decoys of cell-associated receptors. Soluble SCARB2, PSGL-1, sialic acid and heparin or heparin mimetics exhibit inhibitory effects against EV-A71 infection *in vitro* (Nishimura *et al.*, 2009; Yamayoshi *et al.*, 2009; Yang *et al.*, 2009; Pourianfar *et al.*, 2012). Highly sulfated suramin and its analog, NF449, exhibited antiviral activity against EV-A71 infection (Arita *et al.*, 2008b; Wang *et al.*, 2013b). NF449-resistant mutants consist of two mutations in VP1, E98Q and K244R, implying that NF449 inhibited EV-A71 infection by binding to the VP1 protein (Arita *et al.*, 2008b). Similarly, kappa carrageenan, a sulfated polysaccharide from seaweed, also exhibited significant antiviral activity through targeting EV-A71 attachment and entry (Chiu *et al.*, 2012). The possible mechanism of these soluble decoys is through disruption of the integrity of the EV-A71 capsid structure or steric hindrance of receptor interactions.

Receptor antagonists could also be developed as potential antiviral agents. An antimicrobial peptide, lactoferrin, also exhibited anti-EV-A71 properties *in vitro* and *in vivo* through blocking viral attachment to the cell surface (Lin *et al.*, 2002; Weng *et al.*, 2005; Chen *et al.*, 2008a).

2.1.6.2 Therapeutics targeting viral uncoating

Uncoating inhibitors (pocket binders) have been intensively studied as antiviral agents against many picornaviruses, including rhinovirus (Fox *et al.*, 1986), PV (Fox *et al.*, 1986), echovirus (McKinlay *et al.*, 1986) and coxsackievirus (See and Tilles, 1992). The complex of WIN51711 with the EV-A71 hydrophobic pocket underneath the canyon depression has recently been resolved by X-ray crystallography (Plevka *et al.*, 2013). The key success factor of these uncoating inhibitors is their ability to fit into the VP1 hydrophobic pocket, stabilize the capsid structure, and therefore block the receptor-induced uncoating mechanism (Plevka *et al.*, 2013).

A series of modified WIN compounds including BPROZ-194, BPROZ-112, BPROZ-284, BPROZ-103, BPROZ-299, BPROZ-101, BPROZ-033, and BPROZ-074 were effective against EV-A71 infection with IC_{50} values ranging from 0.8 nM to 1550 nM (Shia *et al.*, 2002; Chern *et al.*, 2004; Shih *et al.*, 2004a; Shih *et al.*, 2004b; Chang *et al.*, 2005; Chen *et al.*, 2008b). However, a single point mutation in VP1 V192M was sufficient to confer resistance to BPROZ-194 (Shih *et al.*, 2004b). Other than modified WIN compounds, the broad spectrum enterovirus inhibitor pleconaril also inhibited EV-A71 infection *in vitro* and *in vivo* (Pevear *et al.*, 1999; Zhang *et al.*, 2012). However, pleconaril failed to inhibit the cytopathic effect (CPE) induced by a Taiwan 1998 EV-A71 isolate (Shia *et al.*, 2002). Another group of capsid binders, pyridazinyl oxime ethers chemically derived from pirodavir such as BTA39 and BTA188, significantly inhibited EV-A71 infection (Barnard *et al.*, 2004). Crystallographic studies showed the

pirodavir predecessor R61837 complexed with rhinovirus 14 by binding to the hydrophobic pocket underneath the canyon floor, similar to the mechanism of WIN compounds (Chapman *et al.*, 1991). 4',6-Dichloroflavan (BW683C), previously identified as an anti-rhinovirus compound, was also effective against EV-A71 infection (Genovese *et al.*, 1995; Conti *et al.*, 1998). Mechanistic studies demonstrated that BW683C binds to and stabilizes rhinovirus against heat or acid inactivation, implying that BW682C acts as a viral uncoating inhibitor (Bauer *et al.*, 1981; Tisdale and Selway, 1983; Tisdale and Selway, 1984).

2.1.6.3 Therapeutics targeting viral RNA translation

The antisense-mediated mechanism consists of oligonucleotides (8-50 nucleotides in length) that bind to RNA through Watson-Crick base pairing and modulate the function of the targeted RNA (Kole *et al.*, 2012). RNA interference (RNAi) involves the cleavage of targeted mRNA through the RNA-induced silencing complex. Small interfering RNA (siRNA) targeting highly conserved regions of 5'UTR (Deng *et al.*, 2012), VP1, VP2 (Wu *et al.*, 2009), 2C, 3C, 3D (Sim *et al.*, 2005; Tan *et al.*, 2007b), and 3'UTR (Sim *et al.*, 2005) significantly inhibited EV-A71 infection in a dose-dependent manner. In addition, short hairpin RNA (shRNA) was effective against EV-A71 infection *in vitro* and *in vivo* (Lu *et al.*, 2004; Tan *et al.*, 2007a; Tan *et al.*, 2007b). The use of siRNA in clinical settings is hampered by its short half-life in plasma. Improved siRNA with 2'O methylation and 2' fluoro modifications have recently been demonstrated against EV-A71 infection (Deng *et al.*, 2012). However, siRNA also has poor endosomal uptake which limits the clinical application of these siRNAs. Other translation-suppressing nucleotides, for example, PPMO, showed promising results in inhibiting PV and CV-B3 (Yuan *et al.*, 2006; Stone *et al.*, 2008). Unlike siRNA or shRNA, PPMO interacts with targeted RNA, especially the IRES region, and blocks

ribosome recruitment and therefore inhibits viral translation (Kole *et al.*, 2012). PPMO readily penetrates the cells and is resistant to nuclease degradation.

Compounds that down-regulate the activity of IRES-dependent translation could potentially be developed into antiviral agents. Quinacrine, which impairs IRES-dependent translation by preventing the interaction between polypyrimidine-tract binding protein and IRES, has been demonstrated to act against EV-A71 infection (Wang *et al.*, 2013a). Kaempferol, a flavonoid, was found to inhibit EV-A71 IRES activity by altering the composition of ITAFs (Tsai *et al.*, 2011). Geniposide derived from *Fructus gardeniae* inhibited EV-A71 replication via inhibition of viral IRES activity (Lin *et al.*, 2013b). Amantadine, a tricyclic symmetric amine previously used against influenza A virus infection, was found to suppress EV-A71 IRES-dependent translation (Davies *et al.*, 1965; Hoffmann *et al.*, 1965; Chen *et al.*, 2008c).

2.1.6.4 Therapeutics targeting viral polyprotein processing

Since EV-A71 2A and 3C proteases are involved in multiple roles in EV-A71 infection and evasion of host innate immunity, they are important targets for development of antiviral therapeutics. A pseudosubstrate, LVLQTM peptide, could inhibit EV-A71 infection through binding to the active site of 2A protease (Falah *et al.*, 2012). Rupintrivir (AG7088) is an irreversible peptidomimetic inhibitor of human rhinovirus 3C protease which has reached phase 2 clinical trials with promising outcomes (Patick *et al.*, 1999; Witherell, 2000; Binford *et al.*, 2005; Patick, 2006; Binford *et al.*, 2007). Rupintrivir showed significant inhibition of EV-A71 infection *in vitro* and *in vivo* but with reduced efficacy as compared with human rhinoviruses (Zhang *et al.*, 2010a; Hung *et al.*, 2011; Lu *et al.*, 2011; Zhang *et al.*, 2013). X-ray crystallography of the complex of EV-A71 3C protease with rupintrivir revealed that the half-closed S2 sub-site and the size reduced S1' pocket of EV-A71 3C protease limits the access of the rupintrivir's P1'

group which contains a lactam ring (Wang *et al.*, 2011). A series of 3C protease rupintrivir analogues were designed based on AG7088, with an aldehyde replacement of the α,β-unsaturated ester. Compound 10b significantly inhibited EV-A71 infection (Kuo *et al.*, 2008). An orally bioavailable 3C protease inhibitor, designated as compound 1, also exhibited antiviral activities against multiple rhinovirus serotypes and enteroviruses *in vitro* (Patick *et al.*, 2005). Flavonoids such as fisetin and rutin, have also been identified as EV-A71 3C protease inhibitors (Lin *et al.*, 2012a).

2.1.6.5 Therapeutics targeting viral genomic RNA replication

Viral non-structural proteins such as 2C, 3A and RdRP play important roles in viral replication. Hence, inhibitors that inactivate viral replication proteins or interrupt virus protein-host protein interactions could potentially be developed as effective antiviral agents.

Picornavirus 2C protein possesses nucleoside triphosphatase activity and is involved in the synthesis of the viral negative strand RNA and encapsidation of progeny virions in PV. Metrifudil (N-[2-methylphenyl]methyl-adenosine) and N^6 benzyladenosine, both adenosine receptor agonists, were reported to have inhibitory effects against EV-A71 infection with IC_{50} values of 1.3 μM and 0.1 μM, respectively. EV-A71 2C protein with a single mutation E325G or double mutations H118Y and I324M were resistant to metrifudil and N^6 benzyladenosine, respectively (Arita *et al.*, 2008b). Guanidine hydrochloride is one of the most extensively studied picornavirus inhibitors (Caliguiri and Tamm, 1968a; Caliguiri and Tamm, 1968b). This inhibitor blocks the replication of PVs (Rightsel *et al.*, 1961; Loddo *et al.*, 1962), coxsackieviruses (Herrmann *et al.*, 1982), echoviruses, and FMDV (Saunders *et al.*, 1985). Interestingly, guanidine hydrochloride also inhibited EV-A71 infection and analysis of guanidine-resistant mutants revealed that a single mutation at the 2C protein (M193L) was sufficient to

confer resistance (Sadeghipour *et al.*, 2012). The non-structural protein 2C was identified as the guanidine hydrochloride target, hence guanidine was likely to prevent the association of 2C/2BC with host membrane structures during viral replication (Bienz *et al.*, 1990).

Picornavirus 3A protein has been shown to modulate the host cell's intracellular membrane transport. Protein 3AB, the precursor form of 3A, has RNA-binding properties and stimulates the cleavage of 3CD protease and the activity of RdRP in PV. Enviroxime is an anti-enterovirus compound that targets viral proteins 3A and 3AB and suppresses the replication of enterovirus by an unknown mechanism. Recently, phosphatidylinositol 4-kinase III beta (PI4KIIIβ) was identified as a target of enviroxime-like compounds (T-00127-HEV1 and GW5074) for anti-PV activity (Arita *et al.*, 2011), and by anti-enterovirus compounds including PI4KIIIβ inhibitor, PIK93 (Hsu *et al.*, 2010). Enviroxime is reported to have strong antiviral effects against EV-A71 with an IC_{50} of 0.15 μM (de Palma *et al.*, 2008). A functional analog of enviroxime, GW5074 (3-3,5-dibromo-4-hydroxybenzylidine-5-iodo-1,3-dihydro-indol-2-one), is a Raf-1 inhibitor and inhibited EV-A71 infections with an IC_{50} of 2.0 μM. GW5074-resistant mutants carried similar mutations at 3A protein as enviroxime-resistant mutants (Arita *et al.*, 2008b; Arita *et al.*, 2009). The enviroxime mimetic compound AN-12-H5 was found to have strong inhibitory activity against EV-A71 and PV infections. However, AN-12-H5-resistant mutants carried mutations on the viral capsid protein (VP1 A224T and VP3 R227K). The authors suggested that AN-12-H5 could act as a bifunctional inhibitor targeting EV-A71 replication and an early stage of infection after the binding step (Arita *et al.*, 2010). Interestingly, a recent study of an siRNA sensitization assay targeting PI4Kβ-related genes has identified oxysterol-binding protein (OSBP) as a target of AN-12-H5 (Arita *et al*., 2013). A compound designated as compound 1, 2-fluoro-4-(-methyl-8-(3-(methylsulfony)benzylamino)imidazo[1,2-

a]pyrazin-3-yl)phenol, was found to exhibit broad-spectrum antiviral activity against multiple enteroviruses with IC_{50} ranging between 4 to 71 nM. Resistant mutant analysis revealed substitutions in the 3A protein at the position which interacts with PI4KIIIβ (van der Schaar, *et al*., 2013).

Picornavirus RdRP is involved in incorporation of nucleotides during the synthesis of negative and positive viral RNA strands and other activities such as uridylation of VPg during RNA replication. DTriP-22 (4-1-phenyl-1*H*-pyr-azolo [3,4-d]pyrimidine) is a novel class of compounds with anti-EV-A71 activity with IC_{50} values of 0.15 – 0.98 μM against EV-A71 strains from all genotypes. DTriP-22-resistant mutants showed mutations in the RdRP implying that DTriP-22 interacts with RdRP and inhibits poly (U) elongation activity, but not VPg uridylylation activity (Chen *et al.*, 2009).

Unlike DNA polymerase, RdRP lacks 3'→ 5' proofreading ability. Ribavirin (1-β-D-ribofuranosyl-1,2,4-triazole-3-carboxyamine) is an antiviral compound used in the treatment of infections with HCV and respiratory syncytial viruses. Ribavirin causes transition mutations because of its ability to pair with both uracil and cytosine. Thus, ribavirin exerts its antiviral activity by increasing the "error rate" of viral genome replication past the point of "error catastrophe" whereby the fitness of all members of the viral population is reduced (Airaksinen *et al.*, 2003). Ribavirin inhibited EV-A71 infection with IC_{50} of 266 μM and prevented EV-A71-induced paralysis and death in mice (Li *et al.*, 2008).

2.1.6.6 Other antiviral agents

The type 1 interferon (IFNs) system responds to viral infection and triggers first line antiviral defenses in cells (Basler and Garcia-Sastre, 2002). Type I IFNs including IFN-α4, IFN-α6, IFN-α14 and IFN-α16, provide a protective effect in EV-A71-infected human cell lines and mice (Liu *et al.*, 2005; Yi *et al.*, 2011). However, EV-A71 2A

protease has been shown to play a crucial role in antagonizing the IFN response, which limits the IFN clinical application for treatment of EV-A71 infection (Lu *et al*., 2012).

Chloroquine (4-aminoquinoline) is an anti-malarial agent in clinical use. The antiviral property of chloroquine has been demonstrated against HIV infection, through prevention of glycosylation of the viral envelope protein gp120 occurring in the Golgi apparatus (Savarino *et al.*, 2001a; Savarino *et al.*, 2001b; Savarino *et al.*, 2004; Savarino, 2011). Interestingly, treatment of EV-A71-infected human glioblastoma cells with chloroquine significantly prevented viral-induced apoptosis and resulted in more than a 100-fold reduction of EV-A71 RNA synthesis at 1.2 μM (Shih *et al.*, 2008).

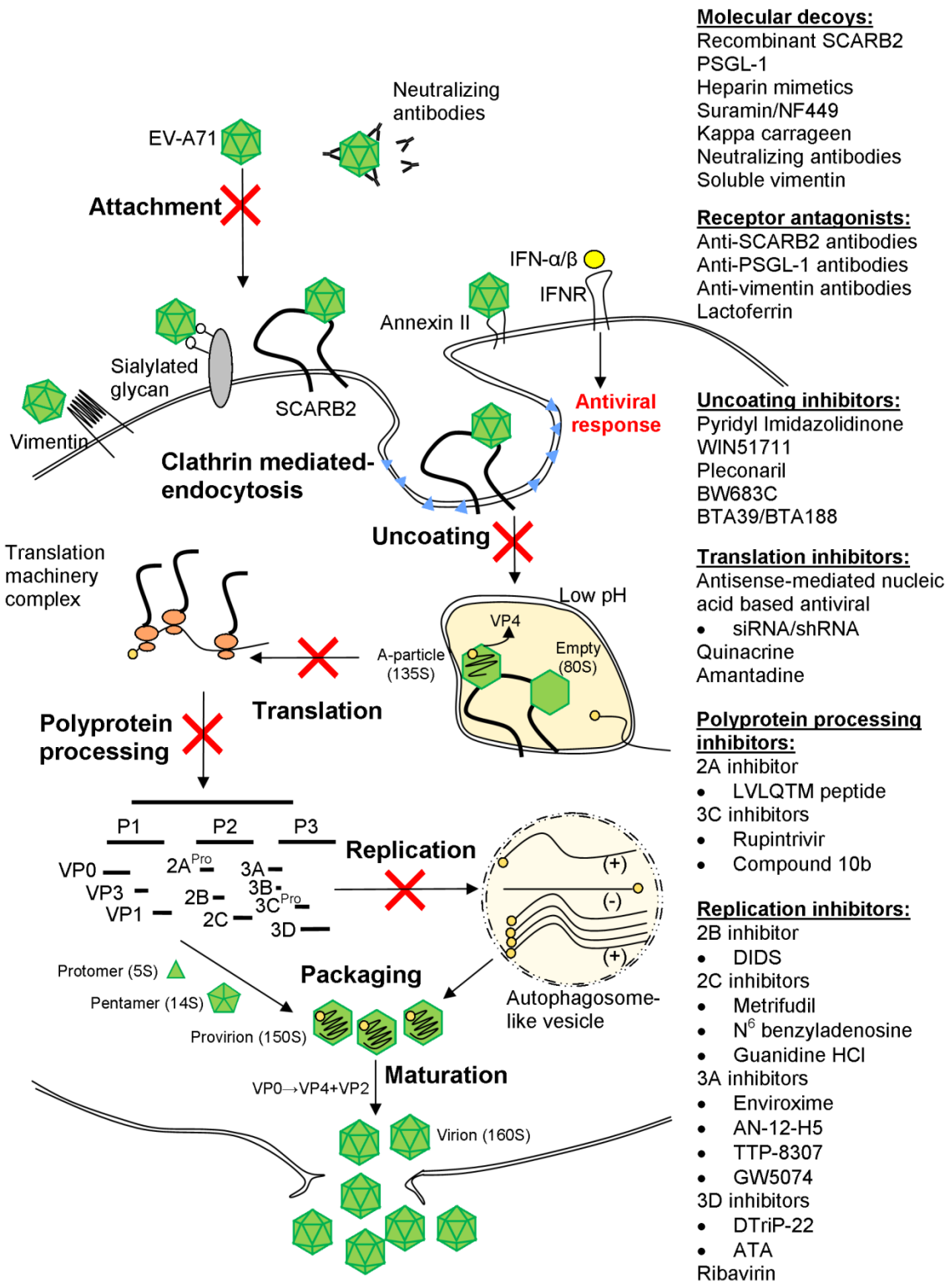

Figure 2.5: Schematic illustration of EV-A71 intracellular infection and summary of the antiviral agents classified according to the mechanisms of action, which include molecular decoys, receptor antagonists, uncoating inhibitors, translation inhibitors, polyprotein processing inhibitors and replication inhibitors.

2.2 Antiviral drug discovery

2.2.1 Antiviral peptides as therapeutics

2.2.1.1 Therapeutic peptides – an overview

Natural and synthetic peptides are promising pharmaceutics with the potential to treat a wide variety of diseases. Peptides are usually composed of up to 50 amino acids that are covalently linked by amide bonds between the amino group of one amino acid and the carboxyl group of another amino acid. Because of their regulatory role and extreme diversity coupled with highly specificity of molecular recognition, peptides are also attractive tools in drug discovery and are making their way into clinical applications. Due to the selective nature and efficacy of the peptide-target interaction, only low concentrations of the peptides are sufficient. The metabolism of peptides is superior to small chemical molecules due to the limited possibility for accumulation and relative non-toxicity to the host. These properties contribute towards a minimal risk of adverse effects. The peptide-based drugs can be receptor agonists or antagonists derived from natural peptides, as well as pathogen proteins. However, the potential of peptides as therapeutics is often hampered by the inability of the peptides to reach the targeted site in its active form *in vivo*, due to inadequacy of absorption through the mucosa and rapid degradation by proteolytic enzymes (Goodwin *et al.*, 2012).

The most important classes of therapeutic peptides that have been investigated include insulin, hormone analogs and antimicrobial peptides. Antimicrobial peptides are typically relatively short with a positive charge (net charge of +2 to +9) and are amphiphilic. To date, hundreds of antimicrobial peptides have been identified. Many antimicrobial peptides are derived from single-cell microorganisms, insects and other invertebrates, plants, amphibians, birds, fishes and mammals including humans (Wang and Wang, 2004). Examples of these antimicrobial peptides are human β-defensin-2,

human lactoferricin, cathelicidin (LL-37) and protegrin (Jenssen *et al.*, 2004b; Jenssen *et al.*, 2006).

2.2.1.2 Antiviral applications of therapeutic peptides

Peptides that can block viral attachment or entry into host cells have therapeutic potential. Enfuvirtide (Fuzeon, Roche) is the first peptide-based inhibitor of viral fusion approved by the FDA in March 2003 for clinical use. Enfuvirtide is a 36 amino acid peptide derived from the HR2 sequence of the transmembrane protein gp41 of HIV-1. It interacts with the $CD4^+$ T-cell receptor and inhibits 6-helix bundle formation required for fusion of viral and cellular membranes. Enfuvirtide is used in combination with other antiretroviral agents in the treatment of patients with resistant HIV (Wild *et al.*, 1994; Kilby *et al.*, 1998). Due to its low bioavailability, short plasma half-life (approximately 2 hours) and easily induced drug resistance, second and third generation peptide-based fusion inhibitors were developed (Ruxrungtham *et al.*, 2004; Zhang *et al.*, 2004). Sifuvirtide was designed to overcome the limitation of enfuvirtide, with a stable secondary structure of the α-helix structure, and increased the plasma half-life up to 22 hours (Wang *et al.*, 2009). To overcome acquired resistance to enfuvirtide, Dwyer *et al.* (2007) synthesized a series of C-peptides with enhanced helical structures, from T2410 to T2635. T2635 was 3,600-fold more active than enfuvirtide and did not generate resistant virus even after more than 70 days in culture (Dwyer *et al.*, 2007). Another anti-HIV peptide was designed according to the α-helical region of the C-terminal domain of HIV-1 capsid, which acts as a molecular decoy to prevent C-terminal domain dimer formation. The α-helical structure of the peptide was stabilized using hydrocarbon stapling technique. *In vitro* assembly assays revealed that the peptide inhibited mature-like virus particle formation and specifically inhibited HIV-1 production in cell-based analysis (Zhang *et al.*, 2011).

An amphipathic 18-mer α-helical peptide (C5A) derived from the membrane anchor domain of the HCV NS5A protein was found to be virucidal for HCV and other flaviviruses, paramyxoviruses and HIV by destabilizing viral membranes (Cheng *et al.*, 2008). Structure activity analysis suggested that C5A permeabilizes viral liposome membranes and leads to release of viral capsids, and exposes the viral genome to nuclease degradation (Cheng *et al.*, 2008). Screening of overlapping peptides covering the HCV E1E2 envelope proteins led to identification of a 16-mer peptide (peptide 75) that exhibited antiviral activities against HCV infection with an IC_{50} of 0.3 μM. Temperature shift experiments suggested that peptide 75 inhibited HCV at the post-binding step (Liu *et al.*, 2010).

A few anti-flavivirus peptides were identified using physio-chemical algorithms and in combination with the Wimley-White interfacial hydrophobicity scale. One of them is DN59, a peptide corresponding to the stem domain of DENV that inhibits DENV and West Nile virus (WNV) at low micromolar concentrations (Hrobowski *et al.*, 2005). Screening of a phage display library derived from murine brain cDNA against WNV envelope protein led to identification of a peptide, designated as peptide 9, that exhibited antiviral activity against WNV and DENV *in vitro*. Mice challenged with WNV that had been pre-incubated with peptide 9 had reduced viremia and fatality (Bai *et al.*, 2007).

A 21-mer synthetic peptide derived from the pre-S1 surface protein of HBV exhibited antiviral activity against HBV at picomolar concentrations. The IC_{50} reported was approximately 20 nM. This peptide is believed to interact with the hepatocyte receptor and therefore blocks HBV binding (Kim *et al.*, 2008). Another study by Zheng *et al.* (2005) identified four 20-mer synthetic peptides derived from the severe acute respiratory syndrome (SARS)-associated coronavirus (SARS-CoV) S protein with

significant antiviral activity against SARS-CoV infection. Pre-incubation with the P8 peptide resulted in over 10,000-fold reduction of SARS-CoV infectivity.

Peptide 6 derived from the Zn^{2+} finger region of the M1 sequence of influenza virus strain A/PR/8/34 centered around amino acids residues 148 to 166 was shown to significantly inhibit multiple influenza viruses at concentrations as low as 0.1 nM. The peptide 6 inhibited influenza viruses infection by inhibiting polymerase activity (Nasser *et al.*, 1996). EB peptide, a 20-mer peptide derived from fibroblast growth factor 4, exhibited significant antiviral activity against influenza viruses including the highly pathogenic H5N1. EB peptide binds to the viral hemagglutinin protein and therefore inhibits viral attachment to the cellular receptor. *In vivo* studies demonstrated that pre-treatment of HK/156 virus with 2 mM EB peptide resulted in 100% survival of infected mice (Jones *et al.*, 2006; Jones *et al.*, 2011). Interestingly, EB peptide also exhibited antiviral activity against multiple viruses including herpes simplex virus type 1 (HSV-1), vaccinia virus, and poxviruses (Bultmann *et al.*, 2001; Altmann *et al.*, 2009; Altmann *et al.*, 2012).

Screening of 138 15-mer peptides covering the ectodomain of the HSV-1 glycoprotein B (gB) identified three peptides (gB94, gB122 and gB131) with 50% effective concentration (EC_{50}) below 20 μM. Studies revealed that gB131 is an entry inhibitor, and gB122 inhibits HSV-1 entry and also causes viral inactivation. The viral inactivation activity was probably a result of either premature triggering or inhibition of conformational change in the gB-1 molecule required for entry. The gB122 or gB131 may be acting by blocking a protein-protein interaction, in particular, inhibiting gB binding to paired immunoglobulin-like type 2 receptor-alpha, gD or gH-gL (Akkarawongsa *et al.*, 2009). Interestingly, highly cationic α-helical peptides that interact with heparan sulfate significantly inhibited HSV-1 and HSV-2 infection. These peptides blocked HSV attachment to the cell surface heparan sulfate. Increasing the net

positive charge of the peptides significantly increased the antiviral activities against HSV-1 infection (Jenssen *et al.*, 2004a). A recent study by Tiwari *et al.* (2011) identified two anti-heparan sulfate peptides, G1 and G2 that exhibited significant anti-HSV-1 activities. These peptides were isolated through phage display peptide library screening by using heparan sulfate as the target. G2 peptide exhibited broad spectrum antiviral activity, as well as inhibitory activity *in vivo* (Tiwari *et al.*, 2011).

2.2.2 Antisense-mediated morpholino oligomers as therapeutics

2.2.2.1 Antisense-mediated mechanism – an overview

The use of a synthetic oligonucleotide to inhibit pathogen replication through an antisense-mediated mechanism was first reported by Zamecnik and Stephenson (1978), using a tridecamer oligodeoxyribonucleotide complementary to Rous sarcoma virus RNA to inhibit production of virus in chick embryo fibroblast cells. The oligodeoxyribonucloetide likely hybridized with the viral RNA and blocked viral protein translation (Zamecnik and Stephenson, 1978). However, unmodified oligodeoxynucleotides are highly susceptible to degradation by endogenous nucleases. Phosphorothioate oligonucleotides (PTOs) were the first oligonucleotide analog derivatives developed to resist nuclease degradation. The only antisense drug that has received approval from FDA for therapeutic application is fomivirsen, a 21-nucleotide PTO antisense drug for intravitreal treatment of cytomegalovirus retinitis in AIDS patients (de Smet *et al.*, 1999; Perry and Balfour, 1999).

In general, antisense-mediated mechanisms can be divided into two categories, targeting RNA cleavage and non-cleavage (Bennett and Swayze, 2010). RNA interference (RNAi) and antisense gapmer oligonucleotides target RNA cleavage while translation-suppressing oligonucleotides do not (Kole *et al.*, 2012). RNAi is a form of post-transcriptional gene silencing.

Small interferencing RNAs (siRNA) are short synthetic double stranded RNAs of 21-22 nucleotide length, which interact with a multi-protein RNA-induced silencing complex (RISC) and hybridize to the targeted mRNA, subsequently leading to mRNA degradation by nucleases. In contrast, antisense gapmer oligonucleotides are modified single-stranded DNA that bind to complementary mRNA by base pairing and induce cleavage of targeted mRNA by ribonuclease H (Kole *et al.*, 2012). Translation-suppressing oligonucleotides are oligonucleotides that pair with mRNA sequences near the translation initiation site and block binding of ribosomes to mRNA, thereby inhibiting translation of the undesirable proteins. Translation-suppressing oligonucleotide-mRNA duplexes are recognized by neither ribonuclease H nor RISC, therefore the mRNA is not cleaved (Kole *et al.*, 2012). The major limitations of these translation-suppressing oligonucleotides include the low knock-down efficacies and off-target effects.

2.2.2.2 Phosphorodiamidate morpholino oligomers

Phosphorodiamidate morpholino oligomers (PMOs) are steric-blocking translation-suppressing oligonucleotides which bind to RNA and block RNA translation. In PMOs, the deoxyribose rings of DNA are replaced with 6-membered morpholine rings, and the phosphodiester linkages are replaced with phosphorodiamidate linkages. PMOs have no electrical charge, do not interact strongly with proteins, and do not require the activity of RNase-H for their activities (Summerton and Weller, 1997; Summerton, 1999). Like siRNA antisense molecules, PMOs do not readily cross cell membranes without delivery techniques, which have prevented their efficacious use in animals. Although the unmodified PMOs are endocytosed, uptake by endocytosis does not mean the PMOs reach the cytoplasm or nucleus of the cell. The PMOs are retained within endosomes with few PMOs escaping from the endosomes to the cytosol or nuclear compartment (Partridge *et al.*, 1996). With the recent identification of cell-penetrating peptide

sequences, PMOs can be easily taken up into cells if conjugated with cell-penetrating peptides. This technology is known as peptide-linked PMOs (PPMOs) (Abes *et al.*, 2006; Abes *et al.*, 2008).

In PPMOs, the PMO is covalently linked with arginine-rich cell-penetrating peptides, which include $(RXR)_4B$-, $(RXR)_4XB$-, $(RXRRBR)_2XB$- and $(RX)_8B$-, with R representing arginine, B representing β-alanine, and X representing 6-aminohexanoic acid (Abes *et al.*, 2006, Moulton and Jiang, 2009). PPMOs are taken up by endocytosis and a fraction of endocytosed PPMOs escape from the endosome, entering the cytosol and nuclear compartment where they can block mRNA translation. Besides PPMOs, vivo-morpholino oligomers (vivo-MOs) are antisense PMO that are covalently linked to a molecular scaffold, a guanidium group at each of its eight tips. Vivo-MOs have been effective in mice, rats, adult zebrafish and various organ explants (Moulton and Jiang, 2009). A schematic illustration of vivo-MOs and PPMOs is shown in Figure 2.6.

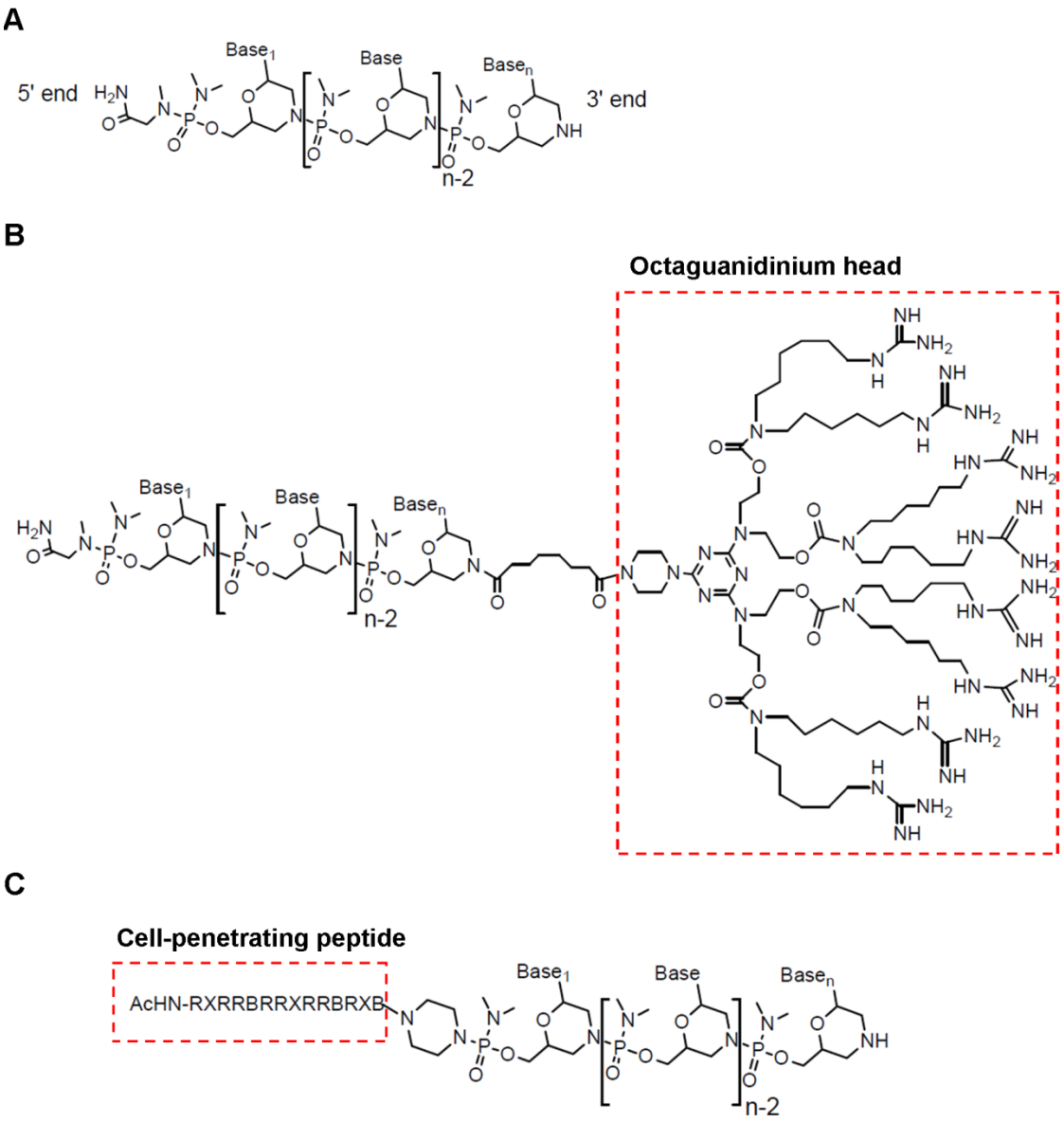

Figure 2.6: Molecular structures of morpholino oligomers: (A) Phosphorodiamidate morpholino oligomer (PMO), (B) octaguanidinium-conjugated morpholino oligomer (vivo-MO) and (C) 5' cell-penetrating peptide-conjugated phosphorodiamidate morpholino oligomer (PPMO). This figure was adapted with modifications from Moulton and Jiang (2009).

2.2.2.3 Antiviral applications of morpholino oligomers

In recent years, PPMOs and vivo-MOs have been shown to be effective antiviral therapeutics. PPMOs are found to inhibit various viruses *in vitro* and *in vivo*, including DENV (Kinney *et al.*, 2005; Holden *et al.*, 2006; Stein *et al.*, 2008), Ebola virus (Enterlein *et al.*, 2006; Warfield *et al.*, 2006; Swenson *et al.*, 2009), influenza virus (Ge *et al.*, 2006; Gabriel *et al.*, 2008; Lupfer *et al.*, 2008; Bottcher-Friebertshauser *et al.*, 2011), coronavirus (Neuman *et al.*, 2004; Neuman *et al.*, 2005; Burrer *et al.*, 2007; Moulton *et al.*, 2007), PV (Stone *et al.*, 2008), FMDV (Vagnozzi *et al.*, 2007), CV-B3 (Yuan *et al.*, 2006) and rhinovirus (Stone *et al.*, 2008). These PPMOs are designed as antisense drugs against positive-sense viruses, often targeting the viral mRNA sequence involved in one or more of the major early events in viral translation.

Antisense-mediated PPMOs targeting several positive-sense picornaviruses have been demonstrated recently. PPMOs targeting type I IRES picornaviruses, including PV, rhinovirus, CV-B2, and CV-B3 IRES stem-loop structures IV-VI caused significant inhibition of viral infection in tissue culture as well as in animal models (Yuan *et al.*, 2006; Stone *et al.*, 2008). In contrast to type I IRES picornaviruses, only PPMOs targeting the AUG start site, but not IRES structure of type II IRES picornaviruses including FMDV, exhibited significant antiviral properties (Vagnozzi *et al.*, 2007). The antisense PPMOs are known to complement the RNA target, either preventing the 48S ribosome formation or disrupting the integrity of the RNA structures required for translation initiation. Viruses acquired resistance to the PPMOs after serial passage in the presence of the PPMOs. Sequence analysis of the mutant viruses revealed a single mutation was sufficient to confer PPMO resistance (Vagnozzi *et al.*, 2007; Stone *et al.*, 2008).

Antisense-mediated PPMOs have also been developed for flaviviruses. PPMOs targeting the DENV 5'UTR stem-loop, 3'UTR cyclization sequence and 3'UTR stem-loop inhibited DENV replication, presumably by blocking critical RNA-RNA or RNA-protein interactions involved in viral translation and replication (Holden *et al.*, 2006). In a different study, PPMOs targeting the DENV 3'UTR cyclization sequences exhibited broad-spectrum antiviral activity against DENV serotypes 1-4 (Kinney *et al.*, 2005). PPMOs targeting the DENV AUG translation start site region have moderate efficacies when compared to those targeting the 5'UTR stem loop or 3'UTR cyclization sequences (Kinney *et al.*, 2005). Both PPMOs targeting the 5'UTR stem-loop and 3'UTR cyclization sequences of DENV-2 increased the average survival time of up to 8 days in DENV-2-infected AG129 mice (Stein *et al.*, 2008). PPMOs targeting the 5' end, the AUG translation start site region, 5'UTR stem-loop and 3'UTR cyclization sequence were found to inhibit WNV infection in BHK-21 cells (Deas *et al.*, 2007). PPMO targeting Japanese encephalitis virus 3'UTR cyclization sequence exhibited significant antiviral activity in tissue culture and mice (Anantpadma *et al.*, 2010).

The inhibitory effects of PPMOs against multiple influenza viruses *in vitro* and *in vivo* have been demonstrated. The $(RXR)_4XB$-conjugated PMOs targeting the start site of viral polymerase subunit PB1 mRNA and the 3' end of the NP virion RNA significantly inhibited viral replication in Balb/c mice when administered through the intranasal route (Gabriel *et al.*, 2008). The PPMO targeting these two regions also inhibited many influenza A virus subtypes, including H1N1, H3N2, H3N8, H7N7 and highly pathogenic H5N1 (Ge *et al.*, 2006).

2.3 Glycosaminoglycans as virus receptors

2.3.1 Heparan sulfate glycosaminoglycan – an overview

Heparin and heparan sulfate are structurally the most complex members of the glycosaminoglycan (GAG) family. Heparin and heparan sulfate are linear polysaccharides that are composed of repeating units of uronic acid (D-glucuronic acid and L-iduronic acid) and D-glucosamine (Kjellen *et al.*, 1980; Kjellen and Lindahl, 1991). Heparin is mainly present in mast cells while heparan sulfate exists in all cell types. Both are predominantly present on the cell surface and in the extracellular matrix (ECM) in the form of proteoglycans. Heparin is highly sulfated whereas heparan sulfate is a low-sulfated chain. Heparan sulfate is negatively-charged through sulfate groups in different positions.

The heparan sulfate chains rarely occur as free entities but are attached to various core proteins. The heparan sulfate-protein conjugate is known as heparan sulfate proteoglycan. There are two major subfamilies of plasma membrane-bound heparan sulfate proteoglycans, syndecans and glypicans (Bernfield *et al.*, 1999). Heparan sulfate is structurally diverse in different cell types. The diversities arise from the disaccharide composition which differs by the presence of variably sulfated or non-sulfated uronic acid and D-glucosamine. Endothelial cells and connective tissue mast cells are rich in D-glucuronic acid-D-glucosamine while kidney is rich in L-iduronic acid-D-glucosamine (Edge and Spiro, 1990; Bourin and Lindahl, 1993; Rosenberg *et al.*, 1997).

The biosynthesis of heparan sulfate involves three basic steps: chain initiation, polymerization and modification (Figure 2.7). During chain initiation, linkage tetrasaccharides are assembled on the serine residues in the core protein. After addition of an N-acetylglucosamine residue, polymerization takes place by alternate addition of glucuronic acid and N-acetylglucosamine residues. As the chain grows, modifying

enzymes introduce sulfate groups at various positions, and some of the glucuronic acid residues are converted into iduronic acid. Glucosaminyl N-deacetylase/N-sulfotransferase (NDST) is the first modifying enzyme that replaces the acetyl group in N-acetylglucosamine residues with a sulfate group. Other modifying enzymes include 2-O-sulfotransferase, 6-O-sulfotransferase and 3-O-sulfotransferase which add 2-O-sulfate, 6-O-sulfate and 3-O-sulfate groups, respectively. The final heparan sulfate biosynthesis product has a cluster of N- and O-sulfated sugar residues separated by non-sulfated regions (Esko and Zhang, 1996; Esko and Lindahl, 2001; Forsberg and Kjellen, 2001; Sugahara and Kitagawa, 2002).

As a result of its diverse structures, heparan sulfate is known to interact with a wide variety of proteins, including growth factors, chemokines, morphogens and enzymes. Many signaling molecules, such as fibroblast growth factor, vascular endothelial growth factor, transforming growth factor-β1 and –β2 bind to cell surface heparan sulfate (Bernfield *et al.*, 1999). Importantly, heparan sulfate serves as an attachment factor for many pathogens.

2.3.2 Heparan sulfate as virus attachment receptors

Heparan sulfate plays its role as a receptor through three major characteristics. First, heparan sulfate is a linear negatively-charged carbohydrate polymer. Most of the heparan sulfate interactions are mediated by electrostatic interactions between clusters of basic amino acids and concentrated negative charges on the sulfated heparan sulfate chain. Second, the domain organization of heparan sulfate places relatively flexible N-acetyl-rich domains adjacent to relatively rigid N-sulfated domains, thus facilitating protein interactions with the sulfate residues. Finally, the micro-sequence diversity and macro-organization are cell type-specific, and do not appear to be core protein-specific,

presumably the result of the cell type-specific repertoires of heparan sulfate chain-modifying enzymes (Zhu *et al.*, 2011).

Besides its functional roles in embryo development and homeostasis, heparan sulfate proteoglycans have been found to serve as receptors for a growing number of viruses from many different families, which include HSV (WuDunn and Spear, 1989; Mardberg *et al.*, 2001; Ali *et al.*, 2012), HPV (Giroglou *et al.*, 2001; Bousarghin *et al.*, 2003; Johnson *et al.*, 2009), HBV (Cooper *et al.*, 2005; Schulze *et al.*, 2007) and HIV (Roderiquez *et al.*, 1995). A summary list of the viruses that utilize cell surface heparan sulfate as an attachment receptor is shown in Table 2.6.

Most of the virus-heparan sulfate binding is mediated by electrostatic interactions between a cluster of basic amino acids arranged in a three-dimensional array on the surface of the virus capsid or envelope protein, and concentrated negative charges on the heparan sulfate polysaccharides chain (McLeish *et al.*, 2012). A stretch of positively-charged amino acids (lysine and arginine) present on the viral envelope or capsid protein is associated with heparan sulfate binding (Roderiquez *et al.*, 1995; Mardberg *et al.*, 2001; Knappe *et al.*, 2007). Cardin and Weintraub (1989) identified two consensus motifs associated with heparan sulfate binding, XBBXBX and XBBBXXBBX, where B represents a basic amino acid, and X represents any amino acid.

2.3.3 Heparan sulfate binding and neurovirulence

Heparan sulfate binding has been postulated to be associated with neurovirulence of a number of viruses. In the case of HIV, involvement of heparan sulfate in HIV infection improves the efficiency of virus binding to brain microvascular endothelial cells and is postulated to facilitate CNS infection (Banks *et al.*, 2004; Bobardt *et al.*, 2004). Heparan sulfate-binding Sindbis virus showed low neurovirulence after subcutaneous

inoculation, but high neurovirulence when inoculated directly into the brain of the mice (Ryman *et al.*, 2007). Highly neurovirulent Theiler's murine encephalomyelitis virus (TMEV) GDVII was associated with heparan sulfate binding. A non-heparan sulfate-binding GDVII mutant with R3126L and N1051S mutations was attenuated in mice, implying that heparan sulfate is associated with neurovirulence of GDVII virus (Reddi and Lipton, 2002; Reddi *et al.*, 2004).

Other than Sindbis virus, natural circulating alphaviruses eastern equine encephalitis virus (EEEV) was found to utilize cell surface heparan sulfate. Ablation of positive charge amino acids in the E2 71-77 region significantly reduced heparan sulfate binding and neurovirulence. The heparan sulfate binding phenotypes were associated with increased EEEV brain replication and neurological disease, but reduced lymphoid tissue replication, signs of illness and cytokine/chemokine induction in mice (Gardner *et al.*, 2011).

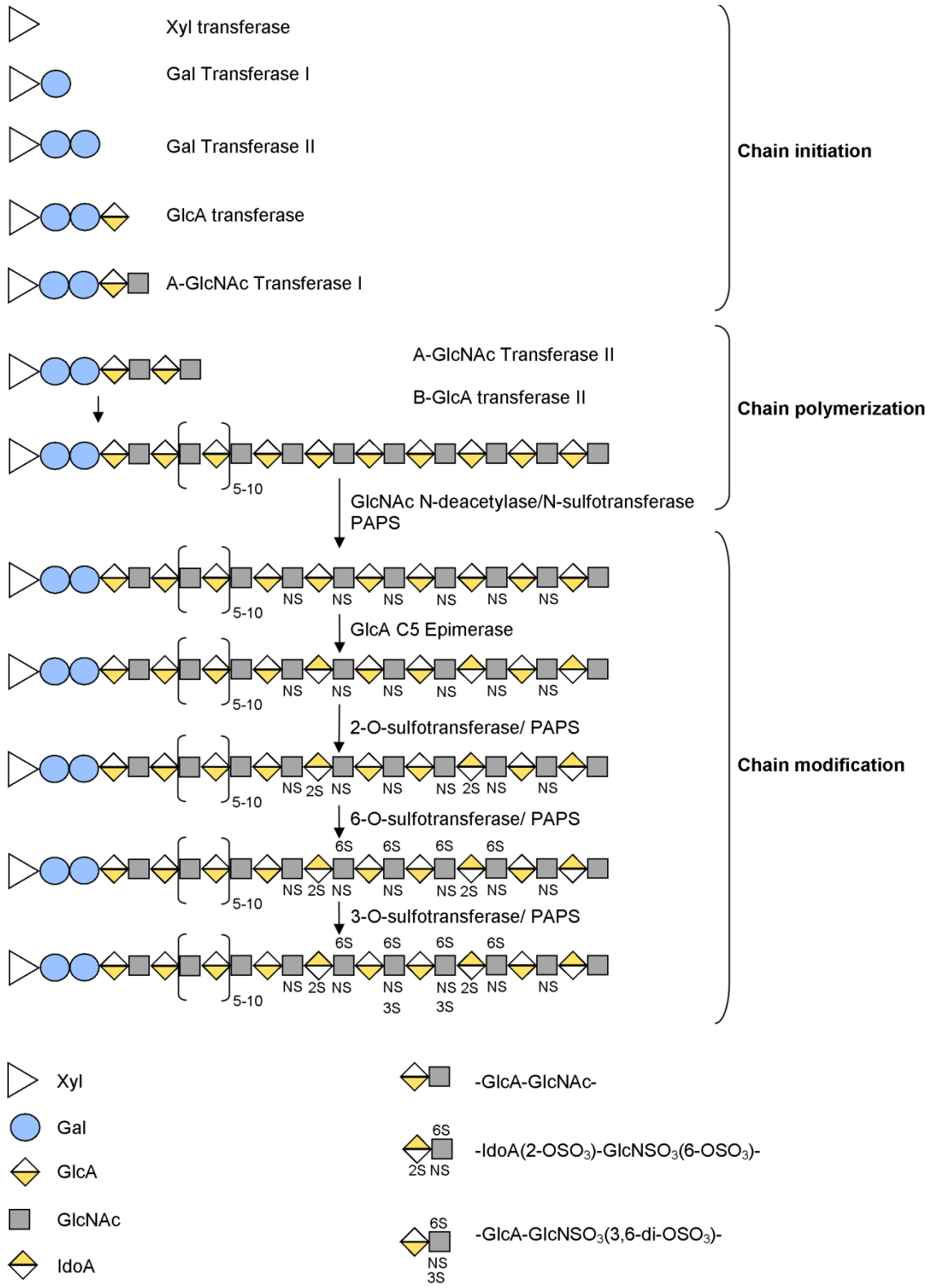

Figure 2.7: Schematic illustration of heparan sulfate chain biosynthesis, modified from Esko and Lindahl (2001).

Table 2.4: Viruses using heparan sulfate as a receptor

Virus family	Virus genus	Virus species	Receptor type	References
Herpesviridae	*Simplexvirus*	Herpes simplex virus	Entry	(WuDunn and Spear, 1989)
	Varicellovirus	Varicella-zoster virus	Unknown	(Jacquet *et al.*, 1998)
	Cytomegalovirus	Human herpesvirus 8	Unknown	(Akula *et al.*, 2001)
		Pseudorabies	Unknown	(Trybala *et al.*, 1996)
Poxviridae	*Orthopoxvirus*	Vaccinia virus	Unknown	(Chung *et al.*, 1998)
Papovaviridae	*Papillomavirus*	Human papillomavirus	Attachment	(Giroglou *et al.*, 2001)
Paramyxoviridae	*Paramyxovirus*	Human parainfluenza virus type 3	Unknown	(Bose and Banerjee, 2002)
	Pneumovirus	Human respiratory syncytial virus	Attachment	(Feldman *et al.*, 2000)
Picornaviridae	*Cardiovirus*	Theiler's virus	Unknown	(Reddi and Lipton, 2002)
	Aphthovirus	Foot-and-mouth disease virus	Attachment	(Jackson *et al.*, 1996)
	Enterovirus	Swine vesicular disease virus	Attachment	(Escribano-Romero *et al.*, 2004)
		Echovirus 6	Attachment	(Goodfellow *et al.*, 2001)
		Coxsackievirus A9	Attachment	(McLeish *et al.*, 2012)
Flaviviridae	*Flavivirus*	Dengue virus	Attachment	(Chen *et al.*, 1997)
		Tick-borne encephalitis virus	Attachment	(Mandl *et al.*, 2001)
	Hepacivirus	Hepatitis C virus	Unknown	(Barth *et al.*, 2003)
	Pestivirus	Swine fever virus	Unknown	(Hulst *et al.*, 2000)
Togaviridae	*Alphavirus*	Sindbis virus	Attachment	(Byrnes and Griffin, 1998)
		Eastern equine encephalitis virus	Attachment	(Gardner *et al.*, 2011)
Retroviridae	*Lentivirus*	Human immunodeficiency virus type 1	Attachment	(Roderiquez *et al.*, 1995)
		Human T-cell leukemia virus	Unknown	(Jones *et al.*, 2005)
	Spumavirus	Human foamy virus	Attachment	(Plochmann *et al.*, 2012)

2.4 Specific aims

As a result of the high morbidity and possible neurological complications of EV-A71 infection, development of effective antiviral agents to counter EV-A71 infection is urgently needed. This study hypothesized that synthetic peptides derived from the EV-A71 capsid protein VP1 can exhibit antiviral activity against EV-A71 attachment or entry, and can eventually lead to discovery of an unknown attachment or entry receptor. With the results of the antiviral peptide work, this study further hypothesized that cell-surface heparan sulfate glycosaminoglycan is used by EV-A71 as an attachment receptor. As an alternative to the antiviral peptide, this thesis also hypothesized that DNA-like morpholino oligomers conjugated with cell-penetrating octaguanidinium dendrimer could act against EV-A71 infection. To test these hypotheses, the specific objectives of this study were as follows:

i. To construct and characterize EV-A71 infectious cDNA clones with and without EGFP gene between the EV-A71 5'UTR and VP4 capsid gene;
ii. To screen overlapping synthetic peptides covering the entire EV-A71 VP1 capsid protein for antiviral peptide(s) against viral attachment during EV-A71 infection *in vitro*;
iii. To investigate and elucidate the role of cell surface heparan sulfate glycosaminoglycan in EV-A71 infection;
iv. To develop antisense-mediated translation-suppressing oligomers targeting the EV-A71 5'UTR IRES stem-loop structure as antiviral inhibiting viral RNA translation; and
v. To isolate vivo-MO-resistant EV-A71 mutants and characterize the degree of tolerance of mismatches by the antisense-mediated translation-suppressing oligomers.

CHAPTER 3

MATERIALS AND METHODS

3.1 Microbiology

3.1.1 Bacterial work

3.1.1.1 Bacterial strains and plasmids

Bacterial strains involved in this study include *E. coli* TOP10 (Invitrogen, USA) (F- mcrA Δ(mrr-hsdRMS-mcrBC) φ80lacZΔM15 ΔlacX74 nupG recA1 araD139 Δ(ara-leu)7697 galE15 galK16 rpsL(Str^R) endA1 λ^-) and *E. coli* XL10-Gold (Agilent Technologies, USA) (endA1 glnV44 recA1 thi-1 gyrA96 relA1 lac Hte Δ(mcrA)183 Δ(mcrCB-hsdSMR-mrr)173 tet^R F'[proAB $lacI^qZ\Delta M15$ Tn10(Tet^R Amy Cm^R)]). The plasmids involved in this study were pCR-XL-TOPO (Invitrogen, USA), pCR-XL-TOPO-EV-A71, pCR-XL-TOPO-EV-A71_EGFP and pET-30a-VP1 (a gift from Dr. Tan Eng Lee, Singapore Polytechnic, Singapore). The restriction map of pCR-XL-TOPO vector is shown in Figure 3.1.

3.1.1.2 Culture and storage of bacterial cells

Luria Bertani (LB) broth was prepared according to Miller (1972). LB broth and agar were autoclaved for 20 minutes at 121℃. *E. coli* strains with recombinant plasmids containing a kanamycin resistance gene were grown and maintained in LB broth or agar supplemented with 50 μg/ml kanamycin. *E. coli* on plates were stored at 4℃ up to 1 month. For long-term storage, bacterial strains were maintained in LB broth supplemented with 20% glycerol (v/v) and stored at -80℃. To revive the bacterial strain from the glycerol stock, a sterile wire loop was placed into the glycerol stock and aseptically streaked on the LB agar plate containing the appropriate antibiotic. The plate was then incubated at 37℃ overnight until colonies were observed.

3.1.1.3 Transformation of competent *Escherichia coli*

E. coli TOP10 and XL10-Gold competent cells were thawed on ice. An aliquot of 1 µl of β-mercaptoethanol was added into 20 µl XL10-Gold competent cells. Two microliters of recombinant plasmids were added to the competent cells, which were then incubated on ice for 30 minutes. The competent cells-plasmid mix was heated at 42 ℃ for 45s and immediately placed on ice for at least 2 minutes. An aliquot of 250 µl of super optimal broth with catabolite repression (SOC) medium was added to the transformed *E. coli* strains and the suspension was shaken at 225 rpm for 1 hour at 37 ℃. Approximately 100 µl of transformed *E. coli* was spread on LB agar plate supplemented with 50 µg/ml kanamycin. The plate was incubated overnight at 37 ℃ and stored at 4 ℃.

Blue white screening was not necessary as the transformed bacteria without the insert of interest were eventually killed by the toxic product expressed by the *ccd*B lethal gene. The recombinant plasmid with the insert of interest was confirmed by both restriction enzyme digestion analysis and colony PCR. The confirmed colonies were then kept as glycerol stock for long-term storage and further downstream analysis.

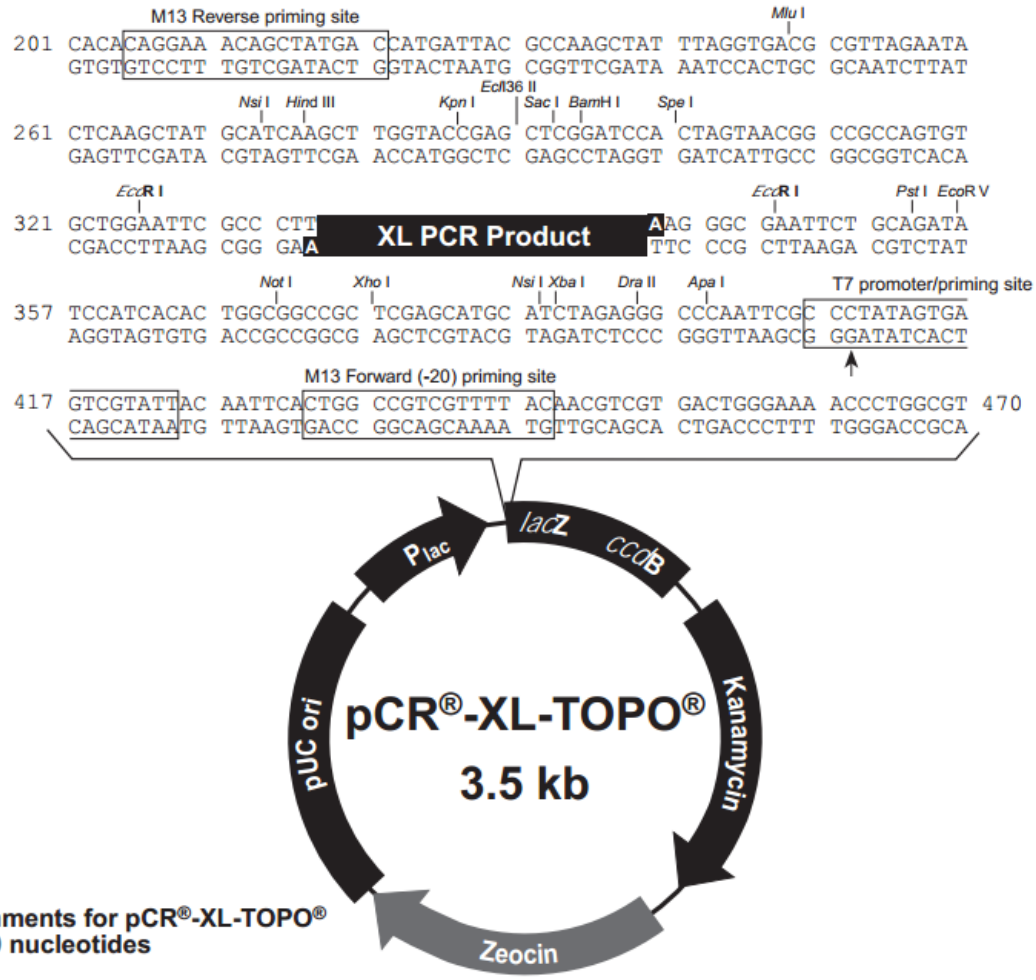

Comments for pCR®-XL-TOPO®
3519 nucleotides

Lac promoter/operator region: bases 95-216
M13 Reverse priming site: bases 205-221
Lac Za ORF: bases 217-576
Multiple Cloning Site: bases 248-399
TOPO® Cloning site: bases 336-337
T7 promoter priming site: bases 406-425
M13 Forward (-20) priming site: bases 433-448
Fusion joint: bases 577-585
*ccd*B lethal gene ORF: bases 586-888
Kanamycin resistance ORF: bases 1237-2031
Zeocin resistance ORF: bases 2238-2612
pUC origin: bases 2680-3393

Figure 3.1: Schematic illustration of pCR-XL-TOPO and the restriction endonuclease recognition sites. The pCR-XL-TOPO allows cloning of DNA fragments of up to 11 kbp using the TA cloning method. This figure is adapted from pCR-XL-TOPO (Invitrogen, USA) user's manual.

3.1.2 Virus work

3.1.2.1 Virus strains

The virus strains used in this study were EV-A71 strain 41 (GenBank accession number AM396587), EV-A71 prototype strain BrCr (GenBank accession number AB204852), EV-A71 strain UH1/PM/1997 (GenBank accession number AM396587), EV-A71 strain SHA66/97 (GenBank accession number AM396586), EV-A71 strain SHA52/97 (GenBank accession number AM396584), PV vaccine strain, CV-A16 strain 22159 (GenBank accession number JN248387), and chikungunya virus (CHIKV) strain MY/08/065 (GenBank accession number FN295485). EV-A71 clinical isolates with minimal passage history (strain names 14716, 35017, 1657640 and 1687413) were all obtained from the Diagnostic Virology Laboratory, University Malaya Medical Center, Kuala Lumpur, Malaysia.

3.1.2.2 Virus propagation and storage

A 75cm^2 tissue culture flask (TPP, Switzerland) with 70-80% confluent rhabdomyosarcoma (RD) cells was infected with 100 µl of virus supernatant. The flask was incubated at room temperature for an hour and replaced with fresh Dulbecco's modification Eagle medium (DMEM) supplemented with 2% fetal bovine serum (FBS). The flask was incubated at 37℃ in 5% CO_2 and observed for CPE, seen as round and shrunken cells which eventually dislodged from the flask surface (Lennette, 1969). The culture supernatants were harvested and freeze-thawed twice, then clarified to remove cell debris by centrifugation at 14,000 x g for 10 minutes at 4℃. The supernatants were then kept at -80℃ until use.

3.1.2.3 Plaque assay

A 24-well plate with 1.5 x 10^5 RD cells/well or a 6-well plate with 6 x 10^5 RD cells/well were prepared and incubated overnight at 37℃ in 5% CO_2. Prior to virus infection, the complete growth medium (DMEM supplemented with 10% FBS) was removed, and appropriate amount of serum-free DMEM was added. An aliquot of 100 µl of virus inoculum was added to the cells for an hour at room temperature with gentle rocking to allow virus attachment. After 1 hour incubation, the inocula were removed and immediately replaced with 500 µl and 2 ml plaque medium (DMEM supplemented with 2% FBS and 1.2% w/v carboxylmethylcellulose) for 24-well plates and 6-well plates, respectively. After 48 to 72 hours incubation, the plaque medium was removed; the cells were fixed with 4% formaldehyde and stained with 0.5% crystal violet. The plaques were visualized against a white background. The plaque forming unit per milliliter (PFU/ml) was calculated with the following formula:

$$\text{PFU/ml} = \frac{\text{Number of plaques x dilution factor}}{\text{Volume of inoculum (ml)}}$$

3.1.2.4 Immunofluorescence assay

Approximately 1.5 x 10^4 cells/well were seeded in chamber slides (Lab-Tek, USA) and CellCarrier-96 black plates (Perkin-Elmer, USA) and incubated overnight at 37℃ in 5% CO_2. EV-A71 at multiplicity of infection (MOI) of 100 was added into each well and incubated at 4℃ for an hour to allow virus to attach. After 1 hour incubation, the inocula were removed and the cells were fixed with 4% formaldehyde and permeabilized using 0.25% Triton X-100 (Sigma, USA) for 5 minutes. The cells were subsequently blocked with Image-iT FX signal enhancer (Invitrogen, USA) for 1 hour. EV-A71 particles were immunostained with mouse anti-EV-A71 monoclonal antibodies (Millipore, USA) as the primary antibodies and 1:200 diluted Alexa Fluor 488 labeled

anti-mouse IgG (Invitrogen, USA) as the secondary antibody for an hour at 37℃. For nuclear visualization, cells were treated with 0.01% 4',6'-diamidino-2-phenylindole (DAPI; Sigma, USA) for 7 minutes at room temperature. Immunofluorescence was detected with Leica TCS SP5 confocal microscope (Leica Microsystems, Germany) and Nikon Eclipse TE2000-E fluorescence microscope. The CellCarrier-96 black plate (PerkinElmer, USA) was evaluated using Cellomics ArrayScan VTI high content screening reader with Spot Detector Bio-application software (Thermo Scientific, USA).

3.2 Cell biology

3.2.1 Mammalian cell lines

3.2.1.1 Cell lines

Human rhabdomyosarcoma cells (RD, ATCC # CCL-136), African green monkey kidney cells (Vero, ATCC # CCL-81), human colon adenocarcinoma cells (HT-29, ATCC # HTB-38), human cervical adenocarcinoma epithelial cells (HeLa, ATCC # CCL-2) and Chinese hamster ovary cells (CHO-K1, ATCC # CCL-61; CHO-pgsD677, ATCC # CRL-2244 and CHO-pgsA745, ATCC # CRL-2242) were used in this study. CHO-pgsD677 cells are deficient in N-acetylglucosaminyltransferase and glucuronosyltransferase activities required for heparan sulfate polymerization and thus completely lack heparan sulfate, but produce 3- to 4-fold higher levels of chondroitin sulfate than wild-type CHO-K1 (Lidholt *et al.*, 1992). CHO-pgsA745 cells are deficient in the enzyme UDP-D-xylose:serine-1,3-D-xylosyltransferase which catalyzes the first sugar transfer reaction in GAG formation, and thus completely lack GAGs (Esko *et al.*, 1985), including heparan sulfate and chondroitin sulfate.

3.2.1.2 Propagation and maintenance

RD and CHO-K1 cells were propagated in DMEM. HeLa and Vero cells were propagated in Eagle minimum essential medium (EMEM). HT-29 cells were propagated in McCoy's medium. CHO-pgsD677 and CHO-pgsA745 were propagated in Kaighn's modification of Ham's F-12 (F-12K) medium. All media were supplemented with 10% FBS, 1% L-glutamine, 1% non-essential amino acids and 1% penicillin/streptomycin, except growth media for CHO-K1 cells which require 1% sodium pyruvate. All cell lines were grown at 37 ℃ in 5% CO_2 until 80-90% confluency.

To passage the cells, growth medium was removed and the cells were rinsed with 0.12% trypsin-EDTA. An aliquot of 2 ml of 0.12% trypsin-EDTA was added to the cells and incubated for 5 minutes at 37 ℃. Upon complete detachment, an equal volume of complete growth medium was added to the trypsinized cells. The cell suspension was split with a ratio of 1:4 to 1:6 into a new 75 cm^2 tissue culture flask and topped up with 10 ml of complete growth medium, followed by incubation in a 37 ℃ incubator in 5% CO_2.

3.2.1.3 Cell seeding

A confluent monolayer of cells in a 75 cm^2 tissue culture flask was rinsed with 0.12% trypsin-EDTA and treated with 2 ml of 0.12% trypsin-EDTA to detach the cells from the flask. An aliquot of cell suspension was mixed with an equal volume of 0.4% trypan blue solution, and the number of cells was enumerated using a hemocytometer or automated cell counter. The cells were added to the desired volume of complete growth medium in a petri dish and resuspended gently. Respective volumes of 100 µl, 500 µl, or 2 ml were added to each well of a 96-well plate, 24-well plate or 6-well plate. The plate was then incubated at 37 ℃ in 5% CO_2.

3.2.1.4 Cell freezing and storage

A confluent monolayer of either RD, CHO-K1, CHO-pgsD677 and CHO-pgsA745 cells in 75 cm^2 tissue culture flasks was washed with 0.12% trypsin-EDTA. The cell monolayer was then treated with 2 ml of trypsin-EDTA for 5 minutes at 37℃ to detach the cells from the flask, followed by the addition of 2 ml of growth media. Then, the cells were pelleted through centrifugation at 150 x g for 5 minutes and the supernatant was discarded. The cell pellet was then resuspended gently in 2 ml of freezing media containing 5% DMSO (Sigma, USA) and an aliquot of 1 ml of cell suspension was transferred into a cryovial (Nunc, USA). The cryovial was then kept in Nalgene Mr. Frosty container (Nalgene, USA) at -80℃ for a day and then transferred into either liquid or vapor phase of liquid nitrogen for long-term storage. The cooling rate of -1℃/minute is the optimal rate for cell preservation.

3.2.1.5 Cell reconstitution

When required, each cryovial of cells was retrieved from the liquid nitrogen and thawed immediately in a 37℃ water bath. When thawed, the cell suspension was transferred slowly into a 25 cm^2 culture flask containing 5 ml of pre-warmed reviving medium (DMEM supplemented with 20% of FBS, 1% L-glutamine, 1% NEAA and 1% penicillin/streptomycin) and the cells were allowed to attach onto the culture flask for not more than 4 hours. After 2 hours incubation at 37℃ in 5% CO_2, the reviving media was removed to eliminate the toxic effects of DMSO present in the freezing media and immediately replaced with fresh reviving media. The cells were allowed to grow to confluency and subsequently maintained in growth medium supplemented with 10% FBS. The cells were subjected to at least two passages before being used for further studies.

3.2.1.6 Cell viability assay

Cell viability analysis was performed using CellTiter 96 Aqueous One Solution Cell Proliferation Assay reagent (Promega, USA) according to the manufacturer's instructions. Briefly, overnight incubated RD cells (1.5 x 10^4 cells/well) were prepared and an aliquot of 100 µl of the medium containing peptide or inhibitors was added to each well. After overnight incubation, an aliquot of 20 µl of the cell viability assay reagent was added to each well, and the plate was incubated for 2 hours at 37℃. The absorbance reading at 490 nm was obtained using the microplate reader and the percentage of cell viability was calculated.

3.3 Molecular biology

3.3.1 Design and synthesis of enterovirus A71 primers and TaqMan probe

The primers and TaqMan probe used for TaqMan real-time PCR were adapted from Tan *et al.* (2008) and shown in Table 3.1. All the primers and TaqMan probe were synthesized by Integrate DNA Technology (IDT, USA). The TaqMan probe with double quenchers was designed with 6-carboxyfluorescein (6-FAM) at the 5' end and Iowa Black fluorescence quencher at the 3' end. An internal ZEN quencher (IDT, USA) reduced the background fluorescence and improved the sensitivity of the TaqMan probe to detect the targeted viral RNA. The TaqMan real-time PCR was used to quantitate virus titer based on RNA copy numbers.

3.3.2 Design and synthesis of synthetic peptides

All synthetic peptides were produced by Mimotopes Pty Ltd (Australia). A set of 95 overlapping peptides spanning the entire sequence of the VP1 capsid protein of EV-A71 strain 41 was synthesized (Appendix IV). Each peptide contained 15 amino acid residues with 12 residues overlapping with the adjacent peptides. Synthetic peptide

SP40, SP40X, G1 and G2 (Table 3.2) were synthesized with >95% purity assessed by high performance liquid chromatography (HPLC). In alanine scanning analysis, a set of 13 peptides with alanine substitution of each amino acid of the SP40 peptide was also synthesized. All the peptides were dissolved in 100% DMSO to achieve a final concentration of 10 mM. The peptides were further diluted to the desired final concentration using serum-free DMEM.

3.3.3 Design and synthesis of morpholino oligomers

All the octaguanidinium-conjugated morpholino oligomers (vivo-MOs) were synthesized by Gene Tools LLC (USA). The 23-mers vivo-MOs were designed to complement the EV-A71 strain 41 5' UTR IRES stem-loop structure V-VI and RdRP. A control vivo-MO with a nonsense sequence was synthesized and used as a negative control throughout the experiment (Table 3.3). All the vivo-MOs were dissolved in phosphate buffer saline (PBS) to a final concentration of 0.5 mM with maintenance medium (DMEM supplemented with 2% FBS) or serum-free DMEM, depending on the time of addition of vivo-MOs.

Table 3.1: Primers and TaqMan probe for TaqMan real-time PCR

Primer name	Sequence	Nucleotide position*
VP1-F	5’ GAGCTCTATAGGAGATAGTGTGAGTAGGG 3’	2468 – 2496
VP1-R	5’ ATGACTGCTCACCTGCGTGTT 3’	2532 – 2552
TaqMan	5’ 6-FAM-ACTTACCCA/ZEN/GGCCCTGCCAGCTCG-Iowa Black FQ-3’	2498 – 2521

*The nucleotide numbering refers to EV-A71 strain 41

Table 3.2: Synthetic peptide sequences

Peptide	**Sequence**	**pI**	**Net charge**	**GRAVY***
SP40	Ac-QMRRKVELFTYMRFD-NH_2	9.98	+2	-0.833
SP40X	Ac-REFTMKRMVLFRQDY-NH_2	9.98	+2	-0.833
G1	Ac-LRSRTKIIRIRH-NH_2	12.48	+5	-0.775
G2	Ac-MPRRRRIRRRQK-NH_2	12.78	+8	-2.842

*Grand average of hydropathicity index (GRAVY) indicates the solubility of protein; a positive GRAVY indicates hydrophobicity and a negative GRAVY indicates hydrophilicity.

Table 3.3: The 23-mers vivo-MOs sequences and target locations in EV-A71 RNA

Vivo-MO	**Sequence (5'- 3')**	**Target location in EV-A71 RNA (nucleotide positions)**
Vivo-MO-1	CAGAGTTGCCCATTACGACACAC	IRES core (512-534)
Vivo-MO-2	GAAACACGGACACCCAAAGTAGT	IRES core (546-568)
Vivo-MO-3	AAACAATTCGAGCCAATTTCTTC	RdRP gene (7303-7325)
Vivo-MO-C	CCTACTCCATCGTTCAGCTCTGA	-

3.3.4 DNA work

This section describes the methodology involved in plasmid DNA extraction, PCR, DNA purification and cloning. These techniques are required for infectious cDNA clones construction.

3.3.4.1 Plasmid extraction

The Hybrid Q mini spin purification kit (GeneAll, Korea) was used for small scale plasmid DNA isolation. This method was based on the alkaline lysis method with an additional column purification step. The anion exchange resin within the column allows the negatively-charged plasmid DNA to bind while the contaminants are washed away by wash buffer. The plasmid DNA purification was carried out according to the manufacturer's instructions. Five mililiters of overnight bacterial culture was pelleted by centrifugation for 5 minutes at 14,000 x g and the pellet was resuspended with 250 µl S1 buffer supplemented with RNase. The bacterial cells were then lysed with 250 µl of S2 lysis buffer and incubated for 5 minutes. The cleared lysate was then neutralized with 350 µl of G3 buffer. The resulting precipitate containing proteins and cellular debris were then removed through centrifugation for 10 minutes at 17,000 x g. The plasmid-containing supernatant was then applied to the DNA binding column and then washed twice with 500 µl of AW buffer, followed by 700 µl of PW buffer. The plasmid DNA was eluted from the column with 40 µl of pre-warmed EB buffer through centrifugation for 2 minutes at 17,000 x g. The plasmid concentration was quantitated using a nano-drop spectrophotometer based on absorbance readings of 260 nm and 280 nm. The integrity of the plasmid DNA was then verified by agarose gel electrophoresis.

3.3.4.2 Restriction endonuclease digestion of DNA

Digestion of DNA was carried out with specific restriction endonuclease (NEB, USA) according to the manufacturer's instructions. In brief, the reaction was carried out in thin-wall PCR tubes with 1-5 µg of DNA, restriction enzyme in the 1X digestion buffer and bovine serum albumin (BSA). All reactions were incubated for at least 1 hour and up to 16 hours at optimal temperatures suggested by the manufacturer.

3.3.4.3 DNA agarose gel electrophoresis

DNA fragments were screened by horizontal gel electrophoresis. The electrophoresis was performed in agarose gel pre-stained with GelRed nucleic acid stain (Biotium, USA) prepared in 0.5X TAE buffer. DNA products were mixed with a gel loading buffer and loaded into the wells. The size of the DNA fragment in the gel was determined based on a 1 kb DNA ladder. Electrophoresis was carried out at 80 V and the DNA bands were visualized under the UV illumination.

3.3.4.4 DNA gel purification

Digested DNA fragments and the PCR products were purified using Expin mini spin purification kit (GeneAll, Korea) according to the manufacturer's instructions. Briefly, the desired DNA fragments were carefully excised from the agarose gel using a clean scalpel blade. An aliquot of GB buffer was added to the excised gel (300 µl per 100 mg of gel) which was then incubated for 10 minutes at 50 ℃. For DNA fragments larger than 5 kbp, an aliquot of isopropanol was added to the mixture at a ratio of 100 µl to 100 mg of gel. The DNA-containing mixture was then added to the column, which was then washed with 700 µl NW buffer. The DNA was eluted from the column using 40 µl of EB buffer and stored at -20 ℃.

3.3.4.5 Phenol chloroform purification of DNA and DNA precipitation

The DNA-containing solution was mixed with an equal volume of phenol/chloroform /isoamyl alcohol (25:24:1, pH 8) (Amresco, USA) and vortexed for 1 minute. The solvent and aqueous phases were separated through centrifugation at 17,000 x g for 10 minutes. The aqueous phase was carefully removed and mixed with an equal volume of chloroform/isoamyl alcohol (24:1) (Sigma, USA). This step was necessary to remove the remaining phenol residues. After 10 minutes centrifugation at 17,000 x g, the aqueous phase was removed, 1/10 volume of 3 M sodium acetate (pH 5.5) was added and mixed well. An aliquot of 2.5 volume of absolute ethanol or 1 volume of isopropyl alcohol was added to the mixture, which was then and incubated at -80 ℃ or -20 ℃, respectively, for 1 hour to precipitate the DNA. The precipitated DNA was pelleted by centrifugation at 17,000 x g for 20 minutes at 4 ℃ and the DNA pellet was washed with 70% ethanol to remove the remaining salts. After air-drying, the pellet was dissolved with TE buffer or nuclease free water.

3.3.4.6 A-tailing of purified PCR product

The gel purified blunt end PCR products were subject to A-tailing using GoTaq DNA polymerase (Promega, USA) according to the manufacturer's instructions. A single A residue overhang at the 3' end was added to the DNA fragment. Briefly, approximately 500 ng of DNA template was added into GoTaq Green master mix containing 0.2 mM dNTP, 1.5 mM $MgCl_2$ and 1.25 U of GoTaq DNA polymerase. The reaction mix was incubated for 30 minutes at 70 ℃. The A-tailed products were then purified by phenol/chloroform/isoamyl alcohol, reconstituted with TE buffer and kept at -20 ℃ until use.

3.3.4.7 TA cloning

The plasmid vector (pCR-XL-TOPO) was supplied as linear form with a single 3' thymidine (T) overhang. The PCR products carrying 3' deoxyadenosine (A) overhangs were cloned into the pCR-XL-TOPO vector according to the manufacturer's instructions. This technology involves the topoisomerase from vaccinia virus. Approximately 10-100 ng/ul of the DNA template was prepared. An aliquot of 4 µl of the DNA template in TE buffer was mixed with 1 µl (10 ng/µl) of plasmid DNA and incubated at room temperature for 30 minutes. Thereafter, the reaction was stopped by adding 1 µl 6X TOPO stop solution. The recombinant plasmid DNA was then transformed into *E. coli* TOP10 competent cells as previously described.

3.3.5 RNA work

This section describes the steps involved in RNA quantification using TaqMan real-time PCR and RNA gel electrophoresis.

3.3.5.1 Viral genomic RNA extraction

EV-A71 RNA genome was extracted from infected tissue culture using QIAamp viral RNA mini kit (QIAGEN, Germany) according to the manufacturer's instructions. Briefly, 140 µl of the virus-containing supernatant was lysed with 560 µl of AVL buffer containing the recommended amount of carrier RNA, followed by addition of 560 µl of absolute ethanol. The viral RNA-containing mixture was then added to the column and washed twice with 500 µl of AW1 and AW2. The viral RNA was eluted with 60 µl AVE buffer and kept at -80℃.

3.3.5.2 TaqMan real-time PCR

The TaqMan real-time PCR was performed using TaqMan Fast Virus 1-Step Master Mix (ABI, USA) with the primers and TaqMan probe as stated in Table 3.1. The reaction mix was prepared (Table 3.4). The PCR reaction was performed with a StepOne Plus real-time PCR system (ABI, USA) with cDNA synthesis by reverse transcription for 5 minutes at 50 ℃, and subsequent amplification for 40 cycles at 95 ℃ for 3 s and 60 ℃ for 30 s. Plasmid DNA containing the EV-A71 VP1 gene was used as the standard to determine the samples copy numbers. The RNA copy number was determined using StepOne Plus software v2.2.

Table 3.4: Master mix preparation for TaqMan real-time PCR.

Reagent	**Volume**	**Final concentration**
VP1-F (10 µM)	0.25 µl	0.25 µM
VP1-R (10 µM)	0.25 µl	0.25 µM
TaqMan probe (5 µM)	1.0 µl	2.0 µM
TaqMan Fast Virus 1-Step Master Mix (4X)	2.5 µl	1X
RNA template	1.0 µl	-
PCR grade water	5.0 µl	-
Total	10.0 µl	

3.3.5.3 RNA non-denaturing agarose gel electrophoresis

RNA fragments were screened by horizontal gel electrophoresis. The electrophoresis was performed in agarose gel pre-stained with GelRed nucleic acid stain (Biotium, USA) prepared in 1X TAE buffer. RNA products were mixed with a 2X RNA loading buffer (NEB, USA) and loaded into the wells. The size of the RNA fragment in the gel was determined based on the standard 0.5-10 kb RNA ladder (Invitrogen, USA). Electrophoresis was carried out at 80 V for 1 hour and the RNA bands were visualized under UV illumination.

3.3.6 Protein work

Protein work is necessary for determination of the protein expression with SDS-PAGE and western blot analysis.

3.3.6.1 Total protein extraction and quantification

The infected RD cells in the 24-well plate were lysed with 100 µl of ReadyPrep Sequential Extraction Kit Reagent 2 (BioRad, USA). The lysate was then clarified by centrifugation at 14,000 x g for 10 minutes at 4 ℃ to remove the cell debris. The protein concentration of the cell lysate was quantitated using MicroBCA Protein Assay (Pierce Biotechnology, USA) according to the manufacturer's instructions. In brief, the microBCA working reagent was prepared accordingly (25:24:1, reagent MA:MB:MC). An aliquot of 150 µl of the standard or unknown sample was mixed with 150 µl of the working reagent and incubated at 37 ℃ for 2 hours. Bovine serum albumin with known concentration was used as the standard. The absorbance reading was measured at 562 nm using a microplate reader. The concentration of the sample was calculated based on the standard curve.

3.3.6.2 Sodium dodecyl sulphate – polyacrylamide gel electrophoresis (SDS-PAGE)

SDS-PAGE was carried out using a vertical slab gel unit in a Mini-Protean tetra cell (Bio-Rad, USA) according to the manufacturer's instructions. The slab gel was cast between two grease-free glass plates, with a 12% (w/v) polyacrylamide separating gel and a 5% (w/v) polyacrylamide stacking gel. The separating gel mixture was poured to 1.5 cm below the bottom of the comb and then carefully overlaid with absolute ethanol to ensure the formation of a straight meniscus. After the separating gel was well polymerized, the ethanol overlay was removed. Thereafter, the stacking gel mixture was layered over the separating gel and the comb was placed in position. The compositions of separating gel and stacking gel are shown in Appendix II. After the gel was polymerized, the comb was removed and the wells were flushed with SDS running buffer. An aliquot of 20 µl of the sample with SDS loading dye was boiled at 100 ℃ for 5 minutes and added into each well. The samples were electrophoresed at 120 V for 2 hours. The gels were then soaked in Coomassie blue staining solution (Appendix II) for 1 hour with constant shaking. The stained gels were soaked in destaining solution (Appendix II) with constant shaking until protein bands could be visualized as blue bands against a clear background.

3.3.6.3 Western blot analysis

The proteins in the resolved SDS-PAGE gel were transferred onto a PVDF membrane (Millipore, USA) using a Trans-Blot SD semi-dry transfer cell (Bio-Rad, USA) according to the manufacturer's instructions. Briefly, the transfer was prepared by assembling the following components from the bottom: two layers of ice-cold anode I buffer-treated filter papers, a layer of ice-cold anode II buffer-treated filter paper, ice-cold anode II buffer-treated PVDF membrane, ice-cold cathode buffer-treated SDS-PAGE gel and three layer of ice-cold cathode buffer-treated filter papers. The buffer

ingredients are shown in Appendix III. The transfer was carried out at 15V for 15 minutes and 10V for 30 minutes for the 0.75 mm and 1.5 mm gels respectively. The membrane was subsequently blocked with 5% skimmed milk in PBS for 1 hour. The membrane was then incubated with 1:100 diluted anti-EV-A71 monoclonal antibodies (Millipore, USA) or 1:5000 diluted β-actin antibodies (Sigma, USA) for 1 hour at room temperature. Thereafter, the membrane was washed twice with PBS-0.05% Tween-20 to remove unbound antibodies. The membrane was then incubated with 1:2000 diluted of HRP-conjugated goat anti-mouse antibody (Gene Tex, USA) for 1 hour at room temperature. The immunoblots were developed with DAB substrate in stable peroxide substrate solution (Pierce Biotechnology, USA). The size of the desired protein bands were determined based on the PageRuler prestained protein marker (Thermo Scientific, USA).

3.3.6.4 Chemiluminescence analysis

For chemiluminescence analysis, the protein resolved in the SDS-PAGE gel was transferred to a nitrocellulose membrane using a Trans-Blot SD semi-dry transfer cell according to the manufacturer's instructions. All the filter papers, nitrocellulose membrane and the SDS-PAGE gel were soaked in transfer buffer (24 mM Tris, 77 mM glycine, 20% methanol) for 15 minutes at 4 ℃. The transfer was prepared by assembling three layers of filter papers, followed by a nitrocellulose membrane, SDS-PAGE gel and three layers of filter papers. The transfer was performed at 15 V for 15 minutes. The membrane was then blocked with 5% skimmed milk in PBS-0.05% Tween-20 for 1 hour. The membrane was then incubated with 1:100 diluted anti-EV-A71 monoclonal antibodies (Millipore, USA) for an hour. Thereafter, the membrane was washed twice with PBS-0.05% Tween-20 to remove unbound antibodies. The membrane was then incubated with 1:2000 diluted HRP-conjugated goat anti-mouse antibody (Gene Tex, USA) for 1 hour at room temperature. The immunoblot was developed with Amersham

ECL Prime Western Blotting Detection Reagent (GE Healthcare, UK) and detected by chemiluminescence. The protein size was determined using Precise Plus Protein WesternC Standard (Bio-Rad, USA).

3.3.7 Construction of enterovirus A71 infectious cDNA clones

3.3.7.1 Design and synthesis of primers

The primers involved in EV-A71 infectious cDNA clone are shown in Table 3.5. The forward primer (EV-A71_MluI/SP6_F) was designed with a restriction enzyme *Mlu*I cutting site (5' ACGCGT 3') and a SP6 promoter sequence (5' ATTTAGGTGACACTATAG 3', with transcription start site underlined). The reverse primer (EV-A71_polyA/EagI_R) was designed with poly$(T)_{50}$ followed by an *Eag*I restriction enzyme cutting site.

3.3.7.2 Reverse transcription

The EV-A71 genomic RNA was reverse transcribed into cDNA using Superscript III reverse transcriptase (Invitrogen, USA) according to the manufacturer's instructions. In brief, the reaction mix was set up with 100 ng of RNA, 2 pmol of EV-A71_polyA/EagI_R and 1 mM dNTP mix in 10 µl reactions. Thereafter, the reaction mix was incubated at 65℃ for 5 minutes and immediately placed on ice for at least 1 minute. The remaining components were then added into the reaction mix (1X RT buffer, 0.01 M DTT, 40 U RNaseOUT and 400 U SuperScript III reverse transcriptase) and incubated at 55℃ for 60 minutes followed by reverse transcriptase inactivation at 70℃ for 15 minutes. The RNA that hybridized to the cDNA was removed by addition of 2 U RNase H and incubated for 20 minutes at 37℃. The cDNA was kept in -80℃ until further experiments.

3.3.7.3 Full-length PCR of enterovirus A71 genome

Full genome PCR was performed using iProof high fidelity DNA polymerase (Bio-Rad, USA) according to the manufacturer's instructions. Briefly, PCR reaction mix was prepared with 0.5 µM of pEV-A71_MluI/SP6_F, pEV-A71_PolyA/EagI_R, and 2 µl of cDNA in 1X high fidelity buffer containing 0.2 mM dNTP and 1 unit of iProof DNA polymerase. The PCR was performed with initial denaturation of 2 minutes at 98℃, followed by 25 cycles of 98℃ for 10 s, 60℃ for 20 s and 72℃ for 4 minutes.

3.3.8 Construction of enhanced green fluorescence protein (EGFP)-expressing enterovirus A71 infectious cDNA clone

3.3.8.1 Design and synthesis of primers

The three sets of primers involved in EV-A71_EGFP infectious cDNA clone construction are shown in Table 3.5. Primer set I was designed to amplify the EV-A71 5'UTR region, flanked by BstB1, SP6 promoter site at the 5' end and EGFP sequence at the 3' end. Primer set II was designed to amplify the EGFP gene, flanked by EV-A71 5'UTR and VP4. Primer set III amplified the EV-A71 P1 region. Primer set IV specifically amplified EV-A71 P2 to the poly(A) tail. Each fragment had at least 30 nucleotides of overlapping sequences.

3.3.8.2 Overlapping extension PCR

Overlapping extension PCR was performed using Q5 high fidelity DNA polymerase (NEB, USA) according to the manufacturer's instructions. The PCR reaction mix was set up with 0.5 µM of each of forward and reverse primers, 1X high fidelity buffer, 0.2 mM dNTP, 1 unit of Q5 DNA polymerase and 10 ng of plasmid DNA containing either EV-A71 full genomic sequence or EGFP gene. The PCR was performed with initial denaturation of 2 minutes at 98℃, followed by 25 cycles of 98℃ for 10 s, 70-72℃ for

20 s and 72℃ for 1-2 minutes. Approximately 100 ng of the gel purified fragments were then overlapped through 15 cycles of 98℃ for 10 s and 72℃ for 1-2 minutes. The fused products were then amplified using pEV-A71_BstBI/SP6_1F and pEV-A71_PolyA/AgeI_4R for 25 cycles of 98℃ for 10 s and 72℃ for 5 minutes.

Table 3.5: Primers involved in EV-A71 infectious cDNA clones construction

Primer	**Sequence (5' → 3')**
pEV-A71_Mlu/SP6_F	GTAACGCGTAGCGATTTAGGTGACACTATAGTTAAAACAGCTGTGGGTTG
pEV-A71_PolyA/EagI_R	CCTACGGCCGT$_{50}$GCTATTCCGGTTATAACAAATTTAC
pEV-A71_BstB1/SP6_1F	GCTTCGAAGCGATTTAGGTGACACTATAGTT
pEV-A71_EGFP/5UTR_1R	GAACAGCTCCTCGCCCTTGCTCACTGAGCCCATGTTTGATTGTATTG
pEV-A71_5UTR/EGFP_2F	CAATACAATCAAACATGGGCTCAGTGAGCAAGGGCGAGGAGCTGTTC
pEV-A71_VP4/EGFP_2R	TGTGAGCCAAGGGTAGTAATGGCCTTGTACAGCTCGTCCATGCCGAG
pEV-A71_EGFP/VP4_3F	GTACAAGGCCATTACTACCCTTGGCTCACAGGTGTCTACTCAGCGAT
pEV-A71_P2_3R	CCCTCACATCAGCAAAACCAACGAG
pEV-A71_P2_4F	CATGGTGTAGTTGGTATAGTGTCCAC
pEV-A71_AgeI/PolyA_4R	GACCGGT$_{50}$GCTATTCCGG

3.3.9 *In vitro* transcription of SP6 promoter

In vitro transcription was performed using RiboMAX large scale RNA production system (Promega, USA) according to the manufacturer's instructions. In brief, 1-5 µg of the linearized DNA template was added to the reaction mix containing 1X SP6 transcription buffer, 25 mM of each of the rNTP and 2 µl of the enzymes mix. *In vitro* transcription was carried out at 37 ℃ for 4-6 hours. Thereafter, the DNA template was removed by DNase treatment for 15 minutes at 37 ℃ at the concentration of 1 U/µg of DNA.

3.3.10 RNA purification

Prior to transfection, the unincorporated free rNTP and the digested DNA was removed using Illustra Microspin G-50 column (GE Healthcare, UK) according to the manufacturer's instructions. The column was prepared by centrifugation at 800 x g for 1 minute to remove the excess storage buffer. An aliquot of 20-50 µl of the *in vitro* transcribed RNA was added to the resin which was then centrifuged at 800 x g for 2 minutes. Purified RNA was collected and stored at -80 ℃ till use.

3.3.11 Transfection of infectious RNA

Overnight grown RD cells (1.5 x 10^5 cells/well in a 24-well plate or 6 x 10^5 cells/well in a 6-well plate) were prepared and used for transfection. Approximately 1 µg and 5 µg of RNA was transfected into a 24-well and 6-well plate, respectively. Prior to transfection, the growth medium was removed and replaced with Opti-MEM (Invitrogen, USA). Transfection mix was prepared with a ratio of 1 µl of Lipofectamine 2000 reagent to 1 µg of RNA. The RNA-containing Opti-MEM was mixed with the Lipofectamine 2000 reagent containing Opti-MEM and incubated at room temperature for 20 minutes. Thereafter, the RNA-lipofectamine mixture was added to the cells drop-by-drop. Two

hours after transfection, the transfection medium was removed and replaced with fresh maintenance medium.

3.3.12 Rescue of infectious viral particles

Infectious RNA-transfected RD cells were harvested 72 hours post-transfection. The harvested cells were freeze-thawed twice. The cell debris was removed through centrifugation at 17,000 x g for 10 minutes at 4℃. The virus-containing supernatant was kept in -80℃ and the virus titers were determined by plaque assay.

3.3.13 Construction of enterovirus A71 mutants

In this study, site-directed mutagenesis is performed to introduce mutations into EV-A71 infectious clone, to study the degree of tolerance of the vivo-MO-1 towards the number and positions of the mutations.

3.3.13.1 Design and synthesis of primers

The primers involved in site-directed mutagenesis are listed in Table 3.6. The primers were designed to carry the desired point mutation flanked by at least 15 nucleotides. Each primer set was complementary to each other. The melting temperature (T_m) of each of the primers was designed to be more than 78℃, determined using the following calculation:

$$\mathbf{T_m = 81.5 + 0.41(\%GC) – (675/N) - \%mismatch}$$

Where N is the primer length in bases and the values for %GC and %mismatch are whole numbers.

3.3.13.2 Site-directed mutagenesis

The QuickChange Lightning Site-Directed Mutagenesis Kit (Agilent Technologies, USA) was used according to the manufacturer's instructions. The pCR-XL-TOPO-EV-

A71 recombinant plasmid was used. The basic procedure utilizes a plasmid DNA vector and the two primers containing the desired mutation. The primers complementary to the opposite strands of the vector were extended during temperature cycling by *Pfu Ultra* HF DNA polymerase without primer displacement. The PCR cycles included initial denaturation for 2 minutes at 95℃, and 18 cycles of denaturation at 95℃ for 20 s, annealing at 60℃ for 10 s and extension at 68℃ for 4 minutes, followed by a final extension at 68℃ for 2 minutes. The extension of the oligonucleotide primers generated a mutated plasmid containing staggered nicks. After the temperature cycling, the parental unmutated plasmid DNA template was removed using *Dpn*I for 30 minutes at 37℃, which specifically cleaved the methylated and hemimethylated targeted sequence 5' Gm^6ATC 3'. An aliquot of 2-3 µl of the mutated plasmid containing the staggered nicks was transformed into *E. coli* XL10-Gold ultracompetent cells (Agilent Technologies, USA) as previously described in section 3.1.1.3.

3.3.14 *In vitro* translation assay

In order to test whether the antisense-mediated morpholino oligomers inhibit viral RNA translation, a cell-free translation assay was performed. *In vitro* translation assay was performed using Human Coupled 1-step *In Vitro* Translation Kit (Pierce Biotechnology, USA) according to the manufacturer's instructions. This kit has been optimized for encephalomyocarditis virus IRES-dependent translation. In brief, approximately 1 µg of *in vitro* transcribed infectious RNA was added to a reaction mix containing HeLa lysate and accessory proteins. *In vitro* translation was carried out at 30℃ for 6 hours. Thereafter, the protein fragments were resolved by SDS-PAGE and EV-A71 proteins were detected through chemiluminescence analysis as previously described in section 3.3.6.4.

Table 3.6: Primers involved in site-directed mutagenesis

Primer	**Sequence (5' → 3')[a]**
pMO-1-mutant 1F	CGTAATGGGCAACTCCGCAGCGGAACCGAC
pMO-1-mutant 1R	GTCGGTTCCGCTGCGGAGTTGCCCATTACG
pMO-1-mutant 2F	GGTAGTGTGTCGTAACGGGCAACTCTGCAG
pMO-1-mutant 2R	CTGCAGAGTTGCCCGTTACGACACACTACC
pMO-1-mutant 3F	GTAGTGTGTCGTAACGGGTAACTCTGCAGCGGAAC
pMO-1-mutant 3R	GTTCCGCTGCAGAGTTACCCGTTACGACACACTAC
pMO-1-mutant 4F	ATCCAGAGGGTAGTGCGTCGTAACGGGTAAC
pMO-1-mutant 4R	GTTACCCGTTACGACGCACTACCCTCTGGAT

[a] Underlined nucleotides indicate substitution mutations.

3.3.15 Small interference RNA transient knockdown

Small interference RNA (siRNA) targeting heparan sulfate modifying enzyme N-deacetylase/N-sulfotransferase-1 (NDST-1) and the heparan sulfate polymerase exostosin-1 (EXT-1) were purchased from Santa Cruz Biotechnology (USA). Different concentrations of siRNAs were incubated with Lipofectamine 2000 reagent in Opti-MEM (Invitrogen, USA) for 20 minutes. The siRNAs were then transfected into 1 x 10^4 RD cells for 24 hours. Before infection, the transfection medium was removed, and washed twice with serum-free DMEM. Thereafter, the cells were infected with EV-A71 at a MOI of 0.1.

3.4 Biochemistry

3.4.1 Heparinase I/II/III and chondroitinase ABC preparation

Heparinase I, II, III, I/III blend from *Flavobacterium heparinum* and chondroitinase ABC from *Proteus vulgaris* were all purchased from Sigma (USA). Heparinase I from recombinant *Bacteroides thetaiotaomicron* was supplied by R&D Systems (USA). Heparinase I, II, III were reconstituted in digestion buffer I (pH 7.5) containing phosphate buffered saline (PBS), 0.05 M sodium acetate and 0.02% bovine serum albumin (BSA). Chondroitinase ABC was reconstituted in digestion buffer II (pH 7.5) containing PBS, 0.5 mM $MgCl_2$, 0.9 mM $CaCl_2$ and 0.1% BSA.

3.4.2 Removal of cell surface heparan sulfate and chondroitin sulfate using enzymatic treatment

Overnight cultured RD cells were pre-treated with various concentrations of heparinase I/II/III and chondroitinase ABC in the respective digestion buffers for an hour at 37℃. Prior to infection, the cells were washed twice with ice cold serum-free DMEM. Thereafter, the treated cells were infected with EV-A71 for an hour at 4℃. After an

hour of infection, the inoculum was removed and the cells were washed twice with ice cold serum-free DMEM. The cells were either replenished with maintenance medium and the viral titers were determined 24 hours post-infection or fixed with 4% formaldehyde for immunofluorescence analysis.

3.5 Antiviral inhibition assay

3.5.1 Cell protection inhibition assay

Approximately 1.5 x 10^4 cells/well of the RD cells were prepared and incubated overnight at 37℃ in 5% CO_2. The growth medium was removed and replaced with serum-free DMEM containing peptides, vivo-MOs and glycosaminoglycans for 1-4 hours. Prior to infection, the cells were washed with serum free DMEM and EV-A71 at a MOI of 0.1 was added to the cells. After 1 hour incubation, the inoculum was removed, the cells were washed with serum-free DMEM and replaced with fresh maintenance medium. The virus was harvested 24 hours post-infection and the titers were determined by plaque assay and TaqMan real-time PCR.

3.5.2 Virus inactivation assay

EV-A71 virus supernatant at MOI of 10 or 0.1 was pre-incubated with peptide or glycosaminoglycans for an hour at 37℃ before infection. For peptide work, the virus-peptide mixture was then diluted 200-fold and added to overnight grown RD cells. For the glycosaminoglycan (GAG) work, the GAG-treated virus was then added to overnight grown RD cells. After 1 hour of incubation, the inoculum was removed and replenished with fresh maintenance medium. The virus was harvested 24 hours post-infection and the titers were determined by plaque assay and TaqMan real-time PCR.

3.5.3 Comprehensive inhibition assay

In the comprehensive inhibition assay, both cells and virus were treated with peptides. In brief, RD cells were pre-treated with various concentrations of peptide for 1 hour at room temperature. At the same time, virus at a MOI of 0.1 was pre-treated with the same amount of peptide for 1 hour at 37℃. After incubation, the peptide-containing supernatant was removed from the cells and the peptide-treated virus was added to the cells. After 1 hour of incubation, the inoculum was removed and replaced with maintenance medium. The virus titers were quantitated 24 hours post-infection by TaqMan real-time PCR and plaque assay.

3.5.4 Virus attachment inhibition assay

In the virus attachment inhibition assay, RD cells were pre-treated with peptide for an hour before infection. A MOI of 100 of ice-cold EV-A71 was added to the pre-cold RD cells and incubated at 4℃ for an hour. After incubation, the inoculum was removed and the cells were washed twice with ice-cold serum-free DMEM. Thereafter, the cells were either fixed with 4% formaldehyde for immunofluorescence assay or replaced with maintenance medium. Virus was harvested 24 hour post-infection and the virus titers were determined by plaque assay and TaqMan real-time PCR.

3.6 Three-dimensional structure and sequence analysis

The crystal structure of EV-A71 with protein data bank (PDB) identification code 4AED was downloaded from the PDB (http://www.rcsb.org/pdb). The three-dimensional structure of EV-A71 was built using the Deep-View Swiss PDB viewer, version 4.0.4 (Swiss Institute of Bioinformatics). For sequence analysis, VP1 sequences from different genotypes were downloaded from GenBank (http://www.ncbi.nlm.nih.gov) and were aligned using ClustalW2 software (http://www.ebi.ac.uk/tools/msa/clustalw2/) (Larkin *et al.*, 2007).

3.7 Statistical analysis

Statistical analysis was performed using GraphPad Prism 5 (GraphPad software Inc., USA). Means ± standard deviations were obtained from at least two independent biological replicates. Statistical significance was calculated using the Mann-Whitney test. A *P* value of < 0.05 was considered as statistically significant.

CHAPTER 4

RESULTS

4.1 Construction of enterovirus A71 and enhanced green fluorescence protein-expressing enterovirus A71 cDNA infectious clones

In this study, infectious clone of EV-A71 was constructed either with or without the enhanced green fluorescence protein (EGFP) reporter gene. These constructs are required to understand the mechanism of antiviral resistance, as well as to characterize the mechanism of action of an antiviral. In this study, EV-A71 infectious cDNA clone is utilized to characterize the degree of mismatch tolerance of the vivo-MO-1 against EV-A71. Desired mutations are introduced into vivo-MO-1 targeted region through site-directed mutagenesis. EV-A71_EGFP is used to study the mechanism of action of vivo-MOs against EV-A71 infection.

4.1.1 Construction and characterization of the enterovirus A71 cDNA clone

4.1.1.1 Amplification and cloning of the full-length enterovirus A71 genome

EV-A71 viral RNA was extracted using QIAamp viral RNA mini kit and subjected to cDNA synthesis. As shown in the agarose gel electrophoresis in Figure 4.1A, the full-length EV-A71 genome size of approximately 7.5 kb was successfully amplified using iProof high fidelity DNA polymerase. The PCR product was then gel purified and subjected to A-tailing using GoTaq DNA polymerase. The product with single 3' adenosine (A) was then cloned into pCR-XL-TOPO plasmid vector and the recombinant plasmid was then transformed into *E. coli* TOP10. The recombinant plasmid was then linearized by *Eag*I. The electrophoresed intact recombinant plasmid pCR-TOPO-XL-EV-A71 is shown in Figure 4.1B.

4.1.1.2 Characterization of enterovirus A71 infectious cDNA clone

The schematic illustration of EV-A71 infectious cDNA clone in pCR-XL-TOPO vector is shown in Figure 4.2. The EV-A71 genome was cloned downstream of the SP6 promoter. Upstream of the SP6 promoter was a *Mlu*I restriction site and downstream of the poly(A) tail was an *Eag*I restriction site. Infectious EV-A71 genomic RNA was synthesized using SP6 RNA polymerase. The *in vitro* transcribed RNA contains an additional G residue at the 5' end and CGGCC residues at the 3' end. As depicted in Figure 4.1C, the size of the *in vitro* transcribed RNA was approximately 7.5 kb. Smearing after the expected band was observed, which was likely due to some RNA degradation occurring during *in vitro* transcription or incomplete denaturation. The presence of non-viral residues at the 5' and 3' ends were found to reduce viral replication efficacy. This correlated well with the results demonstrated in this study. RD cells transfected with the purified viral RNA developed CPE faster than the RD cells transfected with *in vitro* transcribed RNA. The CPE was usually observed 48 to 72 hours post-transfection of the *in vitro* transcribed RNA. Characterization of the plaque morphology and the replication kinetics of the cDNA-derived EV-A71 and the wild-type virus are shown in Figure 4.3. There were no differences in the plaque morphology and the replication kinetics between the viruses produced from the infectious cDNA clone and the wild-type virus.

4.1.2 Construction and characterization of the enterovirus A71 enhanced green fluorescence protein (EGFP) reporter virus

4.1.2.1 Amplification and cloning of full-length enterovirus A71 EGFP genome

In order to avoid alteration of the EV-A71 genome through addition of restriction enzyme cutting sites, overlapping extension PCR was used to fuse the EGFP gene into the EV-A71 genome. The recombinant plasmid pCR-XL-TOPO-EV-A71 and pEGFP-

N1 (Clonetech, USA) were used as the backbone for EV-A71_EGFP construction. The primers were designed with at least 15 nucleotides overlap. A total of four DNA fragments were fused together. Fragment 1 (808 bp) covered the EV-A71 5'UTR which was flanked by the SP6 promoter and part of the EGFP gene. Fragment 2 (777 bp) covered the EGFP gene and was flanked by part of the EV-A71 5'UTR and VP4. Fragment 3 (3037 bp) covered the EV-A71 P1 region which was flanked by part of the EGFP gene and the EV-A71 2A gene. Fragment 4 (3783 bp) covered the entire EV-A71 P2 and P3 regions and was flanked by part of the EV-A71 2A region and a poly(A) tail. The fragments were then fused fragment-by-fragment using overlapping extension PCR (Figure 4.4A). The final full-length EV-A71 genome with EGFP gene (8.2 kb) was then gel purified and cloned into a pCR-XL-TOPO vector. All the PCRs were performed using Q5 high fidelity DNA polymerase, which has > 100X fidelity compared to normal Taq polymerase.

4.1.2.2 Characterization of enterovirus A71 EGFP-expressing infectious cDNA clone

The schematic illustration of EV-A71_EGFP-expressing infectious cDNA clone is depicted in Figure 4.5. The EGFP gene was fused between 5'UTR and VP4 followed by a 2A cleavage site (with amino acid sequence of –AITTL-). After viral polyprotein synthesis, the EGFP which was fused with VP4 will be cleaved off by EV-A71 2A proteases to produce a functional EGFP. The EV-A71_EGFP-expressing infectious cDNA clone was flanked by restriction sites *Bst*B1 upstream of the SP6 promoter sequence and *Age*I located downstream of the poly(A) tail. The *in vitro* transcribed RNA contains an additional G residue at the 5' end and CCGG residues at the 3' end. The *in vitro* transcribed RNA was about 8 kb in length (Figure 4.4B). The GFP signal could be detected 24 hours post-transfection and the CPE was observed 72 days post-transfection. The replication kinetics and the plaque morphology were determined using the P1 stock. As shown in Figure 4.6, EV-A71 expressing EGFP has a smaller plaque

size with a diameter of 1 mm and less well-defined edges compared to wild type EV-A71 with an average 1.5 mm diameter. EV-A71_EGFP infectious virus had slower replication kinetics compared to the wild type EV-A71, which could be a result of inefficiency in RNA genome packaging.

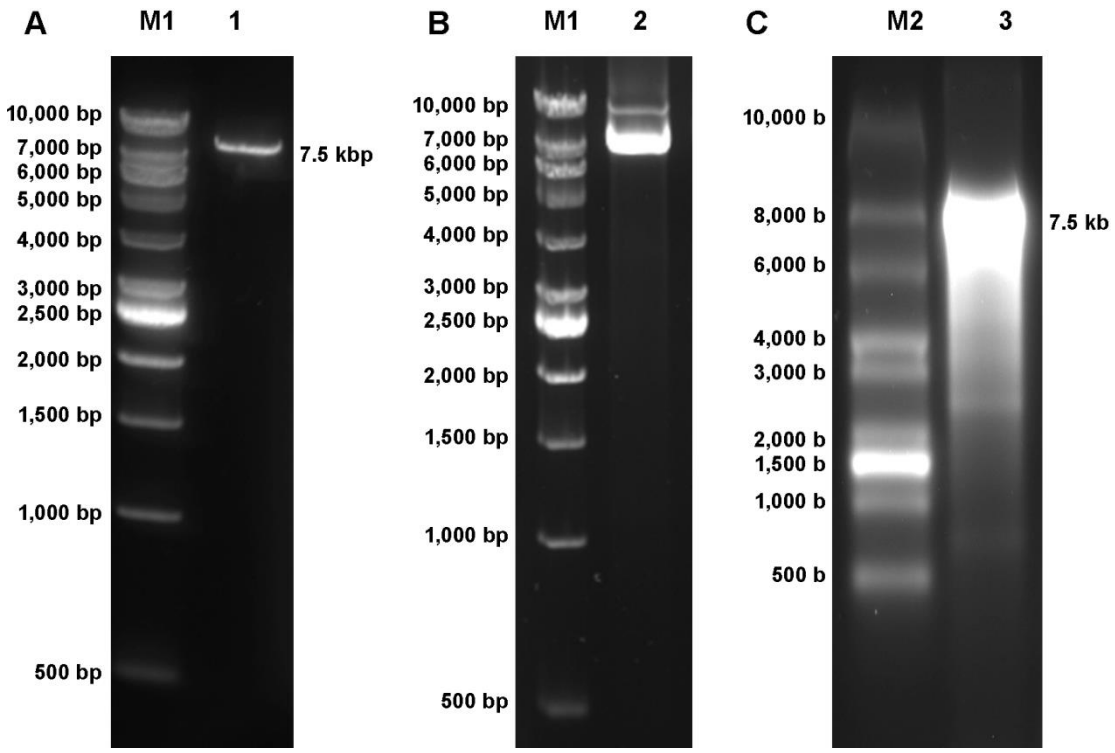

Figure 4.1: Agarose gel electrophoresis of full-length EV-A71 genome. Agarose gel electrophoresis images of (A) full-length EV-A71genomic PCR product (lane 1), (B) purified plasmid pCR-TOPO-XL-EV-A71 from *E.coli* TOP10 (lane 2) and (C) SP6 *in vitro* transcribed RNA (lane 3). Lane M1 contains VC 1 kb DNA ladder and lane M2 contains 0.5-10 kb RNA ladder. The sizes of the DNA and RNA ladders are indicated as base pairs (bp) and bases (b).

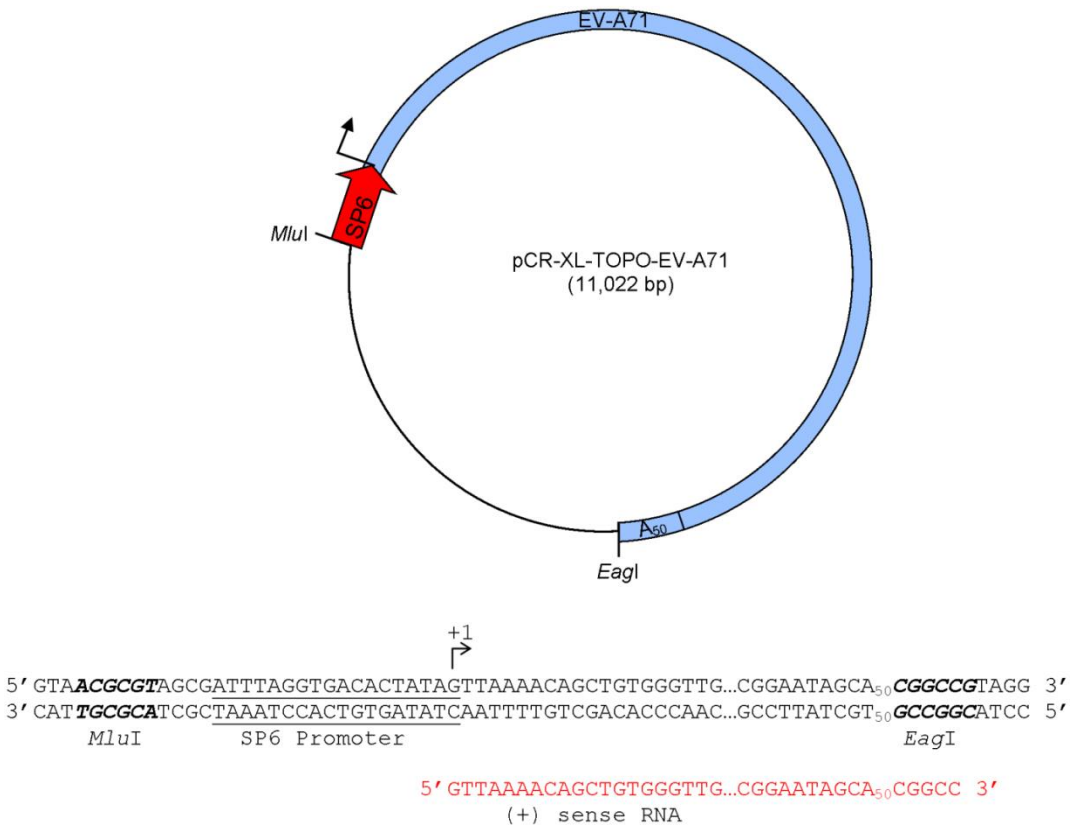

Figure 4.2: Schematic illustration of EV-A71 infectious cDNA clone in pCR-XL-TOPO. EV-A71 genomic cDNA was cloned downstream of a SP6 RNA polymerase promoter. The *in vitro* transcribed positive-sense RNA carried an additional G residue at the 5' end and a poly$(A)_{50}$ tail followed by additional CGGCC residues at the 3' end. The arrow indicates the transcription start site.

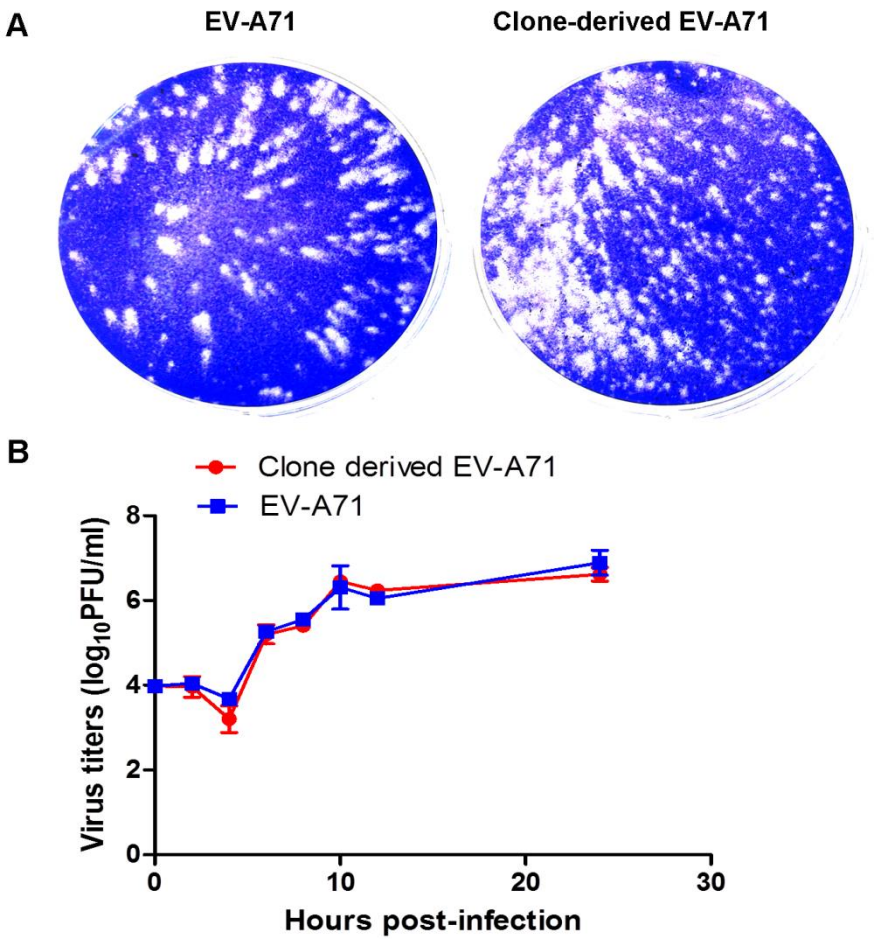

Figure 4.3: Replication kinetics of the EV-A71 infectious cDNA clone. Phenotypic characterization of wild-type EV-A71 and clone-derived EV-A71 based on the (A) plaque morphology after 48 hours post-infection and (B) replication kinetics in RD cells. At each time point, titers are the average of two biological replicates; error bars represent the standard deviation of the mean.

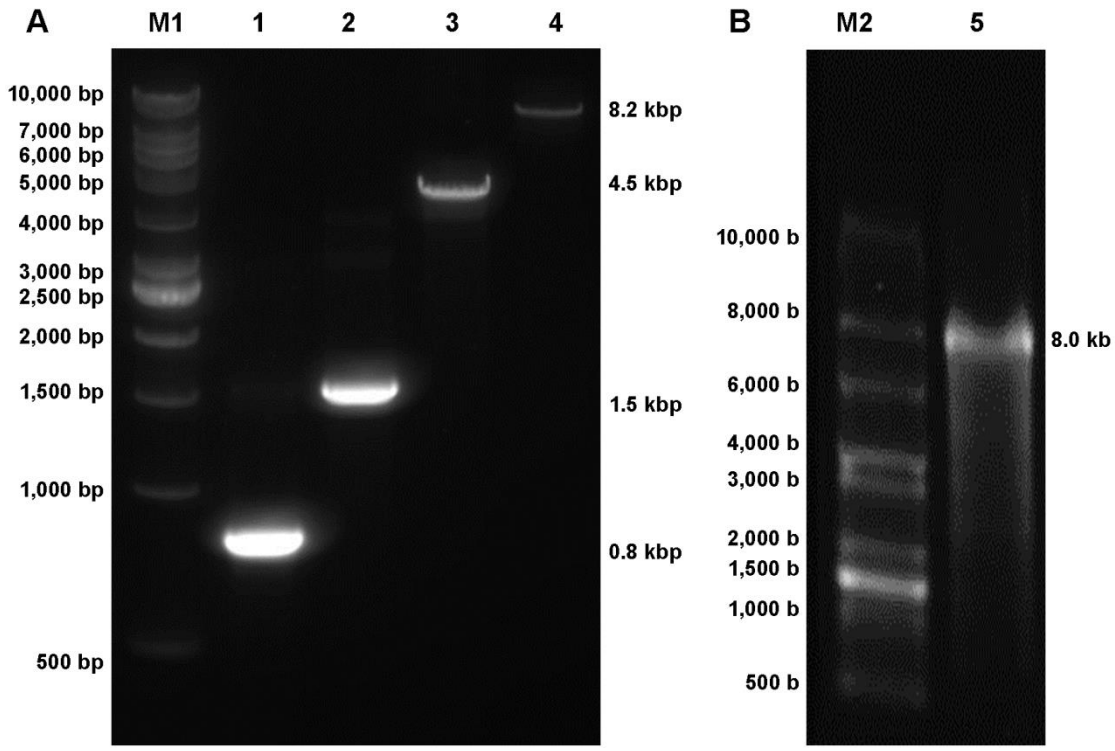

Figure 4.4: Agarose gel electrophoresis of overlapping PCR DNA fragments and *in vitro* transcribed RNA. Agarose gel electrophoresis images of (A) overlapping extension PCR products and (B) SP6 *in vitro* transcribed RNA. Lane M1, 1 kb DNA ladder; Lane 1, fragment 1; lane 2, overlapped product of fragments 1 and 2; lane 3, overlapped product of fragments 1, 2 and 3; lane 4, full-length EV-A71_EGFP; lane M2, 0.5-10 kb RNA ladder; and lane 6, *in vitro* transcribed RNA.

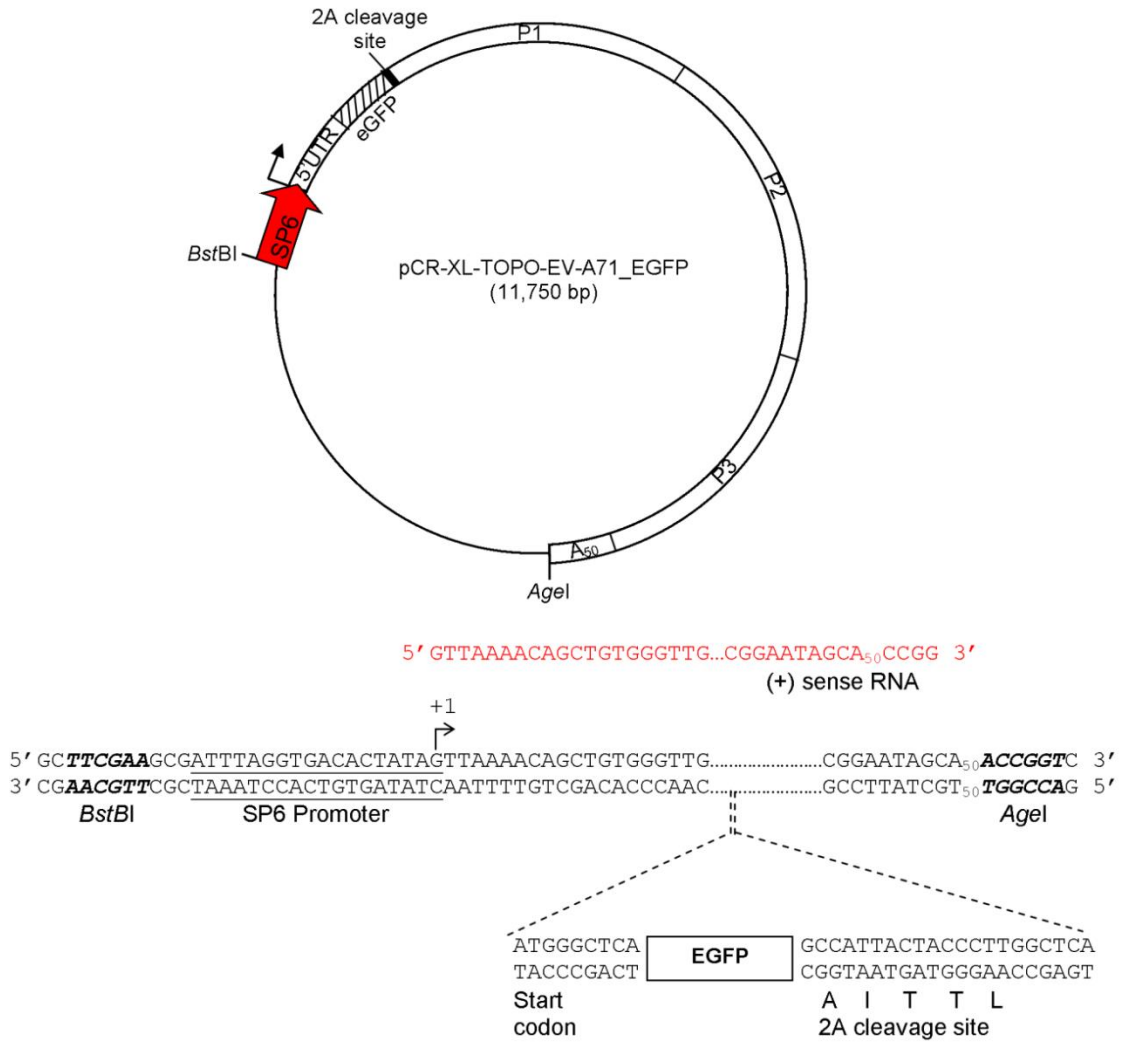

Figure 4.5: Schematic illustration of EV-A71_EGFP-expressing cDNA clone in pCR-XL-TOPO. The EV-A71_EGFP genome was located downstream of bacteriophage SP6 RNA polymerase promoter sequence and upstream of a poly(A)$_{50}$ tail. The EGFP gene was fused in between the EV-A71 5'UTR and VP4 gene, followed by a 2A cleavage site using overlapping extension PCR. The positive-sense RNA derived from the SP6 RNA polymerase consists of an additional G residue at the 5' end and CCGG residues at the 3' end. The arrow indicates the transcription start site.

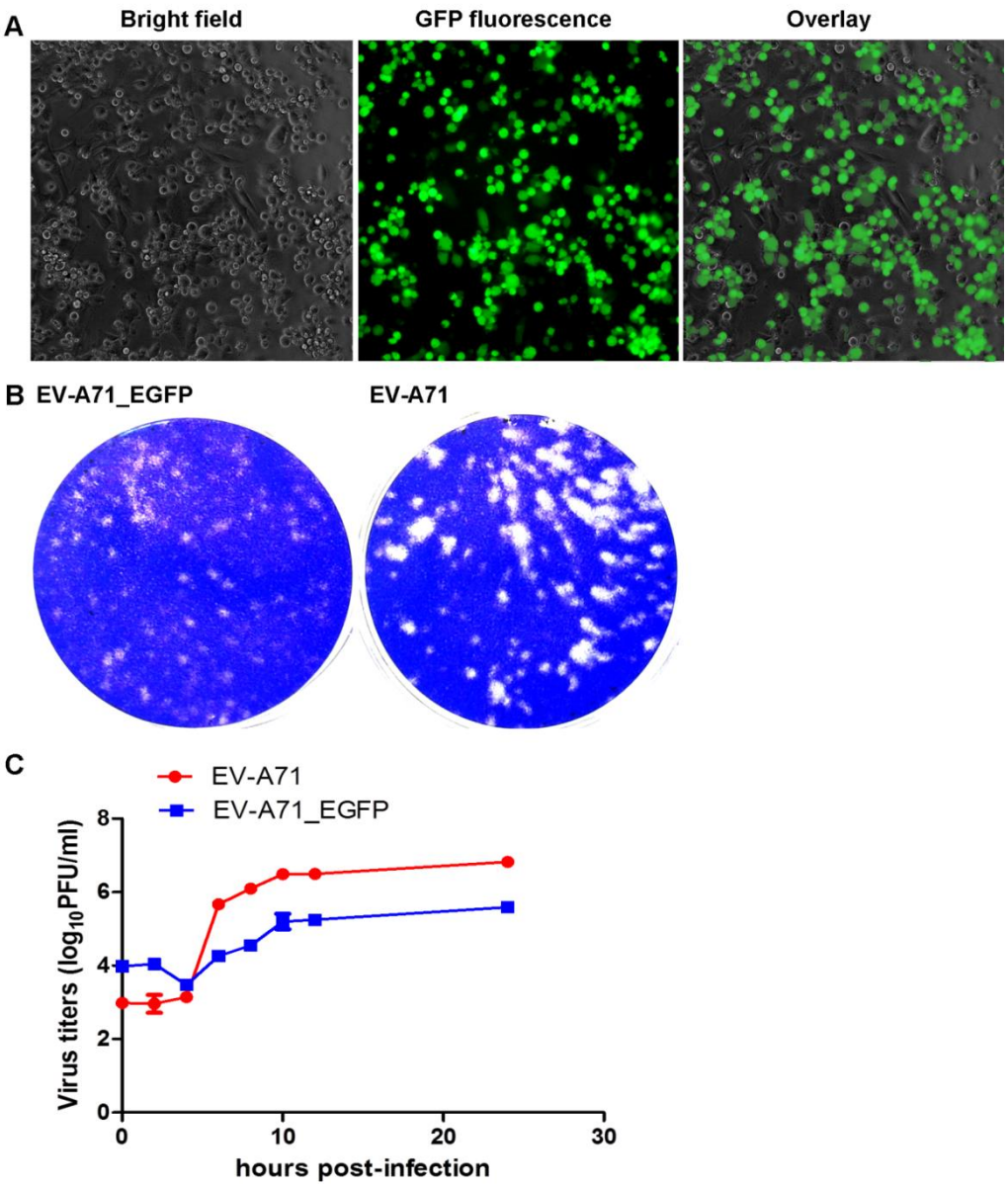

Figure 4.6: Characterization of EV-A71_EGFP-expressing clone. (A) RD cells were infected with rescued EV-A71_EGFP at a MOI of 0.1. The viral-induced CPE and the EGFP expression was observed 24 hours post-infection. The EGFP signal (green) was detected using a fluorescence microscope at an excitation wavelength of 488 nm. Phenotypic characterization of EV-A71 and EV-A71_EGFP based on the (B) plaque formation size after 72 hours post-infection and (C) replication kinetics in RD cells. At each time point, titers are the average of two biological replicates; error bars represent the standard deviation of the mean.

4.2 Inhibition of enterovirus A71 infections by a novel antiviral peptide derived from enterovirus A71 capsid protein VP1

Virus-host receptor interaction is an essential event during virus infection. EV-A71 VP1 is known to carry multiple receptors recognition sites. Therefore, screening of synthetic peptides covering the entire VP1 capsid protein could lead to novel antiviral peptides discovery as well as discovery of an unknown receptor. A library of 95 overlapping peptides was synthesized and screened for potential anti-EV-A71 activity. The following sub-sections describe the outcomes of the antiviral peptides screening, which led to a novel antiviral peptide discovery.

4.2.1 Screening of 95 overlapping peptides against enterovirus A71 infection

In this study, 95 synthetic peptides covering the entire EV-A71 VP1 were synthesized with overlapping 12 residues (6 residues at the C terminal and 6 residues at the N terminal). The peptides used for the initial screening had 60 – 65% purity. All synthetic peptides were dissolved in 100% DMSO followed by dilution using serum-free DMEM. The synthetic peptides were diluted to a final concentration of approximately 100 μM and the inhibitory effects against 100 plaque forming units (PFU) of EV-A71 were evaluated in RD cells using a comprehensive inhibitory assay. A peptide was considered to have antiviral effect if it inhibited at least 80% of plaque formation at a concentration of 100 μM. Of the 95 overlapping synthetic peptides used, four peptides, designated as SP40, SP45, SP81 and SP82, exhibited significant antiviral activity against EV-A71 infection (Figure 4.7). SP40, SP45, SP81 and SP82 reduced plaque formation by 89.3%, 83.7%, 83.7%, and 82.5%, respectively. This study further focused on the SP40 peptide, as it exhibited the highest inhibitory activity. The amino acid sequence of the SP40 peptide (Ac-QMRRKVELFTYMRFD-NH_2) was highly conserved across all EV-A71 genotypes, implying that this region plays a critical role in EV-A71 infection.

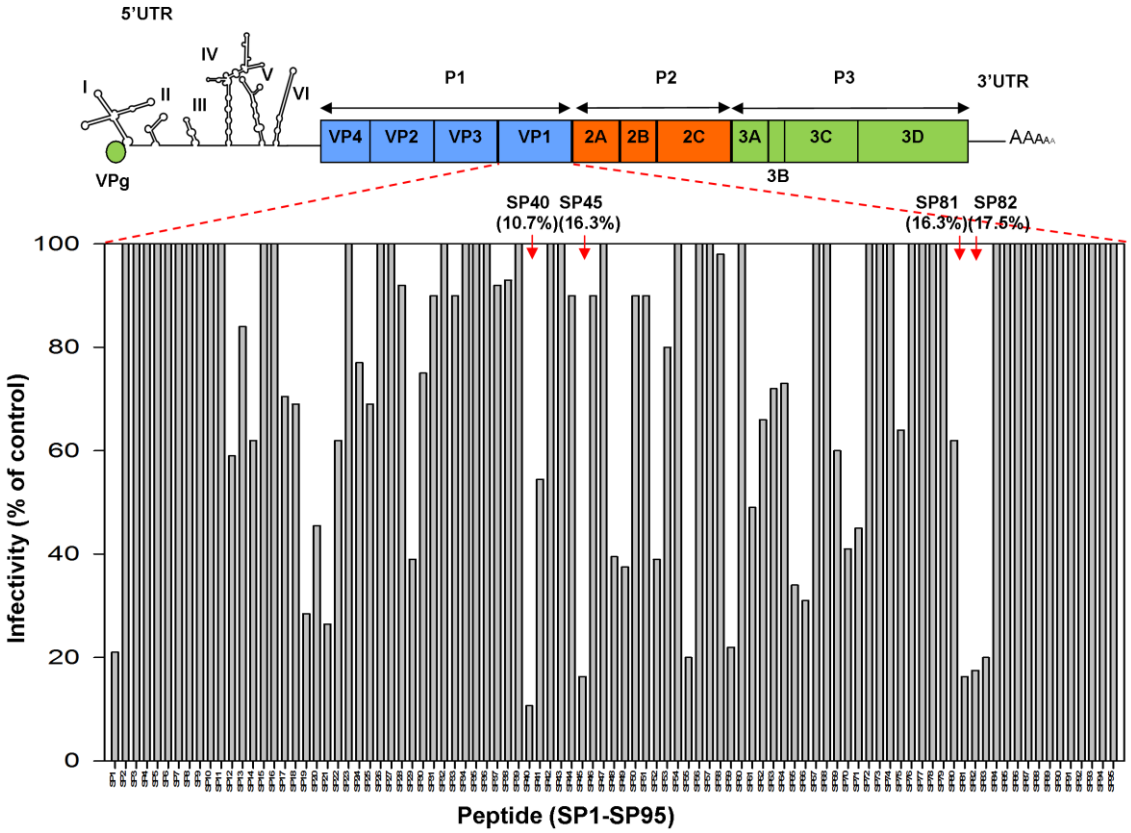

Figure 4.7: Identification of antiviral peptides. A library containing 95 overlapping synthetic peptides (15-mers) covering the entire EV-A71 capsid protein VP1 was synthesized. Each peptide was screened at a concentration of 100 μM for its ability to inhibit EV-A71 infection in a plaque reduction assay. A schematic representation of the EV-A71 genome is shown; and the percentage of EV-A71 infectivity following treatment with each peptide is shown in the bar graph. Arrows denote the four peptides that inhibited > 80% of plaques.

4.2.2 Antiviral analysis of the SP40 peptide

To further investigate the antiviral activities of SP40 peptide, the peptide was re-synthesized at a higher purity of > 95% by HPLC. A scrambled peptide, SP40X (Ac-REFTMKRMVLFRQDY-NH_2) was synthesized and used as a control throughout the experiment. The inhibitory effect of SP40 peptide against EV-A71 at a MOI of 0.1 was determined using a comprehensive inhibition assay. SP40 peptide significantly reduced EV-A71-induced CPE (Figure 4.8A), plaque formation (Figure 4.8B) and viral protein expression (Figure 4.8C). The results also confirmed that SP40 peptide inhibited EV-A71 infection in RD cells, with reduction of viral plaques by 96.3% $\pm$ 0.8 (Figure 4.9A) and viral RNA level by 92.0% $\pm$ 9.3 (Figure 4.9B). The inhibition concentration 50% (IC_{50}) for SP40 peptide was 7.9 μM $\pm$ 3.5. The scramble SP40X did not inhibit EV-A71 infection, except at higher concentration. This is likely due to the accumulation of positively-charged amino acids. Taken together, these data suggests that the amino acid sequence of SP40 is critical for its antiviral activity.

To verify whether the antiviral activity of SP40 peptide was cell-specific, the SP40 peptide was tested against EV-A71 infection in HeLa, Vero and HT-29 cell lines. As depicted in Figure 4.10A and B, SP40 peptide greatly inhibited EV-A71 infection in HeLa, Vero and HT-29 cells in a dose-dependent manner, as determined by CPE observation and TaqMan real-time PCR. However, SP40 peptide exhibited reduced efficacy in HT-29 cells as compared to the HeLa or Vero cells.

This study also further investigated whether SP40 peptide inhibited different EV-A71 genotypes as well as other enteroviruses. As shown in Table 4.1, SP40 peptide also exhibited antiviral activity against EV-A71 BrCr (genotype A), EV-A71 SHA66/97 (genotype B3), EV-A71 SHA52/97 (genotype C2), CV-A16 strain 22159 and PV

vaccine strain. However, reduced antiviral activity was observed against the PV vaccine strain (IC_{50} of 18.2 μM ± 10.4).

4.2.3 Cytotoxicity analysis of the SP40 peptide

To evaluate whether SP40 peptide was cytotoxic to cells, RD cells were treated with increasing concentrations of SP40 peptide from 0 μM to 280 μM. The cell viability was then determined. As depicted in Figure 4.11, SP40 peptide was not toxic to cells when tested up to 280 μM.

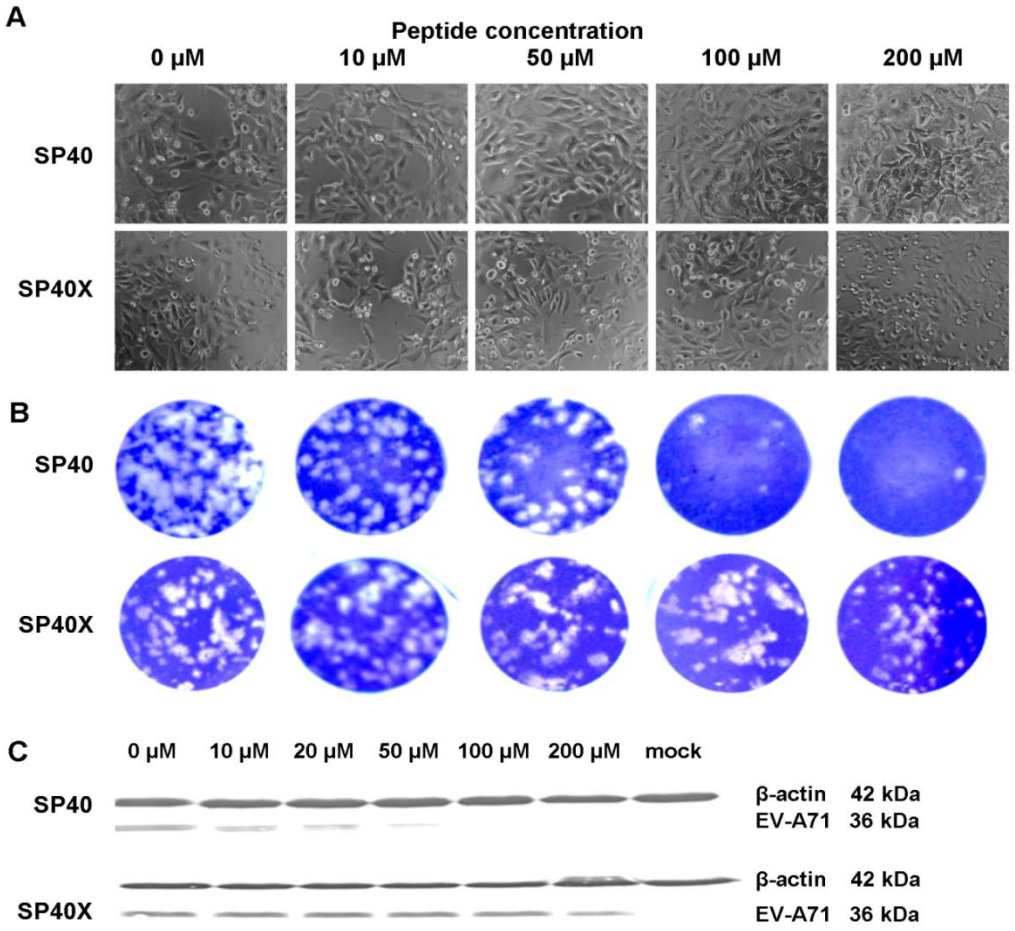

Figure 4.8: Inhibitory effects of SP40 and SP40X peptides on CPE, plaque formation and protein synthesis. (A) For CPE, EV-A71 at a MOI of 0.1 was pre-incubated with peptides for 1 hour before infection of peptide-treated RD cells. The images were taken at 24 hours post-infection. CPE was seen as round and shrunken cells, which eventually dislodged from the surface. (B) For the plaque reduction assay, approximately 100 PFU of EV-A71 were pre-incubated with peptides for 1 hour before infection of the peptide-treated RD cells. The cells were fixed with 4% formaldehyde and stained with 0.5% crystal violet at 48 hours post-infection. (C) Western blot analysis of total protein isolated from virus-infected cells using the anti-EV-A71 monoclonal antibodies and monoclonal anti-β-actin antibodies. The molecular weights of the EV-A71 protein and β-actin are 36 kDa and 42 kDa, respectively.

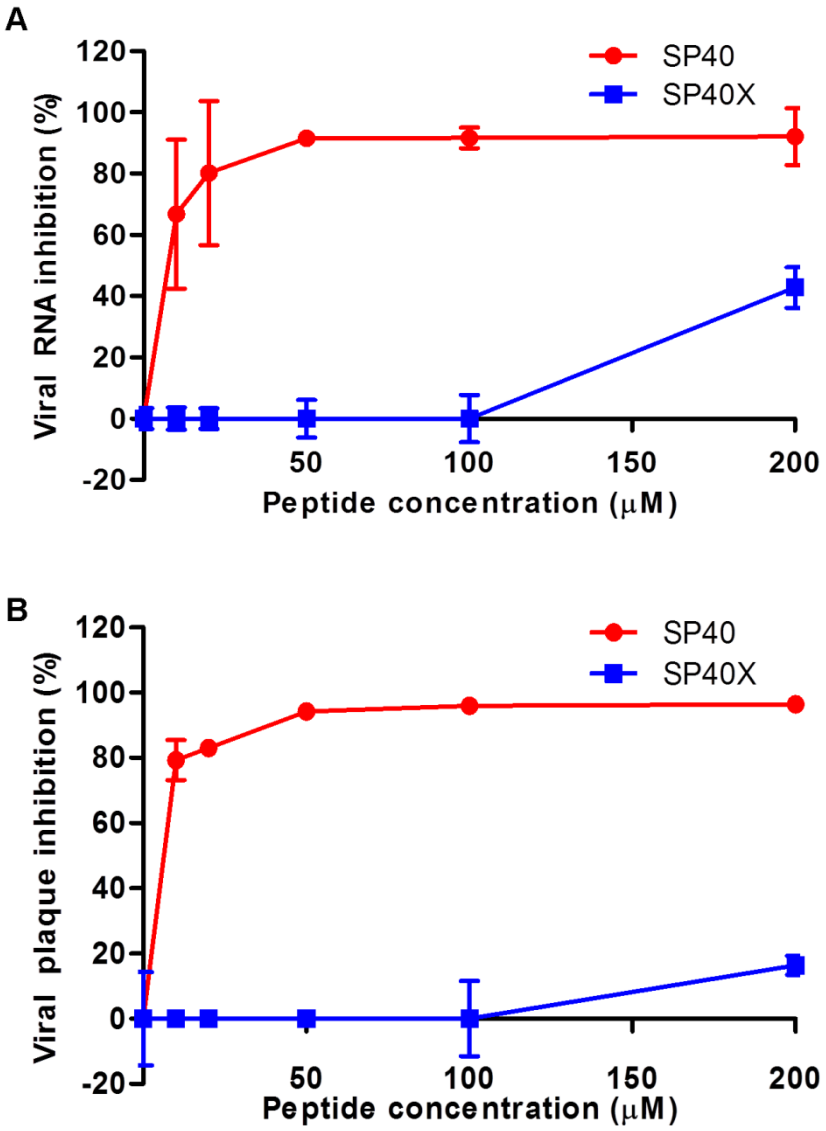

Figure 4.9: Antiviral activities of the SP40 and SP40X peptides. Both RD cells and EV-A71 were separately pre-incubated with increasing concentrations of each peptide for 1 hour before viral inoculation. The inhibitory levels of the peptide were evaluated at 24 hours post-infection by (A) plaque assay and (B) TaqMan real-time PCR. At each peptide concentration, titers are the average of two biological replicates; error bars represent the standard deviation of the mean.

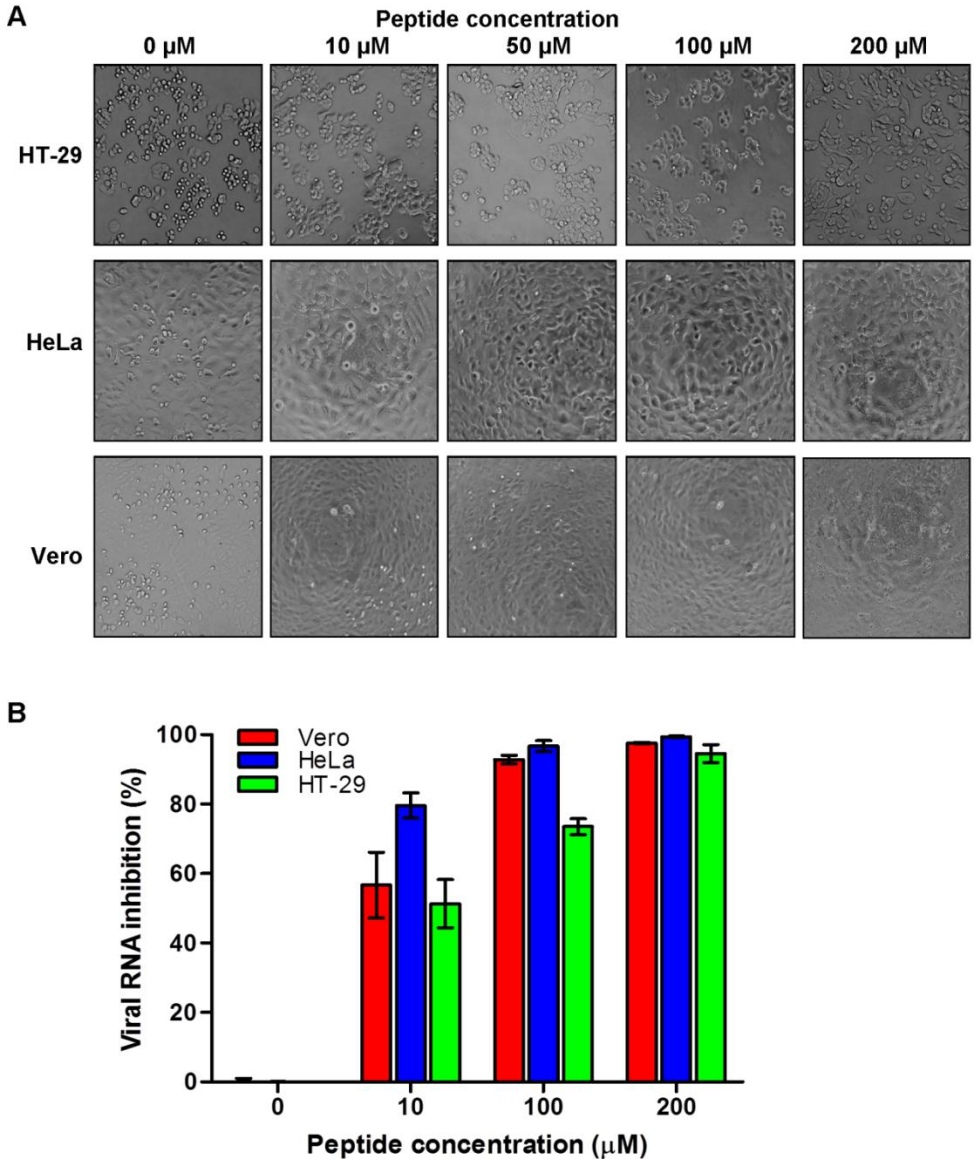

Figure 4.10: The antiviral activities of the SP40 peptide in various cell lines. Vero, HeLa and HT-29 cell lines were pre-treated with the SP40 peptide at various concentrations for 1 hour at room temperature before infection with EV-A71 at a MOI of 0.1. (A) The viral-induced CPE in various cell lines were observed 24 hours post-infection. CPE was seen as round and shrunken cells, which eventually dislodged from the surface. (B) Viral RNA inhibition was quantitated by TaqMan real-time PCR. At each peptide concentration, percentages of inhibition are the average of two biological replicates; error bars represent the standard deviation of the mean.

Table 4.1: Inhibition concentration 50% (IC_{50}) of the SP40 peptide against various enteroviruses

Enterovirus	**Genotype**	**Clinical manifestations**	**IC_{50} (µM)[a]**
EV-A71 BrCr	A	Aseptic meningitis	9.3 ± 2.5
EV-A71 SHA66/97	B3	HFMD	6 ± 0.7
EV-A71 41	B4	Fatal	7.9 ± 3.5
EV-A71 SHA52/97	C2	HFMD	8.5 ± 2.8
CV-A16	-	HFMD	6 ± 0.8
PV vaccine strain	-	-	18.22 ± 10.4

[a]The IC_{50}s are presented as mean ± standard deviation determined from at least two independent experiments

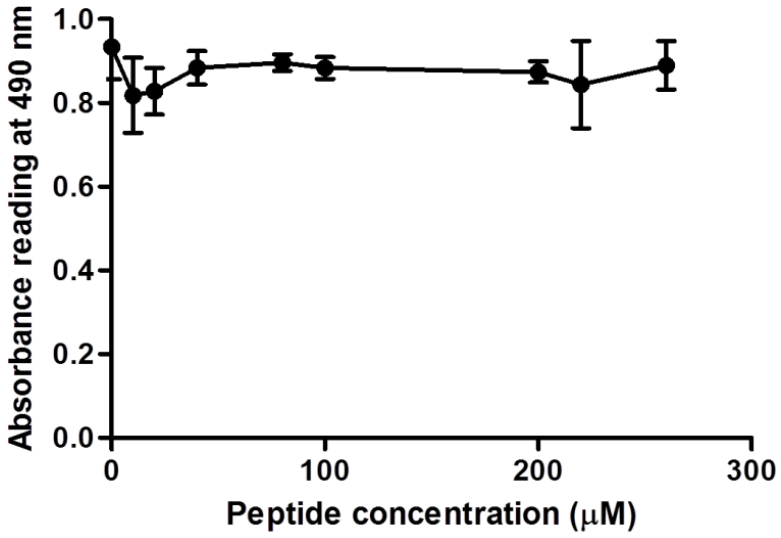

Figure 4.11: Cytotoxicity assay. RD cell monolayers in a 96-well plate were treated with increased concentrations of SP40 peptide. Cell viability was assayed as an absorbance reading at 490 nm. At each peptide concentration, the absorbance readings are averages of two biological replicates; error bars represent the standard deviation of the mean.

4.2.4 Mechanism of action of the SP40 peptide

Since the amino acid sequence of SP40 peptide was critical for its antiviral activity, further understanding of the mechanism of action is required. The data from the comprehensive assay suggests that the SP40 peptide could exert its antiviral activity through inhibition of the viral binding step or inactivation of the virus. To further elucidate the mechanism, either cells or viruses were pre-treated with SP40 peptide before infection. When the viruses at a MOI of 10 were pre-treated with the SP40 peptide, followed by 200-fold dilution prior to infection, the SP40 peptide lost its antiviral activity against EV-A71, and this implied that SP40 peptide did not inactivate the virus (Figure 4.12).

When only the cells were pre-treated with SP40 peptide, significant inhibition of EV-A71 infection was observed with an IC_{50} value of 15 μM. This result suggests that the SP40 peptide could either inhibit EV-A71 at the pre-binding step or post-binding step.

To address this, RD cells were pre-treated with various concentrations of the SP40 peptide at 4℃ for 1 hour, followed by EV-A71 at a MOI of 100 at 4℃ for 1 hour. The EV-A71 viral particles that attached to the cells surface were then determined by immunofluorescence assay and further quantitated by high content screening analysis. As shown in Figure 4.13A, the number of EV-A71 viral particles (with Alexa Fluor 488 green fluorescence) attached to the SP40 peptide-treated cell surface was significantly lower compared to the untreated cells. This result was further verified by Cellomics HCS ArrayScan Spot Detector Bio-Application and TaqMan real-time PCR. As shown in Figure 4.13B, the number of spots per field for SP40 peptide-treated RD cells (68 ± 20 spots/field) was lower compared to the untreated cells (210 ± 39 spots/fields). The results correlated well with TaqMan real-time PCR (Figure 4.13C). To investigate if SP40 peptide inhibited the EV-A71 post-binding step, RD cells were pre-treated with

EV-A71 at 4 ℃ for 1 hour to allow the virus to bind to the cells, followed by addition of SP40 peptide. The cells were washed and then immediately shifted to 37 ℃ for 1 hour to allow the virus to enter the cells. However, SP40 peptide lost its antiviral activity, which implies that SP40 peptide blocked EV-A71 infection at the pre-binding step. These findings suggest that SP40 peptide could interact with the attachment receptor targeted by EV-A71 and hence block the attachment event.

To further verify whether the SP40 peptide still inhibits EV-A71 infection in the post-infection event, SP40 peptide was administered 1 hour after EV-A71 infection. The SP40 peptide was found to be non-inhibitory when added 1 hour after infection, with an IC_{50} value of 200 μM (Figure 4.12).

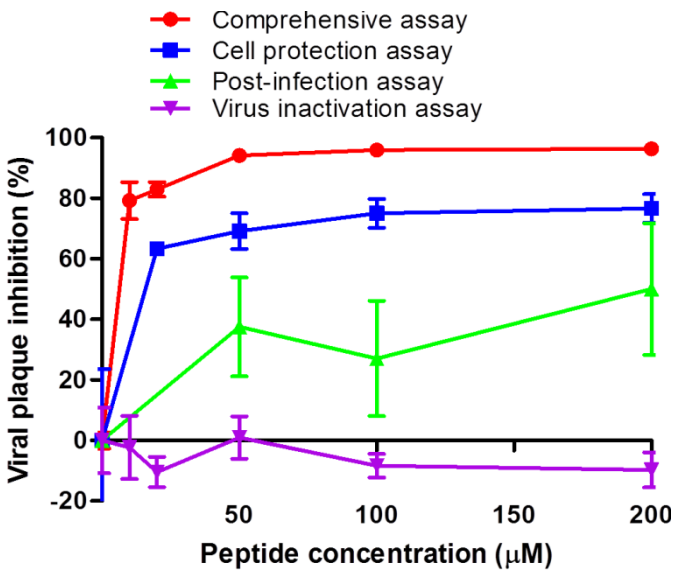

Figure 4.12: Mechanism of action studies of SP40 peptide. The SP40 peptide was administered at different time points relative to viral inoculation, and plaque assay was performed 24 hours post-infection. In the comprehensive assay, both RD cells and EV-A71 were pre-treated with the SP40 peptide for an hour before infection. In the cell protection assay, RD cells were pre-treated with the peptide for an hour before virus inoculation. In the post-infection assay, RD cells were infected with EV-A71 for an hour before addition of the peptide-containing media. In the virus inactivation assay, EV-A71 was pre-treated with the peptide for an hour, and diluted 200-fold before infection of RD cells. At each peptide concentration, percentages of plaque inhibition are the average of two biological replicates; error bars represent the standard deviation of the mean

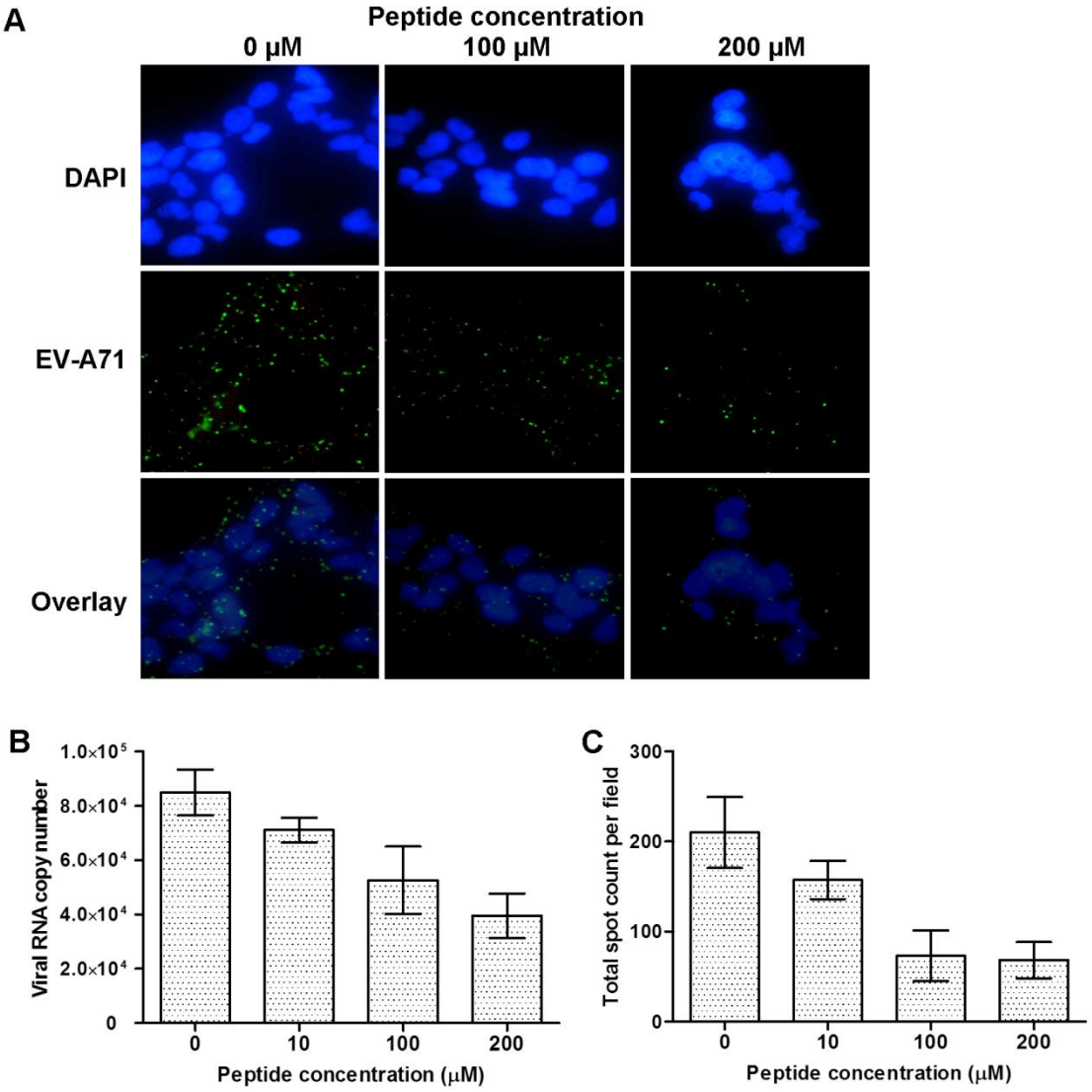

Figure 4.13: Effect of SP40 peptide on EV-A71 attachment. (A) Immunofluorescence analysis of EV-A71 viral particles attached on the RD cell surface. EV-A71 viral particles were probed with anti-EV-A71 antibodies and Alexa Fluor 488; and cell nuclei were stained with DAPI. EV-A71 viral particles and nuclei are shown in green and blue fluorescence, respectively. The number of virus particles attached to the cell surface were quantified by (B) TaqMan real-time PCR assay and (C) Cellomics HCS ArrayScan Spot Detector Bio-Application. At each peptide concentration, titers are the average of two biological replicates; error bars represent the standard deviation of the mean.

4.2.5 Alanine scanning analysis

Identification of the amino acids critical for the antiviral activity of SP40 peptide can determine the mechanism of action, and identify the potential receptor binding site. Alanine scanning is the most common method used to identify the amino acid residues critical for activities. Thirteen peptides with alanine substitutions in each amino acid position of the 15-mer SP40 peptide were synthesized. The inhibitory effects in RD cells at 200 μM of all peptides were evaluated. Reduction of viral RNA levels by each of the peptides were evaluated and are summarized in Figure 4.14. Substitution of an arginine residue at position 3 (P3) with alanine significantly reduced the antiviral activity from 95.9% to 60.8%. Substitution of other positively-charged amino acids (lysine and arginine) at positions 4, 5 and 13 (P4, P5 and P11) of the SP40 peptide with alanine caused a moderate reduction of antiviral activity, from 95.9% to 74.3%, 70.9% and 70.6%, respectively. Substitution of a polar amino acid, methionine, at position 12 (P10) with alanine also reduced the antiviral activity moderately to 74.7%. Alanine substitution of other amino acids at other positions of the SP40 peptide did not alter its antiviral activity. These results indicated that the positively-charged amino acids of SP40 peptide were critical for its antiviral properties. Substitution of a polar methionine also reduced the antiviral properties.

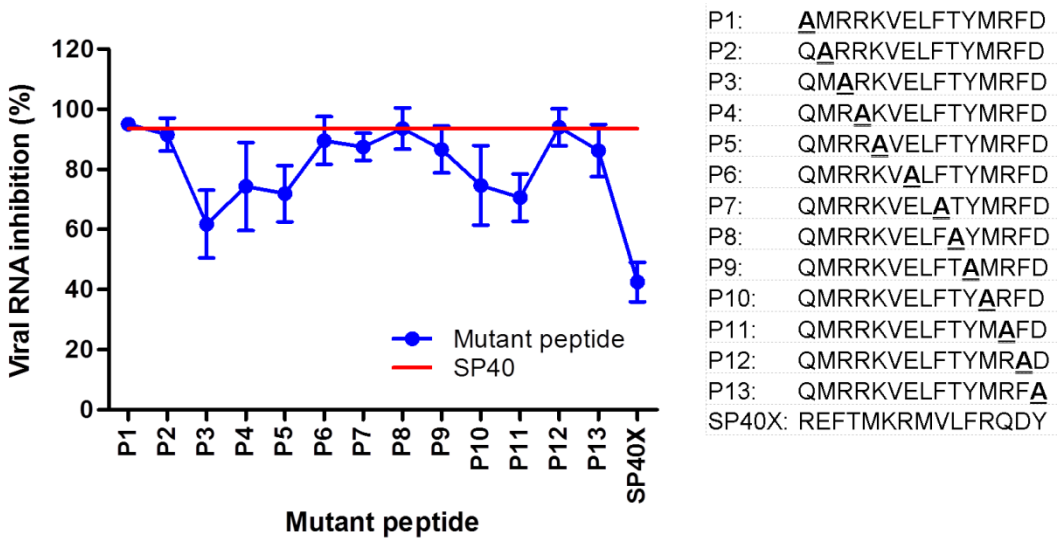

Figure 4.14: Alanine scanning analysis of SP40 peptide. Thirteen different peptides (P1-P13) were synthesized by replacing one residue at a time with an alanine and their inhibitory effect was determined, compared with the original SP40 represented by the red line. SP40X, a scrambled peptide, was used as a negative control. Percentages higher than the red line showed a gain of antiviral activity whereas a lower number represented a loss of antiviral activity. Data presented are mean of two biological replicates; error bars represent the standard deviation of the mean.

4.2.6 Three-dimensional structure analysis

With the recent available crystal structure of EV-A71, the position of the SP40 peptide was located and characterized (Figure 4.15). The SP40 peptide was not positioned on the surface, but the lysine residues of SP81 and SP82, which also exhibited antiviral activity (see section 4.2.1) were highly exposed on the surface.

4.2.7 Synergistic antiviral activities of the SP40 peptide with SP81

To investigate whether the SP40 peptide exhibited synergistic antiviral activities with other peptides, the SP40 peptide was combined with SP45 and SP81 (> 70% purity by HPLC) to a final concentration of 200 μM. The SP40 peptide exhibited synergistic antiviral activity with SP81 peptide to achieve a total viral RNA inhibition of 99.7% when compared to 92.0% inhibition by the SP40 peptide alone. However, the SP40 peptide had less synergistic effect when combined with the SP45 peptide, with viral RNA inhibition of 94.3%. When all the three peptides were combined, viral RNA inhibition achieved was 98.8%. There were only few amino acids difference between SP81 and SP82 peptides, implying that these two peptides could share similar mechanism in action. Therefore, synergistic antiviral activities of SP40 and SP82 peptides were not included in this study. These data suggest that all these peptides could potentially target different host factors that are important for EV-A71 infection.

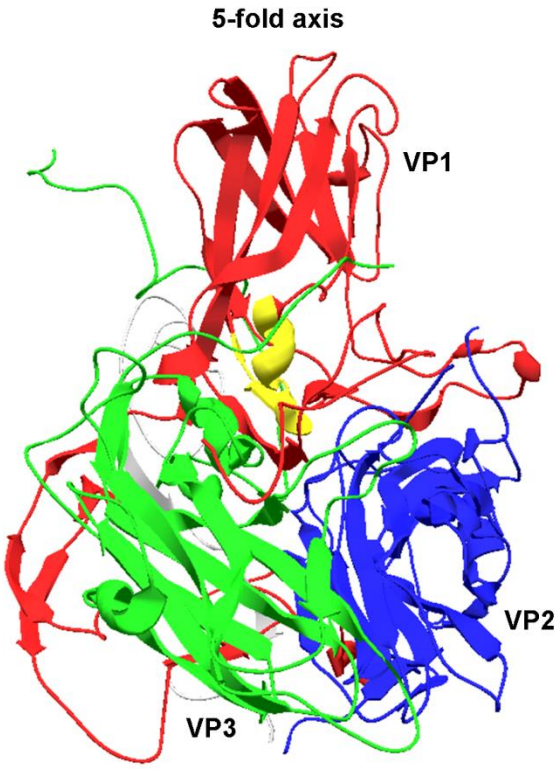

Figure 4.15: Proposed location of the SP40 peptide based on the recently determined EV-A71 crystal structure (PDB accession number 4AED). The molecular structures of EV-A71 VP1, VP2, VP3, and VP4 are represented by red, blue, green and grey, respectively. The SP40 peptide sequence is indicated in yellow.

4.3 Enterovirus A71 uses cell surface heparan sulfate glycosaminoglycan as an attachment receptor

The previous section describes the discovery of an antiviral peptide, SP40 peptide, which exhibited significant antiviral activity against EV-A71 infection. Alanine scanning analysis revealed that the positively-charged amino acids were critical for the antiviral activity. This implies that SP40 peptide may interact with a highly negatively-charged attachment factor present on the cell surface, and block viral attachment. Interestingly, SP40 peptide also carries a heparan sulfate mimetic-binding domain (-RRK-). These findings led to the postulation that EV-A71 may utilize highly negatively-charged cell surface heparan sulfate as an attachment receptor. The following sub-sections provide evidence to support this hypothesis.

4.3.1 Inhibitory effects of heparin, dextran sulfate, chondroitin sulfate and suramin against enterovirus A71 infection

To characterize whether cell surface GAGs play a significant role in viral receptor interaction, various concentrations of heparin and chondroitin sulfate were pre-incubated with EV-A71 at a MOI of 0.1 for 1 hour at 37˚C before infection of RD cells. The viral titers were quantified 24 hours post-infection using quantitative TaqMan real-time PCR and plaque assay. Of the two GAGs evaluated, significant inhibition of EV-A71 by heparin and chondroitin sulfate was observed only at concentrations higher than 500 μg/ml (Figure 4.16A). The inhibitory effect of heparin was most significant at 79.4 ± 2.9% compared to chondroitin sulfate (38.5 ± 6.4%) when tested at a concentration of 1000 μg/ml ($P < 0.05$). A similar inhibitory trend was observed in the plaque assay (Table 4.2).

To further investigate the significance of the carbohydrate backbone on the inhibition of EV-A71, polyanions dextran sulfate (2.3 sulfate groups/glucosyl group) and

polysulfonate suramin (6.0 sulfate groups/molecule) were used. Previous studies have shown that suramin inhibits viruses such as DENV and HBV virus which bind to cell surface heparan sulfate (Chen *et al.*, 1997; Schulze *et al.*, 2007). Viral inhibition increased with concentration of the tested inhibitors, and at 1000 μg/ml the inhibition was 65.8 ± 6.7% for dextran sulfate and 63.4 ± 6.1% for suramin (Table 4.2). However, suramin was more effective as it was able to inhibit EV-A71 infection at a concentration as low as 20 μg/ml (Figure 4.16A). Inhibition of EV-A71 infection by the suramin analog NF449 was previously demonstrated by Arita *et al.* (2008b).

Pre-incubation of RD cells with heparin and dextran sulfate at concentrations from 100-1000 μg/ml before viral infection had no inhibitory effect, but enhanced the virus infectivity. The results demonstrated that the inhibitory effect was due to direct interaction of these compounds with the virus and not to the target cells (Figure 4.16A and 4.16B).

4.3.2 Inhibitory effects of anti-heparan sulfate peptide and poly-D-lysine peptide against enterovirus A71 infection

To assess the important role of negative charges carried on the cell surface in the binding of EV-A71, RD cells were pre-incubated with poly-D-lysine to neutralize cell surface negative charges before EV-A71 infection at a MOI of 0.1. As shown in Figure 4.16C, poly-D-lysine strongly decreased EV-A71 infection in a dose-dependent manner when applied from 1 to 5 μg/ml. At 5 μg/ml, the inhibition was significant, with viral RNA inhibition of 99.1 ± 0.2%. Concentrations higher than 5 mg/ml were found to be cytotoxic to RD cells. To ascertain whether the negative charge carried by heparan sulfate present on the cell surface plays a significant role in viral attachment, two anti-heparan sulfate peptides identified by Tiwari *et al.* (2011), G1 (LRSRTKIIRIRH) and G2 (MPRRRRIRRRQK) were evaluated for their inhibitory effects. The inhibitory

effect of G2 was significant with viral RNA inhibition of 76.5 ± 26.8% at 1000 µg/ml. The G1 peptide did not inhibit EV-A71 infection (Figure 4.16C). These data confirmed that EV-A71 binds to cell surface heparan sulfate.

4.3.3 Inhibitory effect of heparin against enterovirus A71 clinical isolates

Heparan sulfate binding phenotype is often acquired through tissue culture adaptation as previously observed in Sindbis virus and FMDV (Jackson *et al.,* 1996; Klimstra *et al.*, 1998). To verify that the heparan sulfate binding phenotype of EV-A71 is not a result of tissue culture adaptation, the inhibitory effects of heparin against various laboratory EV-A71 strains (BrCr, 41, UH1/97 and SHA66/97) and low passage clinical EV-A71 isolates from the Diagnostic Virology Laboratory, University Malaya Medical Center (EV-A71 strains 14716, 35017, 1657640 and 1687413) was evaluated. Heparin at 2500 µg/ml was observed to have an inhibitory effect on both laboratory strains and low passage EV-A71 isolates (Figure 4.17). The inhibitory effects varied between strains. The inhibition of the laboratory strains ranged from 61.4-98.0%, while inhibition of the low passage isolates ranged from 30.4-78.4%. Interestingly, heparin failed to inhibit the PV vaccine strain even when tested at 2500 µg/ml, implying that PV does not use heparan sulfate as attachment receptor. The data suggested that the heparan sulfate-binding phenotypes were not likely acquired through tissue culture adaptation.

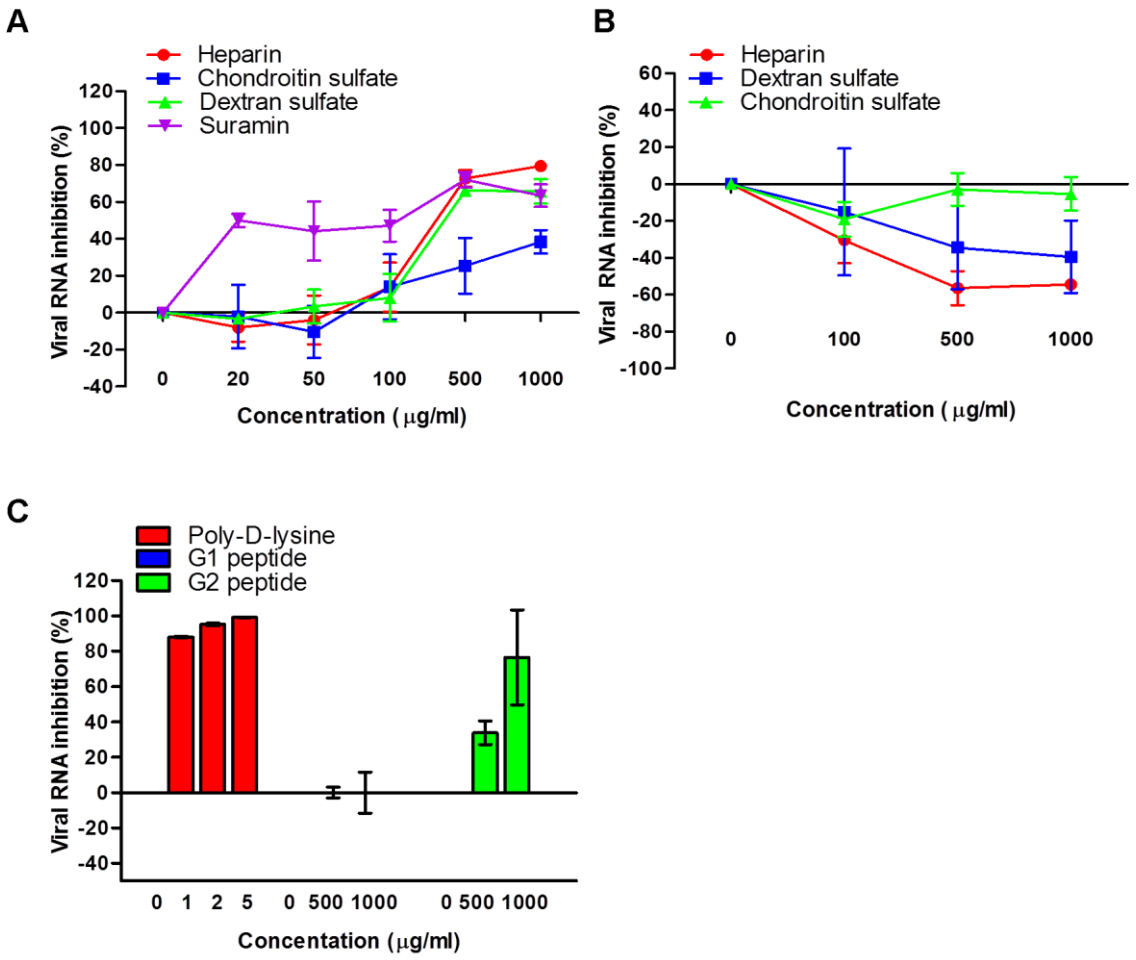

Figure 4.16: Inhibitory effects of GAGs and inhibitors. For the viral inactivation assay, various concentrations of (A) GAGs, polyanionic dextran sulfate and suramin were pre-incubated with EV-A71 for 1 hour at 37℃ before infection of RD cells at room temperature. For the cell protection assay, various concentrations of (B) GAGs, (C) poly-D-lysine and anti-heparan sulfate peptides, designated as G1 and G2 peptides, were pre-incubated with RD cells for 1 hour at 37℃ before EV-A71 infection. The viral RNA was extracted and quantified by TaqMan real-time PCR 24 hours post-infection. The data were obtained from at least two biological replicates and the error bars indicate the standard deviation of the mean.

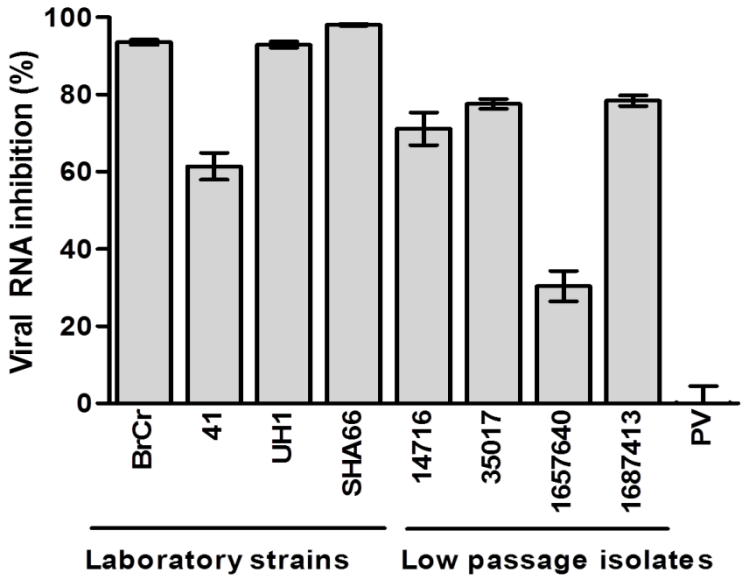

Figure 4.17: Inhibitory effect of heparin against EV-A71 isolates and the PV vaccine strain. EV-A71 and PV viral particles were pre-treated with heparin at a final concentration of 2500 μg/ml for 1 hour at 37℃ before RD cell infections. The low passage EV-A71 isolates (14716, 35017, 1657640 and 1687413) and the PV vaccine strain were obtained from the Diagnostic Virology Laboratory, University Malaya Medical Center. The viral titers of EV-A71 and the PV vaccine strain were quantified 24 hours post-infection by TaqMan real-time PCR and plaque assays, respectively. The data were obtained from at least two biological replicates and the error bars indicate the standard deviation of the mean.

Table 4.2: Effect of GAGs, GAG variants and inhibitors tested on EV-A71 infection

Inhibitors [a]	Inhibition (%)	
	Viral plaque reduction	Viral RNA reduction
Heparin	95.5 ± 0.7	79.4 ± 2.9
Chondroitin sulfate	52.4 ± 16.4	38.4 ± 6.4
De-N-sulfated heparin	70.0 ± 1.1	39.7 ± 15.6
Dextran sulfate	95.2 ± 0.7	65.8 ± 6.7
Suramin	76.3 ± 2.4	63.4 ± 6.1

[a] The concentration of inhibitors used was 1000 μg/ml.

4.3.4 Characterization of the residues critical for the inhibitory properties

To establish if the degree of sulfation of heparin is critical for viral inhibition, different sulfated heparin variants were investigated. N-acetyl-de-O-sulfated heparin, which is completely de-sulfated (0 sulfate group/disaccharide), failed to abolish EV-A71 infection (Figure 4.18A). In contrast, de-N-sulfated heparin (0.8-1.2 sulfate group/disaccharide) showed moderate inhibition (39.7 ± 15.6%) and the wild-type heparin (2.4 sulfate group/disaccharide) exhibited the most significant inhibition (79.4 ± 2.9%) at 1000 μg/ml, indicating that the degree of sulfation within the GAG carbohydrate structure is functionally important. Inhibition of viral plaque formation by these GAGs and inhibitors are shown in Table 4.2.

To further confirm the role of sulfation of heparan sulfate in EV-A71 attachment, EV-A71 infection of RD cells grown in medium containing 0-50 mM of sodium chlorate was carried out. Sodium chlorate inhibits cellular adenosine triphosphate sulfurylase, which reduces sulfation of heparan sulfate by up to 60% (Giroglou *et al.*, 2001; Guibinga *et al.*, 2002). As shown in Figure 4.18B, RD cells treated overnight with sodium chlorate had significantly reduced EV-A71 infection in a dose-dependent manner in all the EV-A71 strains tested. Sodium chlorate inhibited EV-A71 strains 41, UH1, SHA66 and BrCr infections at 50 mM with viral RNA inhibition of 92.7 ± 2.7%, 79.0 ± 3.3%, 83.2 ± 4.2%, and 61.5 ± 5.5%, respectively. To rule out the possibility that the reduction of EV-A71 was due to the cytotoxicity of sodium chlorate, cytotoxicity of sodium chlorate was evaluated by the commercially available MTT assay. Sodium chlorate showed no toxicity at 10 mM and 30 mM, and minimal cytotoxicity at 50 mM (data not shown).

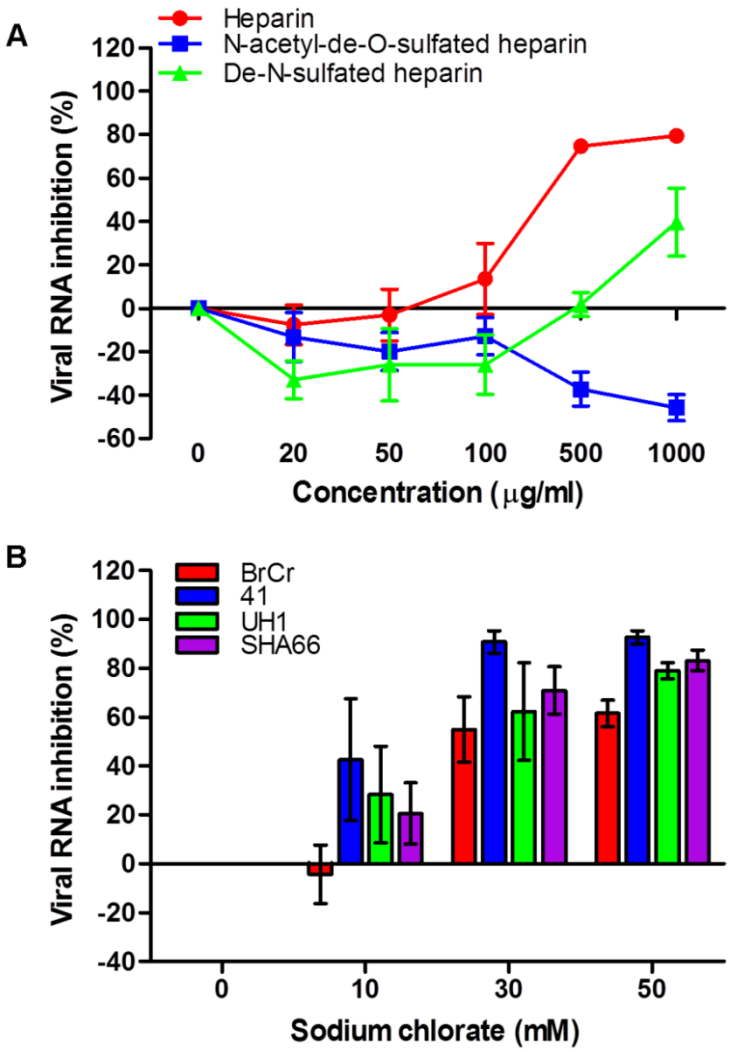

Figure 4.18: Identification of residues critical for the inhibitory effect. (A) EV-A71 was pre-incubated with various concentrations of heparin and heparin variants for 1 hour at 37 ℃ before infection of RD cells. N-acetyl-de-O-sulfated heparin is completely desulfated, and de-N-sulfated heparin is partially desulfated compared to heparin. (B) Inhibitory effect of sodium chlorate on RD cells against different EV-A71 strains. RD cells were pre-treated with increasing concentrations (0 mM, 10 mM, 30 mM and 50 mM) of sodium chlorate for 24 hours before EV-A71 (strains BrCr, 41, UH1 and SHA66) infection at a MOI of 0.1. Data presented are obtained from at least two biological replicates. Error bars indicate standard deviation of the mean.

4.3.5 Removal of cell surface heparan sulfate using enzymatic treatment

To identify the type of GAG which is responsible for EV-A71 binding to RD cells, the binding of EV-A71 to cells after enzymatic removal of cell surface GAGs with chondroitinase ABC and heparinase I/II/III digestion was examined. Heparinase I degrades heparin and highly sulfated domains in heparan sulfate (relative activity about 3:1) at the linkages between hexosamines and O-sulfated iduronic acids. Heparinase II cleaves heparan sulfate, and to a lesser extent heparin (relative activity about 2:1) at the 1-4 linkages between hexosamines and uronic acid residues. Heparinase III specifically degrades heparan sulfate (Ernst *et al.*, 1995; Chen *et al.*, 1997). Treatment of RD cells with each of the heparinases at 2.5 mIU/ml and 5.0 mIU/ml for 1 hour at 37˚C was found to significantly reduce the viral RNA (Figure 4.19A) 24 hours post-infection in a dose-dependent manner. Treatment of RD cells with heparinase I, II and III at 5.0 mIU/ml significantly inhibited EV-A71 viral RNA by 68.6 ± 6.2%, 91.7 ± 4.1% and 82.2 ± 11.7%, respectively (Figure 4.19A). Removal of cell surface chondroitin sulfate by chondroitinase ABC failed to inhibit EV-A71 infection (Figure 4.19A), even when tested at concentrations as high as 20 mIU/ml (data not shown). Removal of cell surface heparan sulfate significantly reduced the infectivity of the different EV-A71 strains tested, but not the PV vaccine strain (Figure 4.19B). Removal of surface heparan sulfate, but not chondroitin sulfate, significantly reduces EV-A71 attachment to the surface of RD cells (Figure 4.19C).

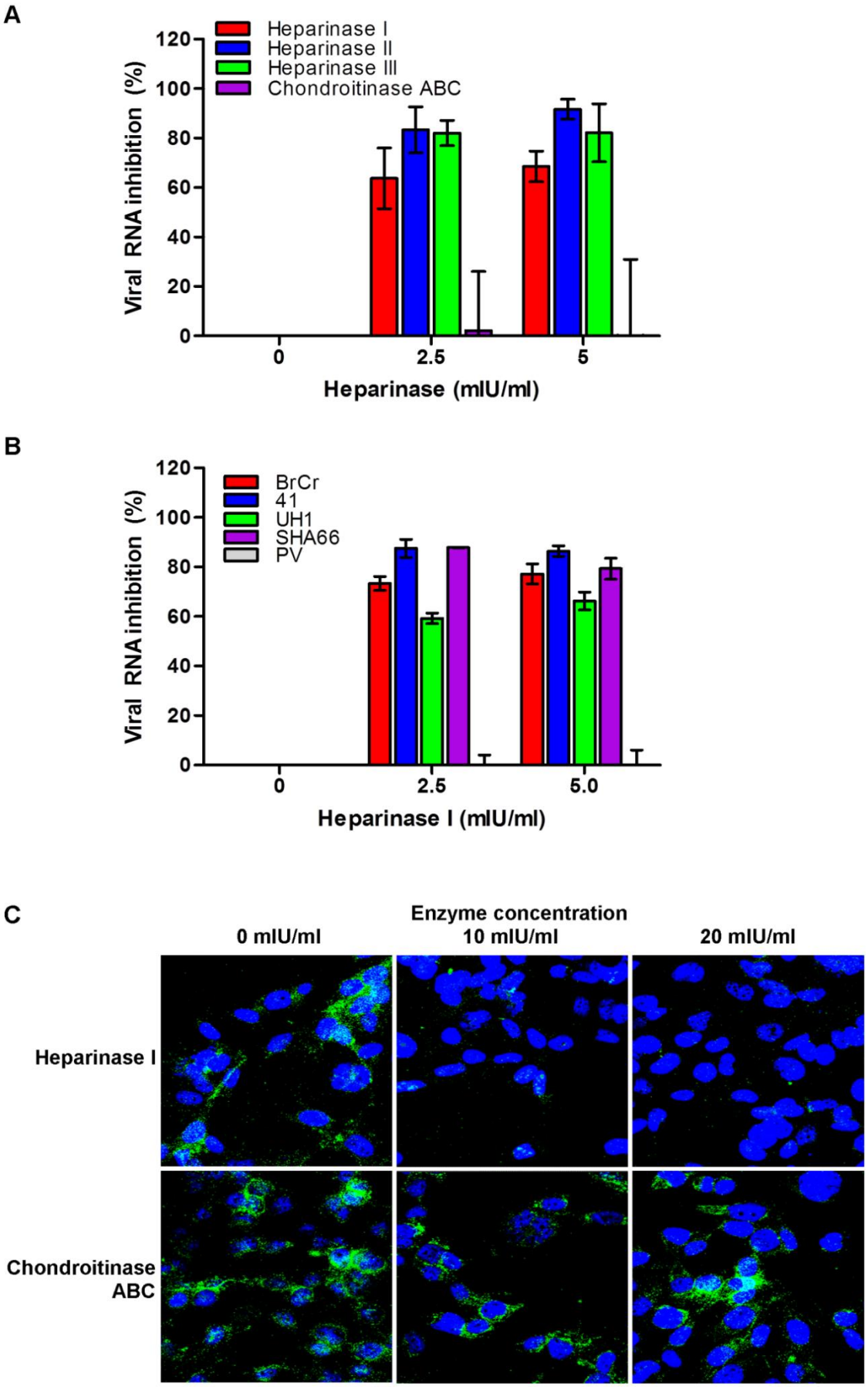

Figure 4.19, continued

Figure 4.19: Effect of heparinases and chondroitinase ABC treatment on EV-A71 infection. (A) Inhibitory effect of heparinase I, II, III and chondroitinase ABC on EV-A71 infection. RD cells were pre-treated with heparinases or chondroitinase ABC for 1 hour at 37˚C before EV-A71 infection at a MOI of 0.1. The viral RNA was extracted and evaluated by TaqMan real-time PCR. (B) Inhibitory effect of heparinase I against different EV-A71 strains and PV vaccine strain. PV vaccine strain was used as a control virus. (C) Confocal microscopy analysis (40X magnification) of EV-A71 binding assay after heparinase I and chondroitinase ABC treatments. EV-A71 viral particles were stained with monoclonal anti-EV-A71 antibody and subsequently stained with Alexa Fluor 488 anti-mouse IgG. Nuclei were stained with DAPI. EV-A71 viral particles and nuclei are shown in green and blue, respectively.

4.3.6 Knockdown of heparan sulfate biosynthesis expression using small interference RNA

To further confirm that heparan sulfate plays an important role in EV-A71 infection, expression of the NDST-1 and EXT-1 genes were transiently knocked down using siRNA. NDST-1 is a heparan sulfate modification enzyme which removes N-acetyl groups from the selected N-acetylglucosamine (GlcNAc) residues and replaces them with sulfate groups (Presto *et al.*, 2008). EXT-1 is a heparan sulfate polymerase that adds alternating units of glucuronic acid (GlcA) and GlcNAc to the non-reducing end of the chain. RD cells were transfected with various concentrations of NDST-1 and EXT-1 siRNAs for 24 hours using Lipofectamine 2000 reagent before infection with EV-A71 at a MOI of 0.1. As shown in Figure 4.20, transient knockdown of both NDST-1 and EXT-1 expression in RD cells significantly reduced EV-A71 infection with inhibition up to 80.1 ± 7.7% and 57.2 ± 19.1% at 20 nM, respectively. However, the scrambled negative control siRNA did not reduce EV-A71 infection.

4.3.7 Binding of enterovirus A71 to Chinese hamster ovary (CHO) cells that are variably deficient in glycosaminoglycan biosynthesis

CHO cells with defects in the biosynthesis of GAGs have been extensively used to demonstrate the involvement of heparan sulfate as the receptor for binding of various viruses (Summerford and Samulski, 1998; Goodfellow *et al.*, 2001; Guibinga *et al.*, 2002; Vlasak *et al.*, 2005; Schulze *et al.*, 2007). The mutant CHO-pgsD677 cells are deficient in N-acetylglucosaminyltransferase and glucuronosyltransferase activities required for heparan sulfate polymerization, and thus completely lack heparan sulfate. These cells also produce three- to four-fold higher levels of chondroitin sulfate when compared to the wild-type CHO-K1 cells (Lidholt *et al.*, 1992). The mutant CHO-pgsA745 cells are deficient in the enzyme UDP-D-xylose:serine-1,3-D-

xylosyltransferase, which catalyses the first sugar transfer reaction in GAG formation, and thus completely lack GAGs (Esko *et al.*, 1985).

To investigate whether EV-A71 binds differently in these cell lines, cells were seeded in CellCarrier-96 and chamber slides, and infected with EV-A71 at an MOI of 100 for 1 hour at 4℃. As shown in Figure 4.21, significantly lower numbers of viral particles were attached to the CHO-pgsD677 and CHO-pgsA745 cells when compared to the wild-type CHO-K1 which expressed normal levels of heparan sulfate (P <0.001). Results from Cellomics HCS VTI array scaning demonstrated that CHO-pgsD677 and CHO-pgsA745 cells showed reduced binding of 46.7% and 41.6%, respectively when compared to CHO-K1 cells. Interestingly, more viral particles were bound to RD when compared to CHO-K1 cells. This could result from the different levels of heparan sulfate expression or the sulfation phenotypes in RD and CHO-K1 cells.

4.3.8 Binding of enterovirus A71 to immobilized heparin sepharose beads

To characterize the interaction of EV-A71 particles to GAGs, virus-containing supernatant was applied to a heparin affinity chromatography column under normal physiological salt conditions (0.14 M NaCl) and eluted with 2M NaCl. The virus in each fraction collected was quantified by TaqMan real-time PCR and plaque assay for EV-A71 and PV, respectively. As depicted in Figure 4.22A, most of the EV-A71 viral particles were detected in all the eluates following application of 2M NaCl. The EV-A71 viral particles present in eluate 1 were concentrated by up to 4.1-fold. In a control experiment, a column packed with sepharose alone showed no binding of EV-A71 viral particles to the column (Figure 4.22B). The results confirm that the EV-A71 particles bind to heparin and were eluted by high salt concentrations. In contrast to EV-A71, the PV vaccine strain did not interact with heparin sepharose and most of the PV viral particles were detected in the flow-through fraction (Figure 4.22A). This result

confirmed that EV-A71 binds to cell surface heparan sulfate, and PV does not.

4.3.9 Enterovirus A71 three-dimensional structuring and prediction of heparan sulfate binding domains

To determine the possible heparan sulfate binding site(s) on the EV-A71 viral particles, the three-dimensional crystal structure of EV-A71 was built using DeepView Swiss PDB viewer (Guex and Peitsch, 1997). As shown in Figure 4.23A, amino acids Arg166, Lys242 and Lys244 are arranged symmetrically in the 5-fold axis of the EV-A71 pentamer structure. These amino acids are also located at positions which are highly exposed on the surface of the EV-A71 viral particle (Figure 4.23B). All these amino acids were highly conserved across all EV-A71 genotypes with the exception of Lys244, where lysine (K) was substituted with glutamic acid (E) in genotype A (Figure 4.23C). These symmetrically arranged clusters of positively-charged amino acids could serve as the major binding site for heparan sulfate.

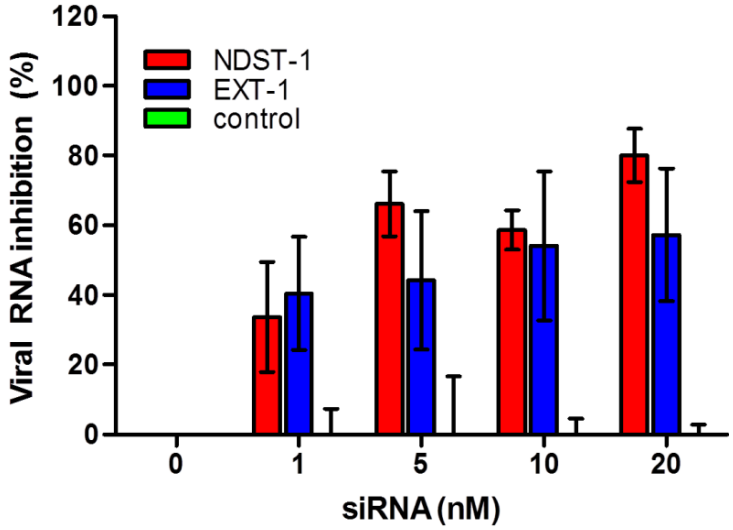

Figure 4.20: Effect of transient siRNA knockdown of NDST-1 and EXT-1 expression on EV-A71 infection. The NDST-1 and EXT-1 siRNA in lipofectamine 2000 reagent was transfected into RD cells for 24 hours before EV-A71 infection. The viral load was determined 24 hours post-infection by TaqMan real-time PCR. An siRNA with a nonsense sequence was used as a control. The data presented are means obtained from at least two biological replicates. Error bars indicate standard deviation of the mean.

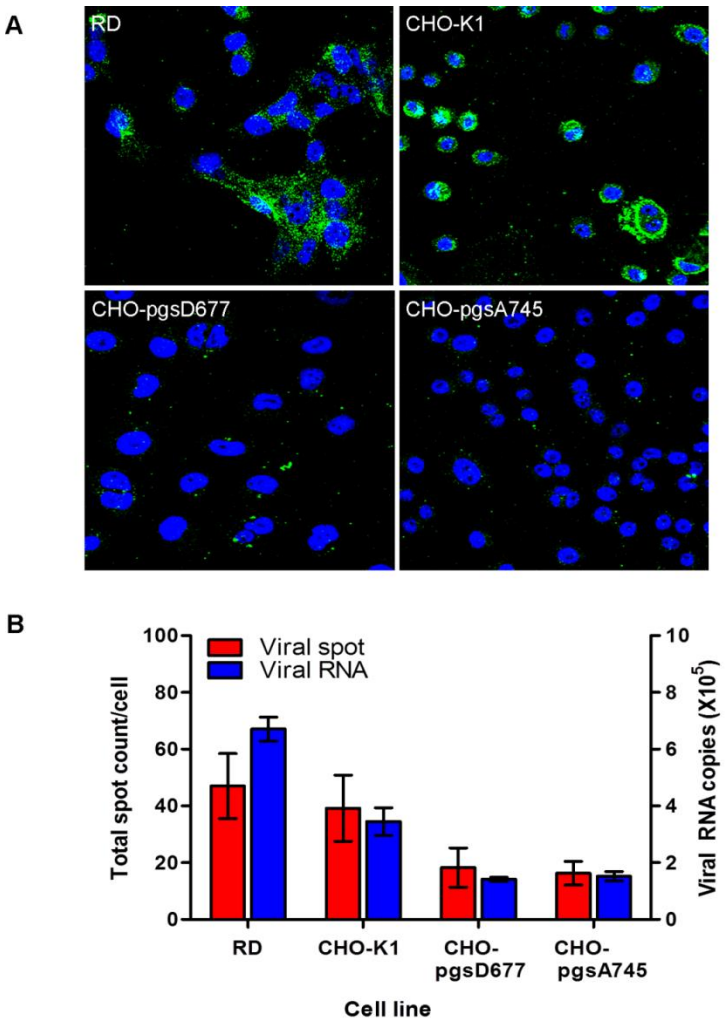

Figure 4.21: Binding of EV-A71 to CHO-K1 and CHO mutant cells. CHO-K1 cells and CHO mutants defective in proteoglycan synthesis were assessed for their ability to bind to EV-A71. Cell line CHO-pgsA745 lacks heparan sulfate and chondroitin sulfate proteoglycans, while CHO-pgsD677 lacks heparan sulfate proteoglycan but produces 15% of normal proteoglycans. Binding of EV-A71 to parental and mutant CHO cells was assayed using (A) confocal microscopic analysis (40X magnification) and (B) Cellomics HCS ArrayScan VTI SpotDetector BioApplication and verified by TaqMan real-time PCR. EV-A71 viral particles and nuclei are shown in green and blue, respectively. The data presented are means obtained from at least two biological replicates. Error bars indicate standard deviation of the mean.

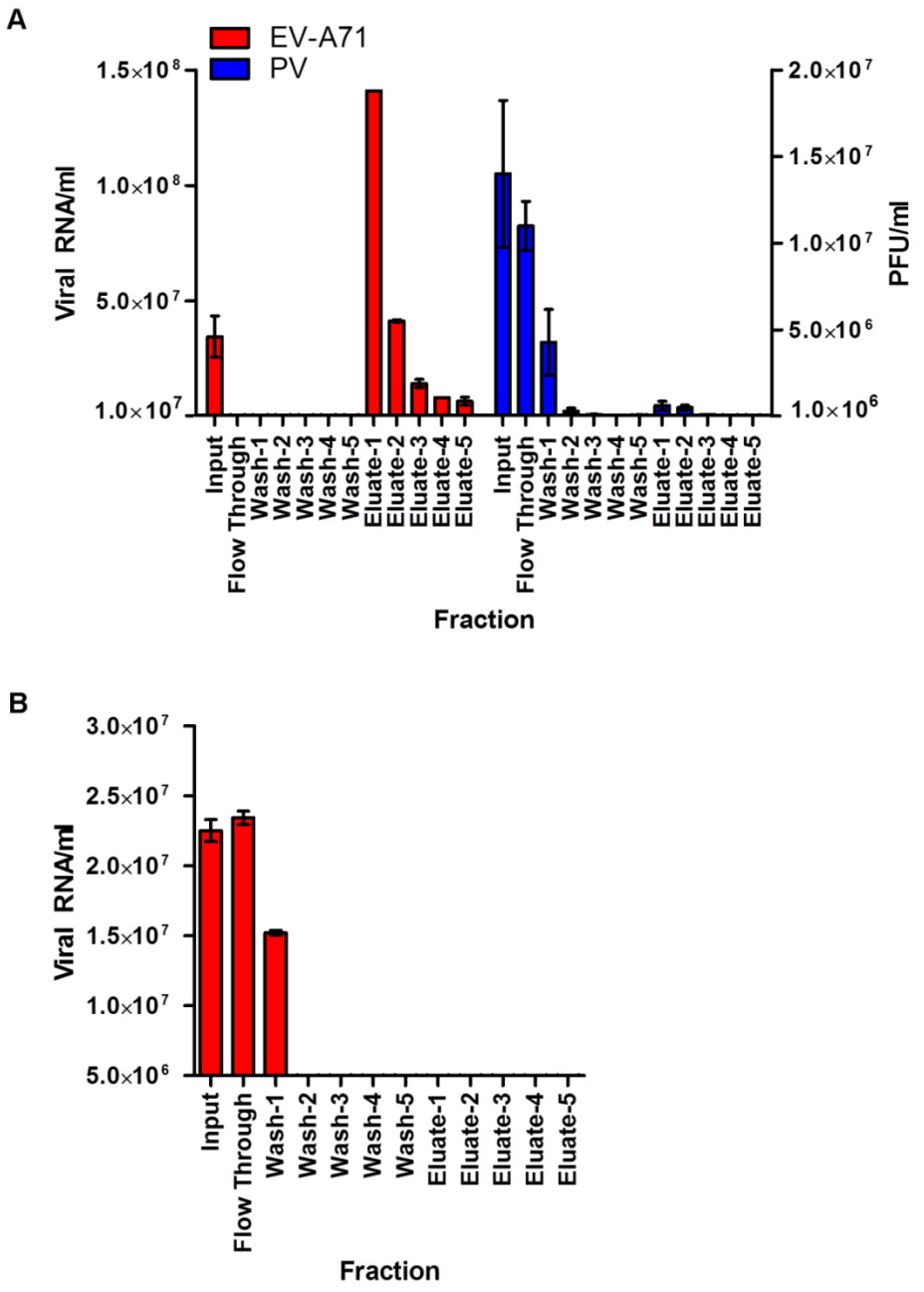

Figure 4.22: Binding of EV-A71 and PV to immobilized heparin-sepharose column. (A) EV-A71 and PV supernatants were passed through a column of immobilized heparin-sepharose and eluted with 2M NaCl. The viral titers of EV-A71 and PV vaccine strain from each fraction were quantified by TaqMan real-time PCR and plaque assay, respectively. EV-A71 is presented as viral RNA/ml and the PV vaccine strain was presented as PFU/ml. (B) Binding of EV-A71 to the sepharose beads. Error bars represent means ± SD of each fraction.

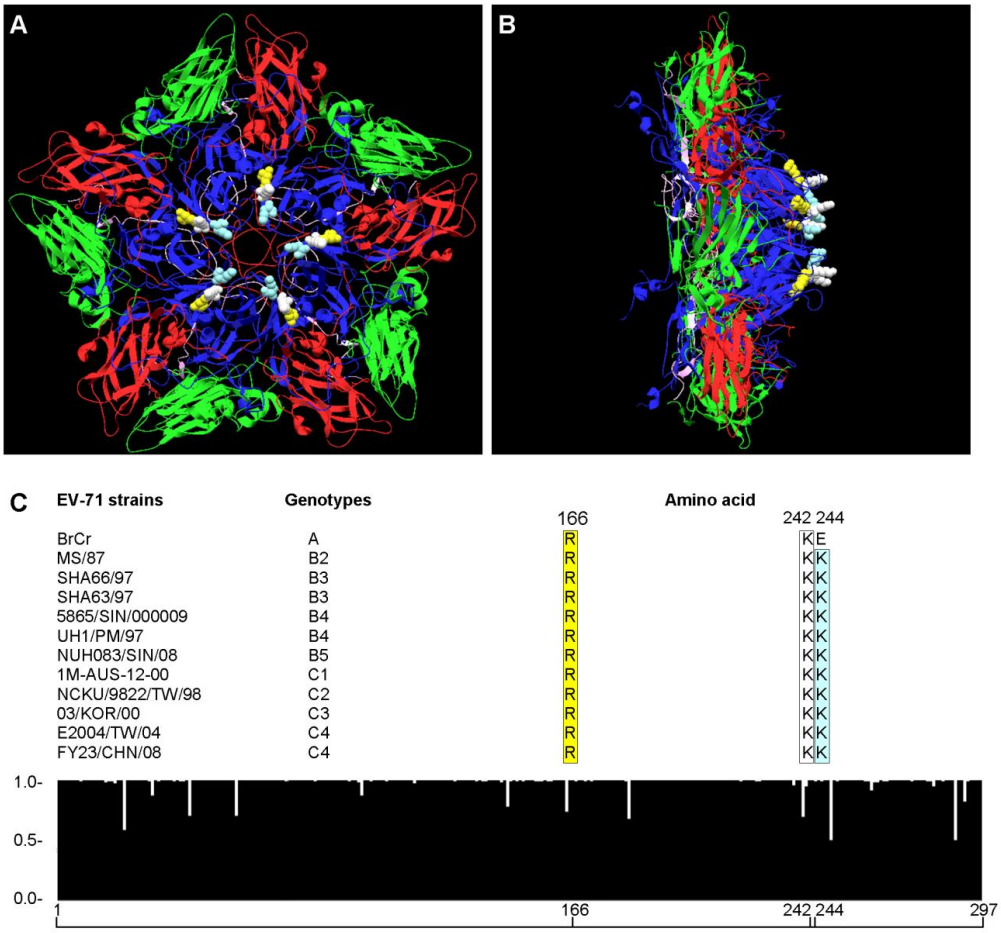

Figure 4.23: Three-dimensional pentameric structure and sequence alignment of EV-A71. The structure of the EV-A71 pentamer was generated using DeepView Swiss PDB viewer. The molecular structure of EV-A71 VP1, VP2, VP3 and VP4 is represented by blue, green, red and purple, respectively. The amino acids Arg166, Lys242 and Lys244 are indicated in yellow, white and light blue, respectively. (A) Top view and (B) side view of the EV-A71 pentamer. (C) Histogram showing sequence consensus in the VP1 region of EV-A71. A total of 174 sequences were aligned and analyzed using ClustalW2. The arbitrary scale is depicted to the left of the histogram and 1.0 denotes perfect consensus at a given amino acid site across all entries. The alignment of Arg166, Lys242 and Lys244 of representative EV-A71 strains from genotypes A, B and C are shown above the histogram.

4.3.10 Enterovirus A71 receptors analysis

Multiple receptors have been discovered for EV-A71 infection, which include human SCARB2, PSGL-1, sialic acid, annexin II and vimentin (Nishimura *et al.*, 2009; Yamayoshi *et al.*, 2009; Yang *et al.*, 2009; Yang *et al.*, 2011; Du *et al.*, 2014). In this study, the sequential events of the SCARB2 and heparan sulfate usage were investigated. RD cells in a chamber slide were incubated with EV-A71 viral particles at an MOI of 100 at 4℃ for an hour. The cells were either immediately fixed or shifted to 37℃ for 15 minutes before being fixed with 4% formaldehyde. The cells were then stained with anti-EV-A71 monoclonal antibodies and either anti-heparan sulfate monoclonal antibodies or anti-SCARB2 monoclonal antibodies. The nuclei were visualized by DAPI stain. At 4℃, most of the virus particles were co-localized with the heparan sulfate receptor (Figure 4.24A). However, when the temperature was shifted to 37℃ for 15 minutes, most of the virus particles were now co-localized with SCARB2 receptor (Figure 4.24B). These results indicated that cell surface heparan sulfate serves as an attachment receptor and virus entry required further interactions with the SCARB2 entry receptor.

Cell surface sialic acid and heparan sulfate were removed using neuraminidase V and heparinase I/III blend, respectively, leading to the reduction of EV-A71 infection (Figure 4.25). Interestingly, the inhibition of EV-A71 infection was higher when cell surface heparan sulfate was removed, suggesting that heparan sulfate is more important compared to sialic acid. When both cell surface sialic acid and heparan sulfate were removed, a greater reduction of EV-A71 infection was observed. This data suggests that EV-A71 selectively binds to cell surface heparan sulfate and sialic acid, and heparan sulfate is functionally more important than sialic acid.

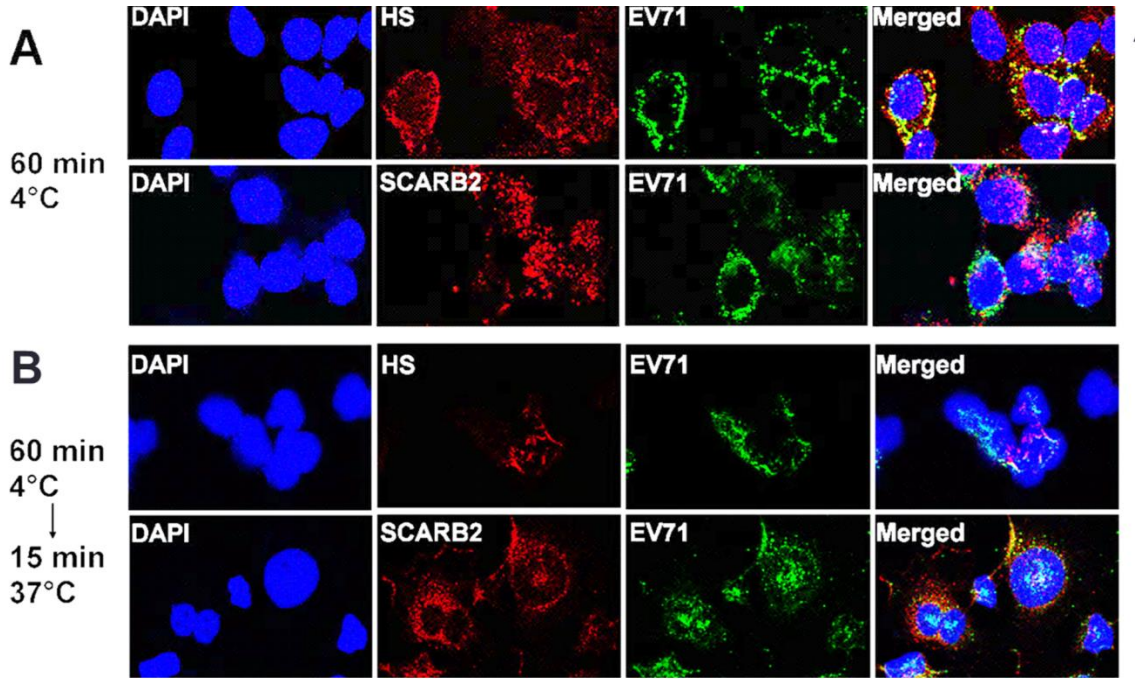

Figure 4.24: Colocalization analyses of EV-A71 receptor interactions. Confocal microscopy analysis (40X magnification) of EV-A71 binding to the RD cells was performed at the (A) attachment stage and (B) entry stage. EV-A71 was allowed to attach to the cell surface at 4℃ for an hour, and viral entry was stimulated at 37℃. EV-A71 viral particles, heparan sulfate and SCARB2 were bound to their respective monoclonal antibodies and stained with the appropriate Alexa Fluor-conjugated IgG antibodies. Nuclei were stained with DAPI. EV-A71 viral particles and nuclei are stained green and blue, respectively. Both heparan sulfate and SCARB2 are stained red. Co-localization is indicated in yellow.

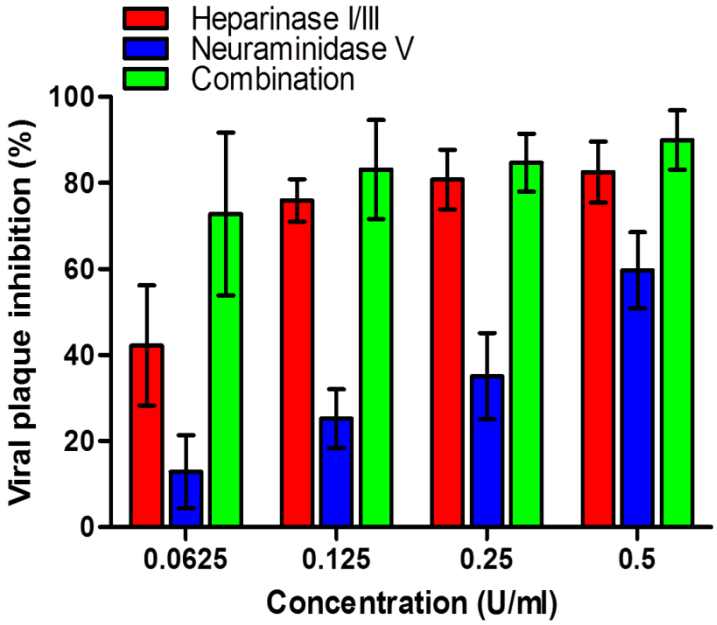

Figure 4.25: Effect of heparinase I/III and neuraminidase V treatment on EV-A71 infection. RD cells were pre-treated with heparinase I/III, neuraminidase V or both for 1 hour before infection of EV-A71 at a MOI of 0.1. The virus titers were determined 24 hours post-infection by plaque assay. The data presented are means of two biological replicates. Error bars indicate standard deviation of mean.

4.4 Inhibition of enterovirus A71 infections by octaguanidinium-conjugated morpholino oligomers

The absence of effective antiviral agents remains a major challenge in treatment of viral infection. The previous section describes the use of SP40 peptide as a receptor antagonist to inhibit EV-A71 infection. Other compounds including suramin and dextran sulfate which serve as molecular decoys also block EV-A71 infection. This study also further characterizes the use of antisense-mediated morpholino oligomers as translation inhibitors. Since the efficacy of the antisense-mediated agent is limited by poor uptake by cells, this study used a morpholino oligomer conjugated with a cell-penetrating molecule, octaguanidinium (Figure 4.26A), as an anti-EV-A71 agent.

4.4.1 Design of octaguanidinium-conjugated morpholino oligomers (vivo-MOs)

Three antisense vivo-MOs were designed to pair with complementary sequences in the IRES regions of the 5' UTR and RdRP gene of EV-A71 positive-sense RNA (Figure 4.26B and Table 4.3). Since EV-A71 translation is highly dependent on the IRES structure, two vivo-MOs (vivo-MO-1 and vivo-MO-2) were designed to target the IRES domains V-IV of 522-577, which are highly conserved across all EV-A71 genotypes. PPMOs targeting these regions were previously shown to be effective against other picornaviruses including PV and CV-B3 (Yuan *et al.*, 2006; Stone *et al.*, 2008). This IRES region was also previously found to interact with important translational factors (Lin *et al.*, 2009b; Huang *et al.*, 2011; Shih *et al.*, 2011), and hence these vivo-MOs were likely to interfere with these interactions. The vivo-MO-3 targeting EV-A71 RdRP was designed according to the siRNA which was previously shown to be effective against EV-A71 infection *in vitro* and *in vivo* (Tan *et al.*, 2007b). A vivo-MO with a nonsense sequence with no homology to any EV-A71 genome was used as a control.

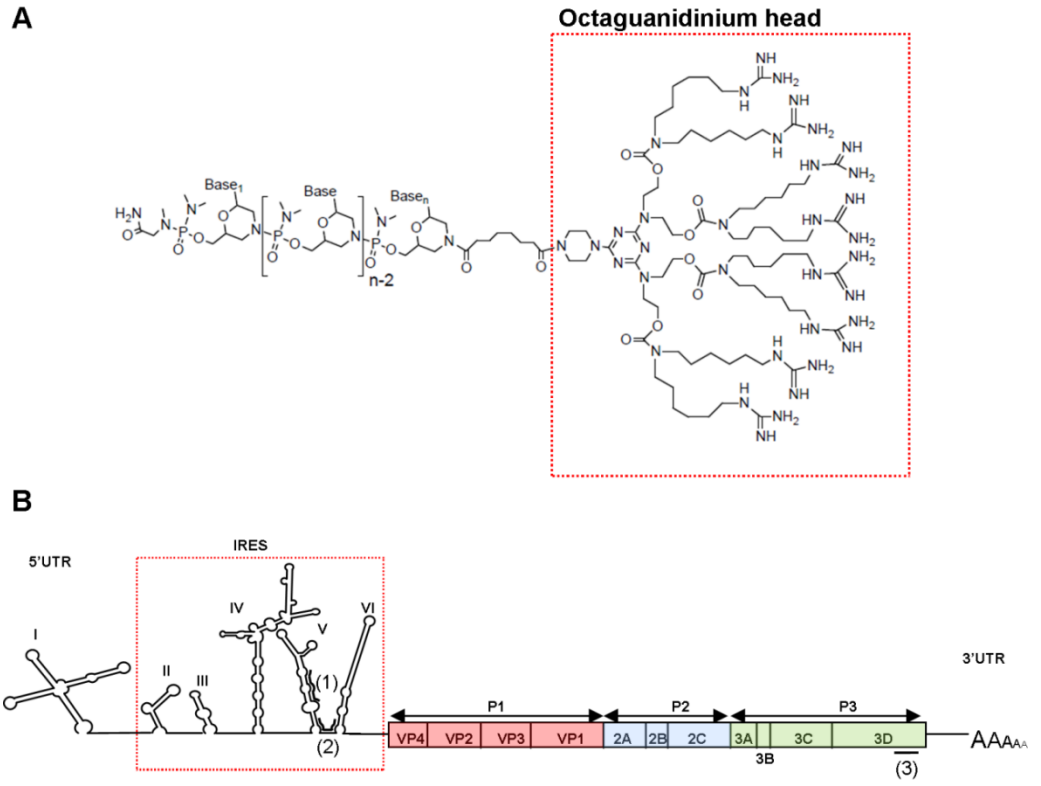

Strains	Genotypes	(1) GTGTGTCGTAATGGGCAACTCTG	(2) ACTACTTTGGGTGTCCGTGTTTC	(3) GAAGAAATTGGCTCGAATTGTTT
BrCr	A	**********C**********	**********	**********G**A***
MS/87	B2	**********	**********	*G**********
SHA66/97	B3	**********C**********	**********	**C*C**********C*A**C
SHA63/97	B3	**********C**********	**********	**C*C**********C*A**C
5865/SIN/000009	B4	**********	**********	**********
UH1/PM/97	B4	**********	**********	**********
NUH083/SIN/08	B5	**********	**********	**********A***
1M-AUS-12-00	C1	**********C**********	**********	**********T**********
SHA52/97	C2	**********	**********	**********
03-KOR-00	C3	**********C**********	**********	**********A***
FY23/CHN/08	C4	**********C***T*******	**********	**C*C**********G**A***
CV-A16	-	*C*C**********T*******	**********	**********G**A***
Poliovirus	-	*CC********C*C*******C*	**********	ACC*CCG******T**C*CA***

Figure 4.26: Schematic illustrations of vivo-MO and the EV-A71 genomic structure. (A) vivo-MO is an antisense structural type in which each subunit consists of a purine or pyrimidine base attached to a morpholino ring with a unique covalently-linked delivery moiety comprised of an octaguanidinium dendrimer (Moulton and Jiang, 2009). (B) Three genomic vivo-MOs target sequences (5' to 3'), labeled (1), (2) and (3), are indicated within the proposed secondary structures of the IRES region and RdRP of EV-A71 RNA (upper part). The sequences of these three targeted regions were aligned across all EV-A71 genotypes, CV-A16 and PV (bottom part). Mismatched nucleotides are shown in red.

Table 4.3: The 23-mers vivo-MOs sequences and target locations in EV-A71 RNA

Vivo-MO	**Sequence (5'- 3')**	**Target location in EV-A71 RNA (nucleotide position)**
Vivo-MO-1	CAGAGTTGCCCATTACGACACAC	IRES core (512-534)
Vivo-MO-2	GAAACACGGACACCCAAAGTAGT	IRES core (546-568)
Vivo-MO-3	AAACAATTCGAGCCAATTTCTTC	RdRP (7303-7325)
Vivo-MO-C	CCTACTCCATCGTTCAGCTCTGA	-

4.4.2 Inhibitory effects of vivo-MOs against enterovirus A71 infection

To evaluate the effects of vivo-MOs on EV-A71 infectivity in RD cells, RD cells were treated with vivo-MOs an hour after infection. As shown in Figure 4.27, both vivo-MOs targeting the EV-A71 IRES stem-loop region exhibited significant antiviral activity against EV-A71 infection with reduction of virus-induced CPE (Figure 4.27A), viral plaque formation (Figure 4.27B), RNA (Figure 4.27C) and protein expression (Figure 4.27D) in a dose-dependent manner. Vivo-MO-1 and vivo-MO-2 significantly reduced EV-A71 plaque formation by up to 2.7 and 3.5 $\log_{10}$ PFU/ml at 10 μM, respectively. Significant inhibition was observed at concentrations higher than 1 μM. The IC_{50} values of vivo-MO-1 and vivo-MO-2 reported in this study were 1.5 μM and 1.2 μM, respectively. However, vivo-MO-3 exhibited less inhibitory effect against EV-A71 infection in RD cells with a plaque reduction of only 1.2 $\log_{10}$ PFU/ml.

Besides RD cells, vivo-MOs also inhibited EV-A71 in neuroepithelial SK-N-MC cells, but with reduced activity when compared to RD cells. This confirms that the antiviral effects are not cell-specific.

4.4.3 Cytotoxicity analysis of vivo-MOs in tissue culture

To measure the effects of vivo-MOs on cell viability, non-infected RD cells were treated with various concentrations of vivo-MOs for 24 hours in maintenance medium. None of the three vivo-MOs caused more than 20% reduction of cell viability at concentrations less than 5 μM as measured by the MTS assay. Overall, vivo-MOs concentrations up to 5 μM showed minimal cytotoxicity to cells (Figure 4.28).

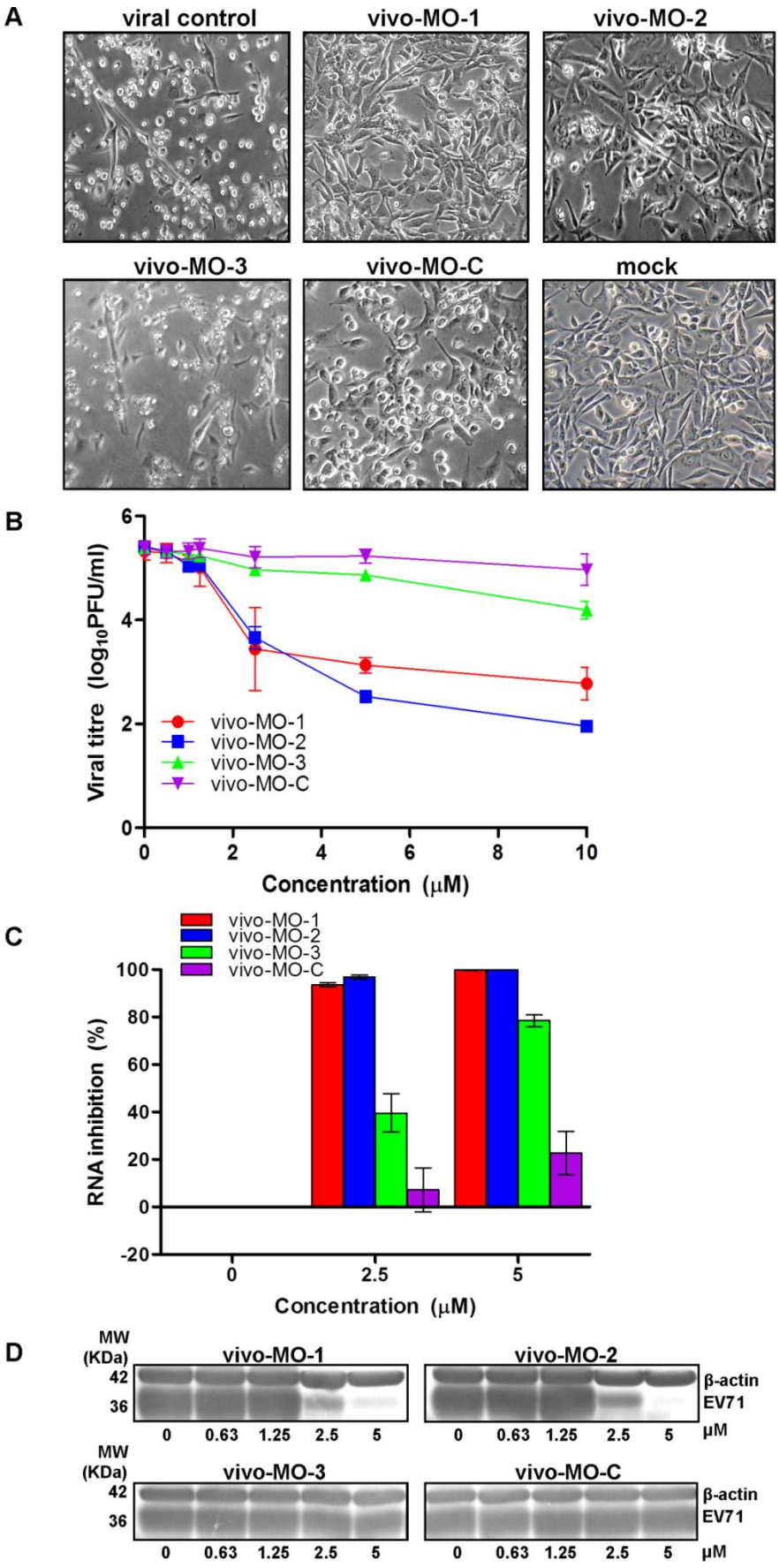

Figure 4.27, continued

Figure 4.27: Inhibitory effects of vivo-MOs in RD cells. Various concentrations of vivo-MOs were applied to RD cells after 1 hour post-infection and (A) virus-induced CPE (20 × magnification) was observed 24 hours post-infection. CPE was seen as round and shrunken cells, which eventually dislodged from the surface. The total infectious particles or total viral proteins were harvested 24 hours post-infection and evaluated by (B) plaque assay, (C) TaqMan real-time PCR and (D) western blot analysis. EV-A71 viral capsid protein was detected by mouse anti-EV-A71 monoclonal antibody and cellular β-actin was detected using mouse anti-β-actin monoclonal antibody. Vivo-MO-C is the negative control with nonsense sequence.

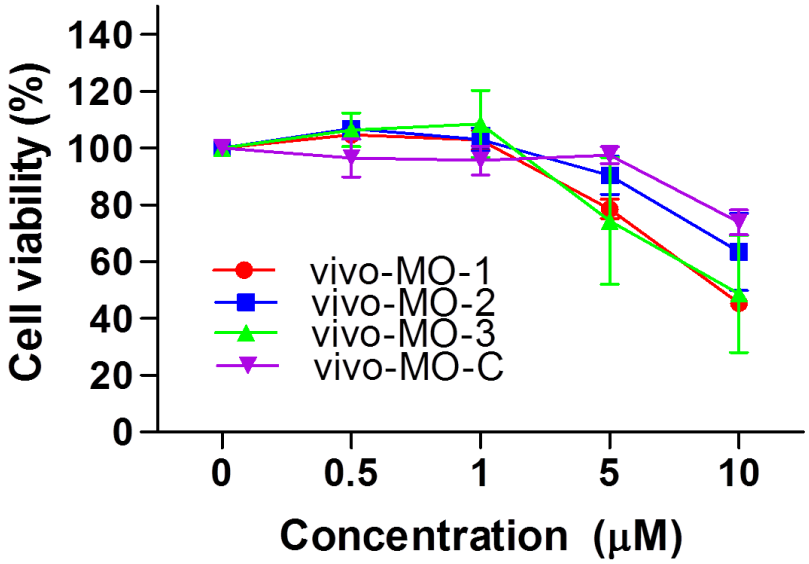

Figure 4.28: Cell viability analysis of vivo-MOs. Various concentrations of vivo-MOs were incubated with RD cells for 24 hours in maintenance medium followed by MTS assay. The absorbance reading at 490 nm was obtained. The percentage of cell viability (%) was determined by dividing the absorbance readings obtained from vivo-MO-treated over non-treated cells. The data presented are means of two biological replicates. Error bars indicate the standard deviation of mean.

4.4.4 Time of addition analysis

To further characterize the efficacy of vivo-MOs at multiple time points relative to EV-A71 infection, vivo-MOs were applied for 4 hours before, or at 0, 1, 2, 4, or 6 hours after EV-A71 infection. Both vivo-MO-1 and vivo-MO-2 remained effective when administered before or after EV-A71 infection. When vivo-MOs and EV-A71 were added together into the RD cells for 1 hour, the inhibitory effect was reduced, which could have resulted from the incomplete uptake of the vivo-MOs by the cells. However, the efficacies of vivo-MO-1 and vivo-MO-2 were reduced when treatments were delayed. Nonetheless, the antiviral effects were retained with 92.8% plaque inhibition, for both vivo-MO-1 and vivo-MO-2 even when administered 6 hours post-infection. Vivo-MO-3 had no observable inhibitory effects on EV-A71 infection when administered 4 hours before infection and 2, 4, or 6 hours after EV-A71 infection (Figure 4.29).

4.4.5 Inhibitory effects of vivo-MOs against other enteroviruses

Next, the ability of the vivo-MOs to inhibit different EV-A71 strains and other picornaviruses were investigated. Each of the vivo-MOs was tested at a final concentration of 5 μM against two other EV-A71 strains (BrCr and UH1/97), PV, CV-A16 and CHIKV as the control virus. The vivo-MO-2 which targets the highly conserved region of the IRES stem-loop structure exhibited significant inhibitory activity against EV-A71 strains BrCr and UH1/97, PV and CV-A16 with viral plaque reduction ranging from 1.8 - 3.1 $\log_{10}$ PFU/ml (Figure 4.30). However, vivo-MO-1 only exhibited antiviral activities against EV-A71 strains BrCr and UH1/97, and CV-A16, but not against PV (Figure 4.30). EV-A71 strain BrCr which has a single nucleotide mismatch in the middle of the vivo-MO-1 targeted site (Figure 4.26B) remained sensitive to the vivo-MO-1 treatment. The efficacy of vivo-MO-1 against CV-A16 (0.95

log_{10}PFU/ml reduction) was significantly lower when compared to EV-A71 (1.86 log_{10}PFU/ml reduction). This could be due to CV-A16 having three nucleotide mismatches with the vivo-MO-1. PV with five nucleotide mismatches was completely resistant to the inhibitory effect of vivo-MO-1. The vivo-MO-C, which has no homologous sequence to the EV-A71 genome, was not inhibitory at all against all EV-A71 strains tested. All the vivo-MOs did not show any inhibition of CHIKV infection. Thus, the antiviral activities of vivo-MOs were sequence-specific.

4.4.6 Mechanism of action analysis of vivo-MOs

To investigate the mechanism of action of the antiviral vivo-MOs, cell-free translation analysis was used. In cell-free analysis, 1 μg of infectious RNA was *in vitro* translated either in the presence or absence of 10 μM of vivo-MOs. The presence of either vivo-MO-1 or vivo-MO-2 significantly blocked the *in vitro* translation of EV-A71 viral capsid proteins when compared to the control without vivo-MOs (Figure 4.31A). Vivo-MO-3 exhibited reduced efficacies as compared to IRES-targeting vivo-MOs (Figure 4.31A). In the EGFP reporter translation inhibition assay, the presence of vivo-MO-1 or vivo-MO-2 greatly reduced EGFP expression in RD cells 6 hours post-infection with EV-A71_EGFP (Figure 4.31B).

4.4.7 Isolation and characterization of vivo-MO-resistant mutants

Enteroviruses may escape antiviral effects through mutations (Shih *et al.*, 2004b, de Palma *et al.*, 2009). To determine whether EV-A71 could become resistant to vivo-MO treatments, EV-A71 was serially passaged in the presence of increasing concentrations of either vivo-MO-1 or vivo-MO-2. Interestingly, only EV-A71 mutants resistant to vivo-MO-1 were isolated after eight passages. EV-A71 mutants that were resistant to vivo-MO-2 could not be isolated, suggesting that the region targeted by vivo-MO-2 is critical for EV-A71 translation initiation.

4.4.8 Characterization of degree of tolerance of vivo-MO mismatches against enterovirus A71 infection

To investigate the determinant(s) of resistance, viral RNA was isolated from the resistant population and the 5' UTR was sequenced. A single point mutation from T to C at position 533 was sufficient to confer resistance to vivo-MO-1 (Figure 4.32A). To characterize the loss of inhibitory activity by vivo-MO-1, EV-A71 mutants carrying various mismatches at the vivo-MO-1 target site were constructed (Table 4.4), and the inhibitory effects of vivo-MO-1 against each of the mutants were evaluated. The mismatched RNA target sequences were designed to reflect the most likely natural variations that would arise in the EV-A71 sequence. As shown in Figure 4.32B, the EV-A71 MO-1-mutant-1, which carried a single point mutation at position 533 (T to C substitution), required higher vivo-MO-1 concentrations to achieve a similar inhibitory effect when compared to the wild type. The EV-A71 MO-1-mutant-2 with a single point mutation in the middle of the targeted sequence (a T to C substitution at position 523) remained sensitive to vivo-MO-1, but vivo-MO-1 had reduced inhibitory efficacy when compared with the wild type. Increasing the number of mutations on the targeted sequence significantly reduced the inhibitory efficacy of vivo-MO-1. The viral plaque inhibition at 2 μM of vivo-MO-1 against EV-A71 MO-1-WT was 98.9% ± 0.1, and reduced to 89.6% ± 3.4 for the MO-1-mutant-1 that carried a point mutation at the 3' end of the target sequence. The viral plaque inhibition by vivo-MO-1 reduced to 78.0% when the number of nucleotide mismatches increased to three.

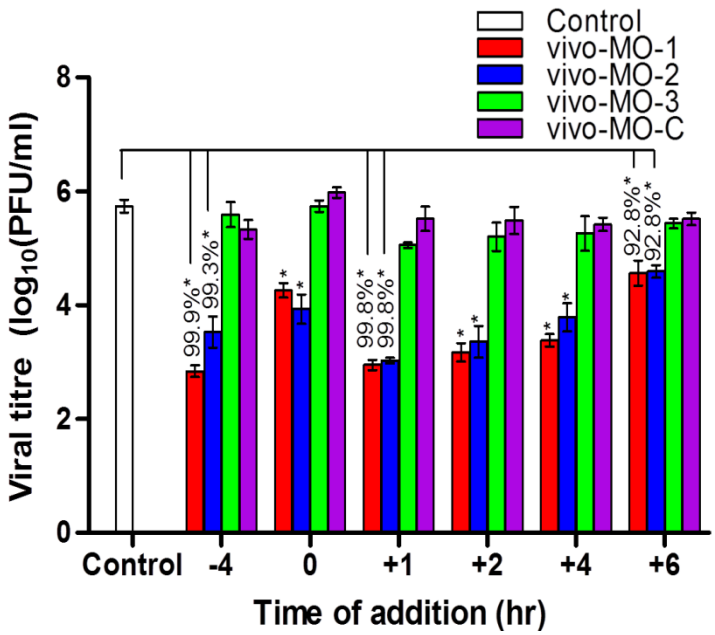

Figure 4.29: The effect of time of addition on the antiviral properties of vivo-MOs. Vivo-MOs at the final concentration of 5 μM were applied to RD cells at 4 hours before or 0, 1, 2, 4, 6 hours after EV-A71 infection at MOI of 0.1. The data presented were obtained from at least two independent biological replicates. Error bars indicate standard deviation of the mean. Percentage of inhibition at the time points -4, +1, and +6 are shown above the respective bars. Asterisks indicate statistically significant differences compared to the control, with $p < 0.05$.

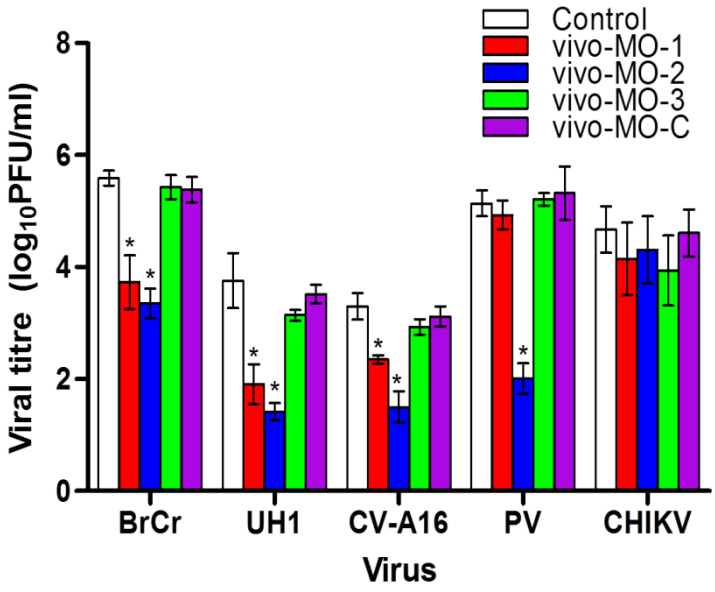

Figure 4.30: The antiviral activities of vivo-MOs against multiple enteroviruses. RD cells were pre-treated with each of the vivo-MOs at a final concentration of 5 μM for 4 hours at 37 ℃ before infection with various enteroviruses (EV-A71 strains BrCr and UH1/97, PV and CV-A16) and CHIKV at MOI of 0.1. The inhibitory effects of each of the vivo-MOs were evaluated by plaque assay 24 hours post-infection. The data presented were obtained from at least two independent biological replicates. Error bars indicate standard deviation of the mean. Asterisks indicate statistically significant differences compared to the control, with $p < 0.05$.

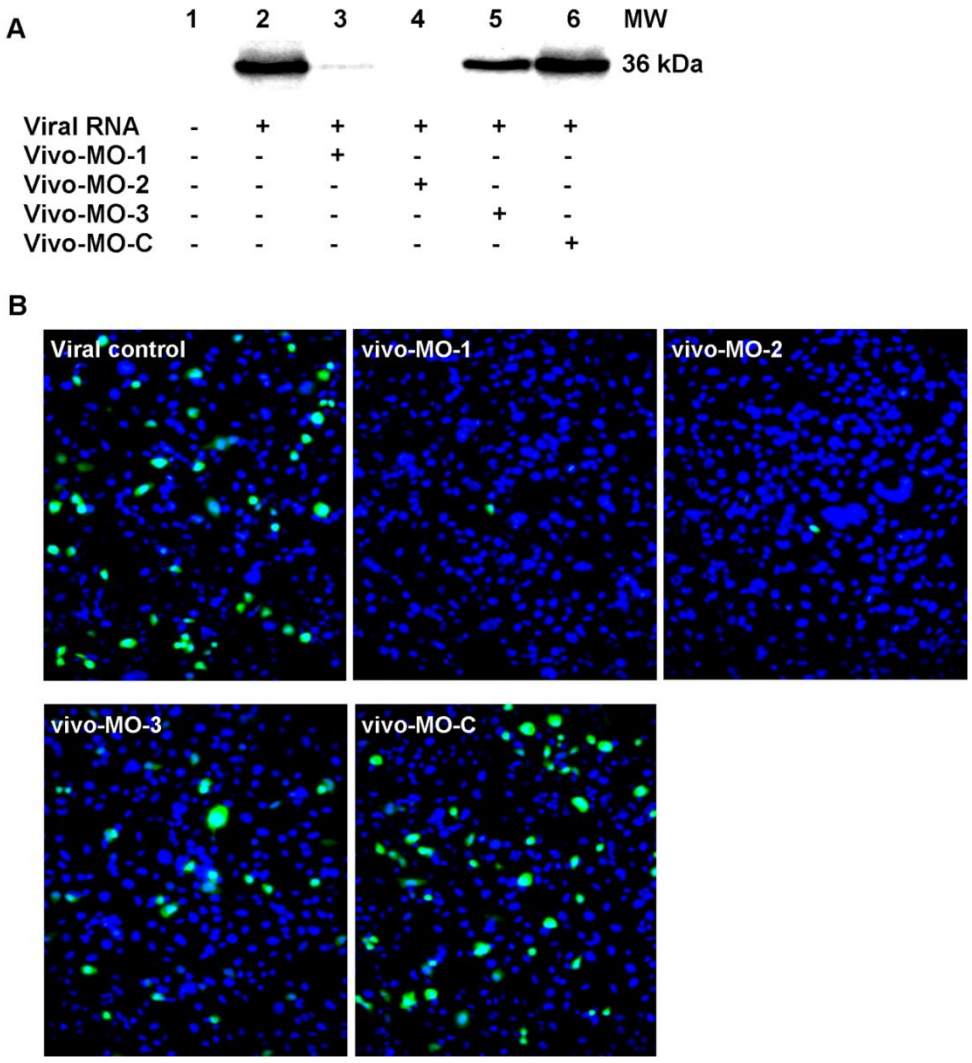

Figure 4.31: Translation inhibition assay. (A) *In vitro* translation was performed with 1 µg of RNA using the 1-Step Human Coupled IVT Kit either in the presence or absence of vivo-MOs at a final concentration of 10 µM. Aliquots of 15 µl of the translated product was subjected to SDS-PAGE and western blot analysis. A 36 KDa band indicates expression of EV-A71 capsid protein. (B) EV-A71_EGFP expression assay. RD cells were infected with EV-A71 at a MOI of 1 for an hour at 37 ℃, followed by treatment of vivo-MOs at the final concentration of 2.5 µM. The EGFP signal was detected 6 hours post-infection using a fluorescence microscope. EGFP expression and cell nuclei are presented as green and blue, respectively.

Table 4.4: The vivo-MO-1 sequence (3’ to 5’) and the *in vitro* transcribed infectious RNA with target sequences (5’ to 3’)

Target	**Sequence**	**Mismatch(es)**
Vivo-MO-1	3′-CACACAGCATTACCCGTTGAGAC-5′	-
MO-1-WT	5′-GTGTGTCGTAATGGGCAACTCTG-3′	0
MO-1-mutant-1	5′-**********C*-3′	1
MO-1-mutant-2	5′-**********C**********-3′	1
MO-1-mutant-3	5′-**********C***T*******-3′	2
MO-1-mutant-4	5′-***C*******C***T*******-3′	3

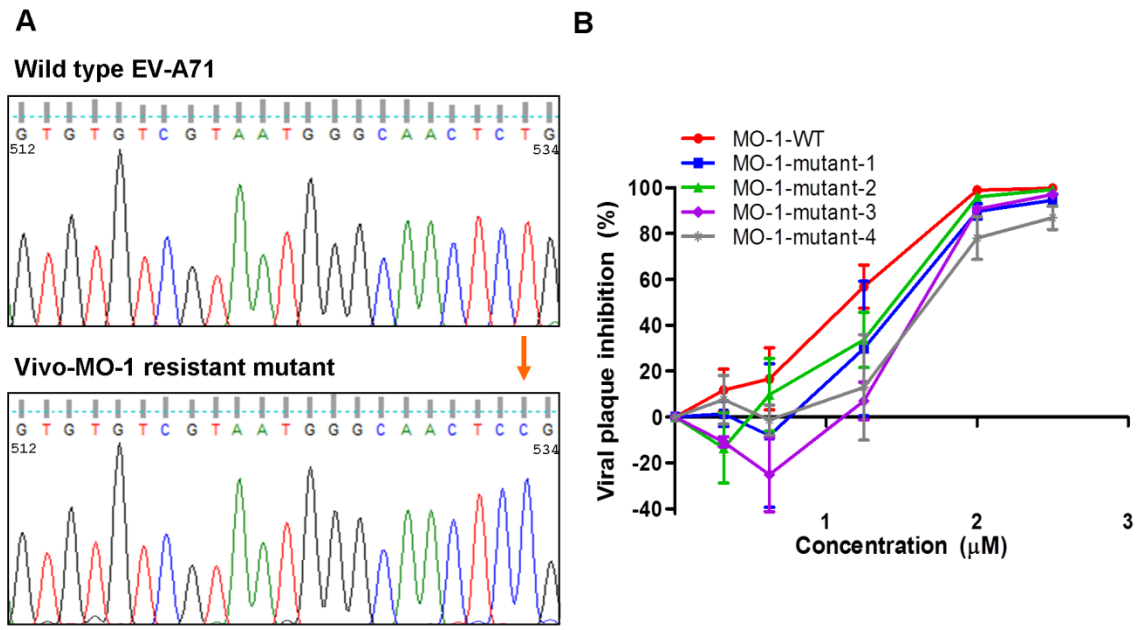

Figure 4.32: Vivo-MO-1 resistant mutant analysis. EV-A71 was serially passaged in the presence of vivo-MO-1 from 1 μM to 5 μM. EV-A71 populations that were resistant to vivo-MO-1 were plaque purified, and subjected to DNA sequencing. (A) The DNA sequences targeted by vivo-MO-1 are shown in the sequencing chromatograms. The arrow indicates the T to C substitution at position 533 of the vivo-MO-1 resistant mutant. (B) The effect of sequence mismatches between vivo-MO-1 and target RNA on the inhibition assay. Several *in vitro* transcribed RNA, each having a different number of nucleotide mismatches in the target region were analyzed. Viral titers were quantitated 24 hours post-infection by plaque assay. The data presented were obtained from at least two independent biological replicates.

CHAPTER 5

DISCUSSION

5.1 Construction of enterovirus A71 infectious cDNA clone

Development of cDNA-derived infectious viruses allows rapid characterization of the molecular biology of a virus (Evans, 1999). This approach is based on the infectious nature of the viral RNA genome in permissive host cells. An infectious cDNA clone of a picornavirus was first demonstrated by Racaniello and Baltimore (1981). Subsequently, infectious cDNA clones of coxsackievirus, hepatitis A virus and other enteroviruses were also constructed (Gow *et al.*, 1996; Tellier *et al.*, 1996a; Tellier *et al.*, 1996b; Martino *et al.*, 1999). In the current study, the full-length infectious cDNA clone of EV-A71 strain 41 was constructed using a long distance RT-PCR technique with high fidelity DNA polymerase. The long distance RT-PCR approach has been implemented to rapidly amplify the full-length cDNA of different enteroviruses (Gow *et al.*, 1996; Leister and Thompson, 1996; Cameron-Wilson *et al.*, 2002). Combination of cDNA fragments into a full-length clone can be technically challenging due to the lack of appropriate restriction enzyme sites. The method could also easily fail due to the combination of cDNA fragments from incompatible quasispecies (Gow *et al.*, 1996). However, a few EV-A71 infectious cDNA clones have been constructed using this approach (Arita *et al.*, 2005; Chua *et al.*, 2008; Phuektes *et al.*, 2011). Construction of EV-A71 infectious cDNA clones using full genome PCR technique have also been previously reported (Han *et al.*, 2010; Yeh *et al.*, 2011). The product was then cloned into the high copy number vector pCR-XL-TOPO and transformed into *E. coli* TOP10. To avoid incorporation of mutations during PCR, iProof high fidelity DNA polymerase was used in this study, which has 52X more fidelity than normal Taq polymerase (4.4×10^{-7} vs 2.28×10^{-5} error rate). Initially, the infectious clone was constructed using

Platinum Taq high fidelity polymerase which has 3X greater fidelity than normal Taq polymerase. However, none of the clones generated were infectious. The loss of infectivity could be a result of generation of lethal mutations during PCR (Yanagi *et al.*, 1997).

The EV-A71 genome was cloned downstream of an SP6 bacteriophage promoter. The SP6 promoter-driven transcription yielded a positive-sense RNA with an additional G residue at the 5' end of EV-A71 RNA. Most enterovirus infectious cDNA clones contain an additional 1, 2 or 3 G residues at the 5' end of the cDNA-derived viral RNA and no alteration of viral infectivity has been reported (Kraus *et al.*, 1995; Martino *et al.*, 1999; Arita *et al.*, 2005). A previous study by Phuektes *et al.* (2011) reported that the infectious EV-A71 strain 6F clone with two G residues at the 5' end was infectious. However, an additional G residue at the 5' end of the *in vitro* transcribed RNA yielded substantially lower rescue viral titers compared to transfection of the purified viral RNA (van der Werf *et al.*, 1986; Boyer and Haenni, 1994).

The length of the poly(A) tail at the 3' end plays a critical role in cDNA-derived enterovirus infectivity and viral RNA replication, allowing poly(A) binding protein interaction and initiation of VPg uridylation (Silvestri *et al.*, 2006). Silvestri *et al.* (2006) demonstrated that increasing the length of poly(A) tail of PV significantly increased PV negative strand RNA synthesis. PV RNA with poly$(A)_{11}$ and poly$(A)_{12}$ had 1-3% of the level of negative-strand RNA synthesis of PV with poly$(A)_{80}$. PV RNA with poly$(A)_{20}$ had a similar level of negative-strand RNA synthesis to poly$(A)_{80}$. Previous studies by Phuektes *et al.* (2011) and Arita *et al.* (2005) demonstrated that EV-A71 infectious cDNA clones with poly$(A)_{25}$ could produce infectious viral particles. The infectious cDNA clone constructed in this study carried poly$(A)_{50}$ which was similar to the EV-A71 infectious cDNA clone constructed by Yeh *et al.* (2011).

The fluorescence protein-based reporting viruses allow high content image-based assays, which allow rapid evaluation of the antiviral activity and cytotoxicity of compounds simultaneously in living cells (Shum *et al.*, 2010). EV-A71 expressing GFP has been constructed previously by Yamayoshi *et al.* (2009) and Shang *et al.* (2013). The EV-A71_EGFP-expressing infectious cDNA clone developed in this study was constructed using the overlapping extension PCR technique, which was simpler than restriction digestion and cloning, and which also allows incorporation of the desired gene into regions lacking suitable restriction digestion sites. With Q5 high fidelity DNA polymerase that has 100X greater fidelity then normal Taq polymerase, incorporation of undesired mutations into the EV-A71 genome during PCR was minimized.

The phenotype of the clone-derived virus was compared with the parental virus. Although transfection of the *in vitro* transcribed RNA produced lower virus yield compared to the purified viral RNA, the rescued EV-A71 had similar plaque morphology and replication kinetics as the parental virus. This could be a result of the restoration of the wild type 5' and 3' ends of the viral genomes after transfection (Eggen *et al.*, 1989; Tacahashi and Uyeda, 1999; Kusov *et al.*, 2005; Liu *et al.*, 2008). The *in vitro* transcribed RNA can be repaired before replication depending on the availability of host enzymes (Kusov *et al.*, 2005). The EGFP-expressing EV-A71 had smaller plaque sizes and lower viral titers compared to the parental virus. Although producing lower titers, the EV-A71_EGFP RNA genome (of 8.2 kb length) remained infectious. A similar observation has been reported by Shang *et al.* (2013). Incorporation of larger foreign genes such as *Renilla* and firefly luciferase (1 kb and 1.6 kb, respectively) in PV infectious cDNA led to low stability and very low viral titers (Song *et al.*, 2012).

In conclusion, full-length infectious cDNA clones of EV-A71 strain 41 (genotype B4) as well as EGFP-expressing EV-A71 were successfully constructed. The availability of such infectious cDNA clones allows study of the pathogenesis of EV-A71 at a

molecular level (Arita *et al.*, 2005; Arita *et al.*, 2008a; Chua *et al.*, 2008; Kung *et al.*, 2010; Yeh *et al.*, 2011; Huang *et al.*, 2012). In the current study, EV-A71 infectious cDNA clones were used to investigate the degree of tolerance of mismatches of vivo-MO-1 towards its targeted sequence within the EV-A71 RNA genome.

5.2 Development of an antiviral peptide against enterovirus A71 infections

EV-A71 infections are not limited to mild HFMD, but in some cases, may lead to severe neurological complications with high mortality rates, and yet treatment remains limited by a lack of effective antivirals (Wu *et al.*, 2010).

Inhibition of viral attachment provides an option for therapeutic intervention. Therapeutic peptides have become an attractive tool in drug discovery due to their active regulatory role in biological systems and their high specificity of recognition. The best characterized therapeutic peptide inhibitor is enfuvirtide, a fusion inhibitor which mimics the N terminal sequence in the HIV fusion protein, gp41 (Kilby *et al.*, 1998). Using peptides offers significant advantages over small chemical molecules or large therapeutic antibodies. Major advantages of peptides are their small size and their high activity and specificity when compared to antibodies. Peptides are better candidates to inhibit protein-protein interactions over a surface area often too large to be inhibited by small chemical molecules. Peptides accumulate in lesser quantities in tissues, and have very low cell toxicity compared to small synthetic molecules (Huther and Dietrich, 2007). Antimicrobial peptides such as lactoferrin, human β-defensin-2 and dermaseptins have been reported to exhibit antiviral properties against various viruses (Gropp *et al.*, 1999; Andersen *et al.*, 2001; Bastian and Schafer, 2001; Belaid *et al.*, 2002; Andersen *et al.*, 2003; Jenssen *et al.*, 2006).

Peptides derived from virus envelope or capsid that play significant roles in surface protein-protein interactions can exert inhibitory activities against viruses like influenza

virus (Jones *et al.*, 2006), HSV-1 (Akkarawongsa *et al.*, 2009; Tiwari *et al.*, 2011), HBV (Kim *et al.*, 2008), HCV (Cheng *et al.*, 2008; Liu *et al.*, 2010), HIV-1 (Kilby *et al.*, 1998), DENV and WNV (Hrobowski *et al.*, 2005). Although the EV-A71 capsid protein VP1 has been reported to be responsible in mediating viral adsorption and the uncoating process, little information is available about the molecular interactions of EV-A71 and cell receptors (Li *et al.*, 2007). Recently, Chen *et al.* (2012) identified several amino acid residues present within position 152-236 in the EV-A71 capsid protein VP1 that were critical for the molecular interaction between EV-A71 and the SCARB2 receptor.

A Pepscan strategy was employed to screen 95-overlapping synthetic peptides corresponding to the VP1 capsid protein for antiviral activity against EV-A71. Four peptides SP40, SP45, SP81 and SP82 were found to exhibit significant antiviral activities. The SP40 peptide was selected for further investigation as the amino acid sequence of SP40 is highly conserved across all EV-A71 genotypes and subgenotypes. The results demonstrated that the SP40 peptide inhibited EV-A71 infection in a dose-dependent manner corresponding to the reduction of viral RNA, viral protein and plaque formation. The IC_{50} values ranged from 6-9.3 μM against all representative strains of EV-A71 genotypes A, B and C. Interestingly, the SP40 peptide also inhibited CV-A16 and PV1 infection *in vitro*, implying that the SP40 peptide could function as a broad-spectrum antiviral agent. However, a higher concentration of SP40 peptide was required to block PV1 infection. This could be due to the high degree of dissimilarity of the amino acid sequences of EV-A71 and PV.

The possible mechanism of action of the SP40 peptide could be either through direct virus inactivation or blocking of viral attachment and entry. This study confirmed that the SP40 peptide was not virucidal, but that it blocked viral attachment to the cell surface and hence prevented EV-A71 infection. Immunofluorescence assay showed the number of viral particles attached to the cell surface was reduced significantly when the

RD cells were pre-treated with the SP40 peptide before addition of virus at 4˚C. This indicated that the SP40 peptide probably first interacted with a cell surface receptor and subsequently prevented EV-A71-cellular receptor interactions. However, the SP40 peptide lost its antiviral activity when the peptide was added 1 hour after EV-A71 infection.

Results also demonstrated the importance of the SP40 amino acid sequence for its antiviral activity. The inhibitory effect of the scrambled peptide SP40X, was significantly lower (42.5%) than the effect observed with the SP40 peptide. The SP40 peptide could prevent viral attachment by interacting with cell receptors present on the surface of RD cells, thereby blocking the availability of receptors for attachment of the EV-A71 viral particles. The observation of a significantly reduced IC_{50} value when RD cells were pre-treated with SP40 before EV-A71 infection strongly supported this view. The cellular receptor that the SP40 peptide interacted with remained unknown. None of the amino acids identified that interact with SCARB2 (Chen *et al.*, 2012) was mapped within the SP40 peptide amino acid sequence. This suggested that the SP40 peptide probably did not interact with the SCARB2 receptor. The SP40 peptide could also inhibit CV-A16 and PV1 infections *in vitro*, indicating that it could interact with a common receptor shared by these viruses.

Since the positively-charged amino acids were critical for antiviral activities, the SP40 peptide could interact with cell surface receptors through electrostatic charge interactions. The antiviral activity of the SP40 peptide was not restricted to a specific cell type, but it could block EV-A71 infection in different cell lines. This indicated that the SP40 peptide was probably interacting with a receptor that was commonly expressed in most cell types. Cell surface GAGs are present ubiquitously on the surface of most animal cells and in the extracellular matrix (Liu and Thorp, 2002). The presence of several arginine residues in SP40 showed similarity to an antiviral peptide against

HSV-1 which bore positively-charged poly-arginine residues, and which was found to interact with heparan sulfate (Tiwari *et al.*, 2011). Sequence analysis of the SP40 peptide revealed that it contained heparan sulfate GAG-specific binding domains (G_1RRRRS_6 and $R_{28}KVR_{31}$) present in bovine and human lactoferrins (Mann *et al.*, 1994; Shimazaki *et al.*, 1998; Jenssen *et al.*, 2006). Several studies have reported that lactoferrin was able to bind to ligands such as heparan sulfate and chondroitin sulfate (van der Strate *et al.*, 2001; Marchetti *et al.*, 2004; Jenssen *et al.*, 2006). It is possible that through this interaction, lactoferrin was able to inhibit EV-A71 infection (Weng *et al.*, 2005). These findings suggest that the SP40 peptide could interact with cell surface GAGs to prevent EV-A71 attachment. The SP40 peptide reported in this study had an even lower IC_{50} value at 15 μg/ml when compared to the IC_{50} value of bovine lactoferrin at 34.5 μg/ml (Weng *et al.*, 2005) or human lactoferrin at 103.3-185.0 μg/ml (Lin *et al.*, 2002; Wu *et al.*, 2010).

Interestingly, the amino acid domains in VP1 that are critical for SCARB2 binding were found in the SP45, SP55, and SP81 peptides. These peptides were able to inhibit EV-A71 infections in a dose-dependent manner with no cytotoxicity to the RD cells. Strong synergistic antiviral activities were observed between the SP40 and the SP81 peptides in RD cells. The additive effects of these two peptides could have significantly reduced the availability of receptors for viral attachment.

Since the SP40 peptide works at a very low micromolar concentrations, is non-cytotoxic to RD cells, and has activity against multiple EV-A71 genotypes, it is potentially an excellent candidate for further development as an antiviral agent. The SP40 peptide was effective when administered before EV-A71 infection and may be of particular use for prophylactic intervention, for example to contacts of a case of neurological EV-A71 disease. The exact cellular receptor(s) that the SP40 peptide interacts with still remains unknown, but it was postulated to interact with cell surface negatively-charged GAGs

such as heparan sulfate. Further *in vivo* studies are needed for development of SP40 as an antiviral agent. Although a major disadvantage of peptides is their low bioavailability due to their rapid degradation in the gastrointestinal system, new formulations, such as the D-isomer peptide and other delivery options are being developed (Huther and Dietrich, 2007).

5.3 Cell surface heparan sulfate as an enterovirus A71 attachment receptor

Virus receptors are one of the determinants of virus host range and tissue tropism (Haywood, 1994). Receptors that are known to bind to EV-A71 have been identified over the past few years. PSGL-1 was the first to be discovered as an EV-A71 receptor. However, PSGL-1 is selectively expressed only in neutrophils, monocytes and most lymphocytes (Nishimura *et al.*, 2009). The second receptor, reported by Yamayoshi *et al.* (2009), was human SCARB2 which is expressed on most types of cells (Yamayoshi *et al.*, 2012). EV-A71 binds to the SCARB2 receptor, and is then internalized through clathrin-mediated endocytosis (Hussain *et al.*, 2011; Lin *et al.*, 2013a). However, blocking of these receptors did not abolish EV-A71 infection and this led to discovery of a third receptor, annexin II. Pre-treatment of host cells with anti-annexin II antibody was found to reduce viral attachment. Pre-incubation of EV-A71 with annexin II also reduced EV-A71 infection (Yang *et al.*, 2011).

Besides these known receptors for EV-A71, Yang *et al.* (2009) reported sialylated glycans as a receptor for EV-A71. Treatment of RD, SK-N-SH and DLD-1 cells with neuraminidase was found to reduce the ability of EV-A71 to bind to the cell surface, confirming that EV-A71 utilizes sialylated glycans as attachment factors (Yang *et al.*, 2009; Su *et al.*, 2012). Recently, vimentin, a type III microfilament, was reported as an EV-A71 attachment receptor. Treatment of EV-A71 with soluble vimentin as molecular decoys or blocking of cell surface with anti-vimentin antibodies reduced EV-A71

binding to the cells (Du *et al*., 2014). Other than these five known receptors, this current study has demonstrated that cell surface heparan sulfate is required for EV-A71 attachment. In this study, EV-A71 infection of RD cells was significantly reduced when EV-A71 viral particles were pre-treated with soluble heparin, dextran sulfate and suramin. However, pre-incubation of RD cells with heparin and dextran sulfate did not inhibit, but unexpectedly enhanced EV-A71 infection. This could be caused by the creation of additional artificial binding sites through accumulation of heparin and dextran sulfate on the surface of cells (Hilgard and Stockert, 2000; Schulze *et al.*, 2007). These findings imply that heparin or dextran sulfate could bind to the positively-charged surface of viral particles, and prevent interaction of viral particles with the cell surface as demonstrated in FMDV (Fry *et al.*, 1999). Removal of cell surface heparan sulfate using each of the heparinases (I, II, III) also reduced the ability of EV-A71 to bind to and infect RD cells which further confirmed the important role of heparan sulfate in EV-A71 infection. The involvement of chondroitin sulfate as a receptor for attachment was excluded as enzymatic removal of chondroitin sulfate did not impair EV-A71 infection.

The present study demonstrated that EV-A71 could bind to CHO cells. However, CHO cells defective in the biosynthesis of heparan sulfate and chondroitin sulfate exhibited a reduced ability to bind to EV-A71, which further supports the role of heparan sulfate in EV-A71 infection. No infection was observed since CHO cells are not susceptible to EV-A71 infection in nature. The inability of EV-A71 to infect CHO cells is likely due to its failure to internalize and initiate infection. In TMEV GDVII, viruses bound to heparan sulfate were postulated to use protein entry receptors for virus internalization (Reddi and Lipton, 2002). A similar mechanism could be utilized by EV-A71. EV-A71 viral particles bound to heparan sulfate may need to interact with known entry receptors such as SCARB2 and PSGL-1, or with an unknown protein entry receptor to gain entry

into the cells. CHO cells of hamster origin may have different SCARB2 since it has been reported that the EV-A71 binding domains in human SCARB2 and murine SCARB2 are different (Chen *et al.,* 2012). Results also showed that EV-A71 was still able to bind to the CHO mutant completely lacking in heparan sulfate and chondroitin sulfate, which further suggests that multiple attachment receptors are involved during EV-A71 infection. This view is similar to what has been reported for several viruses that use heparan sulfate (Delputte *et al.*, 2002; Reddi and Lipton, 2002; Misinzo *et al.*, 2006).

Heparan sulfate is expressed by all cell types. However, they show variations in structure with differences in the degrees of sulfation, modification in chain length and the position of the sulfate group (Shi and Zaia, 2009). The data demonstrated that highly sulfated heparin could inhibit EV-A71 infection whereas decreased sulfation in heparin led to a progressive loss of EV-A71 inhibition. Completely de-sulfated heparin was found to have no inhibitory effect. This suggests that structural variations of heparan sulfate present in different cell types could lead to differences in susceptibility to infection, and may explain the selective tropism of EV-A71 (Jackson *et al.*, 1996).

Heparan sulfate binding could arise from adaptation to the cells in which isolates were propagated. Culture adaptations of heparan sulfate usage in picornaviruses (Sa-Carvalho *et al.*, 1997; Escarmis *et al.*, 1998), flaviviruses (Lee *et al.*, 2004) and alphaviruses (Klimstra *et al.*, 1998) have been demonstrated. *In vitro* cultivation of viruses was shown to rapidly select amino acid substitutions that increase the net positive charge of the envelope protein (Lee and Lobigs, 2002). However, the ability to bind to heparan sulfate was also documented for clinical isolates of porcine circoviruses (Misinzo *et al.*, 2006) and echoviruses (Goodfellow *et al.*, 2001). The present study showed that heparin was able to inhibit clinical isolates of EV-A71 with low passage history, hence the heparan sulfate binding phenotype was not likely due to culture adaptation of EV-A71.

Furthermore, this study has shown that EV-A71 binds to heparin sepharose under physiological salt concentrations, and that the interaction could be disrupted by high salt concentrations. This suggests that EV-A71-heparin interactions involve mainly electrostatic charge interactions. Substitution of a single positively-charged amino acid with another amino acid is sufficient to abolish the heparin-binding phenotype in TMEV GDVII virus and CV-A9 (Reddi and Lipton, 2002; Reddi *et al.*, 2004; McLeish *et al.*, 2012). Thus, positively-charged amino acids present on the surface of viral particles are critical for heparin binding. Sequence analysis of the VP1 capsid protein revealed two possible heparan sulfate mimic binding domains, from residues 120-123 (-RRKV-) and residues 241-244 (-SKSK-). Peptides with these heparan sulfate binding domains exhibited significant antiviral activity against EV-A71 infection in RD cells, suggesting that the inhibitory effect could have resulted from direct binding to heparan sulfate and blocking of viral attachment (Tan *et al.*, 2012). Heparan sulfate-interacting regions could be linear heparan sulfate-binding domains, or are more often formed from clusters of basic residues that are displayed on the three-dimensional crystal structure as shown in FMDV and CV-A9 (Fry *et al.*, 1999; McLeish *et al.*, 2012). With the recent available crystal structure of EV-A71, the electrostatic surface of EV-A71 was determined (Wang *et al.*, 2012b). A few conserved positively-charged amino acids (Arg166, Lys242 and Lys244) were clustered symmetrically at the 5-fold axis of the EV-A71 pentamer. These amino acids were also located on the surface of EV-A71 viral particles. These findings suggests that the interaction could be due to the electrostatic interactions between these clusters of basic amino acids arranged in a three-dimensional array on the virions and concentrated negative charges on the sulfated heparan sulfate chain.

This study demonstrated that EV-A71 viral particles utilized cell surface heparan sulfate as an attachment receptor. Although the exact mechanism of how EV-A71 viral

particles interact with cell surface negatively-charged heparan sulfate remains unclear, determination of the molecular basis of the viral-receptor interaction within target cells will be useful towards understanding the pathogenicity of EV-A71 and development of antiviral agents against EV-A71.

5.4 Development of an antisense-mediated translation inhibitor of enterovirus A71 infections

The use of antisense mechanisms to inhibit pathogen replication has showed promising results. Fomivirsen, used for intravitreal treatment of cytomegalovirus retinitis, is the only antisense agent approved by the FDA to date (de Smet *et al.*, 1999; Perry and Balfour, 1999). Various antisense molecules, mainly siRNA targeting different regions of the EV-A71 RNA genome, have been described (Sim *et al.*, 2005; Tan *et al.*, 2007a; Tan *et al.*, 2007b; Deng *et al.*, 2012; Yang *et al.*, 2012). However, the major limitations of RNA-based antiviral therapeutics are short half-lives in plasma and the need for a delivery reagent which might be cytotoxic to cells (Song *et al.*, 2003; Kole *et al.*, 2012). To overcome these limitations, phosphorodiamidate morpholino oligomers (PMOs), which are highly resistant to nuclease degradation, coupled with a non-peptide cell-penetrating molecule known as octaguanidinium dendrimer was used in this study (Moulton and Jiang, 2009). These have an advantage over peptide-based cell-penetrating molecules, which are susceptible to protease degradation that can impact the effectiveness of PPMOs (Youngblood *et al.*, 2007).

The present study examined the effects of vivo-MOs designed to interfere with the initiation of translation and expression of EV-A71 RdRP in RD cells. Among the three vivo-MOs examined, the two vivo-MOs targeting the EV-A71 IRES stem-loop region exhibited significant antiviral activity. The vivo-MOs blocked EV-A71 viral protein synthesis in a cell-free inhibition assay using HeLa cell extracts, as well as in a cell-

based EV-A71_EGFP inhibition assay. Previous studies have also reported that only PMOs targeting positive strand IRES regions or the AUG start codon sites were effective when compared to the PMOs targeting other regions of the viral RNA (Yuan *et al.*, 2006; Vagnozzi *et al.*, 2007; Stone *et al.*, 2008). The PMO may bind with complementary viral RNA and disrupt the integrity of the IRES stem-loop secondary structures or tertiary structures, hence arresting IRES-dependent translation. These PMOs were likely to block 40S ribosomal subunit binding the viral RNA in the vicinity of stem-loop V in the picornavirus type I IRES. Furthermore, it has been suggested that the IRES stem-loop V-VI of EV-A71 interacts with ITAF such as FBP and hnRNP A1 (Lin *et al.*, 2009b; Lin *et al.*, 2009c; Shih *et al.*, 2011). The mechanism of action of vivo-MOs was likely to be disruption of RNA structure integrity and blocking of the interaction between translational factors and viral RNA. Unlike synthetic double-stranded siRNA or antisense oligonucleotides which involve cleavage of mRNA, PMOs are translation-suppressing oligonucleotides which are not recognized by the RNA-induced silencing complex (RISC) or RNase H and therefore do not lead to RNA degradation (Kole *et al.*, 2012). This could explain why siRNA targeting the same sequence as vivo-MO-3 was effective, not by acting as a translation suppression oligonucleotide, but by down-regulating gene expression via steric hindrance of ribosome access to mRNA (Tan *et al.*, 2007b).

The timing of treatment with vivo-MOs affects their antiviral efficacies. Vivo-MOs retained their antiviral activity when administered either before or shortly after EV-A71 infection. The antiviral properties dropped significantly if the treatment was delayed in a time-dependent manner. These data suggest that delayed treatment may allow viral replication to a level that the vivo-MOs were unable to effectively interfere with viral translation. The cytotoxicity effects of vivo-MOs were observed at concentrations

higher than 5 μM, which could have resulted from the delivery moiety octaguanidinium dendrimer.

Previous studies have shown that many EV-A71 subgenotypes co-circulate during outbreaks in Asia (Chan *et al.*, 2012). The data presented in this study showed that vivo-MO-1 exhibited broad-spectrum antiviral activity against different EV-A71 strains from different subgenotypes, and vivo-MO-2 was found to exhibit broad-spectrum antiviral activities against different enteroviruses, including CV-A16, another common etiological agent of HFMD.

Previous studies have also demonstrated that a single nucleotide mismatch or more were sufficient for PPMO resistance. In this study, an EV-A71 mutant that was resistant to vivo-MO-1 carried a single nucleotide substitution (Vagnozzi *et al.*, 2007; Stone *et al.*, 2008) of T to C at the position 533. This study failed to isolate any EV-A71 resistant to vivo-MO-2 even after eight passages *in vitro*, implying that the vivo-MO-2 targeted region was intolerable to any mutation in nature. Interestingly, vivo-MO-1 remained highly inhibitory even with a single mismatch in the middle of the target RNA of the EV-A71 BrCr strain, but more than one mismatch in the targeted sequence resulted in a substantial loss of inhibition, as seen with CV-A16 and PV. The mutagenesis studies further confirmed that the positions and number of mutations affect the antiviral efficacy in RD cells. A single mismatch present in the middle of the targeted sequence (T to C substitution at position 523) was more tolerable than a mutation appearing at the end of the targeted site (T to C substitution at position 533). These findings correlated well with previous findings that PV and FMDV which showed resistance to PPMO also carried a single point mutation at the extreme end of the PPMO-targeted sequence (Vagnozzi *et al.*, 2007; Stone *et al.*, 2008). A similar observation has been demonstrated in influenza virus as the degree of inhibition was associated with the number of mismatches (Ge *et al.*, 2006). Unlike RNAi machinery that is extremely sensitive to

mutations within the central region and the 3’ end of the target sequence (Gitlin *et al.*, 2005), PMOs remained active even with mismatches at the central region of the targeted region.

In summary, we have established two critical locations that are involved in viral translation initiation in the EV-A71 genome as targets for vivo-MO antiviral intervention. The vivo-MOs worked well at low micromolar concentrations to inhibit EV-A71 infection and showed little cytotoxicity in RD cells. The potent inhibition of several enteroviruses by vivo-MO-2 raises the possibility that it could be developed as a broad-spectrum antiviral agent. Furthermore, the degree of tolerance of mismatches by vivo-MOs is a favorable characteristic for their use as a potential antiviral agent.

CHAPTER 6

CONCLUSION

In this study, screening of 95 overlapping synthetic peptides covering the entire EV-A71 VP1 capsid protein led to discovery of an attachment inhibitor known as SP40 peptide, which could potentially be developed as an antiviral. The SP40 peptide functions as a receptor antagonist, which blocks viral attachment to the targeted receptor. This led to the finding of the role of cell surface heparan sulfate as an EV-A71 attachment receptor. EV-A71 interacts with heparan sulfate via electrostatic interaction. Clustering of positively-charged amino acids at the 5-fold axis of EV-A71 pentamer may be responsible for the heparan sulfate interactions. The outcomes of this study support the hypothesis that screening of overlapping peptides covering the VP1 capsid protein could lead to identification of a viral attachment inhibitor and a previously unknown receptor. This study also identified two antisense-mediated vivo-MOs targeting two highly conserved EV-A71 IRES sites which significantly inhibited EV-A71 infection by arresting IRES-dependent translation. Serial passaging of EV-A71 in the presence of increasing concentrations of the vivo-MOs led to isolation of vivo-MO-1 resistant mutants with a single mutation at the 3' end of the targeted site. No vivo-MO-2 resistant mutant was isolated after 8 passages, implying that the vivo-MO-2 targeted site is intolerant of any mutation. Overall, the attachment receptor antagonist and antisense-mediated translation-suppressing inhibitors could be developed into potential anti-EV-A71 agents.

REFERENCES

Abes R, Moulton HM, Clair P, Yang ST, Abes S, Melikov K, Prevot P, Youngblood DS, Iversen PL, Chernomordik LV, Lebleu B. Delivery of steric block morpholino oligomers by (R-X-R)4 peptides: structure-activity studies. Nucleic Acids Research. 2008; 36(20): 6343-54.

Abes S, Moulton HM, Clair P, Prevot P, Youngblood DS, Wu RP, Iversen PL, Lebleu B. Vectorization of morpholino oligomers by the (R-Ahx-R)4 peptide allows efficient splicing correction in the absence of endosomolytic agents. Journal of Controlled Release. 2006; 116(3): 304-13.

Abubakar S, Chan YF, Lam SK. Outbreaks of enterovirus 71 infection. New England Journal of Medicine. 2000; 342(5): 355-6.

Abubakar S, Sam IC, Yusof J, Lim MK, Misbah S, Matrahim N, Hooi PS. Enterovirus 71 outbreak, Brunei. Emerging Infectious Diseases. 2009; 15(1): 79-82.

Adams MJ, King AM, Carstens EB. Ratification vote on taxonomic proposals to the International Committee on Taxonomy of Viruses (2013). Archives of Virology. 2013; 158(9): 2023-30.

Airaksinen A, Pariente N, Menendez-Arias L, Domingo E. Curing of foot-and-mouth disease virus from persistently infected cells by ribavirin involves enhanced mutagenesis. Virology. 2003; 311(2); 339-49.

Akkarawongsa R, Pocaro NE, Case G, Kolb AW, Brandt CR. Multiple peptides homologous to herpes simplex virus type 1 glycoprotein B inhibit viral infection. Antimicrobial Agents and Chemotherapy. 2009; 53(3): 987-96.

Akula SM, Wang FZ, Vieira J, Chandran B. Human herpesvirus 8 interaction with target cells involves heparan sulfate. Virology. 2001; 282(2): 245-55.

Alexander DA, Dimock K. Sialic acid functions in enterovirus 70 binding and infection. Journal of Virology. 2002; 76(22): 11265-72.

Ali MM, Karasneh GA, Jarding MJ, Tiwari V, Shukla D. A 3-O sulfated heparan sulfate binding peptide preferentially targets herpes simplex virus type-2 infected cells. Journal of Virology. 2012; 86(12): 6434-43.

Altmann SE, Brandt CR, Jahrling PB, Blaney JE. Antiviral activity of the EB peptide against zoonotic poxviruses. Virology Journal. 2012; 9: 6.

Altmann SE, Jones JC, Schultz-Cherry S, Brandt CR. Inhibition of vaccinia virus entry by a broad spectrum antiviral peptide. Virology. 2009; 388(2): 248-59.

Anantpadma M, Stein DA, Vrati S. Inhibition of Japanese encephalitis virus replication in cultured cells and mice by a peptide-conjugated morpholino oligomer. Journal of Antimicrobial Chemotherapy. 2010; 65(5): 953-61.

Andersen JH, Jenssen H, Gutteberg TJ. Lactoferrin and lactoferricin inhibit herpes simplex 1 and 2 infection and exhibit synergy when combined with acyclovir. Antiviral Research. 2003; 58(3): 209-15.

Andersen JH, Osbakk SA, Vorland LH, Traavik T, Gutteberg TJ. Lactoferrin and cyclic lactoferricin inhibit the entry of human cytomegalovirus into human fibroblasts. Antiviral Research. 2001; 51(2): 141-9.

Arita M, Ami Y, Wakita T, Shimizu H. Cooperative effect of the attenuation determinants derived from poliovirus sabin 1 strain is essential for attenuation of enterovirus 71 in the NOD/SCID mouse infection model. Journal of Virology. 2008a; 82(4): 1787-97.

Arita M, Kojima H, Nagano T, Okabe T, Wakita T, Shimizu H. Phosphatidylinositol 4-kinase III beta is a target of enviroxime-like compounds for antipoliovirus activity. Journal of Virology. 2011; 85(5): 2364-72.

Arita M, Kojima H, Nagano T, Okabe T, Wakita T, Shimizu H. Oxysterol-binding protein family is the target of minor enviroxime-like compounds. Journal of Virology. 2013; 87(8): 4252-60.

Arita M, Nagata N, Iwata N, Ami Y, Suzaki Y, Mizuta K, Iwasaki T, Sata T, Wakita T, Shimizu H. An attenuated strain of enterovirus 71 belonging to genotype a showed a broad spectrum of antigenicity with attenuated neurovirulence in cynomolgus monkeys. Journal of Virology. 2007; 81(17): 9386-95.

Arita M, Shimizu H, Nagata N, Ami Y, Suzaki Y, Sata T, Iwasaki T, Miyamura T. Temperature-sensitive mutants of enterovirus 71 show attenuation in cynomolgus monkeys. Journal of General Virology. 2005; 6(Pt 5): 1391-401.

Arita M, Takebe Y, Wakita T, Shimizu H. A bifunctional anti-enterovirus compound that inhibits replication and the early stage of enterovirus 71 infection. Journal of General Virology. 2010; 91(Pt 11): 2734-44.

Arita M, Wakita T, Shimizu H. Characterization of pharmacologically active compounds that inhibit poliovirus and enterovirus 71 infectivity. Journal of General Virology. 2008b; 89(Pt 10): 2518-30.

Arita M, Wakita T, Shimizu H. Cellular kinase inhibitors that suppress enterovirus replication have a conserved target in viral protein 3A similar to that of enviroxime. Journal of General Virology. 2009; 90(Pt 8): 1869-79.

Bai F, Town T, Pradhan D, Cox J, Ashish, Ledizet M, Anderson JF, Flavell, RA, Krueger JK, Koski RA, Fikrig E. Antiviral peptides targeting the West Nile virus envelope protein. Journal of Virology. 2007; 81(4): 2047-55.

Banks WA, Robinson SM, Wolf KM, Bess JW Jr, Arthur LO. Binding, internalization, and membrane incorporation of human immunodeficiency virus-1 at the blood-brain barrier is differentially regulated. Neuroscience. 2004; 128(1): 143-53.

Barnard DL, Hubbard VD, Smee DF, Sidwell RW, Watson KG, Tucker SP, Reece PA. In vitro activity of expanded-spectrum pyridazinyl oxime ethers related to pirodavir: novel capsid-binding inhibitors with potent antipicornavirus activity. Antimicrobial Agents and Chemotherapy. 2004; 48(5): 1766-72.

Barth H, Schafer C, Adah MI, Zhang F, Linhardt RJ, Toyoda H, Kinoshita-Toyoda A, Toida T, van Kuppevelt TH, Depla E, von Weizsacker F, Blum HE, Baumert, T. F. Cellular binding of hepatitis C virus envelope glycoprotein E2 requires cell surface heparan sulfate. Journal of Biological Chemistry. 2003; 278(42): 41003-12.

Basler CF, Garcia-Sastre A. Viruses and the type I interferon antiviral system: induction and evasion. International Reviews of Immunology. 2002; 21(4-5): 305-37.

Bastian A, Schafer H. Human alpha-defensin 1 (HNP-1) inhibits adenoviral infection in vitro. Regulatory Peptides. 2001; 101(1-3): 157-61.

Bauer DJ, Selway JW, Batchelor JF, Tisdale M, Caldwell IC, Young DA. 4',6-Dichloroflavan (BW683C), a new anti-rhinovirus compound. Nature. 1981; 292(5821): 369-70.

Belaid A, Aouni M, Khelifa R, Trabelsi A, Jemmali M, Hani K. In vitro antiviral activity of dermaseptins against herpes simplex virus type 1. Journal of Medical Virology. 2002; 66(2): 229-34.

Belov GA, Ehrenfeld E. Involvement of cellular membrane traffic proteins in poliovirus replication. Cell Cycle. 2007; 6(1): 36-8.

Bennett CF, Swayze EE. RNA targeting therapeutics: molecular mechanisms of antisense oligonucleotides as a therapeutic platform. Annual Review of Pharmacology and Toxicology. 2010; 50: 259-93.

Bergelson JM, Coyne CB. Picornavirus entry. Advance in Experimental Medicine and Biology. 2013; 790: 24-41.

Bergstrom T, Trybala E, Spillmann D. Heparan sulfate and viral tropism. Nature Medicine. 1997; 3: 1177.

Bernfield M, Gotte M, Park PW, Reizes O, Fitzgerald ML, Lincecum J, Zako M. Functions of cell surface heparan sulfate proteoglycans. Annual Reviews of Biochemistry. 1999; 68: 729-77.

Bible JM, Pantelidis P, Chan PK, Tong CY. Genetic evolution of enterovirus 71: epidemiological and pathological implications. Reviews in Medical Virology. 2007; 17(6): 371-9.

Bienz K, Egger D, Troxler M, Pasamontes L. Structural organization of poliovirus RNA replication is mediated by viral proteins of the P2 genomic region. Journal of Virology. 1990; 64(3): 1156-63.

Binford SL, Maldonado F, Brothers MA, Weady PT, Zalman LS, Meador JW 3rd, Matthews DA, Patick AK. Conservation of amino acids in human rhinovirus 3C protease correlates with broad-spectrum antiviral activity of rupintrivir, a novel human rhinovirus 3C protease inhibitor. Antimicrobial Agents and Chemotherapy. 2005; 49(2): 619-26.

Binford SL, Weady PT, Maldonado F, Brothers MA, Matthews DA, Patick AK. In vitro resistance study of rupintrivir, a novel inhibitor of human rhinovirus 3C protease. Antimicrobial Agents and Chemotherapy. 2007; 51(12): 4366-73.

Blomberg J, Lycke E, Ahlfors K, Johnsson T, Wolontis S, von Zeipel G. New enterovirus type associated with epidemic of aseptic meningitis and-or hand, foot, and mouth disease. Lancet. 1974; 304(7872): 112.

Bobardt MD, Salmon P, Wang L, Esko JD, Gabuzda D, Fiala M, Trono D, van der Schueren B, David G, Gallay PA. Contribution of proteoglycans to human immunodeficiency virus type 1 brain invasion. Journal of Virology. 2004; 78(12): 6567-84.

Bose S, Banerjee AK. Role of heparan sulfate in human parainfluenza virus type 3 infection. Virology. 2002; 298(1): 73-83.

Bottcher-Friebertshauser E, Stein DA, Klenk HD, Garten W. Inhibition of influenza virus infection in human airway cell cultures by an antisense peptide-conjugated morpholino oligomer targeting the hemagglutinin-activating protease TMPRSS2. Journal of Virology. 2011; 85(4): 1554-62.

Bourin MC, Lindahl U. Glycosaminoglycans and the regulation of blood coagulation. Biochemical Journal. 1993; 289(2): 313-30.

Bousarghin L, Touze A, Combita-Rojas AL, Coursaget P. Positively charged sequences of human papillomavirus type 16 capsid proteins are sufficient to mediate gene transfer into target cells via the heparan sulfate receptor. Journal of General Virology. 2003; 84(Pt 1): 157-164.

Boyer JC, Haenni AL. Infectious transcripts and cDNA clones of RNA viruses. Virology. 1994; 198(2): 415-26.

Brown BA, Oberste MS, Alexander JP Jr, Kennett ML, Pallansch MA. Molecular epidemiology and evolution of enterovirus 71 strains isolated from 1970 to 1998. Journal of Virology. 1999; 73(12): 9969-75.

Brown BA, Pallansch MA. Complete nucleotide sequence of enterovirus 71 is distinct from poliovirus. Virus Research. 1995; 39(2-3): 195-205.

Bultmann H, Busse JS, Brandt CR. Modified FGF4 signal peptide inhibits entry of herpes simplex virus type 1. Journal of Virology. 2001; 75(6): 2634-45.

Burrer R, Neuman BW, Ting JP, Stein DA, Moulton HM, Iversen PL, Kuhn P, Buchmeier MJ. Antiviral effects of antisense morpholino oligomers in murine coronavirus infection models. Journal of Virology. 2007; 81(11): 5637-48.

Byrnes AP, Griffin DE. Binding of Sindbis virus to cell surface heparan sulfate. Journal of Virology. 1998; 72(9): 7349-56.

Caliguiri LA, Tamm I. Action of guanidine on the replication of poliovirus RNA. Virology. 1968a; 35(3): 408-17.

Caliguiri LA, Tamm I. Distribution and translation of poliovirus RNA in guanidine-treated cells. Virology. 1968b; 36(2): 223-31.

Cameron-Wilson CL, Zhang H, Zhang F, Buluwela L, Muir P, Archard LC. A vector with transcriptional terminators increases efficiency of cloning of an RNA virus by reverse transcription long polymerase chain reaction. Journal of Molecular Microbiology and Biotechnology. 2002; 4(2): 127-31.

Cardin AD, Weintraub HJ. Molecular modeling of protein-glycosaminoglycan interactions. Arteriosclerosis. 1989; 9(1): 21-32.

Cardosa MJ, Krishnan S, Tio PH, Perera D, Wong SC. Isolation of subgenus B adenovirus during a fatal outbreak of enterovirus 71-associated hand, foot, and mouth disease in Sibu, Sarawak. Lancet. 1999; 354(9183): 987-91.

Cardosa MJ, Perera D, Brown BA, Cheon D, Chan HM, Chan KP, Cho H, McMinn P. Molecular epidemiology of human enterovirus 71 strains and recent outbreaks in the Asia-Pacific region: comparative analysis of the VP1 and VP4 genes. Emerging Infectious Diseases. 2003; 9(4): 461-8.

Chan KP, Goh KT, Chong CY, Teo ES, Lau G, Ling AE. Epidemic hand, foot and mouth disease caused by human enterovirus 71, Singapore. Emerging Infectious Diseases. 2003; 9(1): 78-85.

Chan LG, Parashar UD, Lye MS, Ong FG, Zaki SR, Alexander JP, Ho KK, Han LL, Pallansch MA, Suleiman AB, Jegathesan M, Anderson LJ. Deaths of children during an outbreak of hand, foot, and mouth disease in Sarawak, Malaysia: clinical and pathological characteristics of the disease. Clinical Infectious Diseases. 2000; 31(3): 678-83.

Chan YF, Abubakar S. Phylogenetic evidence for inter-typic recombination in the emergence of human enterovirus 71 subgenotypes. BMC Microbiology. 2006; 6: 74.

Chan YF, Sam IC, Abubakar S. Phylogenetic designation of enterovirus 71 genotypes and subgenotypes using complete genome sequences. Infection, Genetics and Evolution. 2010; 10(3): 404-12.

Chan YF, Wee KL, Chiam CW, Khor CS, Chan SY, Wan Nor Amalina WMZ, Sam IC. Comparative genetic analysis of VP4, VP1 and 3D gene regions of enterovirus 71 and coxsackievirus A16 circulating in Malaysia between 1997-2008. Tropical Biomedicine. 2012; 28(3): 451-66.

Chang CS, Lin YT, Shih SR, Lee CC, Lee YC, Tai CL, Tseng SN, Chern JH. Design, synthesis, and antipicornavirus activity of 1-[5-(4-arylphenoxy)alkyl]-3-pyridin-4-ylimidazolidin-2-one derivatives. Journal of Medicinal Chemistry. 2005; 48(10): 3522-35.

Chang LY, Huang LM, Gau SS, Wu YY, Hsia SH, Fan TY, Lin KL, Huang YC, Lu CY, Lin TY. Neurodevelopment and cognition in children after enterovirus 71 infection. New England Journal of Medicine. 2007; 356(12): 1226-34.

Chang LY, Lin TY, Hsu KH, Huang YC, Lin KL, Hsueh C, Shih SR, Ning HC, Hwang MS, Wang HS, Lee CY. Clinical features and risk factors of pulmonary oedema after enterovirus-71-related hand, foot, and mouth disease. Lancet. 1999; 354(9191): 1682-6.

Chapman MS, Minor I, Rossmann MG, Diana GD, Andries K. Human rhinovirus 14 complexed with antiviral compound R 61837. Journal of Molecular Biology. 1999; 217(3): 455-63.

Chen HL, Wang LC, Chang CH, Yen CC, Cheng WT, Wu SC, Hung CM, Kuo MF, Chen CM. Recombinant porcine lactoferrin expressed in the milk of transgenic mice protects neonatal mice from a lethal challenge with enterovirus type 71. Vaccine. 2008a; 26(7): 891-8.

Chen KT, Chang HL, Wang ST, Cheng YT, Yang JY. Epidemiologic features of hand-foot-mouth disease and herpangina caused by enterovirus 71 in Taiwan, 1998-2005. Pediatrics. 2007; 120(2): e244-52.

Chen P, Song Z, Qi Y, Feng X, Xu N, Sun Y, Wu X, Yao X, Mao Q, Li X, Dong W, Wan X, Huang N, Shen X, Liang Z, Li W. Molecular determinants of enterovirus 71 viral entry: a cleft around Q172 on VP1 interacts with a variable region on scavenge receptor B2. Journal of Biological Chemistry. 2012; 287(9): 6406-20.

Chen TC, Chang HY, Lin PF, Chern JH., Hsu JT, Chang CY, Shih SR. Novel antiviral agent DTriP-22 targets RNA-dependent RNA polymerase of enterovirus 71. Antimicrobial Agents and Chemotherapy. 2009; 53(7): 2740-7.

Chen TC, Liu SC, Huang PN, Chang HY, Chern JH, Shih SR. Antiviral activity of pyridyl imidazolidinones against enterovirus 71 variants. Journal of Biomedical Science. 2008b; 15(3): 291-300.

Chen Y, Maguire T, Hileman RE, Fromm JR, Esko JD, Linhardt RJ, Marks RM. Dengue virus infectivity depends on envelope protein binding to target cell heparan sulfate. Nature Medicine. 1997; 3(8): 866-71.

Chen YJ, Zeng SJ, Hsu JT, Horng JT, Yang HM, Shih SR, Chu YT, Wu TY. Amantadine as a regulator of internal ribosome entry site. Acta Pharmacologica Sinica. 2008c; 29(11): 1327-33.

Cheng G, Montero A, Gastaminza P, Whitten-Bauer C, Wieland SF, Isogawa M, Fredericksen B, Selvarajah S, Gallay PA, Ghadiri MR, Chisari FV. A virocidal amphipathic α-helical peptide that inhibits hepatitis C virus infection in vitro. Proceedings of the National Academy of Science U S A. 2008; 105(8): 3088-93.

Chern JH, Shia KS, Hsu TA, Tai CL, Lee CC, Lee YC, Chang CS, Tseng SN, Shih SR. Design, synthesis, and structure-activity relationships of pyrazolo[3,4-d]pyrimidines: a novel class of potent enterovirus inhibitors. Bioorganic and Medicinal Chemistry Letters. 2004; 14(19): 2519-25.

Chiu YH, Chan YL, Tsai LW, Li TL, Wu CJ. Prevention of human enterovirus 71 infection by kappa carrageenan. Antiviral Research. 2012; 95(2): 128-34.

Chu PY, Lin KH, Hwang KP, Chou LC, Wang CF, Shih SR, Wang JR, Shimada Y, Ishiko H. Molecular epidemiology of enterovirus 71 in Taiwan. Archives of Virology. 2001; 146(3): 589-600.

Chua BH, Phuektes P, Sanders SA, Nicholls PK, McMinn PC. The molecular basis of mouse adaptation by human enterovirus 71. Journal of General Virology. 2008; 89(Pt 7): 1622-32.

Chua KB, Kasri AR. Hand foot and mouth disease due to enterovirus 71 in Malaysia. Virologica Sinica. 2011; 26(4): 221-28.

Chumakov M, Voroshilova M, Shindarov L, Lavrova I, Gracheva L, Koroleva G, Vasilenko S, Brodvarova I, Nikolova M, Gyurova S, Gacheva M, Mitov G, Ninov N, Tsylka E, Robinson I, Frolova M, Bashkirtsev V, Martiyanova L, Rodin V. Enterovirus 71 isolated from cases of epidemic poliomyelitis-like disease in Bulgaria. Archives of Virology. 1979; 60(3-4): 329-40.

Chung CS, Hsiao JC, Chang YS, Chang W. A27L protein mediates vaccinia virus interaction with cell surface heparan sulfate. Journal of Virology. 1998; 72(2): 1577-85.

Cifuente JO, Lee H, Yoder JD, Shingler KL, Carnegie MS, Yoder JL, Ashley RE, Makhov AM, Conway JF, Hafenstein S. Structures of the procapsid and mature virion of enterovirus 71 strain 1095. Journal of Virology. 2013; 87(13): 7637-45.

Conti C, Mastromarino P, Sgro R, Desideri N. Anti-picornavirus activity of synthetic flavon-3-yl esters. Antiviral Chemistry and Chemotherapy. 1998; 9(6): 511-15.

Cooper A, Tal G, Lider O, Shaul Y. Cytokine induction by the hepatitis B virus capsid in macrophages is facilitated by membrane heparan sulfate and involves TLR2. Journal of Immunology. 2005; 175(5): 3165-76.

Das S, Ravi V, Desai A. Japanese encephalitis virus interacts with vimentin to facilitate its entry into porcine kidney cell line. Virus Research. 2011; 160(1-2): 404-8.

Davies WL, Grunert RR, Hoffmann CE. Influenza virus growth and antibody response in amantadine-treated mice. Journal of Immunology. 1965; 95(6): 1090-4.

de Palma AM, Thibaut HJ, van der Linden L, Lanke K, Heggermont W, Ireland S, Andrews R, Arimilli M, Al-Tel TH, de Clercq E, van Kuppeveld F, Neyts J. Mutations in the nonstructural protein 3A confer resistance to the novel enterovirus replication inhibitor TTP-8307. Antimicrobial Agents and Chemotherapy. 2009; 53(5): 1850-7.

de Palma AM, Vliegen I, de Clercq E, Neyts J. Selective inhibitors of picornavirus replication. Medicinal Research Reviews. 2008; 28(6): 823-84.

de Smet MD, Meenken CJ, van den Horn GJ. Fomivirsen - a phosphorothioate oligonucleotide for the treatment of CMV retinitis. Ocular Immunology and Inflammation. 1999; 7(3-4): 189-98.

Deas TS, Bennett CJ, Jones SA, Tilgner M, Ren P, Behr MJ, Stein DA, Iversen PL, Kramer LD, Bernard KA, Shi PY. In vitro resistance selection and in vivo efficacy of morpholino oligomers against West Nile virus. Antimicrobial Agents and Chemotherapy. 2007; 51(7): 2470-82.

Delputt PL, Vanderheijden N, Nauwynck HJ, Pensaert MB. Involvement of the matrix protein in attachment of porcine reproductive and respiratory syndrome virus to a heparin-like receptor on porcine alveolar macrophages. Journal of Virology. 2002; 76(9): 4312-20.

Deng JX, Nie XJ, Lei YF, Ma CF, Xu DL, Li B, Xu ZK, Zhang GC. The highly conserved 5' untranslated region as an effective target towards the inhibition of enterovirus 71 replication by unmodified and appropriate 2'- modified siRNAs. Journal of Biomedical Science. 2012; 19(1): 73.

Du N, Cong H, Tian H, Zhang H, Zhang W, Song L, Tien P. Cell surface vimentin is an attachment receptor for enterovirus 71. Journal of Virology. 2014; 88(10): 5816-33.

Dwyer JJ, Wilson KL, Davison DK, Freel SA, Seedorff JE, Wring SA, Tvermoes NA, Matthews TJ, Greenberg ML, Delmedico MK. Design of helical, oligomeric HIV-1 fusion inhibitor peptides with potent activity against enfuvirtide-resistant virus. Proceedings of the National Academy of Science U S A. 2007; 104(31). 12772-7.

Edge AS, Spiro RG. Characterization of novel sequences containing 3-O-sulfated glucosamine in glomerular basement membrane heparan sulfate and localization of sulfated disaccharides to a peripheral domain. Journal of Biological Chemistry. 1990; 265(26): 15874-81.

Eggen R, Verver J, Wellink J, De Jong A, Goldbach R, van Kammen A. Improvements of the infectivity of in vitro transcripts from cloned cowpea mosaic virus cDNA: impact of terminal nucleotide sequences. Virology. 1989; 173(2): 447-55.

Enterlein S, Warfield KL, Swenson DL, Stein DA, Smith JL, Gamble CS, Kroeker AD, Iversen PL, Bavari S, Muhlberger E. VP35 knockdown inhibits Ebola virus amplification and protects against lethal infection in mice. Antimicrobial Agents and Chemotherapy. 2006; 50(3): 984-93.

Ernst S, Langer R, Cooney CL, Sasisekharan R. Enzymatic degradation of glycosaminoglycans. Critical Reviews in Biochemistry and Molecular Biology. 1995; 30(5): 387-444.

Escarmis C, Carrillo EC, Ferrer M, Arriaza JF, Lopez N, Tami C, Verdaguer N, Domingo E, Franze-Fernandez MT. Rapid selection in modified BHK-21 cells of a foot-and-mouth disease virus variant showing alterations in cell tropism. Journal of Virology. 1998; 72(12): 10171-9.

Escribano-Romero E, Jimenez-Clavero MA, Gomes P, Garcia-Ranea JA, Ley V. Heparan sulphate mediates swine vesicular disease virus attachment to the host cell. Journal of General Virology. 2004; 85(Pt 3): 653-63.

Eskelinen EL, Tanaka Y, Saftig P. At the acidic edge: emerging functions for lysosomal membrane proteins. Trends in Cell Biology. 2003; 13(3): 137-45.

Esko JD, Lindahl U. Molecular diversity of heparan sulfate. Journal of Clinical Investigation. 2001; 108(2): 169-73.

Esko JD, Stewart TE, Taylor WH. Animal cell mutants defective in glycosaminoglycan biosynthesis. Proceedings of the National Academy of Science U S A. 1985; 82(10): 3197-201.

Esko JD, Zhang L. Influence of core protein sequence on glycosaminoglycan assembly. Current Opinion in Structural Biology. 1996; 6(5): 663-70.

Evans DJ. Reverse genetics of picornaviruses. Advances in Virus Research. 1999; 53: 209-228.

Falah N, Montserret R, Lelogeais V, Schuffenecker I, Lina B, Cortay JC, Violot S. Blocking human enterovirus 71 replication by targeting viral 2A protease. Journal of Antimicrobial Chemotherapy. 2012; 67(12): 2865-69.

Feldman SA, Audet S, Beeler JA, The fusion glycoprotein of human respiratory syncytial virus facilitates virus attachment and infectivity via an interaction with cellular heparan sulfate. Journal of Virology. 2000; 74(14): 6442-7.

Forsberg E, Kjellen L. Heparan sulfate: lessons from knockout mice. Journal of Clinical Investigation. 2001; 108(2): 175-80.

Fox MP, Otto MJ, Mckinlay MA. Prevention of rhinovirus and poliovirus uncoating by WIN 51711, a new antiviral drug. Antimicrobial Agents and Chemotherapy. 1986; 30(1): 110-6.

Fry EE, Lea SM, Jackson T, Newman JW, Ellard FM, Blakemore WE, Abu-Ghazaleh R, Samuel A, King AM, Stuart DI. The structure and function of a foot-and-mouth disease virus-oligosaccharide receptor complex. EMBO Journal. 1999; 18(3): 543-54.

Fujita H, Takata Y, Kono A, Tanaka Y, Takahashi T, Himeno M, Kato K. Isolation and sequencing of a cDNA clone encoding the 85 kDa human lysosomal sialoglycoprotein (hLGP85) in human metastatic pancreas islet tumor cells. Biochemical and Biophysical Research Communications. 1992; 184(2): 604-11.

Gabriel G, Nordmann A, Stein DA, Iversen PL, Klenk HD. Morpholino oligomers targeting the PB1 and NP genes enhance the survival of mice infected with highly pathogenic influenza A H7N7 virus. Journal of General Virology. 2008; 89(Pt 4): 939-48.

Gamp AC, Tanaka Y, Lullmann-Rauch R, Wittke D, D'hooge R, De Deyn PP, Moser T, Hartmann D, Reiss K, Illert AL, Von Figura K, Saftig P. LIMP-2/LGP85 deficiency causes ureteric pelvic junction obstruction, deafness and peripheral neuropathy in mice. Human Molecular Genetics. 2003; 12(6): 631-46.

Gardner CL, Ebel GD, Ryman KD, Klimstra WB. Heparan sulfate binding by natural eastern equine encephalitis viruses promotes neurovirulence. Proceedings of the National Academy of Science U S A. 2011; 108(38): 16026-31.

Ge Q, Pastey M, Kobasa D, Puthavathana P, Lupfer C, Bestwick RK, Iversen PL, Chen J, Stein DA. Inhibition of multiple subtypes of influenza A virus in cell cultures with morpholino oligomers. Antimicrobial Agents and Chemotherapy. 2006; 50(11): 3724-33.

Genovese D, Conti C, Tomao P, Desideri N, Stein ML, Catone S, Fiore L. Effect of chloro-, cyano-, and amidino-substituted flavanoids on enterovirus infection in vitro. Antiviral Research. 1995; 27(1-2): 123-36.

Ghendon Y, Yakobson E, Mikhejeva A. Study of some stages of poliovirus morphogenesis in MiO cells. Journal of Virology. 1972; 10(2): 261-6.

Giroglou T, Florin L, Schafer F, Streeck RE, Sapp M. Human papillomavirus infection requires cell surface heparan sulfate. Journal of Virology. 2001; 75(3): 1565-70.

Gitlin L, Stone JK, Andino R. Poliovirus escape from RNA interference: short interfering RNA-target recognition and implications for therapeutic approaches. Journal of Virology. 2005; 79(2): 1027-35.

Gladue DP, O'Donnel V, Baker-Branstetter R, Holinka LG, Pacheco JM, Fernandez sainz I, Lu Z, Ambroggio X, Rodriguez L, Borca MV. Foot-and-mouth disease virus modulates cellular vimentin for virus survival. Journal of Virology. 2013; 87(12): 6794-803.

Goodfellow IG, Sioofy AB, Powell RM, Evans DJ. Echoviruses bind heparan sulfate at the cell surface. Journal of Virology. 2001; 75(10): 4918-21.

Goodwin D, Simerska P, Toth I. Peptides as therapeutics with enhanced bioactivity. Current Medicinal Chemistry. 2012; 19(26): 4451-61.

Gow JW, Mcgill MM, Behan WM, Behan PO. Long RT-PCR amplification of full-length enterovirus genome. Biotechniques. 1996; 20(4): 582-4.

Gropp R, Frye M, Wagner TO, Bargon J. Epithelial defensins impair adenoviral infection: implication for adenovirus-mediated gene therapy. Human Gene Therapy. 1999; 10(6): 957-64.

Guex N, Peitsch MC. SWISS-MODEL and the Swiss-PdbViewer: an environment for comparative protein modeling. Electrophoresis. 1997; 18(15): 2714-23.

Guibinga GH, Miyanohara A, Esko JD, Friedmann T. Cell surface heparan sulfate is a receptor for attachment of envelope protein-free retrovirus-like particles and VSV-G pseudotyped MLV-derived retrovirus vectors to target cells. Molecular Therapy. 2002; 5(5): 538-46.

Hagiwara A, Tagaya I, Yoneyama T. Epidemic of hand, foot and mouth disease associated with enterovirus 71 infection. Intervirology. 1978; 9(1): 60-3.

Hall RN, Meers J, Fowler E, Mahony T. Back to BAC: the use of infectious clone technologies for viral mutagenesis. Viruses. 2012; 4(2): 211-35.

Han JF, Cao RY, Tian X, Yu M, Qin ED, Qin CF. Producing infectious enterovirus type 71 in a rapid strategy. Virology Journal. 2010; 7: 116.

Harvala H, Kalimo H, Dahllund L, Santti J, Hughes P, Hyypia T, Stanway G. Mapping of tissue tropism determinants in coxsackievirus genomes. Journal of General Virology. 2002; 83(Pt 7): 1697-706.

Haywood AM. Virus receptors: binding, adhesion strengthening, and changes in viral structure. Journal of Virology. 1994; 68(1): 1-5.

Herrero LJ, Lee CS, Hurrelbrink RJ, Chua BH, Chua KB, McMinn PC. Molecular epidemiology of enterovirus 71 in peninsular Malaysia, 1997-2000. Archives of Virology. 2003; 148(7): 1369-85.

Herrmann EC Jr, Herrmann JA, Delong DC. Prevention of death in mice infected with coxsackievirus A16 using guanidine HCl mixed with substituted benzimidazoles. Antiviral Research. 1982; 2(6): 339-46.

Hilgard P, Stockert R. Heparan sulfate proteoglycans initiate dengue virus infection of hepatocytes. Hepatology. 2000; 32(5): 1069-77.

Ho M, Chen ER, Hsu KH, Twu SJ, Chen KT, Tsai SF, Wang JR, Shih SR. An epidemic of enterovirus 71 infection in Taiwan. New England Journal of Medicine. 1999; 341(13): 929-35.

Hoffmann CE, Neumayer EM, Haff RF, Goldsby RA. Mode of action of the antiviral activity of amantadine in tissue culture. Journal of Bacteriology. 1965; 90(3): 623-8.

Holden KL, Stein DA, Pierson TC, Ahmed AA, Clyde K, Iversen PL, Harris E. Inhibition of dengue virus translation and RNA synthesis by a morpholino oligomer targeted to the top of the terminal 3' stem-loop structure. Virology. 2006; 344(2): 439-52.

Hrobowski YM, Garry RF, Michael SF. Peptide inhibitors of dengue virus and West Nile virus infectivity. Virology Journal. 2005; 2: 49.

Hsu NY, Ilnytska O, Belov G, Santiana M, Chen YH, Takvorian PM, Pau C, van der Schaar H, Kaushik-Basu N, Balla T, Cameron CE, Ehrenfeld E, van Kuppeveld FJM, Altan-Bonnet N. Viral reoganization of the secretory pathway generates distinct organelles for RNA replication. Cell. 2010; 141(5); 799-811.

Huang CC, Liu CC, Chang YC, Chen CY, Wang ST, Yeh TF. Neurologic complications in children with enterovirus 71 infection. New England Journal of Medicine. 1999; 341(13): 936-42.

Huang MC, Wang SM, Hsu YW, Lin HC, Chi CY, Liu CC.Long-term cognitive and motor deficits after enterovirus 71 brainstem encephalitis in children. Pediatrics. 2006; 118(6): e1785-8.

Huang PN, Lin JY, Locker N, Kung YA, Hung CT, Huang HI, Li ML, Shih SR. Far upstream element binding protein 1 binds the internal ribosomal entry site of enterovirus 71 and enhances viral translation and viral growth. Nucleic Acids Research. 2011; 39(22): 9633-48.

Huang SC, Chang CL, Wang PS, Tsai Y, Liu HS. Enterovirus 71-induced autophagy detected in vitro and in vivo promotes viral replication. Journal of Medical Virology. 2009; 81(7): 1241-52.

Huang SC, Hsu YW, Wang HC, Huang SW, Kiang D, Tsai HP, Wang SM, Liu CC, Lin KH, Su IJ, Wang JR. Appearance of intratypic recombination of enterovirus 71 in Taiwan from 2002 to 2005. Virus Research. 2008a; 131(2): 250-9.

Huang SW, Wang YF, Yu CK, Su IJ, Wang JR. Mutations in VP2 and VP1 capsid proteins increase infectivity and mouse lethality of enterovirus 71 by virus binding and RNA accumulation enhancement. Virology. 2012; 422(1): 132-43.

Huang YP, Lin TL, Kuo CY, Lin MW, Yao CY, Liao HW, Hsu LC, Yang CF, Yang JY Chen PJ, Wu HS. The circulation of subgenogroups B5 and C5 of enterovirus 71 in Taiwan from 2006 to 2007. Virus Research. 2008b; 137(2): 206-12.

Hulst MM, van Gennip HG, Moormann RJ. Passage of classical swine fever virus in cultured swine kidney cells selects virus variants that bind to heparan sulfate due to a single amino acid change in envelope protein E(rns). Journal of Virology. 2000; 74(20): 9553-61.

Hung HC, Wang HC, Shih SR, Teng IF, Tseng CP, Hsu JT. Synergistic inhibition of enterovirus 71 replication by interferon and rupintrivir. Journal of Infectious Diseases. 2011; 203(12): 1784-90.

Hussain KM, Leong KL, Ng MM, Chu JJ. The essential role of clathrin-mediated endocytosis in the infectious entry of human enterovirus 71. Journal of Biological Chemistry. 2011; 286(1): 309-21.

Huther A, Dietrich U. The emergence of peptides as therapeutic drugs for the inhibition of HIV-1. AIDS Reviews. 2007; 9(4): 208-17.

Jackson T, Ellard FM, Ghazaleh RA, Brookes SM, Blakemore WE, Corteyn AH, Stuart DI, Newman JW, King AM. Efficient infection of cells in culture by type O foot-and-mouth disease virus requires binding to cell surface heparan sulfate. Journal of Virology. 1996; 70(8): 5282-7.

Jackson WT, Giddings TH Jr, Taylor MP, Mulinyawe S, Rabinovitch M, Kopito RR, Kirkegaard K. Subversion of cellular autophagosomal machinery by RNA viruses. PLoS Biology. 2005: 3: e156.

Jacobson MF, Asso J, Baltimore D. Further evidence on the formation of poliovirus proteins. Journal of Molecular Biology. 1970; 49(3): 657-69.

Jacobson MF, Baltimore D. Morphogenesis of poliovirus. I. Association of the viral RNA with coat protein. Journal of Molecular Biology. 1968; 33(2): 369-78.

Jacquet A, Haumont M, Chellun D, Massaer M, Tufaro F, Bollen A, Jacobs P. The varicella zoster virus glycoprotein B (gB) plays a role in virus binding to cell surface heparan sulfate proteoglycans. Virus Research. 1998; 53(2): 197-207.

Jenssen H, Andersen JH, Mantzilas D, Gutteberg TJ. A wide range of medium-sized, highly cationic, alpha-helical peptides show antiviral activity against herpes simplex virus. Antiviral Research. 2004a; 64(2): 119-26.

Jenssen H, Andersen JH, Uhlin-Hansen L, Gutteberg TJ, Rekdal O. Anti-HSV activity of lactoferricin analogues is only partly related to their affinity for heparan sulfate. Antiviral Research. 2004b; 61(2): 101-9.

Jenssen H, Hamill P, Hancock RE. Peptide antimicrobial agents. Clinical Microbiology Reviews. 2006; 19(3): 491-511.

Johnson KM, Kines RC, Roberts JN, Lowy DR, Schiller JT, Day PM. Role of heparan sulfate in attachment to and infection of the murine female genital tract by human papillomavirus. Journal of Virology. 2009; 83(5): 2067-74.

Jones JC, Settles EW, Brandt CR, Schultz-Cherry S. Identification of the minimal active sequence of an anti-influenza virus peptide. Antimicrobial Agents and Chemotherapy. 2011; 55(4): 1810-3.

Jones JC, Turpin EA, Bultmann H, Brandt CR, Schultz-Cherry S. Inhibition of influenza virus infection by a novel antiviral peptide that targets viral attachment to cells. Journal of Virology. 2006; 80(24): 11960-7.

Jones KS, Petrow-Sadowski C, Bertolette DC, Huang Y, Ruscetti FW. Heparan sulfate proteoglycans mediate attachment and entry of human T-cell leukemia virus type 1 virions into CD4+ T cells. Journal of Virology. 2005; 79(20): 12692-702.

Kapusinszky B, Szomor KN, Farkas A, Takacs M, Berencsi G. Detection of non-polio enteroviruses in Hungary 2000-2008 and molecular epidemiology of enterovirus 71, coxsackievirus A16, and echovirus 30. Virus Genes. 2010; 40(2): 163-73.

Khanh TH, Sabanathan S, Thanh TT, Thoa Le PK, Thuong TC, Hang V, Farrar J, Hien TT, Chau NV, Van Doorn HR. Enterovirus 71-associated hand, foot, and mouth disease, Southern Vietnam, 2011. Emerging Infectious Diseases. 2012; 18(12): 2002-5.

Kilby JM, Hopkins S, Venetta TM, Dimassimo B, Cloud GA, Lee JY, Alldredge L, Hunter E, Lambert D, Bolognesi D, Matthews T, Johnson MR, Nowak MA, Shaw GM, Saag MS. Potent suppression of HIV-1 replication in humans by T-20, a peptide inhibitor of gp41-mediated virus entry. Nature Medicine. 1998; 4(11): 1302-7.

Kim DH, Ni Y, Lee SH, Urban S, Han KH. An anti-viral peptide derived from the preS1 surface protein of hepatitis B virus. BMB Reports. 2008; 41(9): 640-4.

Kim J, Hajjar KA. Annexin II: a plasminogen-plasminogen activator co-receptor. Frontiers in Bioscience. 2002; 7: d341-8.

Kinney RM, Huang CY, Rose BC, Kroeker AD, Dreher TW, Iversen PL, Stein DA. Inhibition of dengue virus serotypes 1 to 4 in vero cell cultures with morpholino oligomers. Journal of Virology. 2005; 79(8): 5116-28.

Kitamura N, Semler BL, Rothberg PG, Larsen GR, Adler CJ, Dorner AJ, Emini EA, Hanecak R, Lee JJ, van der Werf S, Anderson CW, Wimmer E. Primary structure, gene organization and polypeptide expression of poliovirus RNA. Nature. 1981; 291(5816): 547-53.

Kjellen L, Lindahl U. Proteoglycans: structures and interactions. Annual Review of Biochemistry. 1991; 60: 443-475.

Kjellen L, Oldberg A, Hook M. Cell-surface heparan sulfate. Mechanisms of proteoglycan-cell association. Journal of Biological Chemistry. 1980; 255(21): 10407-13.

Klimstra WB, Ryman KD, Johnston RE. Adaptation of Sindbis virus to BHK cells selects for use of heparan sulfate as an attachment receptor. Journal of Virology. 1998; 72(9): 7357-66.

Knappe M, Bodevin S, Selinka HC, Spillmann D, Streeck RE, Chen XS, Lindahl U, Sapp M. Surface-exposed amino acid residues of HPV16 L1 protein mediating interaction with cell surface heparan sulfate. Journal of Biological Chemistry. 2007; 282(38): 27913-22.

Kok CC, Phuektes P, Bek E, McMinn PC. Modification of the untranslated regions of human enterovirus 71 impairs growth in a cell-specific manner. Journal of Virology. 2012; 86(1): 542-52.

Kole R, Krainer AR, Altman S. RNA therapeutics: beyond RNA interference and antisense oligonucleotides. Nature Reviews Drug Discovery. 2012; 11(2): 125-40.

Koudelka KJ, Destito G, Plummer EM, Trauger SA, Siuzdak G, Manchester M. Endothelial targeting of cowpea mosaic virus (CPMV) via surface vimentin. PLoS Pathogens. 2009; 5(5): e1000417.

Kraus W, Zimmermann H, Zimmermann A, Eggers HJ, Nelsen-Salz B. Infectious cDNA clones of echovirus 12 and a variant resistant against the uncoating inhibitor rhodanine differ in seven amino acids. Journal of Virology. 1995; 69(9): 5853-8.

Kung YH, Huang SW, Kuo PH, Kiang D, Ho MS, Liu CC, Yu CK, Su IJ, Wang JR. Introduction of a strong temperature-sensitive phenotype into enterovirus 71 by altering an amino acid of virus 3D polymerase. Virology. 2010; 396(1): 1-9.

Kuo CJ, Shie JJ, Fang JM, Yen GR, Hsu JT, Liu HG, Tseng SN, Chang SC, Lee CY, Shih SR, Liang PH. Design, synthesis, and evaluation of 3C protease inhibitors as anti-enterovirus 71 agents. Bioorganic and Medicinal Chemistry. 2008; 16(15): 7388-98.

Kuronita T, Eskelinen EL, Fujita H, Saftig P, Himeno M, Tanaka Y. A role for the lysosomal membrane protein LGP85 in the biogenesis and maintenance of endosomal and lysosomal morphology. Journal of Cell Science. 2002; 115(21): 4117-31.

Kusov YY, Gosert R, Gauss-Muller V. Replication and in vivo repair of the hepatitis A virus genome lacking the poly(A) tail. Journal of General Virology. 2005; 86(Pt 5): 1363-8.

Laine P, Savolainen C, Blomqvist S, Hovi T. Phylogenetic analysis of human rhinovirus capsid protein VP1 and 2A protease coding sequences confirms shared genus-like relationships with human enteroviruses. Journal of General Virology. 2005; 86(Pt 3): 697-706.

Larkin MA, Blackshields G, Brown NP, Chenna R, McGettigan PA, McWilliam H, Valentin F, Wallace IM, Wilm A, Lopez R, Thompson JD, Gibson TJ, Higgins D G. Clustal W and Clustal X version 2.0. Bioinformatics. 2007; 23(21): 2947-8.

Laszik Z, Jansen PJ, Cummings RD, Tedder TF, Mcever RP, Moore KL. P-selectin glycoprotein ligand-1 is broadly expressed in cells of myeloid, lymphoid, and dendritic lineage and in some nonhematopoietic cells. Blood. 1996; 88(8): 3010-21.

Lee E, Hall RA, Lobigs M. Common E protein determinants for attenuation of glycosaminoglycan-binding variants of Japanese encephalitis and West Nile viruses. Journal of Virology. 2004; 78(15): 8271-80.

Lee E, Lobigs M. Mechanism of virulence attenuation of glycosaminoglycan-binding variants of Japanese encephalitis virus and Murray Valley encephalitis virus. Journal of Virology. 2002; 76(10): 4901-11.

Leister D, Thompson R. Production of full-length cDNA from a picornaviral genome by RT-PCR. Trends in Genetics. 1996; 12(1): 11.

Li C, Wang H, Shih SR, Chen TC, Li ML. The efficacy of viral capsid inhibitors in human enterovirus infection and associated diseases. Current Medicinal Chemistry. 2007; 14(8): 847-56.

Li J, Chen F, Liu T, Wang L. MRI Findings of neurological complications in hand-foot-mouth disease by enterovirus 71 infection. International Journal of Neuroscience. 2012; 122(7): 338-44.

Li ZH, Li CM, Ling P, Shen FH, Chen SH, Liu CC, Yu CK. Ribavirin reduces mortality in enterovirus 71-infected mice by decreasing viral replication. Journal of Infectious Diseases. 2008; 197(6): 854-7.

Lidholt K, Weinke JL, Kiser CS, Lugemwa FN, Bame KJ, Cheifetz S, Massague J, Lindahl U, Esko JD. A single mutation affects both N-acetylglucosaminyltransferase and glucuronosyltransferase activities in a Chinese hamster ovary cell mutant defective in heparan sulfate biosynthesis. Proceedings of the National Academy of Science U S A. 1992; 89(6): 2267-71.

Lin HY, Yang YT, Yu SL, Hsiao KN, Liu CC, Sia C, Chow YH. Caveolar endocytosis is required for human PSGL-1-mediated enterovirus 71 infection. Journal of Virology. 2013a; 87(16): 9064-76.

Lin JY, Chen TC, Weng KF, Chang SC, Chen LL, Shih SR. Viral and host proteins involved in picornavirus life cycle. Journal of Biomedical Science. 2009a; 16: 103.

Lin JY, Li ML, Huang PN, Chien KY, Horng JT, Shih SR. Heterogeneous nuclear ribonuclear protein K interacts with the enterovirus 71 5' untranslated region and participates in virus replication. Journal of General Virology. 2008; 89(Pt 10): 2540-9.

Lin JY, Li ML, Shih SR. Far upstream element binding protein 2 interacts with enterovirus 71 internal ribosomal entry site and negatively regulates viral translation. Nucleic Acids Research. 2009b; 37(1): 47-59.

Lin JY, Shih SR, Pan M, Li C, Lue CF, Stollar V, Li ML. hnRNP A1 interacts with the 5' untranslated regions of enterovirus 71 and Sindbis virus RNA and is required for viral replication. Journal of Virology. 2009c; 83(12): 6106-14.

Lin KH, Hwang KP, Ke GM, Wang CF, Ke LY, Hsu YT, Tung YC, Chu PY, Chen BH, Chen HL, Kao CL, Wang JR, Eng HL, Wang SY, Hsu LC, Chen HY. Evolution of EV71 genogroup in Taiwan from 1998 to 2005: an emerging of subgenogroup C4 of EV71. Journal of Medical Virology. 2006; 78(2): 254-62.

Lin TY, Chu C, Chiu CH. Lactoferrin inhibits enterovirus 71 infection of human embryonal rhabdomyosarcoma cells in vitro. Journal of Infectious Diseases. 2002; 186(8): 1161-4.

Lin YJ, Chang YC, Hsiao NW, Hsieh JL, Wang CY, Kung SH, Tsai FJ, Lan YC, Lin CW. Fisetin and rutin as 3C protease inhibitors of enterovirus A71. Journal of Virological Methods. 2012a; 182(1-2): 93-8.

Lin YJ, Lai CC, Lai CH, Sue SC, Lin CW, Hung CH, Lin TH, Hsu WY, Huang SM, Hung YL, Tien N, Liu X, Chen CL, Tsai FJ. Inhibition of enterovirus 71 infections and viral IRES activity by Fructus gardeniae and geniposide. European Journal of Medicinal Chemistry. 2013b; 62: 206-13.

Lin YW, Lin HY, Tsou YL, Chitra E, Hsiao KN, Shao HY, Liu CC, Sia C, Chong P, Chow YH. Human SCARB2-mediated entry and endocytosis of EV71. PLoS ONE. 2012b; 7: e30507.

Linsuwanon P, Puenpa J, Huang SW, Wang YF, Mauleekoonphairoj J, Wang JR, Poovorawan Y. Epidemiology and seroepidemiology of human enterovirus 71 among Thai populations. Journal of Biomedical Science. 2014; 21:16.

Liu CC, Tseng HW, Wang SM, Wang JR, Su IJ. An outbreak of enterovirus 71 infection in Taiwan, 1998: epidemiologic and clinical manifestations. Journal of Clinical Virology. 2000; 17(1): 23-30.

Liu F, Liu Q, Cai Y, Leng Q, Huang Z. Construction and characterization of an infectious clone of coxsackievirus A16. Virology Journal. 2011; 8: 534.

Liu GQ, Ni Z, Yun T, Yu B, Zhu JM, Hua JG, Chen JP. Rabbit hemorrhagic disease virus poly(A) tail is not essential for the infectivity of the virus and can be restored in vivo. Archives of Virology. 2008; 153(5): 939-44.

Liu J, Dong W, Quan X, Ma C, Qin C, Zhang L. Transgenic expression of human P-selectin glycoprotein ligand-1 is not sufficient for enterovirus 71 infection in mice. Archives of Virology. 2012; 157(3): 539-43.

Liu J, Thorp SC. Cell surface heparan sulfate and its roles in assisting viral infections. Medicinal Research Reviews. 2002; 22(1): 1-25.

Liu ML, Lee YP, Wang YF, Lei HY, Liu CC, Wang SM, Su IJ, Wang JR, Yeh TM, Chen SH, Yu CK. Type I interferons protect mice against enterovirus 71 infection. Journal of General Virology. 2005; 86(Pt 12): 3263-9.

Liu R, Tewari M, Kong R, Zhang R, Ingravallo P, Ralston R. A peptide derived from hepatitis C virus E2 envelope protein inhibits a post-binding step in HCV entry. Antiviral Research. 2010; 86(2): 172-9.

Loddo B, Ferrari W, Brotzu G, Spanedda A. In vitro inhibition of infectivity of polio viruses by guanidine. Nature. 1962; 193: 97-8.

Lu G, Qi J, Chen Z, Xu X, Gao F, Lin D, Qian W, Liu H, Jiang H, Yan J, Gao GF. Enterovirus 71 and coxsackievirus A16 3C proteases: binding to rupintrivir and their substrates and anti-hand, foot, and mouth disease virus drug design. Journal of Virology. 2011; 85(19): 10319-31.

Lu J, Yi L, Zhao J, Yu J, Chen Y, Lin MC, Kung HF, He ML. Enterovirus 71 disrupts interferon signaling by reducing the level of interferon receptor 1. Journal of Virology. 2012; 86(7): 3767-76.

Lu WW, Hsu YY, Yang JY, Kung SH. Selective inhibition of enterovirus 71 replication by short hairpin RNAs. Biochemical and Biophysical Research Communications. 2004; 325(2): 494-9.

Lum LC, Wong KT, Lam SK, Chua KB, Goh AY. Neurogenic pulmonary oedema and enterovirus 71 encephalomyelitis. Lancet. 1998a; 352(9137): 1391.

Lum LC, Wong KT, Lam SK, Chua KB, Goh AY, Lim WL, Ong BB, Paul G, AbuBakar S, Lambert M. Fatal enterovirus 71 encephalomyelitis. Journal of Pediatrics. 1998b; 133(6): 795-8.

Lupfer C, Stein DA, Mourich DV, Tepper SE, Iversen PL, Pastey M. Inhibition of influenza A H3N8 virus infections in mice by morpholino oligomers. Archives of Virology. 2008; 153(5): 929-37.

Malhotra R, Ward M, Bright H, Priest R, Foster MR, Hurle M, Blair E, Bird M. Isolation and characterisation of potential respiratory syncytial virus receptor(s) on epithelial cells. Microbes and Infection. 2003; 5(2): 123-33.

Mandl CW, Kroschewski H, Allison SL, Kofler R, Holzmann H, Meixner T, Heinz FX. Adaptation of tick-borne encephalitis virus to BHK-21 cells results in the formation of multiple heparan sulfate binding sites in the envelope protein and attenuation in vivo. Journal of Virology. 2001; 75(12): 5627-37.

Mann DM, Romm E, Migliorini M. Delineation of the glycosaminoglycan-binding site in the human inflammatory response protein lactoferrin. Journal of Biological Chemistry. 1994; 269(38): 23661-7.

Mao Q, Li N, Yu X, Yao X, Li F, Lu F, Zhuang H, Liang Z, Wang J. Antigenicity, animal protective effect and genetic characteristics of candidate vaccine strains of enterovirus 71. Archives of Virology. 2012; 157(1): 37-41.

Marchetti M, Trybala E, Superti F, Johansson M, Bergstrom T. Inhibition of herpes simplex virus infection by lactoferrin is dependent on interference with the virus binding to glycosaminoglycans. Virology. 2004; 318(1): 405-13.

Mardberg K, Trybala E, Glorioso JC, Bergstrom T. Mutational analysis of the major heparan sulfate-binding domain of herpes simplex virus type 1 glycoprotein C. Journal of General Virology. 2001; 82(Pt 8): 1941-50.

Marongiu ME, Pani A, Corrias MV, Sau M, La Colla P. Poliovirus morphogenesis. I. Identification of 80S dissociable particles and evidence for the artifactual production of procapsids. Journal of Virology. 1981; 39(2): 341-7.

Martino TA, Tellier R, Petric M, Irwin DM, Afshar A, Liu PP. The complete consensus sequence of coxsackievirus B6 and generation of infectious clones by long RT-PCR. Virus Research. 1999; 64(1): 77-86.

McKinlay MA, Frank JA Jr, Benziger DP, Steinberg BA. Use of WIN 51711 to prevent echovirus type 9-induced paralysis in suckling mice. Journal of Infectious Diseases. 1986; 154(4): 676-81.

McLeish NJ, Williams CH, Kaloudas D, Roivainen M, Stanway G. Symmetry-related clustering of positive charges is a common mechanism for heparan sulfate binding in enteroviruses. Journal of Virology. 2012; 86(20): 11163-70.

McMinn PC, Stratov I, Dowse G. Enterovirus 71 outbreak in Western Australia associated with acute flaccid paralysis. Communicable Diseases Intelligence. 1999; 23(7): 199.

McMinn PC. An overview of the evolution of enterovirus 71 and its clinical and public health significance. FEMS Microbiology Reviews. 2002; 26(1): 91-107.

Misinzo G, Delputte PL, Meerts P, Lefebvre DJ, Nauwynck HJ. Porcine circovirus 2 uses heparan sulfate and chondroitin sulfate B glycosaminoglycans as receptors for its attachment to host cells. Journal of Virology. 2006; 80(7): 3487-94.

Moulton HM, Fletcher S, Neuman BW, Mcclorey G, Stein DA, Abes S, Wilton SD, Buchmeier MJ, Lebleu B, Iversen PL. Cell-penetrating peptide-morpholino conjugates alter pre-mRNA splicing of DMD (Duchenne muscular dystrophy) and inhibit murine coronavirus replication in vivo. Biochemical Society Transactions. 2007; 35(4): 826-8.

Moulton JD, Jiang S. Gene knockdowns in adult animals: PPMOs and vivo-morpholinos. Molecules. 2009; 14(3): 1304-23.

Nagy G, Takatsy S, Kukan E, Mihaly I, Domok I. Virological diagnosis of enterovirus type 71 infections: experiences gained during an epidemic of acute CNS diseases in Hungary in 1978. Archives of Virology. 1982; 71(3): 217-27.

Nasri D, Bouslama L, Pillet S, Bourlet T, Aouni M, Pozzetto B. Basic rationale, current methods and future directions for molecular typing of human enterovirus. Expert Review of Molecular Diagnostics. 2007; 7(4): 419-34.

Nasser EH, Judd AK, Sanchez A, Anastasiou D, Bucher DJ. Antiviral activity of influenza virus M1 zinc finger peptides. Journal of Virology. 1996; 70(12): 8639-44.

Neufeld KL, Galarza JM, Richards OC, Summers DF, Ehrenfeld E. Identification of terminal adenylyl transferase activity of the poliovirus polymerase 3Dpol. Journal of Virology. 1994; 68(9): 5811-8.

Neuman BW, Stein DA, Kroeker AD, Churchill MJ, Kim AM, Kuhn P, Dawson P, Moulton HM, Bestwick RK, Iversen PL, Buchmeier MJ. Inhibition, escape, and attenuated growth of severe acute respiratory syndrome coronavirus treated with antisense morpholino oligomers. Journal of Virology. 2005; 79(15): 9665-76.

Neuman BW, Stein DA, Kroeker AD, Paulino AD, Moulton HM, Iversen PL, Buchmeier MJ. Antisense morpholino-oligomers directed against the 5' end of the genome inhibit coronavirus proliferation and growth. Journal of Virology. 2004; 78(11): 5891-9.

Nilsson EC, Jamshidi F, Johansson SM, Oberste MS, Arnberg N. Sialic acid is a cellular receptor for coxsackievirus A24 variant, an emerging virus with pandemic potential. Journal of Virology. 2008; 82(6): 3061-8.

Nishimura Y, Lee H, Hafenstein S, Kataoka C, Wakita T, Bergelson JM, Shimizu H. Enterovirus 71 binding to PSGL-1 on leukocytes: VP1-145 acts as a molecular switch to control receptor interaction. PLoS Pathogens. 2013; 9: e1003511.

Nishimura Y, Shimojima M, Tano Y, Miyamura T, Wakita T, Shimizu H. Human P-selectin glycoprotein ligand-1 is a functional receptor for enterovirus 71. Nature Medicine. 2009; 15(7): 794-7.

Nishimura Y, Wakita T, Shimizu H. Tyrosine sulfation of the amino terminus of PSGL-1 is critical for enterovirus 71 infection. PLoS Pathogens. 2010; 6: e1001174.

O'Donnell V, Larocco M, Baxt B. Heparan sulfate-binding foot-and-mouth disease virus enters cells via caveola-mediated endocytosis. Journal of Virology. 2008; 82(18): 9075-85.

Oh MJ, Akhtar J, Desai P, Shukla D. A role for heparan sulfate in viral surfing. Biochemical and Biophysical Research Communications. 2010; 391(1): 176-81.

Olofsson S, Bergstrom T. Glycoconjugate glycans as viral receptors. Annals of Medicine. 2005; 37(3): 154-72.

Ooi MH, Wong SC, Lewthwaite P, Cardosa MJ, Solomon T. Clinical features, diagnosis, and management of enterovirus 71. Lancet Neurology. 2010; 9(11): 1097-105.

Ooi MH, Wong SC, Podin Y, Akin W, Del Sel S, Mohan A, Chieng CH, Perera D, Clear D, Wong D, Blake E, Cardosa MJ, Solomon T. Human enterovirus 71 disease in Sarawak, Malaysia: a prospective clinical, virological, and molecular epidemiological study. Clinical Infectious Diseases. 2007; 44(5): 646-56.

Pallansch MA, Roos RP. Enteroviruses: Polioviruses, coxsackieviruses, echoviruses and newer enteroviruses. In Knipe DM, Howley PM, Griffin RA, Martin MA, Roizman B, Straus SE, editors. Fields Virology. 5th ed. Philadelphia: Lippincott Williams & Wilkins; 2007. P. 840-893.

Partridge M, Vincent A, Matthews P, Puma J, Stein D, Summerton J. A simple method for delivering morpholino antisense oligos into the cytoplasm of cells. Antisense and Nucleic Acid Drug Development. 1996; 6(3): 169-75.

Patick AK. Rhinovirus chemotherapy. Antiviral Research. 2006; 71(2-3): 391-6.

Patick AK, Binford SL, Brothers MA, Jackson RL, Ford CE, Diem MD., Maldonado F, Dragovich PS, Zhou R, Prins TJ, Fuhrman SA, Meador JW, Zalman LS, Mathews DA, Worland ST. In vitro antiviral activity of AG7088, a potent inhibitor of human rhinovirus 3C protease. Antimicrobial Agents and Chemotherapy. 1999; 43(10): 2444-50.

Perry CM, Balfour JA. Fomivirsen. Drugs. 1999; 57(3): 375-80.

Pevear DC, Tull TM, Seipel ME, Groarke, J. M. Activity of pleconaril against enteroviruses. Antimicrobial Agents and Chemotherapy. 1999; 43(9): 2109-15.

Phuektes P, Chua BH, Sanders S, Bek EJ, Kok CC, McMinn PC. Mapping genetic determinants of the cell-culture growth phenotype of enterovirus 71. Journal of General Virology. 2011; 92(Pt 6): 1380-90.

Plevka P, Perera R, Cardosa J, Kuhn RJ, Rossmann MG. Crystal structure of human enterovirus 71. Science. 2012; 336(6086): 1274.

Plevka P, Perera R, Yap ML, Cardosa J, Kuhn RJ, Rossmann MG. Structure of human enterovirus 71 in complex with a capsid-binding inhibitor. Proceedings of the National Academy of Science U S A. 2013; 110(14): 5463-7.

Plochmann K, Horn A, Gschmack E, Armbruster N, Krieg J, Wiktorowicz T, Weber C, Stirnnagel K, Lindemann D, Rethwilm A, Scheller C. Heparan sulfate is an attachment factor for foamy virus entry. Journal of Virology. 2012; 86(18): 10028-35.

Pourianfar HR, Poh CL, Fecondo J, Grollo L. In vitro evaluation of the antiviral activity of heparan sulphate mimetic compounds against enterovirus 71. Virus Research. 2012; 169(1): 22-9.

Presto J, Thuveson M, Carlsson P, Busse M, Wilen M, Eriksson I, Kusche-Gullberg M, Kjellen L. Heparan sulfate biosynthesis enzymes EXT1 and EXT2 affect NDST1 expression and heparan sulfate sulfation. Proceedings of the National Academy of Science U S A. 2008; 105(12): 4751-6.

Racaniello VR. Picornaviridae: The viruses and their replication. In Knipe DM, Howley PM, Griffin RA, Martin B, Roizman B, Straus SE, editors. 5th ed. Fields virology. Philadelphia: Lippincott Williams & Wilkins; 2007. P. 795-834.

Racaniello VR, Baltimore D. Cloned poliovirus complementary DNA is infectious in mammalian cells. Science. 1981; 214(4523): 916-9.

Reddi HV, Kumar AS, Kung AY, Kallio PD, Schlitt BP, Lipton HL. Heparan sulfate-independent infection attenuates high-neurovirulence GDVII virus-induced encephalitis. Journal of Virology. 2004; 78(16): 8909-16.

Reddi HV, Lipton HL. Heparan sulfate mediates infection of high-neurovirulence Theiler's viruses. Journal of Virology. 2002; 76(16): 8400-7.

Rightsel WA, Dice JR, McAlpine RJ, Timm EA, McLean IW Jr, Dixon GJ, Schabel FM Jr. Antiviral effect of guanidine. Science. 1961; 134(3478): 558-9.

Roderiquez G, Oravecz T, Yanagishita M, Bou-Habib DC, Mostowski H, Norcross MA. Mediation of human immunodeficiency virus type 1 binding by interaction of cell surface heparan sulfate proteoglycans with the V3 region of envelope gp120-gp41. Journal of Virology. 1995; 69(4): 2233-9.

Rohll JB, Moon DH, Evans DJ, Almond JW. The 3' untranslated region of picornavirus RNA: features required for efficient genome replication. Journal of Virology. 1995; 69(12): 7835-44.

Rosenberg RD, Shworak NW, Liu J, Schwartz JJ, Zhang L. Heparan sulfate proteoglycans of the cardiovascular system. Specific structures emerge but how is synthesis regulated? Journal of Clinical Investigation. 1997; 100(11): S67-75.

Rossmann MG. The canyon hypothesis. Viral Immunology. 1989; 2(3): 143-61.

Rossmann MG, He Y, Kuhn RJ. Picornavirus-receptor interactions. Trends in Microbiology. 2002; 10(7): 324-31.

Ruxrungtham K, Boyd M, Bellibas SE, Zhang X, Dorr A, Kolis S, Kinchelow T, Buss N, Patel IH. Lack of interaction between enfuvirtide and ritonavir or ritonavir-boosted saquinavir in HIV-1-infected patients. Journal of Clinical Pharmacology. 2004; 44(7): 793-803.

Ryman KD, Gardner CL, Burke CW, Meier KC, Thompson JM, Klimstra WB. Heparan sulfate binding can contribute to the neurovirulence of neuroadapted and nonneuroadapted Sindbis viruses. Journal of Virology.2007; 81(7): 3563-73.

Sa-Carvalho D, Rieder E, Baxt B, Rodarte R, Tanuri A, Mason PW. Tissue culture adaptation of foot-and-mouth disease virus selects viruses that bind to heparin and are attenuated in cattle. Journal of Virology. 1997; 71(7): 5115-23.

Sadeghipour S, Bek EJ, McMinn PC. Selection and characterisation of guanidine-resistant mutants of human enterovirus 71. Virus Research. 2012; 169(1): 72-9.

Satelli A, Li S. Vimentin as potential molecular target in cancer therapy or vimentin, an overview and its potential as a molecular target for cancer therapy. Cellular and Molecular Life Sciences. 2011; 68(18): 3033-48.

Saunders K, King AM, Mccahon D, Newman JW, Slade WR, Forss S. Recombination and oligonucleotide analysis of guanidine-resistant foot-and-mouth disease virus mutants. Journal of Virology. 1985; 56(3): 921-9.

Savarino A. Use of chloroquine in viral diseases. The Lancet Infectious Diseases. 2011; 11(9): 653-4.

Savarino A, Gennero L, Chen HC, Serrano D, Malavasi F, Boelaert JR, Sperber K. Anti-HIV effects of chloroquine: mechanisms of inhibition and spectrum of activity. AIDS. 2001a; 15(17): 2221-9.

Savarino A, Gennero L, Sperber K, Boelaert JR. The anti-HIV-1 activity of chloroquine. Journal of Clinical Virology. 2001b; 20(3): 131-5.

Savarino A, Lucia MB, Rastrelli E, Rutella S, Golotta C, Morra E, Tamburrini E, Perno CF, Boelaert JR, Sperber K, Cauda R. Anti-HIV effects of chloroquine: inhibition of viral particle glycosylation and synergism with protease inhibitors. Journal of Acquired Immune Deficiency Syndromes. 2004; 35(3): 223-32.

Schmidt NJ, Lennette EH, Ho HH. An apparently new enterovirus isolated from patients with disease of the central nervous system. Journal of Infectious Diseases. 1974; 129(3): 304-9.

Schulze A, Gripon P, Urban S. Hepatitis B virus infection initiates with a large surface protein-dependent binding to heparan sulfate proteoglycans. Hepatology. 2007; 46(6): 1759-68.

See DM, Tilles JG. Treatment of coxsackievirus A9 myocarditis in mice with WIN 54954. Antimicrobial Agents and Chemotherapy. 1992; 36(2): 425-8.

Shang B, Deng C, Ye H, Xu W, Yuan Z, Shi PY, Zhang B. Development and characterization of a stable eGFP enterovirus 71 for antiviral screening. Antiviral Research. 2013; 97(2): 198-205.

Shen WC, Tsai C, Chiu H, Chow K. MRI of enterovirus 71 myelitis with monoplegia. Neuroradiology. 2000; 42(2): 124-7.

Shi X, Zaia J. Organ-specific heparan sulfate structural phenotypes. Journal of Biological Chemistry. 2009; 284(18): 11806-14.

Shia KS, Li WT, Chang CM, Hsu MC, Chern JH, Leong MK, Tseng SN, Lee CC, Lee YC, Chen SJ, Peng KC, Tseng HY, Chang YL, Tai CL, Shih SR. Design, synthesis, and structure-activity relationship of pyridyl imidazolidinones: a novel class of potent and selective human enterovirus 71 inhibitors. Journal of Medicinal Chemistry. 2002; 45(8): 1644-55.

Shih SR, Chen SJ, Hakimelahi GH, Liu HJ, Tseng CT, Shia KS. Selective human enterovirus and rhinovirus inhibitors: an overview of capsid-binding and protease-inhibiting molecules. Medicinal Research Reviews. 2004a; 24(4): 449-74.

Shih SR, Stollar V, Li ML. Host factors in enterovirus 71 replication. Journal of Virology. 2011; 85(19): 9658-66.

Shih SR, Tsai MC, Tseng SN, Won KF, Shia KS, Li WT, Chern JH, Chen GW, Lee CC, Lee YC, Peng KC, Chao YS. Mutation in enterovirus 71 capsid protein VP1 confers resistance to the inhibitory effects of pyridyl imidazolidinone. Antimicrobial Agents and Chemotherapy. 2004b; 48(9): 3523-9.

Shih SR, Weng KF, Stollar V, Li ML. Viral protein synthesis is required for enterovirus 71 to induce apoptosis in human glioblastoma cells. Journal of Neurovirology. 2008; 14(1): 53-61.

Shimazaki K, Tazume T, Uji K, Tanaka M, Kumura H, Mikawa K, Shimo-Oka T. Properties of a heparin-binding peptide derived from bovine lactoferrin. Journal of Dairy Science. 1998; 81(11): 2841-9.

Shimizu H, Utama A, Yoshii K, Yoshida H, Yoneyama T, Sinniah M, Yusof MA, Okuno Y, Okabe N, Shih SR, Chen HY, Wang GR, Kao CL, Chang KS, Miyamura T, Hagiwara A. Enterovirus 71 from fatal and nonfatal cases of hand, foot and mouth disease epidemics in Malaysia, Japan and Taiwan in 1997-1998. Japanese Journal of Infectious Diseases. 1999; 52(1): 12-5.

Shingler KL, Yoder JL, Carnegie MS, Ashley RE, Makhov AM, Conway JF, Hafenstein S. The enterovirus 71 A-particle forms a gateway to allow genome release: a cryoEM study of picornavirus uncoating. PLoS Pathogens. 2013; 9: e1003240.

Shoeman RL, Honer B, Stoller TJ, Kesselmeier C, Miedel MC, Traub P, Graves MC. Human immunodeficiency virus type 1 protease cleaves the intermediate filament proteins vimentin, desmin, and glial fibrillary acidic protein. Proceedings of the National Academy of Sciences of U S A. 1990; 87(16): 6336-40.

Shum D, Smith JL, Hirsch AJ, Bhinder B, Radu C, Stein DA, Nelson JA, Fruh K, Djaballah H. High-content assay to identify inhibitors of dengue virus infection. Assay and Drug Development Technologies.2010; 8(5): 553-70.

Silvestri LS, Parilla JM, Morasco BJ, Ogram SA, Flanegan JB. Relationship between poliovirus negative-strand RNA synthesis and the length of the 3' poly(A) tail. Virology. 2006; 345(2): 509-19.

Sim AC, Luhur A, Tan TM, Chow VT, Poh CL. RNA interference against enterovirus 71 infection. Virology. 2005; 341(1): 72-9.

Solomon T, Lewthwaite P, Perera D, Cardosa MJ, McMinn PC, Ooi MH. Virology, epidemiology, pathogenesis, and control of enterovirus 71. The Lancet Infectious Diseases. 2010; 10(11): 778-90.

Somers WS, Tang J, Shaw GD, Camphausen RT. Insights into the molecular basis of leukocyte tethering and rolling revealed by structures of P- and E-selectin bound to SLe(X) and PSGL-1. Cell. 2000; 103(3): 467-79.

Song E, Lee SK, Wang J, Ince N, Ouyang N, Min J, Chen J, Shankar P, Lieberman J. RNA interference targeting Fas protects mice from fulminant hepatitis. Nature Medicine. 2003; 9(3): 347-51.

Song Y, Paul AV, Wimmer E. Evolution of poliovirus defective interfering particles expressing Gaussia luciferase. Journal of Virology. 2012; 86(4): 1999-2010.

Spear PG, Shieh MT, Herold BC, Wudunn D, Koshy TI. Heparan sulfate glycosaminoglycans as primary cell surface receptors for herpes simplex virus. Advances in Experimental Medicine and Biology. 1992; 313: 341-53.

Stein DA, Huang CY, Silengo S, Amantana A, Crumley S, Blouch RE, Iversen PL, Kinney RM. Treatment of AG129 mice with antisense morpholino oligomers increases survival time following challenge with dengue 2 virus. Journal of Antimicrobial Chemotherapy. 2008; 62(3): 555-65.

Stone JK, Rijnbrand R, Stein DA, Ma Y, Yang Y, Iversen PL, Andino R. A morpholino oligomer targeting highly conserved internal ribosome entry site sequence is able to inhibit multiple species of picornavirus. Antimicrobial Agents and Chemotherapy. 2008; 52(6): 1970-81.

Su PY, Liu YT, Chang HY, Huang SW, Wang YF, Yu CK, Wang JR, Chang CF. Cell surface sialylation affects binding of enterovirus 71 to rhabdomyosarcoma and neuroblastoma cells. BMC Microbiology. 2012; 12(1): 162.

Sugahara K, Kitagawa H. Heparin and heparan sulfate biosynthesis. IUBMB Life. 2002; 54(4): 163-75.

Summerford C, Samulski RJ. Membrane-associated heparan sulfate proteoglycan is a receptor for adeno-associated virus type 2 virions. Journal of Virology. 1998; 72(2): 1438-45.

Summerton J. Morpholino antisense oligomers: the case for an RNase H-independent structural type. Biochimica Biophysica Acta. 1999; 1489(1): 141-58.

Summerton J, Weller D. Morpholino antisense oligomers: design, preparation, and properties. Antisense and Nucleic Acid Drug Development. 1997; 7(2): 187-95.

Swenson DL, Warfield KL, Warren TK, Lovejoy C, Hassinger JN, Ruthel G, Blouch RE, Moulton HM, Weller DD, Iversen PL, Bavari S. Chemical modifications of antisense morpholino oligomers enhance their efficacy against Ebola virus infection. Antimicrobial Agents and Chemotherapy. 2009; 53(5): 2089-99.

Tacahashi Y, Uyeda I. Restoration of the 3' end of potyvirus RNA derived from poly(A)-deficient infectious cDNA clones. Virology. 1999; 265(1): 147-52.

Tan CW, Chan YF, Sim KM, Tan EL, Poh CL. Inhibition of enterovirus 71 (EV-71) infections by a novel antiviral peptide derived from EV-71 capsid protein VP1. PLoS ONE. 2012; 7: e34589.

Tan EL, Tan TM, Chow VT, Poh CL. Enhanced potency and efficacy of 29-mer shRNAs in inhibition of enterovirus 71. Antiviral Research. 2007a; 74(1): 9-15.

Tan EL, Tan TM, Chow VT, Poh, CL. Inhibition of enterovirus 71 in virus-infected mice by RNA interference. Molecular Therapy. 2007b; 15(11): 1931-8.

Tan EL, Yong LL, Quak SH, Yeo WC, Chow VT, Poh CL. Rapid detection of enterovirus 71 by real-time TaqMan RT-PCR. Journal of Clinical Virology. 2008; 42(2): 203-6.

Tan X, Huang X, Zhu S, Chen H, Yu Q, Wang H, Huo X, Zhou J, Wu Y, Yan D, Zhang Y, Wang D, Cui A, An H, Xu W. The persistent circulation of enterovirus 71 in People's Republic of China: causing emerging nationwide epidemics since 2008. PLoS ONE. 2011; 6: e25662.

Tee KK, Lam TT, Chan YF, Bible JM, Kamarulzaman A, Tong CY, Takebe Y, Pybus OG. Evolutionary genetics of human enterovirus 71: origin, population dynamics, natural selection, and seasonal periodicity of the VP1 gene. Journal of Virology. 2010; 84(7): 3339-50.

Tellier R, Bukh J, Emerson SU, Miller RH, Purcell RH. Long PCR and its application to hepatitis viruses: amplification of hepatitis A, hepatitis B, and hepatitis C virus genomes. Journal of Clinical Microbiology. 1996a; 34(12): 3085-91.

Tellier R, Bukh J, Emerson SU, Purcell RH. Amplification of the full-length hepatitis A virus genome by long reverse transcription-PCR and transcription of infectious RNA directly from the amplicon. Proceedings of the National Academy of Science U S A. 1996b; 93(9): 4370-3.

Thoa Le PK, Chiang PS, Khanh TH, Luo ST, Dan TN, Wang YF., Thuong TC, Chung WY, Hung NT, Wang JR, Nhan Le NT, Thinh Le Q, Su IJ, Dung TD, Lee MS. Genetic and antigenic characterization of enterovirus 71 in Ho Chi Minh city, Vietnam, 2011. PLoS ONE. 2013; 8: e69895.

Thompson SR, Sarnow P. Enterovirus 71 contains a type I IRES element that functions when eukaryotic initiation factor eIF4G is cleaved. Virology. 2003; 315(1): 259-66.

Tisdale M, Selway JW. Inhibition of an early stage of rhinovirus replication by dichloroflavan (BW683C). Journal of General Virology. 1983; 64 (Pt 4): 795-803.

Tisdale M, Selway JW. Effect of dichloroflavan (BW683C) on the stability and uncoating of rhinovirus type 1B. Journal of Antimicrobial Chemotherapy. 1984; 14 Suppl A: 97-105.

Tiwari V, Liu J, Valyi-Nagy T, Shukla D. Anti-heparan sulfate peptides that block herpes simplex virus infection in vivo. Journal of Biological Chemistry. 2011; 286(28): 25406-25415.

Trybala E, Bergstrom T, Spillmann D, Svennerholm B, Olofsson S, Flynn SJ, Ryan P. Mode of interaction between pseudorabies virus and heparan sulfate/heparin. Virology. 1996; 218(1): 35-42.

Tsai FJ, Lin CW, Lai CC, Lan YC, Lai CH, Hung CH, Hsueh KC, Lin TH, Chang HC, Wan L, Sheu JJC, Lin YJ. Kaempferol inhibits enterovirus 71 replication and internal ribosome entry site (IRES) activity through FUBP and HNRP proteins. Food Chemistry. 2011; 128(2): 312-22.

Tu PV, Thao NT, Perera D, Truong KH, Tien NTK., Thuong TC, Ooi MH, Cardosa MJ, McMinn PC. Epidemiological and virological investigation of hand, foot and mouth disease, Southern Vietnam, 2005. Emerging Infectious Diseases. 2007; 13(11): 1733-41.

Tuthill TJ, Groppelli E, Hogle JM, Rowlands DJ. Picornaviruses. Current Topics in Microbiology and Immunology. 2010; 343: 43-89.

Vagnozzi A, Stein DA, Iversen PL, Rieder E. Inhibition of foot-and-mouth disease virus infections in cell cultures with antisense morpholino oligomers. Journal of Virology. 2007; 81(21): 11669-80.

van der Schaar HM, Leyssen P, Thibaut HJ, de Palma A, Van der Linden L, Lanke KHW, Lacroix C, Verbeken E, Conrath K, MacLeod AM, Mitchell DR, Palmer NJ, van de Poel H, Andrews M, Neyts J, van Kuppeveld FJ. A novel, broad-spectrum inhibitor of enterovirus replication that targets host cell factor phosphatidylinositol 4-kinase IIIβ. Antimicrobial Agents and Chemotherapy. 2013; 57(10): 4971-81.

van der Strate BW, Beljaars L, Molema G, Harmsen MC, Meijer DK. Antiviral activities of lactoferrin. Antiviral Research. 2001; 52(3): 225-39.

van der Werf S, Bradley J, Wimmer E, Studier FW, Dunn JJ. Synthesis of infectious poliovirus RNA by purified T7 RNA polymerase. Proceedings of the National Academy of Science U S A. 1986; 83(8): 2330-4.

van Ooij MJ, Polacek C, Glaudemans DH, Kuijpers J, van Kuppeveld FJ, Andino R, Agol VI, Melchers WJ. Polyadenylation of genomic RNA and initiation of antigenomic RNA in a positive-strand RNA virus are controlled by the same cis-element. Nucleic Acids Research. 2006; 34(10): 2953-65.

Varki NM, Varki A. Diversity in cell surface sialic acid presentations: implications for biology and disease. Laboratory Investigation. 2007; 87(9): 851-7.

Vives RR, Imberty A, Sattentau QJ, Lortat-Jacob H. Heparan sulfate targets the HIV-1 envelope glycoprotein gp120 coreceptor binding site. Journal of Biological Chemistry. 2005; 280(22): 21353-7.

Vlasak M, Goesler I, Blaas D. Human rhinovirus type 89 variants use heparan sulfate proteoglycan for cell attachment. Journal of Virology. 2005; 79(10): 5963-70.

Wang J, Du J, Wu Z, Jin Q. Quinacrine impairs enterovirus 71 RNA replication by preventing binding of polypyrimidine-tract binding protein with internal ribosome entry sites. PLoS ONE. 2013a; 8: e52954.

Wang J, Fan T, Yao X, Wu Z, Guo L, Lei X, Wang M, Jin Q, Cui S. Crystal structures of enterovirus 71 3C protease complexed with rupintrivir reveal the roles of catalytically important residues. Journal of Virology. 2011; 85(19): 10021-30.

Wang J, Wu Z, Jin Q. COPI is required for enterovirus 71 replication. PLoS ONE. 2012a; 7: e38035.

Wang RR, Yang LM, Wang YH, Pang W, Tam SC, Tien P, Zheng YT. Sifuvirtide, a potent HIV fusion inhibitor peptide. Biochemical and Biophysical Research Communications. 2009; 382(3): 540-4.

Wang SM, Liu CC, Tseng HW, Wang JR, Huang CC, Chen YJ, Yang YJ, Lin SJ, Yeh TF. Clinical spectrum of enterovirus 71 infection in children in Southern Taiwan, with an emphasis on neurological complications. Clinical Infectious Diseases. 1999; 29(1): 184-90.

Wang X, Peng W, Ren J, Hu Z, Xu J, Lou Z, Li X, Yin W, Shen X, Porta C, Walter TS, Evans G, Axford D, Owen R, Rowlands DJ, Wang J, Stuart DI, Fry EE, Rao Z. A sensor-adaptor mechanism for enterovirus uncoating from structures of EV71. Nature Structural and Molecular Biology. 2012b; 19(4) 424-9.

Wang Y, Qing J, Sun Y, Rao Z. Suramin inhibits EV71 infection. Antiviral Research. 2013b; 103C: 1-6.

Wang Z, Wang G. APD: the Antimicrobial Peptide Database. Nucleic Acids Research. 2004; 32: D590-2.

Warfield KL, Swenson DL, Olinger GG, Nichols DK, Pratt WD, Blouch R, Stein DA, Aman MJ, Iversen PL, Bavari S. Gene-specific countermeasures against Ebola virus based on antisense phosphorodiamidate morpholino oligomers. PLoS Pathogens. 2006; 2: e1.

Weng TY, Chen LC, Shyu HW, Chen SH, Wang JR, Yu CK, Lei HY, Yeh TM. Lactoferrin inhibits enterovirus 71 infection by binding to VP1 protein and host cells. Antiviral Research. 2005; 67(1): 31-7.

Wild CT, Shugars DC, Greenwell TK, McDanal CB, Matthews TJ. Peptides corresponding to a predictive alpha-helical domain of human immunodeficiency virus type 1 gp41 are potent inhibitors of virus infection. Proceedings of the National Academy of Science U S A. 1994; 91(21): 9770-4.

Wimmer E, Mueller S, Tumpey TM, Taubenberger JK. Synthetic viruses: a new opportunity to understand and prevent viral disease. Nature Biotechnology. 2009; 27(12): 1163-72.

Witherell G. AG-7088 Pfizer. Current Opinion in Investigational Drugs. 2000; 1(3): 297-302.

Wong KT, Munisamy B, Ong KC, Kojima H, Noriyo N, Chua KB, Ong BB, Nagashima K. The distribution of inflammation and virus in human enterovirus 71 encephalomyelitis suggests possible viral spread by neural pathways. Journal of Neuropathology and Experimental Neurology. 2008; 67(2): 162-9.

Wu KX, Ng MM, Chu JJ. Developments towards antiviral therapies against enterovirus 71. Drug Discovery Today. 2010; 15(23-24): 1041-1051.

Wu Z, Yang F, Zhao R, Zhao L, Guo D, Jin Q. Identification of small interfering RNAs which inhibit the replication of several enterovirus 71 strains in China. Journal of Virological Methods. 2009; 159(2): 233-8.

WuDunn D, Spear PG. Initial interaction of herpes simplex virus with cells is binding to heparan sulfate. Journal of Virology. 1989; 63(1): 52-8.

Yamayoshi S, Iizuka S, Yamashita T, Minagawa H, Mizuta K, Okamoto M, Nishimura H, Sanjoh K, Katsushima N, Itagaki T, Nagai Y, Fujii K, Koike S. Human SCARB2-dependent infection by coxsackievirus A7, A14, and A16 and enterovirus 71. Journal of Virology. 2012; 86(10): 5686-96.

Yamayoshi S, Koike S. Identification of a human SCARB2 region that is important for enterovirus 71 binding and infection. Journal of Virology. 2011; 85(10): 4937-46.

Yamayoshi S, Ohka S, Fujii K, Koike S. Functional comparison of SCARB2 and PSGL1 as receptors for enterovirus 71. Journal of Virology. 2013; 87(6): 3335-47.

Yamayoshi S, Yamashita Y, Li J, Hanagata N, Minowa T, Takemura T, Koike S. Scavenger receptor B2 is a cellular receptor for enterovirus 71. Nature Medicine. 2009; 15(7): 798-801.

Yanagi M, Purcell RH, Emerson SU, Bukh J. Transcripts from a single full-length cDNA clone of hepatitis C virus are infectious when directly transfected into the liver of a chimpanzee. Proceedings of the National Academy of Science U S A. 1997; 94(16): 8738-43.

Yang B, Chuang H, Yang KD. Sialylated glycans as receptor and inhibitor of enterovirus 71 infection to DLD-1 intestinal cells. Virology Journal. 2009; 6: 141.

Yang SL, Chou YT, Wu CN, Ho MS. Annexin II binds to capsid protein VP1 of enterovirus 71 and enhances viral infectivity. Journal of Virology. 2011; 85(22): 11809-20.

Yang Z, Li G, Zhang Y, Liu X, Tien P. A novel minicircle vector based system for inhibiting the replication and gene expression of enterovirus 71 and coxsackievirus A16. Antiviral Research. 2012; 96(22): 234-44.

Yeh MT, Wang SW, Yu CK, Lin KH, Lei HY, Su IJ, Wang JR. A single nucleotide in stem loop II of 5'-untranslated region contributes to virulence of enterovirus 71 in mice. PLoS ONE. 2011; 6: e27082.

Yi L, He Y, Chen Y, Kung HF, He ML. Potent inhibition of human enterovirus 71 replication by type I interferon subtypes. Antiviral Therapy. 2011; 16(1): 51-8.

Yoke-Fun C, AbuBakar S. Recombinant human enterovirus 71 in hand, foot and mouth disease patients. Emerging Infectious Diseases. 2004; 10(8): 1468-70.

Youngblood DS, Hatlevig SA, Hassinger JN, Iversen PL, Moulton HM. Stability of cell-penetrating peptide-morpholino oligomer conjugates in human serum and in cells. Bioconjugate Chemistry. 2007; 18(1): 50-60.

Yu H, Chen W, Chang H, Tang R, Zhao J, Gan L, Liu B, Chen J, Wang M. Genetic analysis of the VP1 region of enterovirus 71 reveals the emergence of genotype A in Central China in 2008. Virus Genes. 2010; 41(1): 1-4.

Yu SF, Lloyd RE. Identification of essential amino acid residues in the functional activity of poliovirus 2A protease. Virology. 1991; 182(2): 615-25.

Yuan J, Stein DA, Lim T, Qiu D, Coughlin S, Liu Z, Wang Y, Blouch R, Moulton HM, Iversen PL, Yang D. Inhibition of coxsackievirus B3 in cell cultures and in mice by peptide-conjugated morpholino oligomers targeting the internal ribosome entry site. Journal of Virology. 2006; 80(23): 11510-9.

Zaini Z, McMinn P. Complete genome sequence of a human enterovirus 71 strain isolated in Brunei in 2006. Genome Announcements. 2013; 1(4): e00522-13.

Zaini Z, Phuektes P, McMinn P. A reverse genetic study of the adaptation of human enterovirus 71 to growth in Chinese hamster ovary cell cultures. Virus Research. 2012; 165(2): 151-6.

Zamecnik PC, Stephenson ML. Inhibition of Rous sarcoma virus replication and cell transformation by a specific oligodeoxynucleotide. Proceedings of the National Academy of Science U S A. 1978; 75(1): 280-4.

Zautner AE, Jahn B, Hammerschmidt E, Wutzler P, Schmidtke M. N- and 6-O-sulfated heparan sulfates mediate internalization of coxsackievirus B3 variant PD into CHO-K1 cells. Journal of Virology. 2006; 80(13): 6629-36.

Zhang G, Zhou F, Gu B, Ding C, Feng D, Xie F, Wang J, Zhang C, Cao Q, Deng Y, Hu W, Yao K. In vitro and in vivo evaluation of ribavirin and pleconaril antiviral activity against enterovirus 71 infection. Archives of Virology. 2012; 157(4): 669-79.

Zhang H, Curreli F, Zhang X, Bhattacharya S, Waheed AA, Cooper A, Cowburn D, Freed EO, Debnath AK. Antiviral activity of alpha-helical stapled peptides designed from the HIV-1 capsid dimerization domain. Retrovirology. 2011; 8: 28.

Zhang X, Lalezari JP, Badley AD, Dorr A, Kolis SJ, Kinchelow T, Patel IH. Assessment of drug-drug interaction potential of enfuvirtide in human immunodeficiency virus type 1-infected patients. Clinical Pharmacology and Therapeutics. 2004; 75(6): 558-68.

Zhang X, Song Z, Qin B, Chen L, Hu Y, Yuan Z. Rupintrivir is a promising candidate for treating severe cases of enterovirus-71 infection: evaluation of antiviral efficacy in a murine infection model. Antiviral Research. 2013; 97(3): 264-9.

Zhang XN, Song ZG, Jiang T, Shi BS, Hu YW, Yuan ZH. Rupintrivir is a promising candidate for treating severe cases of enterovirus-71 infection. World Journal of Gastroenterology. 2010a; 16(2): 201-9.

Zhang Y, Zhu Z, Yang W, Ren J, Tan X, Wang Y, Mao N, Xu S, Zhu S, Cui A, Yan D, Li Q, Dong X, Zhang J, Zhao Y, Wan J, Feng Z, Sun J, Wang S, Li D, Xu W. An emerging recombinant human enterovirus 71 responsible for the 2008 outbreak of hand foot and mouth disease in Fuyang city of China. Virology Journal. 2010b; 7: 94.

Zheng BJ, Guan Y, Hez ML, Sun H, Du L, Zheng Y, Wong KL, Chen H, Chen Y, Lu L, Tanner JA, Watt RM, Niccolai N, Bernini A, Spiga O, Woo PC, Kung HF, Yuen KY, Huang JD. Synthetic peptides outside the spike protein heptad repeat regions as potent inhibitors of SARS-associated coronavirus. Antiviral Therapy. 2005; 10(3): 393-403.

Zhu W, Li J, Liang G. How does cellular heparan sulfate function in viral pathogenicity? Biomedical and Environmental Sciences. 2011; 24(1): 81-7.

APPENDICES

Appendix I Reagents for growth media

DMEM growth medium

2X DMEM	500 ml
FBS	100 ml
Penicillin/streptomycin	10 ml
NEAA	10 ml
L-glutamine	10 ml
MiliQ H_2O	370 ml

The media was stored at 4 ℃ until use.

DMEM maintenance medium

2X DMEM	500 ml
FBS	20 ml
Penicillin/streptomycin	10 ml
NEAA	10 ml
L-glutamine	10 ml
MiliQ H_2O	450 ml

The media was stored at 4 ℃ until use.

Plaque medium (1.2% w/v carboxymethylcellulose)

2X DMEM	500 ml
FBS	20 ml
Penicillin/streptomycin	10 ml
NEAA	10 ml
L-glutamine	10 ml
MiliQ H_2O	450 ml
Carboxymethylcellulose	12 g

The media was stored at 4 ℃ until use.

Super optimal broth with catabolite repression (SOC) medium

Tryptone	2 %
Yeast extract	0.5 %
NaCl	10 mM
KCl	2.5 mM
$MgCl_2$	10 mM
$MgSO_4$	10 mM
Glucose	20 mM

Appendix II Materials for SDS-PAGE

Polyacrylamide gel

	5% separating gel (5 ml)	12% resolving gel (8 ml)
30% acrylamide/ 0.8% bisacrylamide	0.83 ml	3.20 ml
1.5 M Tris-HCl, pH 8.8	-	2.00 ml
1.0M Tris-HCl, pH 6.8	1.25 ml	-
10% SDS	50 µl	80 µl
10% Ammonium persulphate	50 µl	80 µl
TEMED	5 µl	8 µl
MiliQ H_2O	2.82 ml	1.32 ml

6x SDS loading buffer

1 M Tris-HCl, pH 6.8	3.75 ml
SDS	1.2 g
Glycerol	6 ml
DTT	0.93 g
Bromophenol Blue	6 mg

Top up to 25 ml with miliQ H_2O and stored at -20 ℃ until use.

SDS running buffer

Tris-Base	25 mM
Glycine	192 mM
SDS	0.1 %

SDS staining solution

Ethanol	40 %
Acetic acid	10 %
Coomassive Brilliant Blue	0.1 %
miliQ H_2O	50 %

SDS destaining solution

Ethanol	40 %
Acetic acid	10 %
Distilled water	50 %

Appendix III Material for western blot

Anode buffer I	
Tris-base	0.3 M
Methanol	10 %
pH	10.4

Anode buffer II	
Tris-base	25 mM
Methanol	10%
pH	10.4

Cathode buffer	
Tris-base	25 mM
Glycine	40 mM
Methanol	10 %
pH	9.4

Appendix IV List of 95 overlapping synthetic peptides covering the VP1 capsid protein

1 : GDRVADVIESSIGDS
2 : VADVIESSIGDSVSR
3 : VIESSIGDSVSRALT
4 : SSIGDSVSRALTQAL
5 : GDSVSRALTQALPAP
6 : VSRALTQALPAPTGQ
7 : ALTQALPAPTGQNTQ
8 : QALPAPTGQNTQVSS
9 : PAPTGQNTQVSSHRL
10 : TGQNTQVSSHRLDTG
11 : NTQVSSHRLDTGEVP
12 : VSSHRLDTGEVPALQ
13 : HRLDTGEVPALQAAE
14 : DTGEVPALQAAEIGA
15 : EVPALQAAEIGASSN
16 : ALQAAEIGASSNTSD
17 : AAEIGASSNTSDESM
18 : IGASSNTSDESMIET
19 : SSNTSDESMIETRCV
20 : TSDESMIETRCVLNS
21 : ESMIETRCVLNSHST
22 : IETRCVLNSHSTAET
23 : RCVLNSHSTAETTLD
24 : LNSHSTAETTLDSFF
25 : HSTAETTLDSFFSRA
26 : AETTLDSFFSRAGLV
27 : TLDSFFSRAGLVGEI
28 : SFFSRAGLVGEIDLP
29 : SRAGLVGEIDLPLEG
30 : GLVGEIDLPLEGTTN
31 : GEIDLPLEGTTNPNG
32 : DLPLEGTTNPNGYAN
33 : LEGTTNPNGYANWDI
34 : TTNPNGYANWDIDIT
35 : PNGYANWDIDITGYA
36 : YANWDIDITGYAQMR
37 : WDIDITGYAQMRRKV
38 : DITGYAQMRRKVELF
39 : GYAQMRRKVELFTYM
40 : QMRRKVELFTYMRFD
41 : RKVELFTYMRFDAEF
42 : ELFTYMRFDAEFTFV
43 : TYMRFDAEFTFVACT
44 : RFDAEFTFVACTPTG
45 : AEFTFVACTPTGEVV
46 : TFVACTPTGEVVPQL
47 : ACTPTGEVVPQLLQY
48 : PTGEVVPQLLQYMFV
49 : EVVPQLLQYMFVPPG
50 : PQLLQYMFVPPGAPK
51 : LQYMFVPPGAPKPES
52 : MFVPPGAPKPESRES
53 : PPGAPKPESRESLAW
54 : APKPESRESLAWQTA
55 : PESRESLAWQTATNP
56 : RESLAWQTATNPSVF
57 : LAWQTATNPSVFVKL
58 : QTATNPSVFVKLTDP
59 : TNPSVFVKLTDPPAQ
60 : SVFVKLTDPPAQVSV
61 : VKLTDPPAQVSVPFM
62 : TDPPAQVSVPFMSPA
63 : PAQVSVPFMSPASAY
64 : VSVPFMSPASAYQWF
65 : PFMSPASAYQWFYDG
66 : SPASAYQWFYDGYPT
67 : SAYQWFYDGYPTFGE
68 : QWFYDGYPTFGEHKQ
69 : YDGYPTFGEHKQEKD
70 : YPTFGEHKQEKDLEY
71 : FGEHKQEKDLEYGAC
72 : HKQEKDLEYGACPNN
73 : EKDLEYGACPNNMMG
74 : LEYGACPNNMMGTFS
75 : GACPNNMMGTFSVRT
76 : PNNMMGTFSVRTVGS
77 : MMGTFSVRTVGSSKS
78 : TFSVRTVGSSKSKYP
79 : VRTVGSSKSKYPLVV
80 : VGSSKSKYPLVVRIY
81 : SKSKYPLVVRIYMRM
82 : KYPLVVRIYMRMKHV
83 : LVVRIYMRMKHVRAW
84 : RIYMRMKHVRAWIPR
85 : MRMKHVRAWIPRPMR
86 : KHVRAWIPRPMRNQN
87 : RAWIPRPMRNQNYLF
88 : IPRPMRNQNYLFKAN
89 : PMRNQNYLFKANPNY
90 : NQNYLFKANPNYAGN
91 : YLFKANPNYAGNSIK
92 : KANPNYAGNSIKPTG
93 : PNYAGNSIKPTGTSR
94 : AGNSIKPTGTSRTAI
95 : SIKPTGTSRTAITTL

PUBLICATIONS

Publications related to thesis

Tan CW, Chan YF, Quah YW, Poh CL. Inhibition of enterovirus 71 infections by octaguanidinium dendrimer-conjugated morpholino oligomers. Antiviral Research. 2014; 107: 35-41.

Tan CW, Poh CL, Sam IC, Chan YF. Enterovirus 71 uses cell surface heparan sulfate glycosaminoglycan as an attachment receptor. Journal of Virology. 2013; 87(1): 611-20.

Tan CW, Chan YF, Sim KM, Tan EL, Poh CL. Inhibition of enterovirus 71 (EV-71) infections by a novel antiviral peptide derived from EV-71 VP1 capsid protein. PLoS ONE. 2012; 7: e34589.

Publication not related to thesis

Lee JJ, Koh YZ, Quak SH, Chow VTK, Tan CW, Poh CL, Chu JJH, Tan EL. Seroproteomics reveals cross-reactivity of anti-enterovirus 71 antibodies with cytoplasmid actin. International Journal of Virology and Molecular Biology. 2012; 1: 12-7.

Editorial

Tan CW, Chan YF. Enterovirus 71 receptor: Promising drug target? Expert Review of Anti-Infective Therapy. 2013; 11: 547-9.

Review article

Tan CW, Lai JKF, Sam IC, Chan YF. Recent development of antiviral agents against enterovirus 71 infection. Journal of Biomedical Science. 2014; 21: 14.

Proceedings:

Poh CL, Chan YF, Quah YW, Tan CW. Inhibition of enterovirus 71 infection by antisense octaguanidinium dendrimer-conjugated morpholino oligomers. 30th Annual Clinical Virology Symposium. Daytona Beach, Florida, USA, 27th April, 2014 – 30th April, 2014.

Tan CW, Chan YF, Quah YW, Poh CL. In vitro antiviral and resistance selection of octaguanidinium conjugated morpholino oligomers against enterovirus 71 infections. Europic 2014, 18th International Picornavirus Meeting. Blankenberge, Belgium, 9th March, 2014 – 14th March, 2014.

Tan CW, Poh CL, Sam IC, Chan YF. Enterovirus 71 uses cell surface heparan sulfate glycosaminoglycan as an attachment receptor. Keystone Symposium on Positive Strand RNA viruses. Boston, Massachusetts, USA, 28th April, 2013 – 3rd May, 2013.

Tan CW, Poh CL, Sam IC, Chan YF. Enterovirus 71 uses cell surface heparan sulfate glycosaminoglycan as an attachment receptor. 19th Scientific Meeting of Malaysian Society for Molecular Biology and Biotechnology. Kuala Lumpur, 31 october, 2012- 1 November 2012.

Tan CW, Chan YF, Sim KM, Tan EL, Poh CL. Inhibition of enterovirus 71 (EV-71) infections by a novel antiviral peptide derived from EV-71 capsid protein VP1. 2011 International Symposium on Infectious Disease and Signal Transduction. Taiwan, 19-20 November, 2011.

Intellectual properties:

Chan YF, Tan CW, Sim KM and Poh CL 2013. Enterovirus 71 antiviral peptide. Malaysia patent application PI2013700382, filed on March 2013. Patent pending.

Poh CL, Chan YF, Tan CW 2014. Agents for the treatment of viral infections. Malaysia patent application PI2014700090, filed on January 2014. Patent pending.

OPEN ACCESS Freely available online

PLoS one

Inhibition of Enterovirus 71 (EV-71) Infections by a Novel Antiviral Peptide Derived from EV-71 Capsid Protein VP1

Chee Wah Tan[1], Yoke Fun Chan[1], Kooi Mow Sim[2], Eng Lee Tan[3], Chit Laa Poh[4]*

1 Department of Medical Microbiology, Faculty of Medicine, University of Malaya, Kuala Lumpur, Malaysia, **2** Department of Chemical Science, Faculty of Science, Universiti Tunku Abdul Rahman, Kampar, Malaysia, **3** Centre for Biomedical and Life Sciences, Singapore Polytechnic, Singapore, Singapore, **4** School of Health and Natural Sciences, Sunway University, Petaling Jaya, Malaysia

Abstract

Enterovirus 71 (EV-71) is the main causative agent of hand, foot and mouth disease (HFMD). In recent years, EV-71 infections were reported to cause high fatalities and severe neurological complications in Asia. Currently, no effective antiviral or vaccine is available to treat or prevent EV-71 infection. In this study, we have discovered a synthetic peptide which could be developed as a potential antiviral for inhibition of EV-71. Ninety five synthetic peptides (15-mers) overlapping the entire EV-71 capsid protein, VP1, were chemically synthesized and tested for antiviral properties against EV-71 in human Rhabdomyosarcoma (RD) cells. One peptide, SP40, was found to significantly reduce cytopathic effects of all representative EV-71 strains from genotypes A, B and C tested, with IC_{50} values ranging from 6–9.3 μM in RD cells. The *in vitro* inhibitory effect of SP40 exhibited a dose dependent concentration corresponding to a decrease in infectious viral particles, total viral RNA and the levels of VP1 protein. The antiviral activity of SP40 peptide was not restricted to a specific cell line as inhibition of EV-71 was observed in RD, HeLa, HT-29 and Vero cells. Besides inhibition of EV-71, it also had antiviral activities against CV-A16 and poliovirus type 1 in cell culture. Mechanism of action studies suggested that the SP40 peptide was not virucidal but was able to block viral attachment to the RD cells. Substitutions of arginine and lysine residues with alanine in the SP40 peptide at positions R3A, R4A, K5A and R13A were found to significantly decrease antiviral activities, implying the importance of positively charged amino acids for the antiviral activities. The data demonstrated the potential and feasibility of SP40 as a broad spectrum antiviral agent against EV-71.

Citation: Tan CW, Chan YF, Sim KM, Tan EL, Poh CL (2012) Inhibition of Enterovirus 71 (EV-71) Infections by a Novel Antiviral Peptide Derived from EV-71 Capsid Protein VP1. PLoS ONE 7(5): e34589. doi:10.1371/journal.pone.0034589

Editor: Jianming Qiu, University of Kansas Medical Center, United States of America

Received November 4, 2011; **Accepted** March 2, 2012; **Published** May 1, 2012

Funding: This work was supported by grants from UTAR (Universiti Tunku Abdul Rahman) Research Fund (6200/P04), University of Malaya Research Grant (RG245/10HTM), Sunway University Research Grant (INT-SHNS-0111-01) awarded to CLP and High Impact Research Grant (UM.C/625/1/HIR/014) awarded to YFC. The funders had no role in study design, data collection and analysis, decision to publish, or preparation of the manuscript.

Competing Interests: The authors have declared that no competing interests exist.

* E-mail: chitlaa.poh@gmail.com

Introduction

Enterovirus 71 (EV-71) belongs to the Human Enterovirus A species of the genus Enterovirus within the family *Picornaviridae* [1]. EV-71 is composed of a single-stranded, positive-sense RNA of approximately 7411 nucleotides enclosed within an icosahedral capsid assembled from 60 copies of each of the four structural proteins, VP1–VP4 [2].

EV-71 is one of the main etiological agents of hand, foot and mouth disease (HFMD) which is generally regarded as a mild childhood disease. HFMD is characterized by the development of mild febrile illness with papulovesicular lesions on the hand, foot and mouth. Several epidemics with high mortalities have occurred in Europe in the 1970s (Bulgaria 1975 and Hungary in 1978) [3,4]. However, in recent years, it has emerged as a pathogen capable of causing severe neurological complications such as brain stem encephalitis and acute flaccid paralysis in infants and young children (<6 years old) in Asia [5–7]. The impact of high fatalities and long-term neurological sequelae in severely infected children isolated from large scale HFMD outbreaks in Malaysia (1997),Taiwan (1998) and China (2009) indicated that EV-71 should be regarded as the most feared neurotrophic enterovirus after the eradication of poliovirus [8–10]. Currently, there is no vaccine for prevention or antiviral to treat EV-71 infections [6,11]. Thus, there is a need to develop better and effective antiviral agents to treat future EV-71 infections.

Peptides that can block viral attachment or entry into host cells have therapeutic potentials. Enfuvirtide is the first peptide-based inhibitor of viral fusion approved by the FDA in March, 2003 for clinical use. Enfuvirtide is a 36-amino acid peptide derived from the HR2 sequence of the transmembrane protein gp41 of HIV-1 and is the prototype of new antivirals [12,13]. Recent studies have discovered potential antiviral peptides against Hepatitis C by screening 441 overlapping peptides (18-mers) covering the entire HCV polyprotein [14] and a peptide derived from the pre-S1 surface protein of Hepatitis B virus was able to exhibit antiviral properties against Hepatitis B virus infection [15]. Shih *et al.* (2004) showed that BPROZ-194 binds to VP1 and was effective in inhibiting viral attachment or viral uncoating. This indicated that VP1 is a good target to derive potentially antiviral peptide sequences [16].

In the present study, 95-overlapping peptides (15-mers) covering the entire EV-71 capsid protein, VP1, were chemically synthesized. These peptides were screened for their ability to inhibit EV-71 infection in Rhabdomyosarcoma (RD) cells. Four peptides were found to inhibit EV-71 infection by more than 80% when

screened at 100 μM. One peptide, SP40, was selected for further studies as it was able to inhibit EV-71 infection at 89% in RD cells and it mimics the sequence that is highly conserved in all EV-71 genotypes.

Materials and Methods

Cell and Viruses

Rhabdomyosarcoma (RD, ATCC # CCL-136) cells, African green monkey kidney (Vero, ATCC # CCL-81) cells, human cervical adenocarcinoma Epithelial (HeLa, ATCC # CCL-2) cells and human colon adenocarcinoma (HT-29, ATCC # HTB-38) cells were obtained from American Type Culture Collection (ATCC, USA). RD cells were grown in Dulbecco's Modified Eagle's Medium (DMEM) supplemented with 10% fetal bovine serum (FBS). Vero and HeLa cell lines were grown in Eagle Minimal Essential Medium (EMEM) supplemented with 10% FBS. HT-29 cells were grown in McCoy's Medium supplemented with 10% FBS. EV-71 strain 41 (5865/SIN/000009) (GenBank accession number: AF316321), SHA66/97 (GenBank accession number: AM396586); BrCr (GenBank accession number: AB204852) and SHA52 (GenBank accession number: AM396584) were propagated in RD cells supplemented with 2% FBS. Coxsackievirus A16 (strain 22159) and poliovirus type 1 used were clinical isolates and were propagated in RD and Vero cells supplemented with 2% FBS, respectively.

Peptides

A set of 95 overlapping synthetic peptides spanning the entire sequence of the VP1 capsid protein of Enterovirus 71 strain 41 (GenBank accession no. AF316321) was synthesized by Mimotopes Pty Ltd. (Clayton Victoria, Australia). Each peptide contains 15-amino acid residues with 12 residues overlapping with the adjacent peptides. All the peptides were reconstituted in 100% dimethyl sulfoxide (DMSO) and stored at −80°C. The peptide stock solution was diluted to the final concentration of 100 μM in the maintenance medium for initial screening. The final concentration of the DMSO was less than 1%. The peptide that showed inhibition of cytopathic effects was identified and synthesized in larger amounts with >95% HPLC purity grade.

In vitro EV-71 Inhibitory Assay of 95-overlapping Synthetic Peptides

Approximately 1.5×10^4 of RD cells were seeded into each well of a 96-well plate and incubated overnight in a CO_2 incubator supplemented with 5% CO_2. Prior to virus infection, EV-71 (100 PFU) were incubated with 100 μM of each synthetic peptide for 1 hour at room temperature with gentle rocking and then transferred to the plate containing RD cells. After adsorption for 1 hour, the inoculum was removed, and the cells were washed twice with the serum free medium. An aliquot of 100 μl of the fresh maintenance medium supplemented with 2% FBS was added and the infected RD cells were incubated at 37°C for 24 hours. After 24-hour post infection, total infectious viral particles were harvested and titrated with plaque assay.

EV-71 Plaque Assay

The plaque assay was carried out according to Sim *et al.* (2005) with some modifications [17]. In brief, approximately $1.5X10^5$ RD cells were seeded into each well of a 24-well plate, and maintained in the complete growth medium. Prior to viral infection, the complete growth medium was removed. After adsorption for 1 hour, the inocula were removed, and the cells were washed twice, overlaid with 500 μl plaque medium (containing 1.2% carboxymethylcellulose and 2% FBS). After 48 hours of incubation, cells were fixed with 4% formaldehyde and stained with 0.5% crystal violet.

Inhibition Concentration 50% (IC_{50}) Determination

The IC_{50} values of SP40 against EV-71 strains, CV-A16 and poliovirus type 1 were determined using comprehensive assay. In brief, various concentrations of the peptide were prepared and mixed with an equal volume of virus supernatant. The virus-peptide mixtures were then used to infect peptide treated RD cells at a MOI of 0.1. For EV-71, the viral titer was determined by the plaque assay and total viral RNA was quantitated by the RT TaqMan Real-time PCR assay. For CV-A16 and poliovirus type 1, the total infectious viral particles were harvested 24-hour post infection and quantitated by $TCID_{50}$ using Reed and Muench method [18].

Reverse Transcription (RT) TaqMan Real-time PCR Assay

The primers and probe were designed according to Tan *et al.* [19]. The forward primer employed was 5′-GAGCTCTATAGGAGA-TAGTGTGAGTAGGG-3′, the reverse primer was 5′-AT-GACTGCTCACCTGCGTGTT-3′ and the TaqMan probe used was 5′6-FAM-ACTTACCCA/ZEN/GGCCCTGCCAGCTCC-lowa Black FQ-3′. The viral RNA samples were extracted using QIAamp Viral RNA mini kit (QIAGEN, Hilden, Germany) according to the manufacturer's instructions. The RT TaqMan real-time PCR assay was performed with the OneStep™Plus Real Time System (ABI, Carlsbad, USA) using TaqMan® Fast virus 1-step master mix (ABI, Carlsbad, USA) with cDNA synthesis by reverse transcription for 5 minutes at 50°C and subsequently amplified for 40 cycles at 95°C for 3 s, 60°C for 30 s.

SDS-PAGE and Western Blot Analysis

RD cells were seeded at 7.5×10^5 cells/well in a 6-well plate and followed by overnight incubation at 37°C in a CO_2 incubator. Prior to infection, both RD cells and virus were pre-treated with various concentrations of the peptides for 1 hour. At 24-hour post-infection, the cells and viruses were harvested. The cells were lysed using 100 μl of ReadyPrep Sequential Extraction Kit Reagent 2 (Bio-Rad, USA). The protein concentration was determined using the MicroBCA protein assay (Pierce, Rockford, USA). An aliquot of 30 μg of each lysate was electrophoresed in a denaturing 12.5% polyacrylamide gel. The proteins were transferred onto a PVDF membrane (Millipore, Billerica, USA), and the membrane was subsequently blocked in 5% skimmed milk powder in phosphate buffered saline (PBS) with 0.05% Tween-20 for 1 hour in room temperature. The membrane was incubated with 1:1000 diluted anti-EV-71 monoclonal antibody (Millipore, Billerica, USA) or 1:1000 diluted β-actin antibody (Sigma, St. Louis, USA) for 1 hour at room temperature. After the membrane was washed, it was incubated with 1:1000 diluted secondary antibody (HRP-conjugated rabbit anti-mouse antibody, Sigma, St. Louis, USA) for 1 hour at room temperature. The immunoblots were developed with the DAB substrate in stable peroxide substrate solution (Pierce, Rockford, USA).

Mechanism of Action of SP40

RD cells were seeded at 1.5×10^4 cells per well in a 96-well plate and incubated overnight at 37°C in a CO_2 incubator before EV-71 infection with a MOI of 0.1 per well. Peptides were added at various concentrations under the following conditions: (i) Cell protection assay: RD cells were treated with various concentra-

tions of peptide (50 µl/well). After 1 hour, the cells were washed twice with serum free medium and infected with 100 µl/well of EV-71 (1.5×10^4 PFU/ml) for 1 hour. The medium containing virus was replaced with fresh maintenance medium and the viral titer was determined 24-hour post-infection using plaque assay. (ii) Post-infection assay: RD cells were first infected with EV-71 for 1 hour before addition of the peptide. The inocula were replaced with fresh maintenance medium containing various concentrations of peptide (50 µl/well) and the viral titer was determined 24 hours later. (iii) Virucidal assay: EV-71 (1×10^6 PFU/ml) was treated with various concentrations of peptide in 100 µl of maintenance medium for 1 hour. The treated virus was then diluted 200-fold and used to infect cells for 1 hour. The diluted virus-peptide mixtures were replaced with fresh maintenance medium, and the plaque forming unit was determined 24 hours later. (iv) Viral attachment assay: RD cells in the chamber slide (Lab-tek, Rochester, USA) or a 96-well plate or a CellCarrier-96 optic black plate (Perkin-Elmer, Waltham, USA) were pre-treated with the peptide for 1 hour at 4°C and subsequently infected with EV-71 at the MOI of 100 for 1 hour at 4°C. The infected cells in the 96-well plate were washed twice to remove unbound viral particles, the attached EV-71 viral RNA were extracted and quantitated by the RT TaqMan Real-time PCR assay. The infected cells in the chamber slide and the CellCarrier-96 optic black plate were fixed with 4% paraformaldehyde and permeabilized with 0.25% Triton-X. The slide was first blocked with Image-iT^{TM} FX Signal Enhancer (Invitrogen, San Diego, USA) for 1 hour. Subsequently, anti-Enterovirus 71 monoclonal antibody (Millipore, Billerica, USA) was added into the cell-coated well followed by 1:200 diluted Alexa Fluor 488 anti-mouse IgG (Invitrogen, USA) as a secondary antibody. The nuclei of the RD cells were stained with 4,6-diamidino-2-phenylindole (DAPI). The slide was observed under Nikon Eclipse TE2000-E Fluorescence Microscope and the CellCarrier-96 optic black plate was analyzed by Cellomics High Content Screening ArrayScan VTI (Thermo Fisher Scientific, USA) using Spot Detector Bio-Application. The number of spots per field was determined.

Cytotoxicity Assay

Peptide cytotoxicity was determined by a commercially available assay (Celltiter 96 AQueous One Solution Cell Proliferation Assay Reagent, Promega, Madison, WI) following the manufacturer's instructions. Briefly, RD cells ($1.5X10^4$ cells/well) were seeded in a 96-well plate, and the plate was incubated for 24 hours at 37°C. An aliquot of 20 µl of the medium containing the desired concentration of the SP40 peptide was added to the cells. The final concentration of DMSO for all peptide dilutions was adjusted to 0.6% to eliminate the effect of DMSO variation on cell cytotoxicity. After incubation of the cells in the presence of the SP40 peptide overnight at 37°C, 20 µl of the 96 AQ_{queous} One Solution cell proliferation assay reagent were added to each well. The plate was then incubated for 2 hours at 37°C and the absorbance at 490 nm was determined with a 96-well plate reader.

Sequence Alignment and Structure Homology Prediction

The genome sequences of the EV-71 strain 41 (GenBank accession number: AAK13008) and the Mahoney poliovirus strain (GenBank accession number:1PO2_1) were searched using the NCBI Protein website (http://www.ncbi.nlm.nih.gov/protein/). The sequence of the EV-71, VP1 protein was aligned using Clustal W2 program (http://www.ebi.ac.uk/Tools/Clustalw2/index.html). The three-dimensional structure of the VP1-VP4 protein complex of Mahoney strain poliovirus (PDB ID: 1HXS) was selected to predict the possible position of SP40 by homology modeling.

Results

Screening of the VP1 Capsid Protein Peptide Library

To test the potential of using peptides as an antiviral agent, a library of 15-mer peptides (purity at 60–65%) corresponding to residues 1 to 297 of the VP1 capsid protein and overlapping with each other by 12 residues (6 residues on the C-terminal and N-terminal, respectively) were synthesized. All the 95-overlapping peptides were evaluated for their ability to reduce cytopathic effects caused by EV-71 in RD cells, followed by plaque reduction assay as described in the materials and methods. The criterion for designating a peptide as antiviral is the inhibition of at least 80% of plaque formation at a concentration of 100 µM. Fig. 1 shows the locations of the peptides in the EV-71 genome and their antiviral activities in the initial screen. Of the 95-overlapping peptides in the library, there were four peptides, designated as SP40, SP45, SP81 and SP82 that were found to exhibit inhibitory effects against EV-71 plaque formation at 89.3%, 83.7%, 83.7%, and 82.5%, respectively (Fig. 1). The SP40 peptide was selected for further analysis as SP40 showed the highest inhibition of both cytopathic effect and plaque reduction. The amino acid sequence of the SP40 peptide was highly conserved across all genotypes of EV-71 (Table S1). SP40 is a 15-mer peptide (Ac-QMRRKVELF-TYMRFD-NH_2) spanning from position 118 to 132 in the VP1 capsid region. A scrambled-SP40 peptide, designated as SP40X (Ac-REFTMKRMVLFRQDY-NH_2), was synthesized and used as a control throughout the experiments.

Synergistic Antiviral Activities of the SP40 Peptide with SP81

To investigate whether the SP40 peptide exhibited synergistic antiviral activities with other peptides, the SP40 peptide was mixed with SP45, SP55 and SP81 (<70% purities) to a final concentration of 200 µM. Our results demonstrated that the SP40 peptide could best exhibit synergistic antiviral activities with the SP81 peptide to achieve a total viral RNA inhibition of 99.7% when compared to 92.0% being exhibited by 200 µM of the SP40 peptide alone. However, the SP40 peptide had less synergistic effect when combined with the SP45 peptide or the SP55 peptide, with viral RNA inhibitions of 94.3% and 96.0%, respectively. When all the 4 peptides were combined, viral RNA inhibition achieved was at 98.8%.

Antiviral Properties of SP40

To further confirm that the SP40 peptide inhibited EV-71 infection in RD cells, the peptide was synthesized on a larger scale with >95% purity. The peptide was tested in the comprehensive assay against EV-71 at a MOI of 0.1. The results confirmed that SP40 inhibited viral plaque formation and RNA synthesis with inhibition levels achieved at 96.3%±0.8 and 92.0%±9.3, respectively when the peptide was applied at 200 µM (Fig. 2B, Fig.3A and 3B). The SP40 peptide also significantly reduced viral cytopathic effect and protein synthesis when tested in RD cells (Fig. 2A, Fig. 2C). To determine whether the amino acid sequence of the SP40 peptide is critical for the antiviral activities, the antiviral property of the scrambled SP40X peptide was evaluated. The data indicated that the SP40X peptide showed no significant inhibition of EV-71 infection at 200 µM. Two independent experiments confirmed that the SP40 peptide inhibited EV-71 strain 41 infection with an IC_{50} of 7.9 µM±3.5 (Table 1). Interestingly, the SP40 peptide also inhibited all three genotypes of

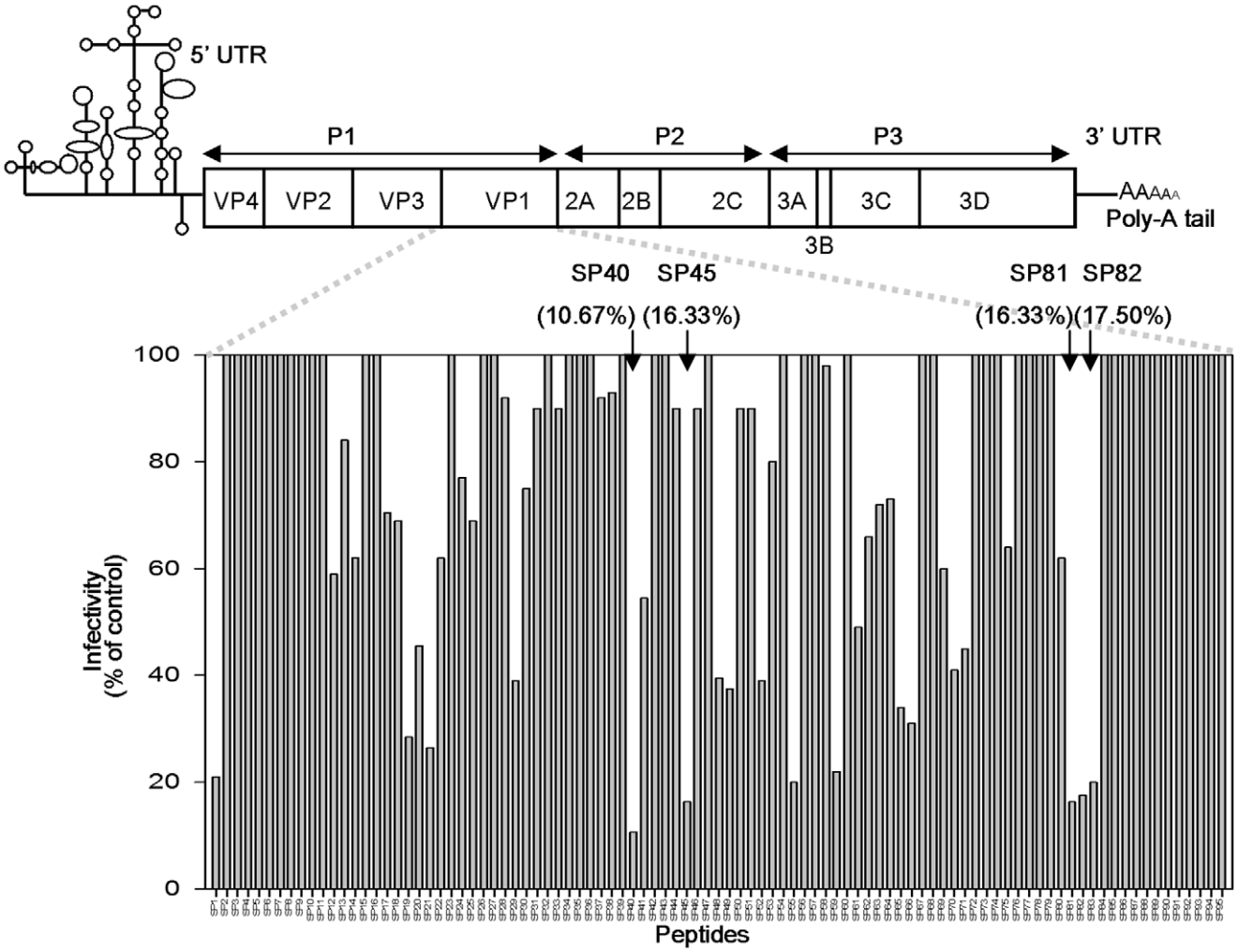

Figure 1. Identification of antiviral peptides. A library consisting of 95-overlapping peptides (15 mers) covering the entire EV-71 capsid protein, VP1 was synthesized. Each peptide was screened at a presumptive concentration of 100 μM for its ability to inhibit EV-71 infection in plaque reduction assay. The top line showed a schematic representation of the EV71 genome, and the activities of the peptides were shown at the bottom. Arrows denote the four peptides that were positive in the assay.
doi:10.1371/journal.pone.0034589.g001

EV-71 (genotypes A, B and C) with IC_{50} values ranging from 6–9.3 μM (Table 1, Fig. 3C). The SP40 peptide was found to inhibit EV-71 induced cytopathic effects and viral RNA synthesis in Vero, HeLa and HT-29 cell lines in a dose-dependent manner (Fig. 4A and 4B). The SP40 peptide also exhibited antiviral activities against CV-A16 and poliovirus type 1 with IC_{50} values of 6 μM±0.8 and 18.22 μM±10.4, respectively. However, the IC_{50} value against poliovirus type 1 was observed at a higher value (Table 1). Hence, we concluded that the SP40 peptide exhibited a broad-spectrum antiviral activity against all EV-71 genotypes as well as other enteroviruses in various cell lines.

Mechanism of Action of SP40

We have found that the SP40 peptide exhibited the strongest inhibitory effect when tested in the comprehensive assay with an IC_{50} of 7.9 μM where both RD cells and EV-71 viral particles were first pre-treated with the SP40 peptide separately before infection (Fig. 3D). This suggested that the SP40 peptide could exert its inhibition at the viral binding step in EV-71 infection or it was virucidal to EV-71 viral particles.

To determine if the SP40 peptide could inactivate EV-71 viral particles, viral supernatant at a MOI of 10 was incubated with the SP40 peptide for 1 hour at room temperature, and subsequently diluted 200-folds and viable viral particles were quantitated by the plaque assay. The results demonstrated that the SP40 peptide could not inactivate EV-71 even when the peptide tested was present at a concentration as high as 200 μM. Hence, SP40 peptide was not virucidal to EV-71 viral particles (Fig. 3D).

To elucidate whether the SP40 peptide could inhibit the viral binding step in EV-71 infection, RD cells were pre-incubated with the SP40 peptide for 1 hour at room temperature before EV-71 infection. The IC_{50} value observed was 15 μM (Fig. 3D). The data indicated that the SP40 peptide could disrupt or interfere the binding of the EV-71 viral particles to cells or it could interfere with post-binding steps. To address this, RD cells were pre-treated with various concentrations of the SP40 peptide at 4°C for 1 hour, followed by EV-71 inoculation at a MOI of 100 at 4°C. The EV-71 viral particles that were attached to the RD cell surface were determined by immunofluorescence assay as described in the Materials and Methods. As shown in Fig. 5A, the number of EV-71 viral particles (green fluorescence) attached to the RD cell

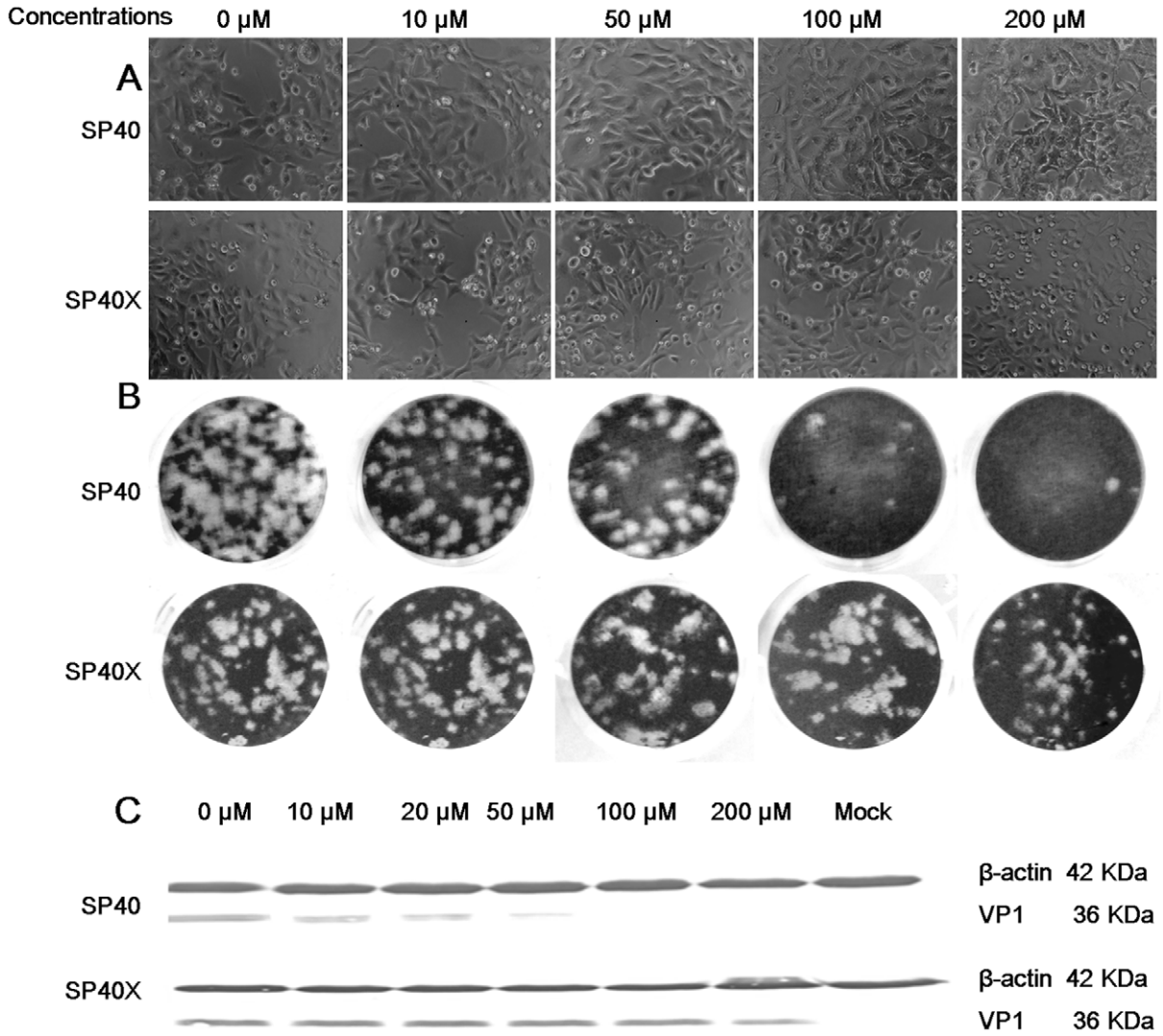

Figure 2. Inhibitory effects of SP40 and SP40X peptides in cytopathic effect, plaque formation and protein synthesis. (A) For cytopathic effect, EV-71 at a MOI of 0.1 was pre-incubated with peptides for 1 hour before infection of peptide-treated RD cells. The images were taken at 24-hour post-infection. (B) For plaque reduction assay, approximately 100 PFU of EV-71 were pre-incubated with peptides for 1 hour before infection of peptide-treated RD cells. The cells were fixed with 4% formaldehyde and stained with 0.5% crystal violet at 48-hour post-infection. (C) Western blot analysis of total protein isolated from virus-infected cells using the EV-71 monoclonal antibody (Millipore, Billerica, USA) and monoclonal anti β-actin antibody (Sigma, St. Louis, USA).
doi:10.1371/journal.pone.0034589.g002

Table 1. IC_{50} of the SP40 peptide against various enteroviruses.

EV-71 strains	Genotypes	Clinical manifestations	IC_{50} (μM)[b]
BrCr	A	Aseptic meningitis	9.3±2.5
SHA66/97	B3	HFMD[a]	6±0.7
41	B4	Fatal	7.9±3.5
SHA52	C2	HFMD	8.5±2.8
Coxsackievirus A16	–	HFMD	6±0.8
Poliovirus type 1	–	–	18.22±10.4

[a]HFMD denotes hand, foot and mouth disease.
[b]The IC_{50}s are the mean ± standard deviations determined from at least two independent experiments.
doi:10.1371/journal.pone.0034589.t001

surface was observed to be reduced when tested in the presence of the SP40 peptide. The results from the Cellomics HCS ArrayScan Spot Detector BioApplication assay showed that the number of viral particles that were attached to the cell surface were reduced from 210±39 viral spots per field to 68±20 viral spots per field in a dose dependent manner (Fig. 5B). Total viral RNA determined by real-time RT-PCR assay confirmed significant reduction of viral RNA following treatment with the SP40 peptide before infection with EV-71 at 4°C (Fig. 5C). To investigate if SP40 inhibited a post-binding step in EV-71 entry to the cells, RD cells were incubated with EV-71 for 1 hour at 4°C, followed by the addition of SP40. The cells were washed and immediately shifted to 37°C for 1 hour to allow post-binding event. No inhibition of plaque formation was observed (data not shown). The results demonstrated that the SP40 peptide disrupted the binding of the EV-71 viral particles to RD cells rather than at the EV-71 during post-binding stage.

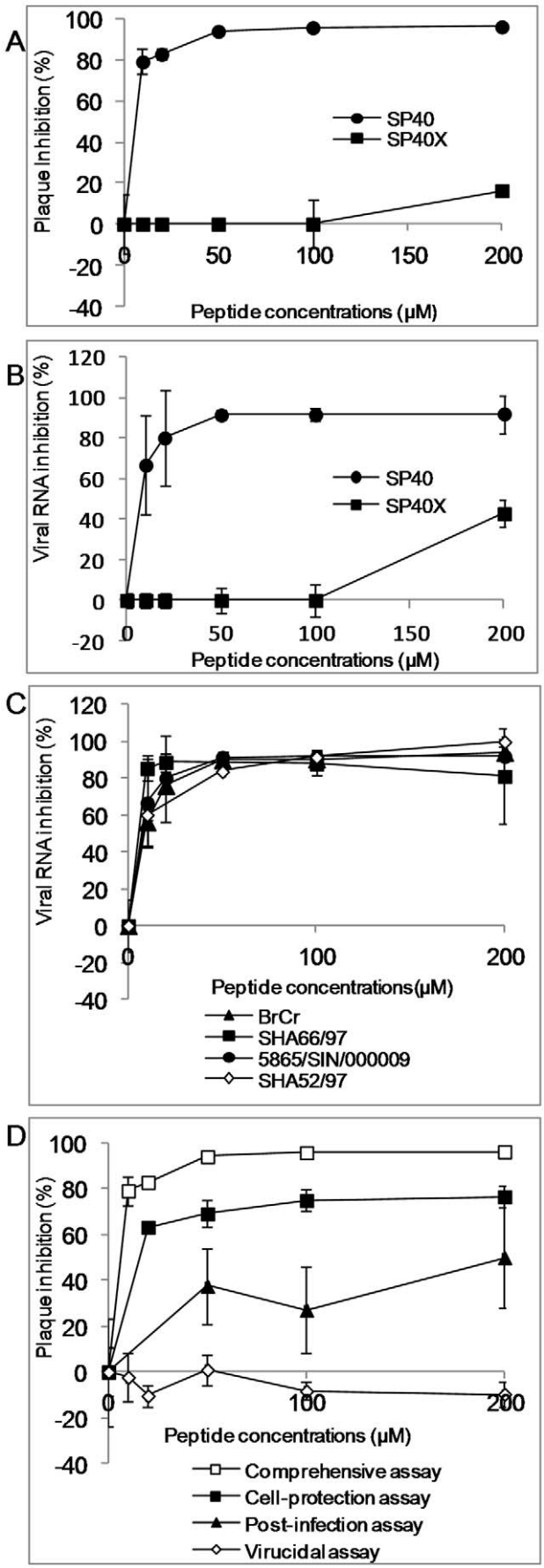

Figure 3. Antiviral activities of the SP40 and SP40X peptides. Both RD cells and EV-71 were separately pre-incubated with increasing concentrations of each peptide for 1 hour before viral inoculation. The inhibitory levels of the peptides were evaluated at 24-hour post-infection by (A) plaque assay and (B) RT TaqMan real-time PCR. (C) Antiviral properties of the SP40 peptide against different EV-71 strains in the comprehensive assay and (D) Mechanism of action studies: The SP40 peptide was added to EV-71 infection at different time points relative to viral inoculation as previously described in the Materials and Methods.
doi:10.1371/journal.pone.0034589.g003

The SP40 peptide was found to be non-inhibitory when added one hour after RD cells were infected with EV-71. The IC_{50} of SP40 peptide after 1 hour post-infection was established to be 200 μM (Fig. 3D).

Residues Critical for Antiviral Activity of SP40

To identify the residues in the SP40 peptide that are critical for antiviral activity, 13 peptides with alanine substitution in each of the amino acid position in the 15-mer SP40 peptide were synthesized. The inhibitory effects in RD cells at 200 μM of all peptides were evaluated. Reduction of viral RNA levels by each of the peptides being evaluated was summarized in Fig. 6. Substitution of the arginine residue at position 3 (P3) with alanine in the SP40 peptide was found to significantly decrease the inhibitory activity (from 95.9% to 61.8%) when compared to substitution at other positions. When positively charged arginine or lysine residues at positions 4, 5 and 13 (P4, P5 and P11) of the SP40 peptide were substituted with alanine, there were moderate losses of activities (from 95.9% reduced to 74.3%, 70.9% and 70.6%, respectively). With only one exception, substitution of the polar methionine residue at position 12 with alanine in the SP40 peptide also reduced the antiviral activity moderately to 74.7%. Alanine substitutions of amino acids at other positions of the SP40 peptide did not alter the antiviral activities when compared to the SP40 peptide. Our data indicated that the positively charged amino acids were critical for the antiviral activities of the SP40 peptide.

Cytotoxicity Assay

To evaluate whether the SP40 peptide was cytotoxic to cells, RD cells were treated with increasing concentrations of the SP40 peptide from 0 μM to 280 μM, and cell viability was determined using CellTiter 96 AQueous One Solution Cell Proliferation Assay Reagent (Promega, Madison, WI). We found that the SP40 peptide was non-cytotoxic to RD cells when tested at the concentration of up to 280 μM. The SP40 peptide was also non-cytotoxic to HeLa, Vero, HT-29 cell lines (data not shown).

Homology Modeling of EV-71

The EV-71 VP1 amino acid sequence was aligned with Mahoney poliovirus using Cluster W2 program and the three dimensional structure of the EV-71 capsid protein based on the poliovirus model was analyzed by the NCBI Cn3D 4.3 software (Fig. 7). The amino acid sequence of the SP40 in the 3D structure is indicated in yellow. The 3D-homology structure of EV-71 indicated that part of the SP40 peptide was exposed on the surface.

Discussion

A Pepscan strategy was employed to screen 95-overlapping synthetic peptides corresponding to the VP1 capsid protein for antiviral activity against EV-71. Four peptides SP40, SP45, SP81 and SP82 were found to exhibit significant antiviral activities. The SP40 peptide was selected for further investigation as the amino

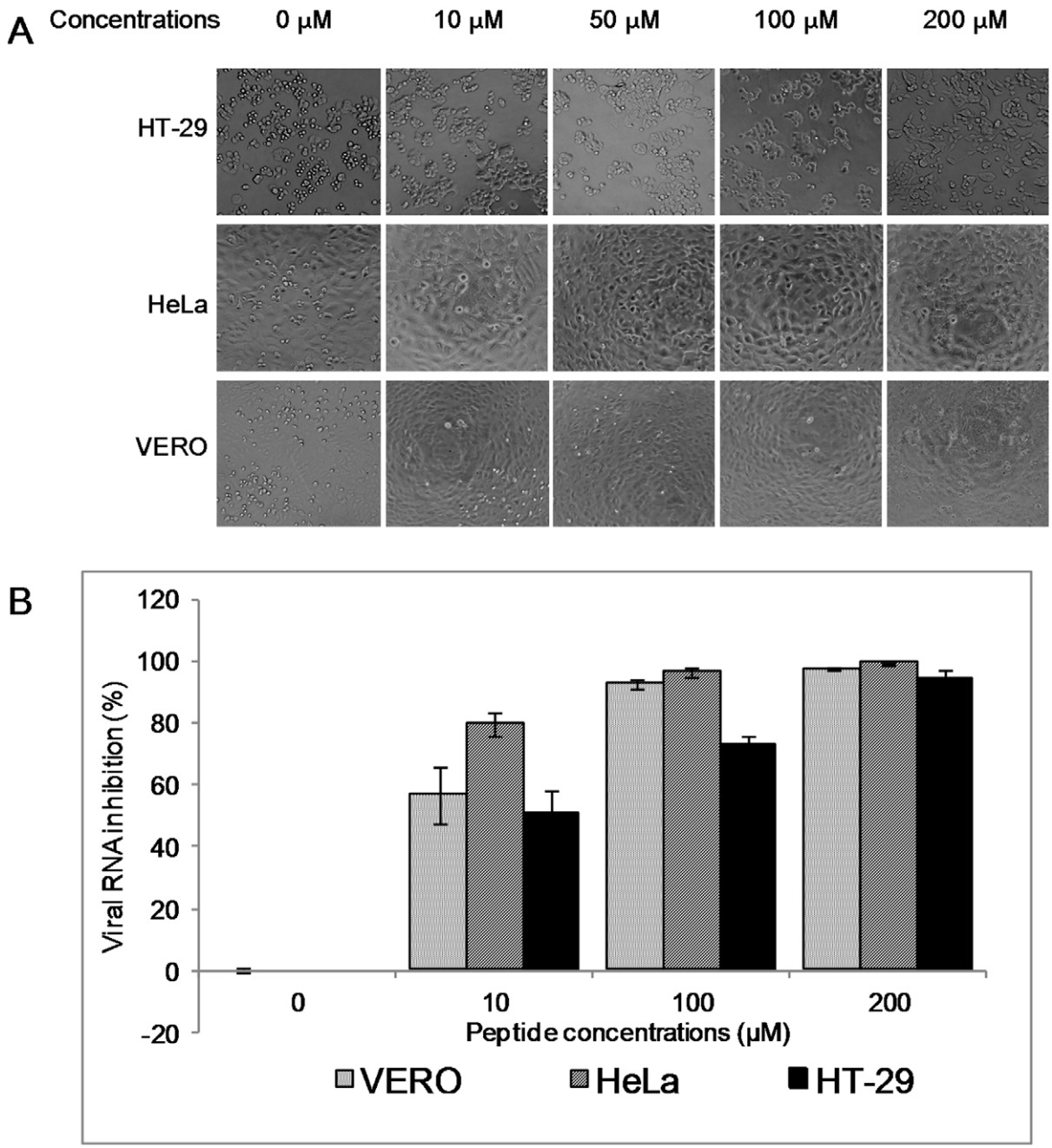

Figure 4. The antiviral activities of the SP40 peptide in various cell lines. Vero, HeLa and HT-29 cell lines were pre-treated with the SP40 peptide at various concentrations for 1 hour at room temperature before infection with EV-71 at a MOI of 0.1. (A) The viral induced cytopathic effects in various cell lines were observed 24-hour post-infection. (B) The viral RNA inhibition that were quantitated by RT TaqMan real-time PCR assay.
doi:10.1371/journal.pone.0034589.g004

acid sequence of SP40 is highly conserved across all EV-71 genotypes and sub-genotypes. Our results demonstrated that the SP40 peptide inhibited EV-71 infection in a dose-dependent manner corresponding to the reduction of viral RNA, VP1 protein and plaque formation. The IC_{50} values reported in our studies ranged from 6–9.3 μM against all representative strains of EV-71 genotypes A, B and C. Interestingly, the SP40 peptide also inhibited CV-A16 and poliovirus type 1 infection *in vitro*, implying that the SP40 peptide could function as a broad-spectrum antiviral agent. However, a higher concentration of SP40 peptide was required to block poliovirus type 1 infection. This could be due to the high degree of dissimilarity of the amino acid sequence present in EV-71 and poliovirus.

The possible mechanism of action of the SP40 peptide could be either through direct viral inactivation or it could block viral attachment and entry. Our data confirmed that the SP40 peptide was not virucidal, but it blocked viral attachment to the cell-surface and hence prevented EV-71 infection. Our immunofluorescence assay and Cellomics HCS ArrayScan showed the number of viral particles attached to the cell surface was reduced significantly when the RD cells were pre-treated with the SP40 peptide before addition of virus at 4°C. The results indicated that

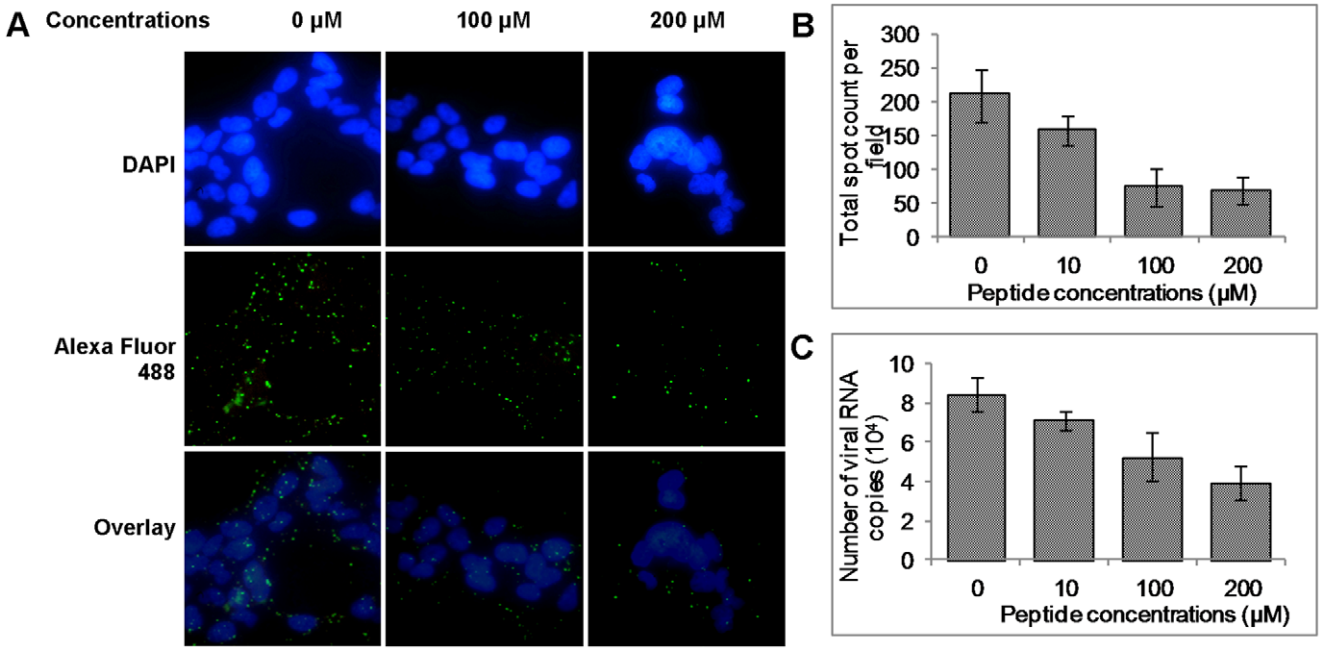

Figure 5. Viral attachment assay. (A) RD cells were grown in the chamber slides (Lab-tek, Rochester, USA) and incubated at room temperature for 1 hour with or without the SP40 peptide. This was followed by the incubation of the cells in the cold with EV-71 for 1 hour and washing off the unbound virions with PBS. RD cell monolayers were fixed with 4% paraformaldehyde and subsequently blocked with Image-iT^{TM} FX Signal Enhancer (Invitrogen, San Diego, USA). The EV-71 particles were probed with anti-EV-71 monoclonal antibody (Millipore, Billerica, USA) and Alexa Fluor 488 anti-mouse IgG (Invitrogen, San Diego, USA). The nuclei were stained with DAPI for 7°minutes at room temperature. The images were obtained from the fluorescent microscopy. EV-71 viral particles and cell nuclei were shown in green and blue fluorescence, respectively. The number of virus particles that was attached to the cell surface were quantitated by (B) Cellomics HCS ArrayScan Spot Detector Bio-Application and (C) RT TaqMan real-time PCR assay
doi:10.1371/journal.pone.0034589.g005

the SP40 peptide probably first interacted with a cell-surface receptor and subsequently prevented EV-71-cellular receptor interactions. However, the SP40 peptide lost its antiviral activity when the peptide was added 1 hour after EV-71 infection.

Previous studies have shown that peptides could play a significant role in surface protein-protein interactions and could exert inhibitory activities against viruses like influenza virus [20], Herpes Simplex virus-1 [21,22], Hepatitis B virus [15], Hepatitis C virus [14,23], HIV-1 [12], Dengue virus and West Nile virus

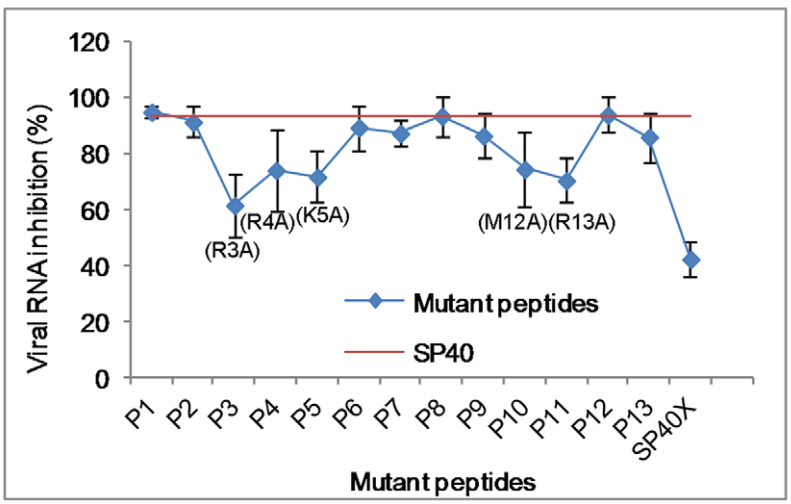

P1: AMRRKVELFTYMRFD
P2: QARRKVELFTYMRFD
P3: QMARKVELFTYMRFD
P4: QMRAKVELFTYMRFD
P5: QMRRAVELFTYMRFD
P6: QMRRKVALFTYMRFD
P7: QMRRKVELATYMRFD
P8: QMRRKVELFAYMRFD
P9: QMRRKVELFTAMRFD
P10: QMRRKVELFTYARFD
P11: QMRRKVELFTYMAFD
P12: QMRRKVELFTYMRAD
P13: QMRRKVELFTYMRFA
SP40X: REFTMKRMVLFRQDY

Figure 6. Alanine scanning analysis. Alanine scanning was performed on the SP40 peptide. Thirteen different peptides were synthesized by replacing one residue at a time with an A and their inhibitory effect was determined as described above. Activity of each peptide was compared with the wild-type SP40, which was represented by the red line. Numbers higher than the red line showed a gain of activity whereas a lower number represented a loss of activity.
doi:10.1371/journal.pone.0034589.g006

A

```
EV71          GDRVADVIESSIGDSVSRALTQALPAPTGQNTQVSSHRLDTGEVPALQAAEIGASSNTSD 60
Poliovirus    --GLGQMGSSSTDNTVRETVGAATSRDALPNTEASGP-THSKEIPALTAVETGATNPLVP 57
                 :.:: .** .::* .::  * .  :  **:.*.   .: *:*** *.* **:.

EV71          ESMIETRCVLNSHSTAETTLDSFFSR--AGLVGEIDLPLEGTTNPNGYANWDIDITGYAQ 118
Poliovirus    SDTVQTRHVVQHRSRSESSIESFFARGACVTIMTVDNPASTTNKDKLFAVWKITYKDTVQ 117
              .. ::** *:: :* :*::::***:*  .  :  :* * . *.: : :* *.*  .. .*
                    SP40
EV71          MRRKVELFTYMRFDAEFTFVACT-----PTGEVVPQLLQYMFVPPGAPKPESRESLAWQT 173
Poliovirus    LRRKLEFFTYSRFDMELTFVVTANFTETNNGHALNQVYQIMYVPPGAPVPEKWDDYTWQT 177
              :***:*:*** *** *:***. :      .*..: *: * *:****** **. :. :***

EV71          ATNPSVFVKLTDPPAQVSVPFMSPASAYQWFYDGYPTFGEHKQ---EKDLEYGACPNNMM 230
Poliovirus    SSNPSIFYTYGTAPARISVPYVGISNAYSHFYDGFSKVPLKDQSAALGDSLYGAASLNDF 237
              ::***:* .   .**::***::. :.**. ****:...  :.*     *  ***.. * :

EV71          GTFSVRTVGSSK-SKYPLVVRIYMRMKHVRAWIPRPMRNQNYLFKANPNYAGNSIKPTGT 289
Poliovirus    GILAVRVVNDHNPTKVTSKIRVYLKPKHIRVWCPRPPRAVAYYGPG-VDYKDGTLTPLST 296
              * ::**.*.. : :* .  :*:*:: **:*.* *** *   *   .  :* ..::.* .*

EV71          SRTAITTL 297
Poliovirus    KDLTTY-- 302
              .  :
```

B

Figure 7. Proposed locations of the SP40 peptide based on sequence alignment and molecular modeling of poliovirus structure. (A) The EV-71 strain 41 was aligned with Mahoney poliovirus strain using Clustal W2 program and (B) The molecular structure of poliovirus VP1, VP2, VP3, and VP4 is represented by purple, blue, brown and green, respectively. The SP40 sequence is indicated in yellow.
doi:10.1371/journal.pone.0034589.g007

[24]. Although the EV-71 capsid protein VP1 has been reported to be responsible in mediating viral adsorption and uncoating process, little information is available about the molecular interactions of EV-71 and cell receptors [25]. Recently, Chen *et al.* [26] had identified several amino acid residues present in the EV-71 capsid protein VP1 that were critical for the molecular interaction between EV-71 and the SCARB2 receptor. These amino acid residues were found within the residues 152–236 of the VP1 protein. None of the amino acids identified was mapped within the SP40 peptide amino acid sequence. This finding suggested that the SP40 peptide probably did not interact with the SCARB2 receptor.

We have demonstrated the importance of the SP40 amino acid sequence for antiviral activities by comparison with a peptide carrying scrambled sequence. The inhibitory effect of the scrambled peptide, SP40X, was significantly lower (at 42.5%) than the effect observed with the SP40 peptide. Since the amino acid sequence of the SP40 peptide was highly conserved across all EV-71 genotypes and was exposed on the surface, this sequence might carry important motif/domain that interacted with an unidentified cell-surface receptor. The SP40 peptide could prevent viral attachment by interacting with cell receptors present on the surfaces of the RD cells, thereby blocking the availability of the receptor for attachment of the EV-71 viral particles. The observation of a significantly reduced IC_{50} value when RD cells were pre-treated with SP40 before EV-71 infection strongly supports this view. The cellular receptor that the SP40 peptide interacted with remained unknown. However, the SP40 peptide could also inhibit CV-A16 and poliovirus type 1 infections *in vitro*, indicating that the SP40 peptide could interact with a common receptor that was probably shared by these viruses.

Since the positively charged amino acids were critical for antiviral activities, the SP40 peptide could interact with cell surface receptors through electrostatic charge interactions. The antiviral activity of the SP40 peptide was not restricted to a specific cell type, but it could block EV-71 infection in different cell lines. This indicated that the SP40 peptide was probably interacting with the receptor that was commonly expressed in most cell types. Interestingly, cell surface glycosaminoglycans are present ubiquitously on the surface of most animal cells and in the extracellular matrix [27]. The presence of several arginine residues in SP40 draws similarity to the antiviral peptide displaying positively charged poly-arginine residues against herpes simplex virus-I (HSV-I) [22]. The antiviral property of the poly-arginine peptide against HSV-I infection in mice was due to an interaction with heparan sulfate. Sequence analysis of the SP40 peptide revealed that it consisted of heparan sulfate glycosaminoglycan specific binding domains (G_1RRRRS$_6$ and R_{28}KVR$_{31}$) present in bovine and human lactoferrins [28–30]. Several studies have reported that lactoferrin was able to bind to ligands such as heparan sulfate and chondroitin sulfate [28,31,32]. It is possible that through this interaction lactoferrin was able to inhibit EV-71 infection [33]. These findings suggested that the SP40 peptide could have interacted with cell surface glycosaminoglycans and prevented EV-71 attachment.

This is the first time that a small novel viral-based peptide (15-mer) derived from VP1 is reported to exhibit antiviral activities against all genotypes and sub-genotypes of EV-71 infection *in vitro*. The development and use of antivirals like enviroxime [34], pleconaril [35], nucleoside analog ribavirin [36] and 3C protease inhibitors [37] for treating enteroviral infection showed variable efficacies against the neurotrophic EV-71 virus [38]. Our results showed that some EV-71 strains were even resistant to ribavirin at 800 μM (unpublished data), this contradicts with the finding of an IC_{50} of 266 μM reported by Li *et al.* [36]. This indicated that ribavirin might not serve as an effective antiviral agent against all EV-71 strains. Other antiviral agents like the viral capsid-binding pyridyl imidazolidinones were found to be ineffective when a single amino acid mutation occurred at position 192 of the hydrophobic pocket of the VP1 capsid protein [16]. The SP40 peptide was found to exhibit very similar antiviral properties with bovine and human lactoferrins which were predicted to prevent viral attachment, possibly by blocking an unknown cellular receptor [33,39]. However, the exact antiviral mechanism of lactoferrin remains to be determined and the SP40 peptide reported in our study has an even lower IC_{50} value at 15 μg/ml when compared to the IC_{50} value of bovine lactoferrin at 34.5 μg/ml [33] or human lactoferrin at 103.3–185.0 μg/ml [39,40]. Thus, SP40 is a good antiviral candidate.

The peptides that blocked the SCARB2 receptor could also be developed as antiviral agents. Chen *et al.* [26] have discovered the amino acid residues in the VP1 capsid protein that are critical for SCARB2 receptor binding. Interestingly, the amino acids in VP1 that are critical for SCARB2 binding were found in the SP45, SP55, and SP81 peptides. The amino acid residues that are important for SCARB2 binding in the SP45, SP55 and SP81 peptides were illustrated in Fig. S1. These peptides were able to inhibit EV-71 infections in a dose-dependent manner with no cytotoxicity to the RD cells (unpublished data). Strong synergistic antiviral activities were observed between the SP40 and the SP81 peptides in RD cells. Since the amino acids critical for binding to SCARB2 were not present in the SP40 peptide, the data suggested that the SP40 peptide could have interacted with a different receptor compared with the SP81 peptide. The additive effects of these two peptides could have significantly reduced the availability of receptors for viral attachment.

Inhibition of viruses at the stage of viral attachment provides a target for therapeutic intervention. Therapeutic peptides have become an attractive tool in drug discovery due to their active regulatory role in the biological system and their extreme high specificity of recognition. The best characterized therapeutic peptide inhibitor is Enfuvirtide (fusion inhibitor) which mimics the N terminal sequence in HIV fusion protein, gp41 [12]. Using peptides as therapeutic agents offer some significant advantages over small chemical molecules or large therapeutic antibodies. A major advantage of peptides is their small size and their high activity and specificity when compared to the antibodies. Peptides are better candidates to inhibit protein-protein interactions that comprise a surface area often too large to be inhibited by small chemical molecules. Peptides accumulate in lesser quantity in tissues, and have very low cell toxicity when compared to small synthetic molecules [41]. Antimicrobial peptides such as lactoferrin, human β-defensin-2 and dermaseptins have been reported to exhibit antiviral properties against various viruses [28,42–46]. Therefore, therapeutic peptides have some advantages over the smaller chemical compounds as antiviral agents.

Since the SP40 peptide works at a very low micromolar concentration and is non-cytotoxic to RD cells, it is potentially an excellent candidate for further development as an antiviral agent. The SP40 peptide was effective when administered before EV-71 infection and could be considered as an excellent candidate for prophylactic intervention. The exact cellular receptor(s) that the SP40 peptide interacted with still remained unknown. Further *in vivo* studies are needed for development of the SP40 as an antiviral agent. Although a major disadvantage of peptides is their low bioavailability due to their rapid degradation in the gastrointestinal system, new formulations, such as the D-isomer peptide and other delivery options are being developed to circumvent these disadvantages [41].

Supporting Information

Figure S1 Diagrammatic illustration of EV-71 VP1 secondary structure. Cylinder and arrow represent α-helix structure and β-sheet, respectively. The effects of mutations examined as to which amino acids were interacting with the SCARB2 receptor was marked as follows: Filled circle indicates those most effective residues for viral binding and infection; open circle indicates partial effective residues [26]. The amino acid sequences of SP40, SP45, SP55 and SP81-83 were shown to

correspond to their secondary structure and location within the VP1 capsid protein.
(TIF)

Table S1 VP1 protein sequences among enteroviruses.
(DOC)

Acknowledgments

We would like to thank our colleagues for their suggestions and technical assistance.

Author Contributions

Conceived and designed the experiments: CWT YFC KMS CLP. Performed the experiments: CWT. Analyzed the data: CWT YFC CLP. Contributed reagents/materials/analysis tools: YFC ELT KMS CLP. Wrote the paper: CWT. Provided EV-71 strain 5865/SIN/000009: ELT. Provided EV-71 strains SHA66, SHA52 and BrCr: YFC.

References

1. Stanway G, Brown F, Christian P, Hovi T, Tyypia T, et al. (2005) Family *Picornaviridae*. In virus taxonomy. In: Fauquet CM, Mayo MA, Maniloff J, Desselberger U, Ball LA, eds. Eighth Report of the International Committee on Taxonomy of viruses. San Diego: Elsevier Academic Pres. pp 757–778.
2. Brown BA, Pallansch MA (1995) Complete nucleotide sequence of Enterovirus 71 distinct from poliovirus. Virus Res 39: 195–205.
3. Shindarov LM, Chumakov MP, Voroshilova MK, Bojinov S, Vasilenko SM, et al. (1979) Epidemiological, clinical, and pathomorphological characteristics of epidemic poliomyelitis-like disease caused by Enterovirus 71. J Hyg Epidemiol Microbiol Immunol 23: 12.
4. Nagy G, Takatsy S, Kukan E, Mihaly I, Domok I (1982) Virological diagnosis of Enterovirus type 71 infections: experiences gained during an epidemic of acute CNS diseases in Hungary in 1978. Arch Virol 71: 217–227.
5. McMinn PC (2002) An overview of the evolution of Enterovirus 71 and its clinical and public health significance. FEMS Microbiol Rev 26: 91–107.
6. Chan YF, Sam IC, Wee KL, AbuBakar S (2011) Enterovirus 71 in Malaysia: A decade later. Neurol Asia 16: 1–15.
7. Chang LY (2008) Enterovirus 71 in Taiwan. Pediatr Neonatol 49: 103–112.
8. Lum LC, Wong KT, Lam SK, Chua KB, Goh AY, et al. (1998) Fatal Enterovirus 71 encephalomyelitis. J Pediatr 133: 795–798.
9. Ho M, Chen ER, Hsu KH, Twu SJ, Chen KT, et al. (1999) An epidemic of Enterovirus 71 infection in Taiwan. Taiwan Enterovirus Epidemic Working Group. N Engl J Med 341: 929–935.
10. Yang F, Ren L, Xiong Z, Li J, Xiao Y, et al. (2009) Enterovirus 71 outbreak in the People's Republic of China in 2008. J Clin Microbiol 47: 2351–2352.
11. Yi L, Lu J, Kung HF, He ML (2011) The virology and developments toward control of human Enterovirus 71. Crit Rev Microbiol 37: 313–327.
12. Kilby JM, Hopkins S, Venetta TM, DiMassimo B, Cloud GA, et al. (1998) Potent suppression of HIV-1 replication in humans by T-20, a peptide inhibitor of gp41-mediated virus entry. Nat Med 4: 1302–1307.
13. Matthews T, Salgo M, Greenberg M, Chung J, DeMasi R, et al. (2004) Enfuvirtide: the first therapy to inhibit the entry of HIV-1 into host CD4 lymphocytes. Nat Rev Drug Discov 3: 215–225.
14. Cheng G, Montero A, Gastaminza P, Whitten-Bauer C, Wieland SF, et al. (2008) A virocidal amphipathic a-helical peptide that inhibits Hepatitis C virus infection in vitro. Proc Natl Acad Sci U S A 105: 3088–3093.
15. Kim DH, Ni Y, Lee SH, Urban S, Han KH (2008) An anti-viral peptide derived from the preS1 surface protein of Hepatitis B virus. BMB Rep 41: 640–644.
16. Shih SR, Tsai MC, Tseng SN, Won KF, Shia KS, et al. (2004) Mutation in Enterovirus 71 capsid protein VP1 confers resistance to the inhibitory effects of pyridyl imidazolidinone. Antimicrob Agents Chemother 48: 3523–3529.
17. Sim AC, Luhur A, Tan TM, Chow VT, Poh CL (2005) RNA interference against Enterovirus 71 infection. Virology 341: 72–79.
18. Reed LJ, Muench H (1983) A simple method of estimating fifty per cent endpoints. The Am J Hyg 27: 493–497.
19. Tan EL, Yong LL, Quak SH, Yeo WC, Chow VT, et al. (2008) Rapid detection of Enterovirus 71 by real-time TaqMan RT-PCR. J Clin Virol 42: 203–206.
20. Jones JC, Turpin EA, Bultmann H, Brandt CR, Schultz-Cherry S (2006) Inhibition of Influenza virus infection by a novel antiviral peptide that targets viral attachment to cells. J Virol 80: 11960–11967.
21. Akkarawongsa R, Pocaro NE, Case G, Kolb AW, Brandt CR (2009) Multiple peptides homologous to Herpes Simplex Virus type 1 glycoprotein B inhibit viral infection. Antimicrob Agents Chemother 53: 987–996.
22. Tiwari V, Liu J, Valyi-Nagy T, Shukla D (2011) Anti-heparan sulfate peptides that block Herpes Simplex Virus infection in vivo. J Biol Chem 286: 25406–25415.
23. Liu R, Tewari M, Kong R, Zhang R, Ingravallo P, et al. (2010) A peptide derived from Hepatitis C virus E2 envelope protein inhibits a post-binding step in HCV entry. Antiviral Res 86: 172–179.
24. Hrobowski YM, Garry RF, Michael SF (2005) Peptide inhibitors of Dengue Virus and West Nile Virus infectivity. Virol J 2: 49.
25. Li C, Wang H, Shih SR, Chen TC, Li ML (2007) The efficacy of viral capsid inhibitors in human enterovirus infection and associated diseases. Curr Med Chem 14: 847–856.
26. Chen P, Song Z, Qi Y, Feng X, Xu N, et al. (2012) Molecular determinants of Enterovirus 71 viral entry: a cleft around Q172 on VP1 interacts with a variable region on scavenge receptor B 2. J Biol Chem 287: 6406–6420.
27. Liu J, Thorp SC (2002) Cell surface heparan sulfate and its roles in assisting viral infections. Med Res Rev 22: 1–25.
28. Jenssen H, Hamill P, Hancock RE (2006) Peptide antimicrobial agents. Clin Microbiol Rev 19: 491–511.
29. Mann DM, Romm E, Migliorini M (1994) Delineation of the glycosaminoglycan-binding site in the human inflammatory response protein lactoferrin. J Biol Chem 269: 23661–23667.
30. Shimazaki K, Tazume T, Uji K, Tanaka M, Kumura H, et al. (1998) Properties of a heparin-binding peptide derived from bovine lactoferrin. J Dairy Sci 81: 2841–2849.
31. Van der Strate BW, Beljaars L, Molema G, Harmsen MC, Meijer DK (2001) Antiviral activities of lactoferrin. Antiviral Res 52: 225–239.
32. Marchetti M, Trybala E, Superti F, Johansson M, Bergstrom T (2004) Inhibition of Herpes Simplex Virus infection by lactoferrin is dependent on interference with the virus binding to glycosaminoglycans. Virology 318: 405–413.
33. Weng TY, Chen LC, Shyu HW, Chen SH, Wang JR, et al. (2005) Lactoferrin inhibits Enterovirus 71 infection by binding to VP1 protein and host cells. Antiviral Res 67: 31–37.
34. Heinz BA, Vance LM (1995) The antiviral compound enviroxime targets the 3A coding region of Rhinovirus and Poliovirus. J Virol 69: 4189–4197.
35. Pevear DC, Tull TM, Seipel ME, Groarke JM (1999) Activity of pleconaril against Enteroviruses. Antimicrob Agents Chemother 43: 2109–2115.
36. Li ZH, Li CM, Ling P, Shen FH, Chen SH, et al. (2008) Ribavirin reduces mortality in Enterovirus 71-infected mice by decreasing viral replication. J Infect Dis 197: 854–857.
37. Patick AK, Ford C, Binford S, Fuhrman S, Brothers M, et al. (1997) Evaluation of the antiviral activity and cytotoxicity of peptide inhibitors of Human Rhinoviurs 3C protease, a novel target for antiviral intervention. Abstracts of the 10th International Conference on Antiviral Research: Antiviral Res. A75 p.
38. Rotbart HA, O'Connell JF, McKinlay MA (1998) Treatment of Human Enterovirus infections. Antiviral Res 38: 1–14.
39. Lin TY, Chu C, Chiu CH (2002) Lactoferrin inhibits Enterovirus 71 infection of human embryonal rhabdomyosarcoma cells in vitro. J Infect Dis 186: 1161–1164.
40. Wu KX, Ng MM, Chu JJ (2010) Developments towards antiviral therapies against Enterovirus 71. Drug Discov Today 15: 1041–1051.
41. Huther A, Dietrich U (2007) The emergence of peptides as therapeutic drugs for the inhibition of HIV-1. AIDS Rev 9: 208–217.
42. Gropp R, Frye M, Wagner TO, Bargon J (1999) Epithelial defensins impair adenoviral infection: implication for adenovirus-mediated gene therapy. Hum Gene Ther 10: 957–964.
43. Andersen JH, Osbakk SA, Vorland LH, Traavik T, Gutteberg TJ (2001) Lactoferrin and cyclic lactoferricin inhibit the entry of human cytomegalovirus into human fibroblasts. Antiviral Res 51: 141–149.
44. Bastian A, Schafer H (2001) Human alpha-defensin 1 (HNP-1) inhibits adenoviral infection in vitro. Regul Pept 101: 157–161.
45. Belaid A, Aouni M, Khelifa R, Trabelsi A, Jemmali M, et al. (2002) In vitro antiviral activity of dermaseptins against herpes simplex virus type 1. J Med Virol 66: 229–234.
46. Andersen JH, Jenssen H, Gutteberg TJ (2003) Lactoferrin and lactoferricin inhibit Herpes simplex 1 and 2 infection and exhibit synergy when combined with acyclovir. Antiviral Res 58: 209–215.

Journal of Virology

Enterovirus 71 Uses Cell Surface Heparan Sulfate Glycosaminoglycan as an Attachment Receptor

Chee Wah Tan, Chit Laa Poh, I-Ching Sam and Yoke Fun Chan

J. Virol. **2013, 87(1):611. DOI: 10.1128/JVI.02226-12.**
Published Ahead of Print 24 October 2012.

JVI Journals.ASM.org

Enterovirus 71 Uses Cell Surface Heparan Sulfate Glycosaminoglycan as an Attachment Receptor

Chee Wah Tan,[a] Chit Laa Poh,[b] I-Ching Sam,[a,c] Yoke Fun Chan[a,c]

Department of Medical Microbiology, Faculty of Medicine, University Malaya, Kuala Lumpur, Malaysia[a]; Faculty of Science and Technology, Sunway University, Selangor, Malaysia[b]; Tropical Infectious Disease Research and Education Center (TIDREC), Faculty of Medicine, University Malaya, Kuala Lumpur, Malaysia[c]

Enterovirus 71 (EV-71) infections are usually associated with mild hand, foot, and mouth disease in young children but have been reported to cause severe neurological complications with high mortality rates. To date, four EV-71 receptors have been identified, but inhibition of these receptors by antagonists did not completely abolish EV-71 infection, implying that there is an as yet undiscovered receptor(s). Since EV-71 has a wide range of tissue tropisms, we hypothesize that EV-71 infections may be facilitated by using receptors that are widely expressed in all cell types, such as heparan sulfate. In this study, heparin, polysulfated dextran sulfate, and suramin were found to significantly prevent EV-71 infection. Heparin inhibited infection by all the EV-71 strains tested, including those with a single-passage history. Neutralization of the cell surface anionic charge by polycationic poly-D-lysine and blockage of heparan sulfate by an anti-heparan sulfate peptide also inhibited EV-71 infection. Interference with heparan sulfate biosynthesis either by sodium chlorate treatment or through transient knockdown of *N*-deacetylase/*N*-sulfotransferase-1 and exostosin-1 expression reduced EV-71 infection in RD cells. Enzymatic removal of cell surface heparan sulfate by heparinase I/II/III inhibited EV-71 infection. Furthermore, the level of EV-71 attachment to CHO cell lines that are variably deficient in cell surface glycosaminoglycans was significantly lower than that to wild-type CHO cells. Direct binding of EV-71 particles to heparin-Sepharose columns under physiological salt conditions was demonstrated. We conclude that EV-71 infection requires initial binding to heparan sulfate as an attachment receptor.

Human enterovirus 71 (EV-71) belongs to the *Enterovirus* genus within the family *Picornaviridae*. The EV-71 genome is a positive-sense, single-stranded RNA enclosed in an icosahedral capsid assembled from 60 copies of each of the four structural proteins, VP1 to VP4 (1).

EV-71 infections usually cause mild hand, foot, and mouth disease (HFMD), characterized by the development of fever with rashes on the palms and feet and with oral ulcers (2). EV-71 also causes severe neurological manifestations, such as aseptic meningitis, brain stem encephalitis, and poliomyelitis-like acute flaccid paralysis (3). In recent years, EV-71 has emerged as an important cause of epidemic viral encephalitis in Asia, resulting in high fatalities among children below the age of 6 years (3, 4).

Receptor binding is an essential event during viral infection. The ability to recognize and interact with specific receptors is one of the factors that contribute to the host range and tissue tropism of a virus (5). To date, at least four EV-71 receptors have been reported. The first receptor to be discovered was the human P-selectin glycoprotein ligand-1 (PSGL-1). PSGL-1 is a sialomucin membrane protein expressed mainly in leukocytes and was hypothesized to facilitate the viremic phase of EV-71 infection (6). The second receptor reported was the human scavenger receptor class B-2 (SCARB2), a type III double-transmembrane protein located primarily in endosomes but also expressed on the cell surface (7–9). Sialylated glycan was also reported as one of the possible receptors for EV-71 infection. Removal of sialic acid residues from plasma membranes was able to protect DLD-1, RD, and SK-N-SH cells from EV-71 infection (10, 11). Annexin II has recently been identified as another possible receptor for EV-71 in RD cells. Pretreatment of EV-71 with soluble annexin II resulted in reduced viral attachment to the cell surface (12). However, inhibitors that blocked all of the receptors identified failed to inhibit EV-71 infection completely (13). This may imply the involvement of one or more EV-71 receptors that have yet to be discovered.

Our previous study identified a novel antiviral peptide, SP40, derived from the VP1 capsid protein (14). This peptide was found to contain a heparan sulfate-specific glycosaminoglycan (GAG) binding domain (-RRKV-), and the positively charged amino acids were found to be critical for antiviral properties. We postulated that SP40 interacted with heparan sulfate and blocked EV-71 attachment (14). Similarly, bovine and human lactoferrin exhibited antiviral activities against EV-71 when tested *in vitro* and *in vivo*, possibly due to direct interaction with heparan sulfate, resulting in interference with EV-71 binding (15, 16). In a recent study, heparin and heparan sulfate were reported to exhibit antiviral activities against EV-71 infection (17). These findings led us to hypothesize that surface heparan sulfate might play an important role in EV-71 attachment.

GAGs are negatively charged linear polysaccharides composed of hexosamine/hexuronic acid repeats. GAGs acquire negative charges through N- and O-sulfation of the carbohydrate moieties (18). The types of GAG include heparin, heparan sulfate, and chondroitin sulfate. GAG-ligand interactions are complex and are characterized either by merely electrostatic forces or by specific interactions (19). Many viral pathogens, such as herpes simplex virus (20, 21), HIV (22, 23), dengue virus (24), human papillomavirus (25), vaccinia virus (26), Theiler's murine encephalomyelitis

Received 19 August 2012 **Accepted** 17 October 2012
Published ahead of print 24 October 2012
Address correspondence to Yoke Fun Chan, chanyf@ummc.edu.my.

doi:10.1128/JVI.02226-12

virus (TMEV) (27), adeno-associated virus type 2 (28, 29), hepatitis B virus (30), hepatitis C virus (31), Sindbis virus (32), echovirus (33), coxsackievirus B3 and A9 (34, 35), and foot-and-mouth disease virus (36, 37), are known to utilize cell surface heparan sulfate as an attachment or entry receptor.

In the present study, we investigate the role of heparan sulfate in the binding of EV-71 to the surface of rhabdomyosarcoma (RD) cells. We provide evidence that the ability of EV-71 to bind to RD cells was reduced after the enzymatic removal of cell surface heparan sulfate and through the obstruction of heparan sulfate biosynthesis. Our results show that cell surface heparan sulfate, and not chondroitin sulfate, serves as an attachment receptor for EV-71.

MATERIALS AND METHODS

Reagents. Soluble GAGs (heparin sodium salt from porcine intestinal mucosa, chondroitin sulfate sodium salt from shark cartilage, *N*-acetyl-de-O-sulfated heparin sodium salt, and de-N-sulfated heparin sodium salt), dextran sulfate sodium salt from *Leuconostoc mesenteroides*, suramin, heparinase I/II/III from *Flavobacterium heparinum*, chondroitinase ABC from *Proteus vulgaris*, and sodium chlorate were all purchased from Sigma. Heparinase I from recombinant *Bacteroides thetaiotaomicron* was supplied by R&D Systems. An anti-EV-71 monoclonal antibody and poly-D-lysine were purchased from Millipore, and Alexa Fluor 488-labeled anti-mouse IgG was purchased from Invitrogen. Anti-heparan sulfate peptides G1 (LRSRTKIIRIRH) and G2 (MPRRRRIRRRQK) (underlining indicates positively charged amino acids), described previously (38), were synthesized by Mimotopes Pty Ltd. (Australia) with >92% purity as determined by high-performance liquid chromatography (HPLC). All the primers and probes were synthesized by IDT.

Cell lines and viruses. All the cell lines used in this experiment were obtained from the American Type Culture Collection (ATCC). Human rhabdomyosarcoma (RD; ATCC no. CCL-136) and Chinese hamster ovary (CHO-K1; ATCC no. CCL-61) cells were grown in Dulbecco's modified Eagle medium (DMEM) (HyClone) supplemented with 10% fetal bovine serum (FBS). Mutant CHO-pgsD677 (ATCC no. CRL-2244) and CHO-pgsA745 (ATCC no. CRL-2242) cells were grown in Kaighn's modification of Ham's F-12 (F-12K) medium (ATCC) supplemented with 10% FBS. All the experiments were carried out using 1.5×10^4 RD cells, unless otherwise stated. EV-71 laboratory strains BrCr (GenBank accession number AB204852), 41 (a gift from Tan Eng Lee, Singapore Polytechnic, Singapore) (GenBank accession number AF316321), UH1/PM/97 (GenBank accession number AM396587), and SHA66/97 (GenBank accession number AM396586) were propagated in RD cells in maintenance medium supplemented with 2% FBS. All the other EV-71 isolates (14716, 35017, 1687413, and 1657640) and the poliovirus (PV) vaccine strain were obtained from the Diagnostic Virology Laboratory, University Malaya Medical Center, Kuala Lumpur, Malaysia. Isolates 14716, 1687413, and 1657640 were all passaged once in tissue culture, while isolate 35017 had been passaged twice. Throughout the study, EV-71 strain 41 was used, unless otherwise stated.

TaqMan quantitative real-time PCR assay. TaqMan quantitative real-time PCR was performed as described previously (14). Forward primer 5′-GAGCTCTATAGGAGATAGTGTGAGTAGGG-3′, reverse primer 5′-ATGACTGCTCACCTGCGTGTT-3′, and TaqMan probe 5′-6-carboxyfluorescein (FAM)-ACTTACCCA/ZEN/GGCCCTGCCAGCT CC-Iowa Black FQ-3′ were used. Viral RNA samples were extracted by using a QIAamp viral RNA minikit (Qiagen, Germany) according to the manufacturer's instructions. The TaqMan real-time reverse transcription (RT)-PCR assay was performed with the StepOnePlus real-time system (ABI) using the TaqMan Fast Virus 1-step master mix (ABI), with cDNA synthesis from RNA by reverse transcription for 5 min at 50°C and subsequent amplification for 40 cycles at 95°C for 3 s and 60°C for 30 s.

Evaluation of the role of GAGs and inhibitors in EV-71 infection of RD cells. Viral inactivation experiments were performed by preincubation of EV-71 particles with various concentrations of GAGs (heparin, chondroitin sulfate, de-N-sulfated heparin, and *N*-acetyl-de-O-sulfated heparin) and inhibitors (dextran sulfate and suramin) for 60 min at 37°C before inoculation of the RD cells. For cell protection studies, RD cells were preincubated with GAGs, poly-D-lysine, or anti-heparan sulfate peptides at various concentrations for 60 min at 37°C. The cells were washed twice and were subsequently infected with various EV-71 isolates for 1 h at a multiplicity of infection (MOI) of 0.1. Viral infectivity was evaluated and quantified by TaqMan real-time PCR and a plaque assay after 24 h postinfection.

Inhibition of cellular GAG sulfation by sodium chlorate. Sodium chlorate inhibition experiments were carried out in DMEM supplemented with 10% FBS. RD cells were cultured for 24 h in the presence of sodium chlorate at concentrations ranging from 0 mM to 50 mM, followed by infection using different EV-71 strains at an MOI of 0.1. The viral titers were quantified by TaqMan quantitative real-time PCR.

siRNA silencing of the gene involved in heparan sulfate biosynthesis. Small interfering RNAs (siRNAs) targeting the heparan sulfate-modifying enzyme *N*-deacetylase/*N*-sulfotransferase 1 (NDST-1) and the heparan sulfate polymerase exostosin-1 (EXT-1) were purchased from Santa Cruz Biotechnology. Negative-control siRNA with no homology to any known mammalian gene was obtained from Bioneer. Different concentrations of the siRNAs (0 nM, 1 nM, 5 nM, 10 nM, and 20 nM in 50 μl of Opti-MEM) were incubated with Lipofectamine 2000 in Opti-MEM I (Invitrogen) for 20 min. The siRNA was then transfected into 1.0×10^4 RD cells for 24 h. Prior to EV-71 infection, the transfection medium was removed, and the cells were washed twice with growth medium (DMEM with 10% FBS) and were then incubated with the growth medium for at least 3 h. The cells transfected with the respective siRNAs were infected with EV-71 at an MOI of 0.1 for 1 h at room temperature. After 1 h of incubation, the inoculum was removed, washed twice, and replaced with maintenance medium (DMEM with 2% FBS). The viral titers were determined at 24 h postinfection by using TaqMan quantitative real-time PCR.

Enzymatic removal of GAGs from the surfaces of RD cells. Chondroitinase ABC and heparinase I/II/III were reconstituted in digestion buffer I (phosphate-buffered saline [PBS] containing 0.05 M sodium acetate and 0.02% bovine serum albumin [BSA] [pH 7.5]) and digestion buffer II (PBS containing 0.5 mM $MgCl_2$, 0.9 mM $CaCl_2$, and 0.1% BSA [pH 7.5]), respectively, and various concentrations of the enzymes (50 μl/well) were added to RD cells, which were then incubated for 1 h at 37°C. Cells were then washed with the respective digestion buffers and were subsequently infected with EV-71 for 1 h at 4°C. After the incubation, the cells were washed twice with serum-free medium, and infectivity was determined 24 h postinfection by TaqMan real-time RT-PCR.

Binding of EV-71 to GAG-deficient cell lines. RD, CHO-K1, CHO-pgsD677, and CHO-pgsA745 cells in chamber slides (Lab-Tek) and CellCarrier-96 plates (Perkin-Elmer) were infected with EV-71 (MOI, 100) at 4°C for an hour. After 1 h of incubation, the inocula were removed and the cells were fixed with 4% formaldehyde. The fixed cells were permeabilized using 0.25% Triton X-100 (Sigma) for 5 min and were subsequently blocked with Image-iT FX signal enhancer (Invitrogen) for 1 h. EV-71 particles were immunostained with mouse anti-EV-71 monoclonal antibodies (Millipore) as the primary antibodies and 1:200-diluted Alexa Fluor 488-labeled anti-mouse IgG (Invitrogen) as the secondary antibody for 1 h at 37°C. For nuclear visualization, cells were treated with 0.01% 4′,6-diamidino-2-phenylindole (DAPI; Sigma) for 7 min at room temperature. Immunofluorescence was detected with a Leica TCS SP5 confocal microscope (Leica Microsystems, Germany). The CellCarrier-96 plate was evaluated using a Cellomics ArrayScan VTI HCS reader with Spot Detector BioApplication software (Thermo Scientific). The data are presented as the total viral spot count per cell (calculated as the total number of fluorescent

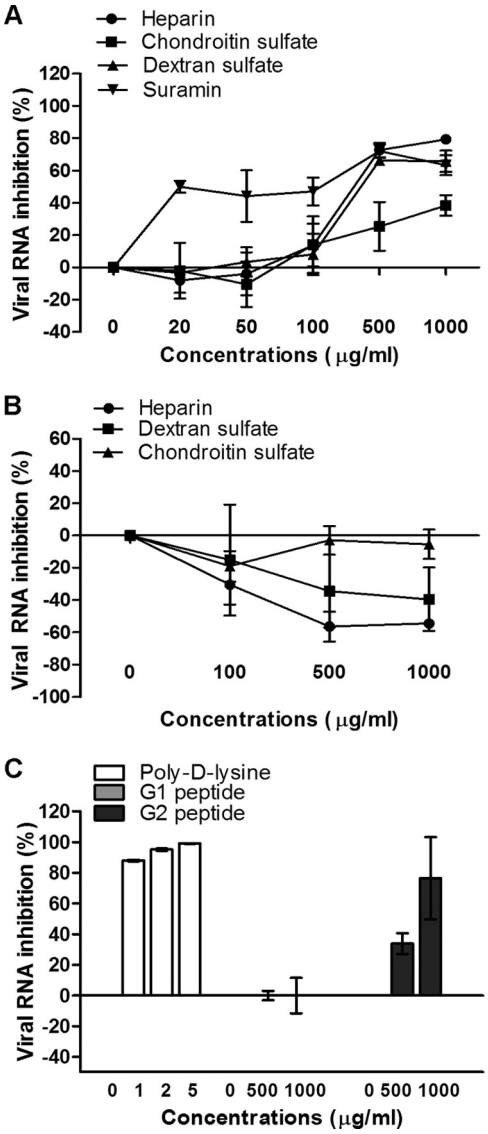

FIG 1 Inhibitory effects of GAGs and inhibitors. (A) For the viral inactivation assay, various concentrations of GAGs, polyanionic dextran sulfate, and suramin were preincubated with EV-71 particles for 1 h at 37°C before infection of RD cells at room temperature. (B and C) For the cell protection assay, various concentrations of GAGs (B) or of poly-D-lysine or anti-heparan sulfate peptides, designated peptides G1 and G2 (C), were preincubated with RD cells for 1 h at 37°C before EV-71 infection. The viral RNA was extracted and quantified by quantitative real-time PCR 24 h postinfection.

viral spots divided by the total number of cells in the same field) and were subsequently verified by TaqMan quantitative real-time PCR.

Binding of EV-71 particles to immobilized heparin-Sepharose beads. Six milliliters of EV-71 or PV vaccine strain supernatant was applied to a 1-ml HiTrap Heparin HP column (GE Healthcare, Sweden) previously equilibrated with the binding buffer (0.02 M Tris-HCl, 0.14 M NaCl [pH 7.4]) at a flow rate of approximately 0.5 ml/min. After loading, the column was washed with at least 5 to 10 column volumes of binding buffer. The bound viral particles were eluted using the elution buffer (0.02 M Tris-HCl, 2 M NaCl [pH 7.4]). Fractions of 1 ml were collected and analyzed by TaqMan quantitative real-time PCR and plaque assays for EV-71 and the PV vaccine strain, respectively.

Cytotoxicity analysis. The cytotoxicities of heparin, dextran sulfate, anti-heparan sulfate peptides, and sodium chlorate were determined using the CellTiter 96 AQueous One solution cell proliferation assay reagent (Promega). Briefly, various concentrations of these compounds were added to overnight-cultured RD cells, which were then incubated overnight. Then 20 μl of the CellTiter 96 AQueous One solution cell proliferation assay reagent was added to each well. The plate was then analyzed at an absorbance of 490 nm after 2 h of incubation at 37°C.

Three-dimensional crystal structure and sequence analysis. The crystal structure of EV-71 (Protein Data Bank [PDB] identification code 4AED) (39) was obtained from the PDB (http://www.rcsb.org/pdb). The 3-dimensional structure of the EV-71 pentamer was built using the DeepView-Swiss PDB Viewer, version 4.0.4 (Swiss Institute of Bioinformatics) (40). For sequence analysis, 174 VP1 sequences from different genotypes (41) were downloaded from GenBank (http://www.ncbi.nlm.nih.gov/protein/) and were aligned using ClustalW2 software (http://www.ebi.ac.uk/tools/msa/clustalw2/).

Statistical analysis. The data presented are the means ± standard deviations (SD) obtained from at least two independent biological replicates. Error bars represent the SD. Statistical significance was calculated using the Mann-Whitney test. A P value of <0.05 was considered statistically significant.

RESULTS

Inhibition of EV-71 infection by heparin, dextran sulfate, and suramin. To determine whether surface GAGs play a significant role in virus-receptor interactions, various concentrations of different GAGs were preincubated with EV-71 at an MOI of 0.1 for 1 h at 37°C before infection of RD cells. The viral titers were quantified 24 h postinfection by using TaqMan quantitative real-time PCR and plaque assays. Of the two GAGs evaluated, significant inhibition of EV-71 by heparin and chondroitin sulfate was observed only at concentrations above 500 μg/ml (Fig. 1A). The inhibitory effect of heparin was more significant, at 79.4% ± 2.9%, than that of chondroitin sulfate (38.5% ± 6.4%) when they were tested at a concentration of 1,000 μg/ml ($P < 0.05$). A similar inhibitory trend was observed in the plaque assays (Table 1).

To further investigate the significance of the carbohydrate backbone for the inhibition of EV-71, polyanionic dextran sulfate (2.3 sulfate groups/glucosyl group) and the polysulfonate pharmaceutical suramin (6.0 sulfate groups/molecule) were used. Previous studies have shown that suramin inhibits viruses such as dengue virus (24) and hepatitis B virus (30), which bind to cell surface heparan sulfate. Viral inhibition increased with the concentration of the inhibitors tested, and at 1,000 μg/ml, the levels of inhibition were 65.8% ± 6.7% for dextran sulfate and 63.4% ± 6.1% for suramin (Table 1). However, suramin was more effective, since it was able to inhibit EV-71 infection at a concentration as low as 20 μg/ml (Fig. 1A).

Preincubation of RD cells with heparin or dextran sulfate at concentrations from 100 to 1,000 μg/ml before viral infection had

TABLE 1 Effects of GAGs, GAG variants, and other inhibitors on EV-71 infection

Inhibitor[a]	Inhibition (%)	
	Viral plaque	Viral RNA
Heparin	95.5 ± 0.7	79.4 ± 2.9
Chondroitin sulfate	52.4 ± 16.4	38.4 ± 6.4
De-N-sulfated heparin	70.0 ± 1.1	39.7 ± 15.6
Dextran sulfate	95.2 ± 0.7	65.8 ± 6.7
Suramin	76.3 ± 2.4	63.4 ± 6.1

[a] The concentration of inhibitors used was 1,000 μg/ml.

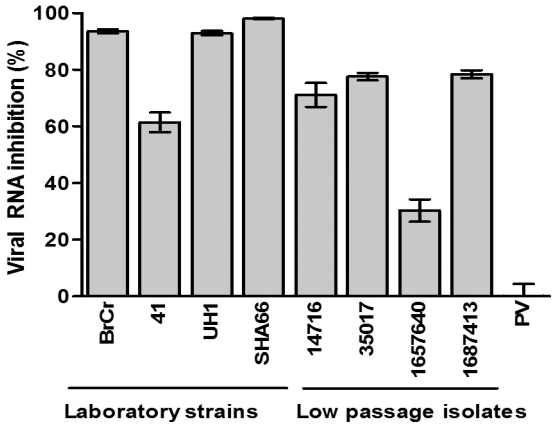

FIG 2 Inhibitory effects of heparin on EV-71 isolates and the PV vaccine strain. EV-71 and PV particles were pretreated with heparin at a final concentration of 2,500 μg/ml for 1 h at 37°C before infection of RD cells. The low-passage-number EV-71 isolates (14716, 35017, 1657640, and 1687413) and the PV vaccine strain were obtained from the Diagnostic Virology Laboratory, University Malaya Medical Center. The titers of EV-71 and the PV vaccine strain were quantified 24 h postinfection by TaqMan quantitative real-time PCR and plaque assays, respectively.

no inhibitory effect but enhanced virus infectivity. The results demonstrated that the inhibitory effect was due to direct interaction of these compounds with the virus and not with the target cells (Fig. 1A and B).

Neutralization of negative charges on cell surfaces reduces EV-71 infection. To assess the important role of negative charges carried on the cell surface in the binding of EV-71, we preincubated RD cells with poly-D-lysine to neutralize negative charges on cell surfaces before infection. As shown in Fig. 1C, poly-D-lysine strongly decreased the level of EV-71 infection when applied at concentrations from 1 to 5 μg/ml. At 5 μg/ml, the inhibition was 99.1% ± 0.2%. To ascertain whether the negative charge carried by heparan sulfate present on the cell surface plays a significant role in viral attachment, two anti-heparan sulfate peptides, G1 (LRSRTKIIRIRH) and G2 (MPRRRRIRRRQK), were evaluated for their inhibitory effects. The inhibitory effect of G2 was significant, with viral RNA inhibition of 76.5% ± 26.8% at 1,000 μg/ml. The G1 peptide did not inhibit EV-71 infection (Fig. 1C).

Heparin reduces the infectivity of both laboratory strains and low-passage-number isolates. Heparin at 2,500 μg/ml was observed to have inhibitory effects both on the laboratory strains and on the low-passage-number EV-71 isolates tested (Fig. 2). The inhibitory effects differed between strains. The level of inhibition of the laboratory strains ranged from 61.4% to 98.0%, while that of the low-passage-number isolates ranged from 30.4% to 78.4%. Interestingly, heparin failed to inhibit the PV vaccine strain even when tested at 2,500 μg/ml.

N- and O-sulfation on heparan sulfate are critical for EV-71 infection. To establish whether the degree of sulfation of heparin is critical for viral inhibition, different sulfated heparin variants were investigated. Completely desulfated heparin failed to abolish EV-71 infection (Fig. 3A). In contrast, de-N-sulfated heparin showed moderate inhibition (39.7% ± 15.6%) at 1,000 μg/ml, indicating that the degree of sulfation within the GAG carbohydrate structure is functionally important. The inhibition of viral plaque formation by these GAGs and inhibitors is shown in Table 1.

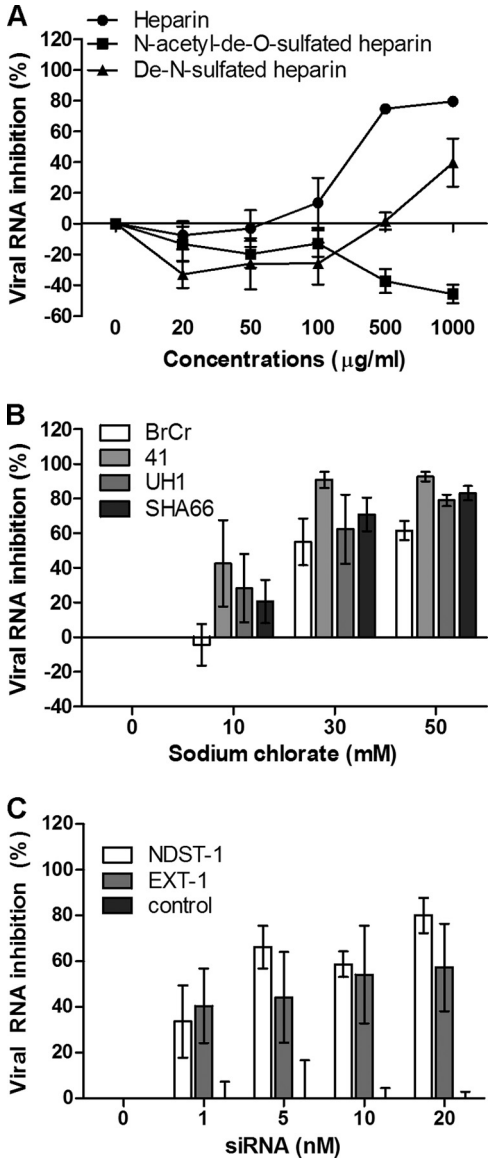

FIG 3 (A) EV-71 was preincubated with various concentrations of heparin and desulfated heparin variants for 1 h at 37°C before infection of RD cells. (B) Inhibitory effect of sodium chlorate on different EV-71 strains in RD cells. RD cells were pretreated with increasing concentrations (0 mM, 10 mM, 30 mM, and 50 mM) of sodium chlorate for 24 h before EV-71 infection at an MOI of 0.1. (C) Transient siRNA knockdown of NDST-1 and EXT-1 expression. NDST-1, EXT-1, and negative-control siRNAs in the Lipofectamine 2000 reagent were transfected into RD cells for 24 h before EV-71 infection. The viral load was determined 24 h postinfection by TaqMan quantitative real-time PCR.

To further confirm the role of the sulfation of heparan sulfate in EV-71 attachment, we carried out EV-71 infection of RD cells grown in a medium containing 0 to 50 mM sodium chlorate. The growth of cells in the presence of sodium chlorate, which inhibits cellular ATP-sulfurylase, has been shown previously to reduce the extent of sulfation of heparan sulfate by as much as 60%, and cells with such modified cell surfaces have been used to examine the role of GAGs in attachment by other viruses (25, 42). As shown in Fig. 3B, sodium chlorate was found to reduce the level of EV-71 infection of RD cells significantly, in a dose-dependent manner,

with all strains tested. At 50 mM, sodium chlorate inhibited infection with EV-71 strains 41, UH1, SHA66, and BrCr; the percentages of viral RNA inhibition were 92.7% ± 2.7%, 79.0% ± 3.3%, 83.2% ± 4.2%, and 61.5% ± 5.5%, respectively. To rule out the possibility that the reduction in the level of EV-71 infection was due to cytotoxicity, the cytotoxicity of sodium chlorate was evaluated by the commercially available 3-(4,5-dimethyl-2-thiazolyl)-2,5-diphenyl-2H-tetrazolium bromide (MTT) assay. The data revealed that sodium chlorate has minimal cytotoxicity at 50 mM.

To further confirm that heparan sulfate plays an important role in EV-71 infection, expression of the NDST-1 and EXT-1 genes was transiently knocked down using siRNA. NDST-1 is a heparan sulfate modification enzyme that removes *N*-acetyl groups from selected *N*-acetylglucosamine (GlcNAc) residues and replaces them with sulfate groups (43). EXT-1 is a heparan sulfate polymerase that adds alternating units of glucuronic acid (GlcA) and GlcNAc to the nonreducing end of the chain. As shown in Fig. 3C, transient knockdown of NDST-1 and EXT-1 expression in RD cells significantly reduced the level of EV-71 infection, with percentages of inhibition as high as 80.1% ± 7.7% and 57.2% ± 19.1%, respectively, at 20 nM siRNA. However, the negative-control siRNA was unable to reduce EV-71 infection.

Enzymatic removal of heparan sulfate from the cell surface reduces the levels of EV-71 binding and infection of RD cells. To identify the type of GAG that is responsible for the binding of EV-71 to RD cells, we examined EV-71 binding to cells after enzymatic removal of cell surface GAGs by chondroitinase ABC and heparinase I/II/III digestion. Heparinase I degrades heparin and highly sulfated domains in heparan sulfate, while heparinase II cleaves both heparin and heparan sulfate, and heparinase III specifically degrades heparan sulfate (24). Treatment of RD cells with each of the heparinases at 2.5 mIU/ml and 5.0 mIU/ml for 1 h at 37°C was found to reduce viral RNA levels and plaque formation significantly (data not shown), in a dose-dependent manner, 24 h postinfection. Treatment of RD cells with heparinases I, II, and III at 5.0 mIU/ml significantly inhibited EV-71 RNA levels by 68.6% ± 6.2%, 91.7% ± 4.1%, and 82.2% ± 11.7%, respectively (Fig. 4A). Removal of cell surface chondroitin sulfate by chondroitinase ABC failed to inhibit EV-71 infection (Fig. 4A), even when chondroitinase ABC was tested at concentrations as high as 20 mIU/ml (data not shown). Removal of cell surface heparan sulfate significantly reduced the infectivities of the different EV-71 strains tested, but not that of the PV vaccine strain (Fig. 4B). Removal of surface heparan sulfate, but not chondroitin sulfate, was found to significantly reduce EV-71 attachment to the surfaces of RD cells (Fig. 4C).

Significant reduction in the level of EV-71 binding to GAG-deficient CHO cells. CHO cells with defects in the biosynthesis of GAGs have been used extensively to demonstrate the involvement of heparan sulfate as the receptor for the binding of various viruses (29, 30, 33, 42, 44). Mutant CHO-pgsD677 cells are deficient in *N*-acetylglucosaminyltransferase and glucuronosyltransferase activities, which are required for heparan sulfate polymerization, and thus completely lack heparan sulfate; these cells also produce levels of chondroitin sulfate 3- to 4-fold higher than those in wild-type CHO-K1 cells (45). Mutant CHO-pgsA745 cells are deficient in the enzyme UDP-D-xylose:serine-1,3-D-xylosyltransferase, which catalyzes the first sugar transfer reaction in GAG formation, and thus completely lack GAGs (46). To investigate whether EV-71 binds differently to these cell lines, cells were seeded in CellCarrier-96 plates and chamber slides and were infected with EV-71 at an MOI of 100 for 1 h at 4°C. As shown in Fig. 5A and B, significantly fewer viral particles were attached to CHO-pgsD677 and CHO-pgsA745 cells than to wild-type CHO-K1 cells, which expressed heparan sulfate ($P < 0.001$). CHO-pgsD677 and CHO-pgsA745 cells showed reduced binding levels of 46.7% and 41.6%, respectively, compared to 100% for CHO-K1 cells. Interestingly, more viral particles were bound to RD cells than to CHO-K1 cells.

Binding of EV-71 to immobilized heparin-Sepharose. To characterize the interaction of EV-71 particles with GAGs, a virus-containing supernatant was applied to a heparin affinity chromatography column. EV-71 particles bound to immobilized heparin-Sepharose under physiological salt conditions (0.14 M NaCl) and were eluted by 2 M NaCl. The virus titers in each fraction collected were quantified by TaqMan quantitative real-time PCR. As shown in Fig. 6, most of the EV-71 particles were detected in all the eluates following the application of 2 M NaCl. The EV-71 particles present in eluate 1 were concentrated as much as 4.1-fold. In a control experiment, we used a column packed with Sepharose alone and found no binding of EV-71 particles to the column (data not shown). The results confirm that EV-71 particles bind to heparin and were eluted by high salt concentrations. In contrast to EV-71, the PV vaccine strain did not interact with heparin-Sepharose, and most of the PV particles were detected in the flow-through fraction (Fig. 6).

Symmetry clustering of highly conserved amino acids Arg166, Lys242, and Lys244 of VP1 in the EV-71 pentamer structure. To determine the possible heparan sulfate binding site(s) on EV-71 particles, the 3-dimensional crystal structure of EV-71 was built using the DeepView-Swiss PDB viewer (40). As shown in Fig. 7A, amino acids Arg166, Lys242, and Lys244 are arranged symmetrically in the 5-fold axis of the EV-71 pentamer structure. These amino acids are also located at positions that are highly exposed on the surface of the EV-71 particle (Fig. 7B). All these amino acids were highly conserved across all EV-71 genotypes except for Lys244, where lysine (K) was replaced by glutamic acid (E) in genotype A (Fig. 7C). This symmetrically arranged clustering of positively charged amino acids could serve as the binding site for heparan sulfate.

DISCUSSION

Virus receptors may be one of the determinants of virus host range and tissue tropism (5). Receptors that are known to bind to EV-71 have been identified over the past few years. P-selectin glycoprotein ligand-1 (PSGL-1) was the first to be discovered as the EV-71 receptor. However, PSGL-1 is selectively expressed only in neutrophils, monocytes, and most lymphocytes (6). The second receptor, reported by Yamayoshi et al. (9), was human SCARB2, which is expressed on most types of cells (7). EV-71 binds to the SCARB2 receptor and is then internalized through clathrin-mediated endocytosis (47, 48). However, blocking of these receptors did not abolish EV-71 infection, and this finding led to the discovery of the third receptor, annexin II. Pretreatment of host cells with an anti-annexin II antibody was found to reduce the level of viral attachment. Preincubation of EV-71 with annexin II also reduced the level of EV-71 infection (12).

Besides these known receptors for EV-71, sialylated glycans were reported by Yang et al. (11) as receptors for EV-71. Treatment of RD, SK-N-SH, and DLD-1 cells with neuraminidase was found to reduce the ability of EV-71 to bind to the cell surface,

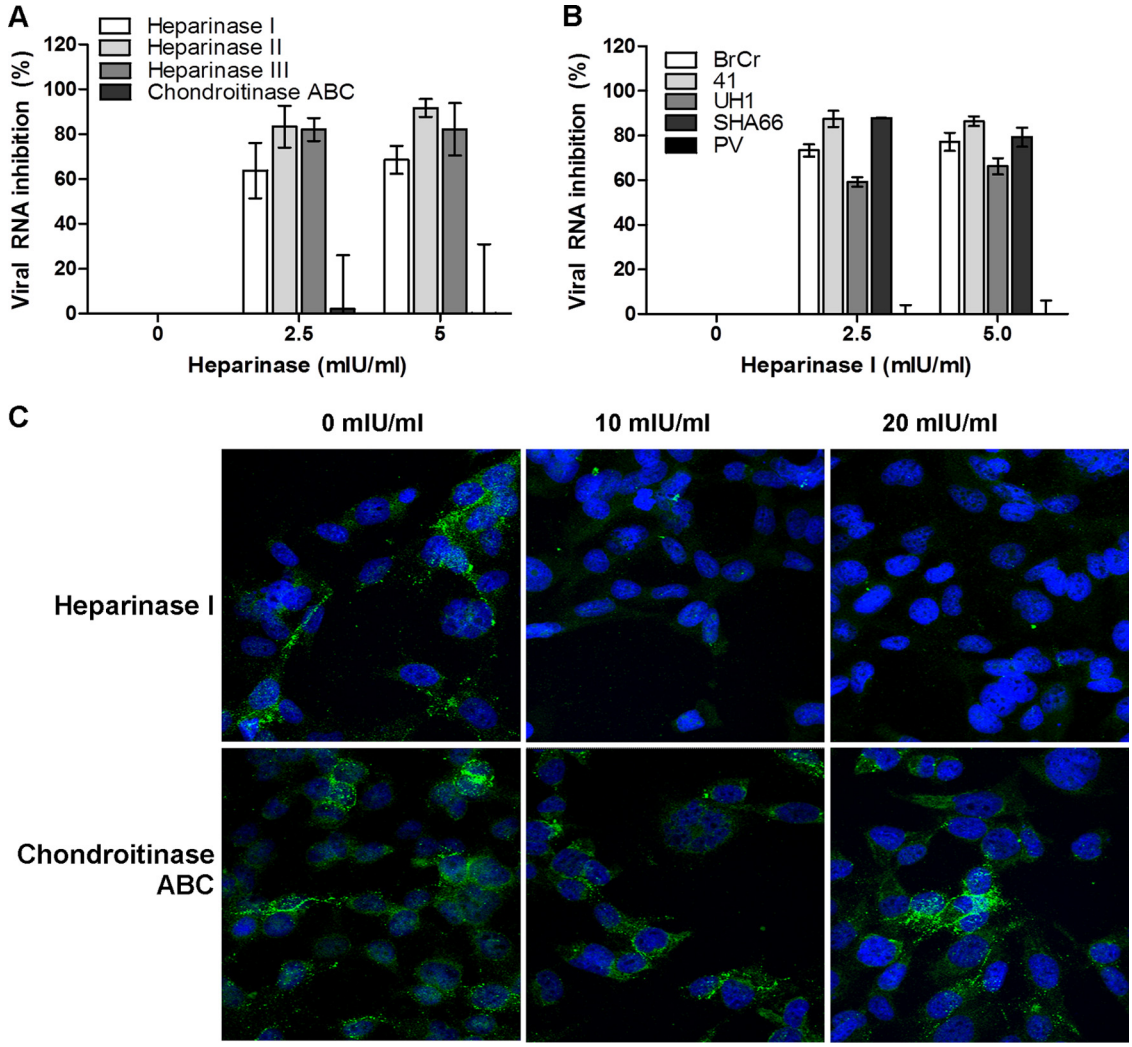

FIG 4 Treatment of RD cells with heparinase or chondroitinase ABC. (A) Inhibitory effects of heparinase I/II/III and chondroitinase ABC on EV-71 infection. RD cells were pretreated with heparinase or chondroitinase ABC for 1 h at 37°C before EV-71 infection at an MOI of 0.1. The viral RNA was extracted and evaluated by TaqMan quantitative real-time PCR. (B) Inhibitory effect of heparinase I on different EV-71 strains and the PV vaccine strain. (C) Confocal microscopy analysis (with a 40× objective) of EV-71 binding assays after heparinase I or chondroitinase ABC treatment. EV-71 particles were stained with a monoclonal anti-EV-71 antibody and were subsequently stained with Alexa Fluor 488-labeled anti-mouse IgG. Nuclei were stained with DAPI. EV-71 particles and nuclei are shown in green and blue, respectively.

confirming that EV-71 utilizes sialylated glycans as attachment factors (10). We have shown in this study that, in addition to the four receptors published to date, cell surface heparan sulfate is required for EV-71 attachment. The level of EV-71 infection of RD cells was significantly reduced when EV-71 particles were pretreated with soluble heparin, dextran sulfate, or suramin. However, preincubation of RD cells with heparin or dextran sulfate did not inhibit EV-71 infection but unexpectedly enhanced it. This may be caused by the creation of artificial binding sites through accumulation of heparin and dextran sulfate on the surfaces of cells (30, 49). These findings imply that heparin or dextran sulfate could bind to the positively charged surfaces of viral particles and prevent the interaction of viral particles with the cell surface, as demonstrated for foot-and-mouth disease virus (50). Removal of cell surface heparan sulfate using each of the heparinases (I, II, and III) also reduced the ability of EV-71 to bind to and infect RD cells, further confirming the important role of heparan sulfate in EV-71 infection. The possible involvement of chondroitin sulfate as a receptor for attachment was excluded based on the evidence that enzymatic removal of chondroitin sulfate did not impair EV-71 infection.

In the present study, we demonstrated that EV-71 can bind to CHO cells. However, CHO cells defective in the biosynthesis of heparan sulfate and chondroitin sulfate exhibited a reduced ability to bind to EV-71, further supporting the role of heparan sulfate in EV-71 infection. While EV-71 could bind to the CHO-K1 cells, no infection was observed, suggesting that EV-71 failed to internalize so as to initiate infection. TMEV GDVII bound to heparan sulfate has been postulated to use protein entry receptors for virus internalization (27). A similar mechanism could be utilized by EV-71. EV-71 particles bound to heparan sulfate may need to interact with known receptors, such as SCARB2 and sialylated glycan, or with an unknown protein entry receptor, to gain entry into cells. CHO cells, of hamster origin, may have a different

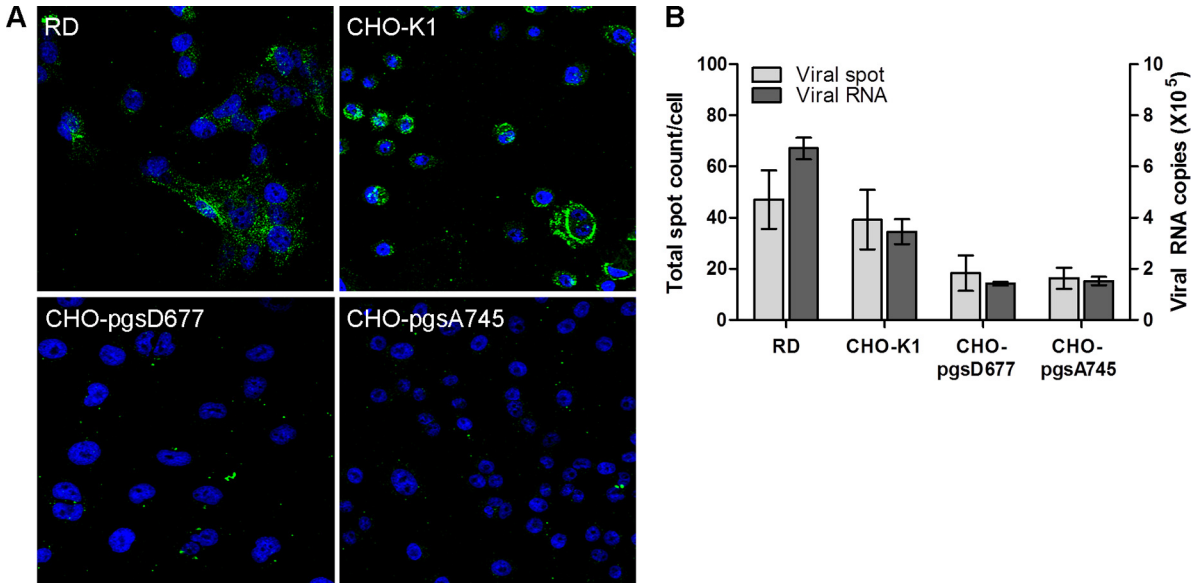

FIG 5 Binding of EV-71 to CHO-K1 and CHO mutant cells. CHO-K1 cells and cells of CHO mutants defective in proteoglycan synthesis were assessed for their abilities to bind to EV-71. The CHO-pgsA745 cell line lacks heparan sulfate and chondroitin sulfate proteoglycans, while the CHO-pgsD677 cell line lacks heparan sulfate proteoglycan but produces 15% of normal proteoglycans. The binding of EV-71 to parental and mutant CHO cells was assayed by using confocal microscopic analysis (A) and a Cellomics ArrayScan VTI HCS reader with Spot Detector BioApplication software (B) and was verified by TaqMan quantitative real-time PCR.

SCARB2, since it has been reported that EV-71 binding domains in human SCARB2 and murine SCARB2 are different (51). In this study, we also showed that EV-71 was still able to bind to the CHO mutant completely lacking in heparan sulfate and chondroitin sulfate, which further suggests that multiple receptors are involved during EV-71 infection. This view is similar to what has been reported for several viruses that use heparan sulfate (27, 52, 53).

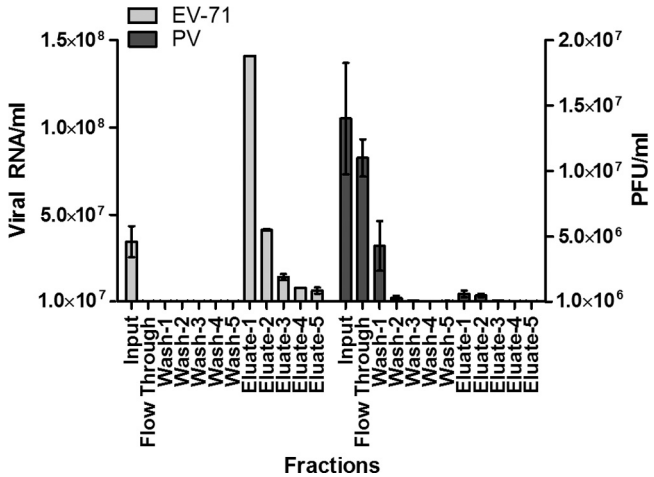

FIG 6 Binding of EV-71 and PV to an immobilized heparin-Sepharose column. EV-71 and PV supernatants were passed through a column of immobilized heparin-Sepharose and were eluted with 2 M NaCl. The titers of EV-71 and the PV vaccine strain from each fraction were quantified by TaqMan quantitative real-time PCR and plaque assays, respectively. EV-71 levels are presented as viral RNA copies per milliliter, and levels of the PV vaccine strain are presented as PFU per milliliter. Error bars represent means ± SD for each fraction.

Heparan sulfate is expressed by all cell types. However, heparan sulfate expressed on different types of cells shows variations in structure, with differences in the degrees of sulfation, chain length, and the position of the sulfate group (54). Our data demonstrated that highly sulfated heparin could inhibit EV-71 infection, whereas decreased sulfation on heparin led to a loss of EV-71 inhibition. Completely desulfated heparin was found to have no inhibitory effect. These findings suggest that structural differences in the heparan sulfate present in different cell types could lead to differences in susceptibility to infection, which may contribute to the selective tropism of EV-71 (37).

Heparan sulfate binding could arise from adaptation to the cells in which isolates were propagated. Culture adaptations of heparan sulfate usage in picornaviruses (55, 56), flaviviruses (57), and alphaviruses (58) have been demonstrated. *In vitro* cultivation of viruses has been shown to rapidly select amino acid substitutions that increase the net positive charge of the envelope protein (59). However, the heparan sulfate binding phenotype has also been documented for clinical isolates of the porcine circoviruses (53) and echoviruses (33). In the present study, we showed that heparin was able to inhibit EV-71 isolates that had been passaged only once in tissue culture, suggesting that heparan sulfate binding phenotypes are not likely to be due to culture adaptation of EV-71. We also provide evidence that heparin failed to inhibit the infection of RD cells with the PV vaccine strain, further strengthening our view that EV-71 binds to heparan sulfate.

Furthermore, we also presented evidence that EV-71 binds to heparin-Sepharose under physiological salt concentrations and that the interaction could be disrupted by high salt concentrations. This finding suggests that EV-71–heparin interactions involve mainly electrostatic charge interactions. Replacement of a single positively charged amino acid with another amino acid is sufficient to retard the heparin binding phenotype in TMEV GDVII

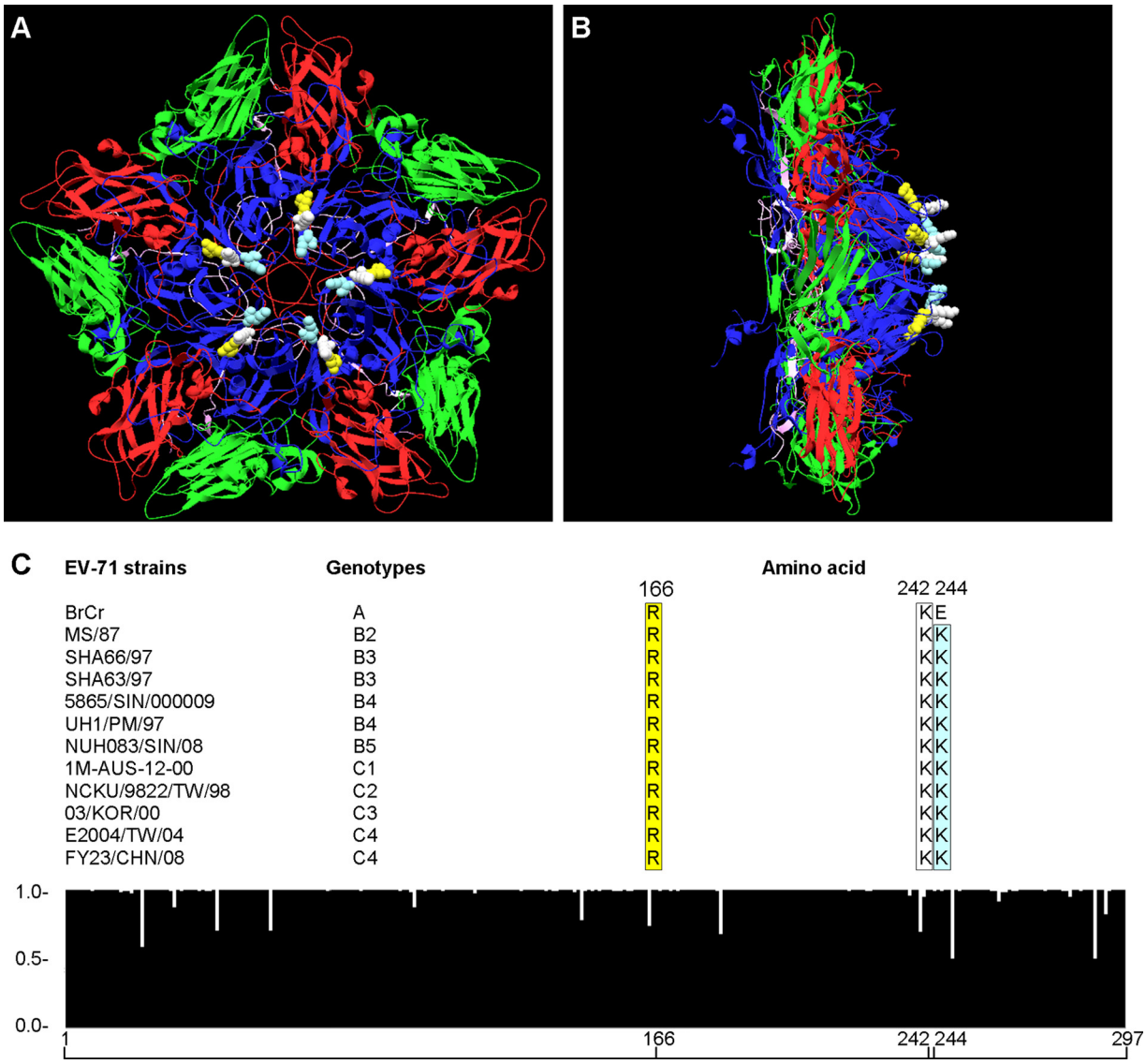

FIG 7 Three-dimensional pentameric structure and sequence alignment of EV-71. The structure of the EV-71 pentamer was generated using the DeepView-Swiss PDB viewer. The molecular structures of EV-71 VP1, VP2, VP3, and VP4 are presented in blue, green, red, and purple, respectively. The amino acids Arg166, Lys242, and Lys244 are presented in yellow, white, and light blue, respectively. (A) Top view of the EV-71 pentamer. (B) Side view of the EV-71 pentamer. (C) Histogram showing sequence consensus in the VP1 region of EV-71. A total of 174 sequences were aligned and analyzed using ClustalW2. The arbitrary scale is shown at the left of the histogram; 1.0 denotes perfect consensus at a given amino acid site across all entries. The alignments of Arg166, Lys242, and Lys244 in representative EV-71 strains from genotypes A, B, and C are shown above the histogram.

and coxsackievirus A9 (27, 34, 60). Thus, positively charged amino acids on the surfaces of viral particles are critical for the heparin binding phenotype. Sequence analysis of the VP1 capsid protein revealed two possible heparan sulfate mimic binding domains, from residues 120 to 123 (-RRKV-) and residues 241 to 244 (-SKSK-). Interestingly, our previous study has shown that peptides with these heparan sulfate binding domains exhibited significant antiviral activities against EV-71 infection in RD cells (14), suggesting that the inhibitory effect could have resulted from direct binding to heparan sulfate and blocking of viral attachment. Heparan sulfate-interacting regions could be linear heparan sulfate binding domains, as well as clusters of basic residues that arise as a result of the 3-dimensional structure, as shown for foot-and-mouth disease virus and coxsackievirus A9 (34, 50). With the recently available crystal structure of EV-71, the electrostatic surface of EV-71 was determined (61). A few conserved positively charged amino acids (Arg166, Lys242, and Lys244) were clustered symmetrically at the 5-fold axis of the EV-71 pentamer. The linear arrangement of these amino acids in the cluster could also be significant for the interactions. These amino acids were also located on the surfaces of EV-71 particles. These findings suggest that the interaction could be due to the electrostatic interactions between these clusters of basic amino acids arranged in a 3-dimensional array on the virions and concentrated negative charges on the sulfated heparan sulfate chain.

In this study, we have shown that EV-71 particles utilized cell surface heparan sulfate as an attachment receptor. Although the exact mechanism of interaction of EV-71 particles with negatively

charged heparan sulfate on the cell surface remains unclear, determination of the molecular basis of the virus-receptor interaction in target cells will be useful for understanding the pathogenicity of EV-71 and for the development of antiviral agents against EV-71.

ACKNOWLEDGMENTS

We acknowledge Lim Fei Tieng (Hi-Tech Instruments Sdn Bhd, Malaysia) for assistance in the confocal microscopy analysis.

This work was supported by University of Malaya research grants (RG245/10HTM and RG298/11HTM), University of Malaya High Impact research grants (E000013-20001 and UM.C/625/1/HIR/014), a Fundamental Research Grant Scheme (FP015/2012A) from the Ministry of Education, Malaysia, a postgraduate research grant (PV013/2012A) from the University of Malaya, and a Sunway University research grant (SHNS-0111-01).

REFERENCES

1. **Brown BA, Pallansch MA.** 1995. Complete nucleotide sequence of enterovirus 71 is distinct from poliovirus. Virus Res. **39**:195–205.
2. **Chan YF, Sam IC, Wee KL, AbuBakar S.** 2011. Enterovirus 71 in Malaysia: a decade later. Neurol. Asia **16**:1–15.
3. **Ooi MH, Wong SC, Lewthwaite P, Cardosa MJ, Solomon T.** 2010. Clinical features, diagnosis, and management of enterovirus 71. Lancet Neurol. **9**:1097–1105.
4. **Solomon T, Lewthwaite P, Perera D, Cardosa MJ, McMinn P, Ooi MH.** 2010. Virology, epidemiology, pathogenesis, and control of enterovirus 71. Lancet Infect. Dis. **10**:778–790.
5. **Haywood AM.** 1994. Virus receptors: binding, adhesion strengthening, and changes in viral structure. J. Virol. **68**:1–5.
6. **Nishimura Y, Shimojima M, Tano Y, Miyamura T, Wakita T, Shimizu H.** 2009. Human P-selectin glycoprotein ligand-1 is a functional receptor for enterovirus 71. Nat. Med. **15**:794–797.
7. **Yamayoshi S, Iizuka S, Yamashita T, Minagawa H, Mizuta K, Okamoto M, Nishimura H, Sanjoh K, Katsushima N, Itagaki T, Nagai Y, Fujii K, Koike S.** 2012. Human SCARB2-dependent infection by coxsackievirus A7, A14, and A16 and enterovirus 71. J. Virol. **86**:5686–5696.
8. **Yamayoshi S, Koike S.** 2011. Identification of a human SCARB2 region that is important for enterovirus 71 binding and infection. J. Virol. **85**:4937–4946.
9. **Yamayoshi S, Yamashita Y, Li J, Hanagata N, Minowa T, Takemura T, Koike S.** 2009. Scavenger receptor B2 is a cellular receptor for enterovirus 71. Nat. Med. **15**:798–801.
10. **Su PY, Liu YT, Chang HY, Huang SW, Wang YF, Yu CK, Wang JR, Chang CF.** 2012. Cell surface sialylation affects binding of enterovirus 71 to rhabdomyosarcoma and neuroblastoma cells. BMC Microbiol. **12**:162. doi:10.1186/1471-2180-12-162.
11. **Yang B, Chuang H, Yang KD.** 2009. Sialylated glycans as receptor and inhibitor of enterovirus 71 infection to DLD-1 intestinal cells. Virol. J. **6**:141. doi:10.1186/1743-422X-6-141.
12. **Yang SL, Chou YT, Wu CN, Ho MS.** 2011. Annexin II binds to capsid protein VP1 of enterovirus 71 and enhances viral infectivity. J. Virol. **85**:11809–11820.
13. **Wu KX, Ng MM, Chu JJ.** 2010. Developments towards antiviral therapies against enterovirus 71. Drug Discov. Today **15**:1041–1051.
14. **Tan CW, Chan YF, Sim KM, Tan EL, Poh CL.** 2012. Inhibition of enterovirus 71 (EV-71) infections by a novel antiviral peptide derived from EV-71 capsid protein VP1. PLoS One **7**:e34589. doi:10.1371/journal.pone.0034589.
15. **Lin TY, Chu C, Chiu CH.** 2002. Lactoferrin inhibits enterovirus 71 infection of human embryonal rhabdomyosarcoma cells in vitro. J. Infect. Dis. **186**:1161–1164.
16. **Weng TY, Chen LC, Shyu HW, Chen SH, Wang JR, Yu CK, Lei HY, Yeh TM.** 2005. Lactoferrin inhibits enterovirus 71 infection by binding to VP1 protein and host cells. Antiviral Res. **67**:31–37.
17. **Pourianfar HR, Poh CL, Fecondo J, Grollo L.** 2012. *In vitro* evaluation of the antiviral activity of heparan sulfate mimetic compounds against enterovirus 71. Virus Res. **169**:22–29.
18. **Honke K, Taniguchi N.** 2002. Sulfotransferases and sulfated oligosaccharides. Med. Res. Rev. **22**:637–654.
19. **Hileman RE, Fromm JR, Weiler JM, Linhardt RJ.** 1998. Glycosaminoglycan-protein interactions: definition of consensus sites in glycosaminoglycan binding proteins. Bioessays **20**:156–167.
20. **Laquerre S, Argnani R, Anderson DB, Zucchini S, Manservigi R, Glorioso JC.** 1998. Heparan sulfate proteoglycan binding by herpes simplex virus type 1 glycoproteins B and C, which differ in their contributions to virus attachment, penetration, and cell-to-cell spread. J. Virol. **72**:6119–6130.
21. **WuDunn D, Spear PG.** 1989. Initial interaction of herpes simplex virus with cells is binding to heparan sulfate. J. Virol. **63**:52–58.
22. **Mondor I, Ugolini S, Sattentau QJ.** 1998. Human immunodeficiency virus type 1 attachment to HeLa CD4 cells is CD4 independent and gp120 dependent and requires cell surface heparans. J. Virol. **72**:3623–3634.
23. **Roderiquez G, Oravecz T, Yanagishita M, Bou-Habib DC, Mostowski H, Norcross MA.** 1995. Mediation of human immunodeficiency virus type 1 binding by interaction of cell surface heparan sulfate proteoglycans with the V3 region of envelope gp120-gp41. J. Virol. **69**:2233–2239.
24. **Chen Y, Maguire T, Hileman RE, Fromm JR, Esko JD, Linhardt RJ, Marks RM.** 1997. Dengue virus infectivity depends on envelope protein binding to target cell heparan sulfate. Nat. Med. **3**:866–871.
25. **Giroglou T, Florin L, Schafer F, Streeck RE, Sapp M.** 2001. Human papillomavirus infection requires cell surface heparan sulfate. J. Virol. **75**:1565–1570.
26. **Chung CS, Hsiao JC, Chang YS, Chang W.** 1998. A27L protein mediates vaccinia virus interaction with cell surface heparan sulfate. J. Virol. **72**:1577–1585.
27. **Reddi HV, Lipton HL.** 2002. Heparan sulfate mediates infection of high-neurovirulence Theiler's viruses. J. Virol. **76**:8400–8407.
28. **Dechecchi MC, Melotti P, Bonizzato A, Santacatterina M, Chilosi M, Cabrini G.** 2001. Heparan sulfate glycosaminoglycans are receptors sufficient to mediate the initial binding of adenovirus types 2 and 5. J. Virol. **75**:8772–8780.
29. **Summerford C, Samulski RJ.** 1998. Membrane-associated heparan sulfate proteoglycan is a receptor for adeno-associated virus type 2 virions. J. Virol. **72**:1438–1445.
30. **Schulze A, Gripon P, Urban S.** 2007. Hepatitis B virus infection initiates with a large surface protein-dependent binding to heparan sulfate proteoglycans. Hepatology **46**:1759–1768.
31. **Barth H, Schafer C, Adah MI, Zhang F, Linhardt RJ, Toyoda H, Kinoshita-Toyoda A, Toida T, Van Kuppevelt TH, Depla E, Von Weizsacker F, Blum HE, Baumert TF.** 2003. Cellular binding of hepatitis C virus envelope glycoprotein E2 requires cell surface heparan sulfate. J. Biol. Chem. **278**:41003–41012.
32. **Byrnes AP, Griffin DE.** 1998. Binding of Sindbis virus to cell surface heparan sulfate. J. Virol. **72**:7349–7356.
33. **Goodfellow IG, Sioofy AB, Powell RM, Evans DJ.** 2001. Echoviruses bind heparan sulfate at the cell surface. J. Virol. **75**:4918–4921.
34. **McLeish NJ, Williams CH, Kaloudas D, Roivainen M, Stanway G.** 2012. Symmetry-related clustering of positive charges is a common mechanism for heparan sulfate binding in enteroviruses. J. Virol. **86**:11163–11170.
35. **Zautner AE, Jahn B, Hammerschmidt E, Wutzler P, Schmidtke M.** 2006. N- and 6-O-sulfated heparan sulfates mediate internalization of coxsackievirus B3 variant PD into CHO-K1 cells. J. Virol. **80**:6629–6636.
36. **Harwood LJ, Gerber H, Sobrino F, Summerfield A, McCullough KC.** 2008. Dendritic cell internalization of foot-and-mouth disease virus: influence of heparan sulfate binding on virus uptake and induction of the immune response. J. Virol. **82**:6379–6394.
37. **Jackson T, Ellard FM, Ghazaleh RA, Brookes SM, Blakemore WE, Corteyn AH, Stuart DI, Newman JW, King AM.** 1996. Efficient infection of cells in culture by type O foot-and-mouth disease virus requires binding to cell surface heparan sulfate. J. Virol. **70**:5282–5287.
38. **Tiwari V, Liu J, Valyi-Nagy T, Shukla D.** 2011. Anti-heparan sulfate peptides that block herpes simplex virus infection in vivo. J. Biol. Chem. **286**:25406–25415.
39. **Plevka P, Perera R, Cardosa J, Kuhn RJ, Rossmann MG.** 2012. Crystal structure of human enterovirus 71. Science **336**:1274. doi:10.1126/science.1218713.
40. **Guex N, Peitsch MC.** 1997. SWISS-MODEL and the Swiss-PdbViewer: an environment for comparative protein modeling. Electrophoresis **18**:2714–2723.
41. **Chan YF, Sam IC, AbuBakar S.** 2010. Phylogenetic designation of enterovirus 71 genotypes and subgenotypes using complete genome sequences. Infect. Genet. Evol. **10**:404–412.
42. **Guibinga GH, Miyanohara A, Esko JD, Friedmann T.** 2002. Cell surface

heparan sulfate is a receptor for attachment of envelope protein-free retrovirus-like particles and VSV-G pseudotyped MLV-derived retrovirus vectors to target cells. Mol. Ther. **5**:538–546.
43. **Presto J, Thuveson M, Carlsson P, Busse M, Wilen M, Eriksson I, Kusche-Gullberg M, Kjellen L.** 2008. Heparan sulfate biosynthesis enzymes EXT1 and EXT2 affect NDST1 expression and heparan sulfate sulfation. Proc. Natl. Acad. Sci. U. S. A. **105**:4751–4756.
44. **Vlasak M, Goesler I, Blaas D.** 2005. Human rhinovirus type 89 variants use heparan sulfate proteoglycan for cell attachment. J. Virol. **79**:5963–5970.
45. **Lidholt K, Weinke JL, Kiser CS, Lugemwa FN, Bame KJ, Cheifetz S, Massague J, Lindahl U, Esko JD.** 1992. A single mutation affects both *N*-acetylglucosaminyltransferase and glucuronosyltransferase activities in a Chinese hamster ovary cell mutant defective in heparan sulfate biosynthesis. Proc. Natl. Acad. Sci. U. S. A. **89**:2267–2271.
46. **Esko JD, Stewart TE, Taylor WH.** 1985. Animal cell mutants defective in glycosaminoglycan biosynthesis. Proc. Natl. Acad. Sci. U. S. A. **82**:3197–3201.
47. **Hussain KM, Leong KL, Ng MM, Chu JJ.** 2011. The essential role of clathrin-mediated endocytosis in the infectious entry of human enterovirus 71. J. Biol. Chem. **286**:309–321.
48. **Lin YW, Lin HY, Tsou YL, Chitra E, Hsiao KN, Shao HY, Liu CC, Sia C, Chong P, Chow YH.** 2012. Human SCARB2-mediated entry and endocytosis of EV71. PLoS One **7**:e30507. doi:10.1371/journal.pone.0030507.
49. **Hilgard P, Stockert R.** 2000. Heparan sulfate proteoglycans initiate dengue virus infection of hepatocytes. Hepatology **32**:1069–1077.
50. **Fry EE, Lea SM, Jackson T, Newman JW, Ellard FM, Blakemore WE, Abu-Ghazaleh R, Samuel A, King AM, Stuart DI.** 1999. The structure and function of a foot-and-mouth disease virus-oligosaccharide receptor complex. EMBO J. **18**:543–554.
51. **Chen P, Song Z, Qi Y, Feng X, Xu N, Sun Y, Wu X, Yao X, Mao Q, Li X, Dong W, Wan X, Huang N, Shen X, Liang Z, Li W.** 2012. Molecular determinants of enterovirus 71 viral entry: cleft around GLN-172 on VP1 protein interacts with variable region on scavenge receptor B2. J. Biol. Chem. **287**:6406–6420.
52. **Delputte PL, Vanderheijden N, Nauwynck HJ, Pensaert MB.** 2002. Involvement of the matrix protein in attachment of porcine reproductive and respiratory syndrome virus to a heparin like receptor on porcine alveolar macrophages. J. Virol. **76**:4312–4320.
53. **Misinzo G, Delputte PL, Meerts P, Lefebvre DJ, Nauwynck HJ.** 2006. Porcine circovirus 2 uses heparan sulfate and chondroitin sulfate B glycosaminoglycans as receptors for its attachment to host cells. J. Virol. **80**:3487–3494.
54. **Shi X, Zaia J.** 2009. Organ-specific heparan sulfate structural phenotypes. J. Biol. Chem. **284**:11806–11814.
55. **Escarmis C, Carrillo EC, Ferrer M, Arriaza JF, Lopez N, Tami C, Verdaguer N, Domingo E, Franze-Fernandez MT.** 1998. Rapid selection in modified BHK-21 cells of a foot-and-mouth disease virus variant showing alterations in cell tropism. J. Virol. **72**:10171–10179.
56. **Sa-Carvalho D, Rieder E, Baxt B, Rodarte R, Tanuri A, Mason PW.** 1997. Tissue culture adaptation of foot-and-mouth disease virus selects viruses that bind to heparin and are attenuated in cattle. J. Virol. **71**:5115–5123.
57. **Lee E, Hall RA, Lobigs M.** 2004. Common E protein determinants for attenuation of glycosaminoglycan-binding variants of Japanese encephalitis and West Nile viruses. J. Virol. **78**:8271–8280.
58. **Klimstra WB, Ryman KD, Johnston RE.** 1998. Adaptation of Sindbis virus to BHK cells selects for use of heparan sulfate as an attachment receptor. J. Virol. **72**:7357–7366.
59. **Lee E, Lobigs M.** 2002. Mechanism of virulence attenuation of glycosaminoglycan-binding variants of Japanese encephalitis virus and Murray Valley encephalitis virus. J. Virol. **76**:4901–4911.
60. **Reddi HV, Kumar AS, Kung AY, Kallio PD, Schlitt BP, Lipton HL.** 2004. Heparan sulfate-independent infection attenuates high-neurovirulence GDVII virus-induced encephalitis. J. Virol. **78**:8909–8916.
61. **Wang X, Peng W, Ren J, Hu Z, Xu J, Lou Z, Li X, Yin W, Shen X, Porta C, Walter TS, Evans G, Axford D, Owen R, Rowlands DJ, Wang J, Stuart DI, Fry EE, Rao Z.** 2012. A sensor-adaptor mechanism for enterovirus uncoating from structures of EV71. Nat. Struct. Mol. Biol. **19**:424–429.

Antiviral Research 107 (2014) 35–41

Contents lists available at ScienceDirect

Antiviral Research

journal homepage: www.elsevier.com/locate/antiviral

Inhibition of enterovirus 71 infection by antisense octaguanidinium dendrimer-conjugated morpholino oligomers

Chee Wah Tan [a], Yoke Fun Chan [a,b], Yi Wan Quah [c], Chit Laa Poh [c,*]

[a] Department of Medical Microbiology, Faculty of Medicine, University of Malaya, 50603 Kuala Lumpur, Malaysia
[b] Tropical Infectious Disease Research and Education Center, University of Malaya, 50603 Kuala Lumpur, Malaysia
[c] Faculty of Science and Technology, Sunway University, 46150 Petaling Jaya, Selangor, Malaysia

ARTICLE INFO

Article history:
Received 9 January 2014
Revised 25 March 2014
Accepted 13 April 2014
Available online 24 April 2014

Keywords:
Enterovirus 71
Hand, foot and mouth disease
Enterovirus
Morpholino oligomers
Antiviral agent

ABSTRACT

Enterovirus 71 (EV-71) infections are generally manifested as mild hand, foot and mouth disease, but have been reported to cause severe neurological complications with high mortality rates. Treatment options remain limited due to the lack of antivirals. Octaguanidinium-conjugated morpholino oligomers (vivo-MOs) are single-stranded DNA-like antisense agents that can readily penetrate cells and reduce gene expression by steric blocking of complementary RNA sequences. In this study, inhibitory effects of three vivo-MOs that are complementary to the EV-71 internal ribosome entry site (IRES) and the RNA-dependent RNA polymerase (RdRP) were tested in RD cells. Vivo-MO-1 and vivo-MO-2 targeting the EV-71 IRES showed significant viral plaque reductions of 2.5 and 3.5 $\log_{10}$PFU/ml, respectively. Both vivo-MOs reduced viral RNA copies and viral capsid expression in RD cells in a dose-dependent manner. In contrast, vivo-MO-3 targeting the EV-71 RdRP exhibited less antiviral activity. Both vivo-MO-1 and 2 remained active when administered either 4 h before or within 6 h after EV-71 infection. Vivo-MO-2 exhibited antiviral activities against poliovirus (PV) and coxsackievirus A16 but vivo-MO-1 showed no antiviral activities against PV. Both the IRES-targeting vivo-MO-1 and vivo-MO-2 inhibit EV-71 RNA translation. Resistant mutants arose after serial passages in the presence of vivo-MO-1, but none were isolated against vivo-MO-2. A single T to C substitution at nucleotide position 533 was sufficient to confer resistance to vivo-MO-1. Our findings suggest that IRES-targeting vivo-MOs are good antiviral candidates for treating early EV-71 infection, and vivo-MO-2 is a more favorable candidate with broader antiviral spectrum against enteroviruses and are refractory to antiviral resistance.

1. Introduction

Enterovirus 71 (EV-71) is a single-strand, positive-sense RNA virus. EV-71 usually cause mild hand, foot and mouth disease (HFMD) characterized by fever with papulovesicular rash on the palms and soles (Ooi et al., 2010). In recent years, EV-71 infections were also associated with neurological complications with high mortalities among infants and young children < 6 years old (Solomon et al., 2010). To date, no effective antiviral agent is available for clinical use (Shang et al., 2013b; Tan et al., 2014). Thus, there is an urgent need to develop effective antiviral agents to treat EV-71 infection.

Considering the morbidity caused by EV-71, new approaches to the development of therapeutics are needed. A number of promising RNA-based therapeutics designed to inhibit EV-71 infections have shown promising results, including siRNA and shRNA (Deng et al., 2012; Sim et al., 2005; Tan et al., 2007a,b; Wu et al., 2009). However, the limitations of RNA-based therapeutics are short half-life and it required a delivery agent which might be toxic to the host. Therefore, nucleic acid-based therapeutics should be designed to possess favorable pharmacological properties such as in *vivo* stability and low toxicity.

A phosphorodiamidate morpholino oligomer (PMO) is a single-stranded DNA-like compound that has the ability to bind to the mRNA and inhibit gene expression by steric blockage of complementary RNA. PMOs are highly nuclease-resistant and do not require the RNase H or other catalytic proteins for their activity (Kole et al., 2012; Summerton, 1999). PMOs have been conjugated with various cell-penetrating compounds such as cell-penetrating peptides and octaguanidinium dendrimers which are able to enhance their uptake by cells (Moulton and Jiang, 2009). Peptide conjugated-PMOs (PPMO) have been demonstrated to inhibit various viral infections, including Ebola virus (Warfield et al., 2006), West Nile virus (Deas et al., 2005), dengue virus (Kinney et al., 2005), sindbis virus (Paessler et al., 2008), coronavirus (Neuman

* Corresponding author. Tel.: +60 3 7491 8622x3837; fax: +60 3 5635 8633.
E-mail address: pohcl@sunway.edu.my (C.L. Poh).

http://dx.doi.org/10.1016/j.antiviral.2014.04.004
0166-3542/

et al., 2004), herpes simplex virus 1 (Moerdyk-Schauwecker et al., 2009), porcine reproductive and respiratory syndrome virus (Opriessnig et al., 2011; Patel et al., 2008), foot-and-mouth disease virus (Vagnozzi et al., 2007), poliovirus, rhinovirus (Stone et al., 2008), and coxsackievirus B3 (Yuan et al., 2006).

In this study, three octaguanidinium dendrimer conjugated-morpholino oligomers (vivo-MOs) targeting the EV-71 internal ribosome entry site (IRES) core sequence and the RNA-dependent RNA polymerase (RdRP) were tested for their inhibitory effects against EV-71. We demonstrated that the two vivo-MOs targeting the IRES core sequence showed significant inhibition of EV-71 infection.

2. Materials and methods

2.1. Cells and viruses

Rhabdomyosarcoma (RD, ATCC) cells were grown in Dulbecco's modified Eagle's medium (DMEM, Hyclone) supplemented with 10% fetal bovine serum (FBS). EV-71 strains 41 (GenBank accession number: AF316321), BrCr (GenBank accession number: AB204852) and UH1/97 (GenBank accession number: AM396587); coxsackievirus A16 (CV-A16), PV and chikungunya virus (CHIKV) strain MY/08/065 (GenBank accession number: FN295485) were propagated in RD cells.

2.2. Vivo-MOs

All vivo-MOs were synthesized by Gene Tools LLC (USA). The 23-mer vivo-MOs were designed to be complementary to the EV-71 (strain 41) IRES stem-loop V-VI and the RdRP gene (Table 1, Fig. 1). All the vivo-MOs were dissolved in phosphate buffer saline (PBS) at concentration of 0.5 mM. The cytotoxicity of the vivo-MOs were evaluated using Cell Titer 96 AQueous cell proliferation reagent (Promega) according to the manufacturer's instructions.

Table 1
Sequence of the 23-mer vivo-MOs and target locations in EV-71 RNA.

Vivo-MOs	Sequence (5'–3')	Target location in EV-71 RNA (nucleotide position)
1	CAGAGTTGCCCATTACGACACAC	IRES core (512–534)
2	GAAACACGGACACCCAAAGTAGT	IRES core (546–568)
3	AAACAATTCGAGCCAATTTCTTC	3D Pol gene (7303–7325)
Control	CCTACTCCATCGTTCAGCTCTGA	–

2.3. In vitro inhibitory effects of vivo-MOs in RD cells

RD cells were seeded at 1.5×10^4 cells or 1.5×10^5 cells within each well of a 96-well plate or 24-well plate, respectively and incubated overnight at 37 °C in 5% CO_2. After overnight incubation, the growth medium was removed and replaced with EV-71 inoculum with a multiplicity of infection (MOI) of 0.1 (PFU per cell) and incubated at 37 °C for 1 h. After incubation, the inoculum was removed and replenished with maintenance medium (DMEM with 2% FBS) with or without vivo-MOs. The inhibitory effects of the vivo-MOs were evaluated by plaque assay, TaqMan real-time RT-PCR and western blot analysis 24 h post-infection (hpi) as previously described (Tan et al., 2012, 2013). The western blot signal was enhanced using SuperSignal® western blot enhancer (Pierce Biotechnology).

2.4. Time of addition assay

Vivo-MOs were added to RD cells at various time points relative to viral inoculation. RD cells were pre-incubated with vivo-MOs at final concentration of 5 μM for 4 h before EV-71 inoculation at a MOI of 0.1. In concurrent studies, both vivo-MOs and EV-71 were added into RD cells for 1 h followed by replacement of medium without vivo-MO. For post-infection studies, RD cells were infected with EV-71 for 1, 2, 4 and 6 h before vivo-MOs were applied. The viral titers for each experiment were quantitated 24 hpi by plaque assays.

2.5. In vitro inhibitory effects of vivo-MOs against various enteroviruses

To evaluate the efficacy of vivo-MOs against different enteroviruses including CV-A16 and PV, RD cells were pre-incubated with vivo-MOs at the final concentration of 5 μM for 4 h before viral

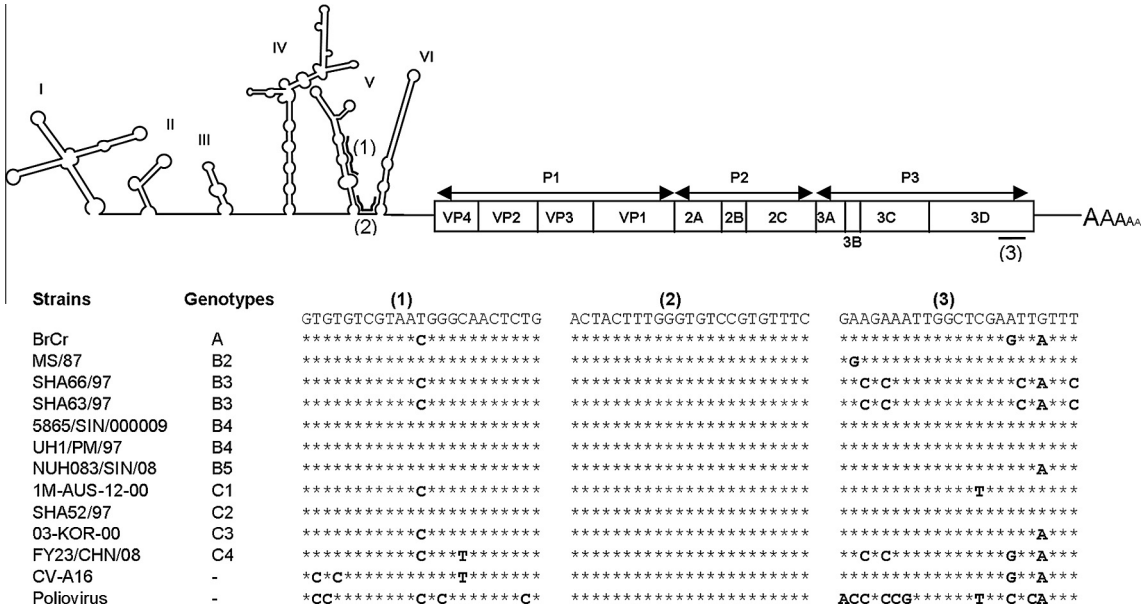

Fig. 1. Schematic illustration of the EV-71 genomic structure. Three genomic vivo-MOs target sequences (5' to 3') are indicated as (1)–(3) within the proposed secondary structures of the IRES region and the RdRP gene of EV-71 RNA. The sequences of these three targeted regions were aligned across all EV-71 genotypes, CV-A16 and PV.

inoculation at a MOI of 0.1 for 1 h at 37 °C. The viral titers were determined 24 hpi by plaque assay. CHIKV was used as a negative control virus in this experiment.

2.6. Construction of EV-71 infectious cDNA clones

EV-71 strain 41 infectious clone was constructed using the full-length genome PCR approach according to Yeh et al. (2011) with modifications. The primers involved in the infectious clone constructions were listed in Table S1. Full-length genome RT-PCR was performed with Superscript III reverse transcriptase (Invitrogen) and iProof High-Fidelity polymerase (Bio-Rad) using pT50/*Eag*I-R and pSP6/EV71-F primers. EV-71 expressing enhanced green fluorescence protein (EGFP) was constructed by overlapping extension PCR strategy using Q5 High-Fidelity polymerase (NEB). The EGFP gene was fused into the EV-71 genome between the 5' UTR and VP4 gene followed by the 2A cleavage site (-AITTL-) as previously described (Shang et al., 2013a). The full-length PCR product was then cloned into pCR-XL-TOPO (Invitrogen). *In vitro* transcription was performed with linearized DNA using RiboMAX-SP6 large scale RNA production system (Promega) and the RNA was transfected into RD cells using Lipofectamine 2000 (Invitrogen) according to the manufacturer's instructions.

2.7. Cell free translation inhibition assay

Cell free translation assay was performed with 1 μg of *in vitro* transcribed RNA using 1-step human coupled IVT kit (Pierce Biotechnology) either in the presence or absence of vivo-MOs according to the manufacturer's instructions. An aliquot of 20 μl of *in vitro* translated sample was subjected to SDS–PAGE and western blot analysis as described previously. The immunoblot was developed with Clarity™ Western ECL substrate (Bio-Rad) and detected by chemiluminescence.

2.8. EV-71–EGFP inhibition assay

RD cells in a 96-well plate were infected with EV-71–EGFP for an hour at 37 °C. After incubation, the inoculum was removed and replaced with maintenance medium containing 2.5 μM of vivo-MOs. The EGFP expression was observed at 6 hpi using fluorescence microscopy.

2.9. Generation of vivo-MOs resistant viruses

EV-71 was passaged in RD cells with increasing concentrations of either vivo-MO-1 or vivo-MO-2. For the first passage, RD cells were infected with EV-71 at a MOI of 0.1 for 1 h at 37 °C and the inoculum was removed and replaced with maintenance medium containing 1 μM of vivo-MO-1 or vivo-MO-2. Each selection was passaged by adding 100 μl of the supernatant into new RD cells. Viruses were passaged once at each of the concentrations ranging from 1 μM to 4 μM, followed by passaging four times at 5 μM. To identify the mutation(s) which conferred resistance to vivo-MOs, viral RNA of an individual plaque population was amplified and subjected to DNA sequencing.

2.10. Reverse genetic analysis of vivo-MO resistant viruses

Point mutations were incorporated into the EV-71 infectious clone by using QuickChange Lightning site-directed mutagenesis kit (Agilent Technologies) according to the manufacturer's instructions. Four mutants were constructed with different nucleotide substitutions at the vivo-MO-1 targeted region (Table 2). The degree of resistance was evaluated using inhibitory assay as described in Section 2.3.

Table 2
Sequence of vivo-MO-1 and the *in vitro* transcribed infectious RNA with target sequences.

Target	Sequences	Mismatch(es)
Vivo-MO-1	3'-CAGAGTTGCCCATTACGACACAC-3'	–
MO-1-WT	5'-GTGTGTCGTAATGGGCAACTCTG-3'	0
MO-1-mutant-1	5'-GTGTGTCGTAATGGGCAACTC**C**G-3'	1
MO-1-mutant-2	5'-GTGTGTCGTAA**C**GGGCAACTCTG-3'	1
MO-1-mutant-3	5'-GTGTGTCGTAA**C**GGG**T**AACTCTG-3'	2
MO-1-mutant-4	5'-GTG**C**GTCGTAA**C**GGG**T**AACTCTG-3'	3

2.11. Statistical analysis

The data presented are the means ± standard deviations (SD) obtained from at least two independent biological replicates. Error bars represent the SD. Statistical significance was calculated using the Mann–Whitney test. A P value of <0.05 was considered statistically significant.

3. Result

3.1. Vivo-MOs complementary to EV-71 IRES stem-loop structures exhibited significant inhibitory activities

To evaluate the effects of vivo-MOs on EV-71 infectivity in RD cells, RD cells were treated with vivo-MOs an hour after infection. As shown in Fig. 2, both vivo-MOs targeting the EV-71 IRES stem-loop region exhibited significant antiviral activity against EV-71 infection with reduction of virus-induced CPE (Fig. 2A), plaque formation (Fig. 2B), RNA (Fig. 2C) and capsid expression (Fig. 2D) in a dose-dependent manner. The vivo-MO-1 and vivo-MO-2 significantly reduced EV-71 plaque formation by up to 2.7 and 3.5 $\log_{10}$-PFU/ml at 10 μM, respectively. Significant inhibition was observed at concentrations higher than 1 μM. The IC_{50} values of vivo-MO-1 and vivo-MO-2 were 1.5 μM and 1.2 μM, respectively. However, vivo-MO-3 exhibited less inhibitory effect against EV-71 infection in RD cells with a plaque reduction of only 1.2 $\log_{10}$PFU/ml (Fig. 2B). The vivo-MO-C which has no homologous sequence to the EV-71 genome has no inhibitory effects at all against all EV-71 strains tested. None of the vivo-MOs caused more than 20% reduction of cell viability at concentrations less than 5 μM as measured by the MTS assay (Fig. 3).

3.2. Vivo-MOs blocked EV-71 infections at multiple time points

To further characterize the efficacy of vivo-MOs at multiple time points relative to EV-71 infection, vivo-MOs were applied for 4 h before, or 1, 2, 4, or 6 h after EV-71 infection. Both vivo-MO-1 and vivo-MO-2 remained effective when administered before or after EV-71 infection. However, the efficacies were reduced when treatments were delayed. When vivo-MOs and EV-71 were added together into the RD cells for 1 h, the inhibitory effect was reduced, which could have resulted from the incomplete uptake of the vivo-MOs by the cells. Nonetheless, the antiviral effects were retained for both IRES-targeting vivo-MOs even when administered 6 hpi, with 92.8% plaque inhibition. Vivo-MO-3 had no observable inhibitory effects on EV-71 infection when administered 4 h before infection and 2, 4, or 6 hpi (Fig. 4A).

3.3. Vivo-MO-2 exhibited broad-spectrum antiviral activities against various enteroviruses

Next, we investigate whether any of the vivo-MOs could inhibit different EV-71 strains as well as other picornaviruses. We evaluated each of the vivo-MOs against two other EV-71 strains (BrCr

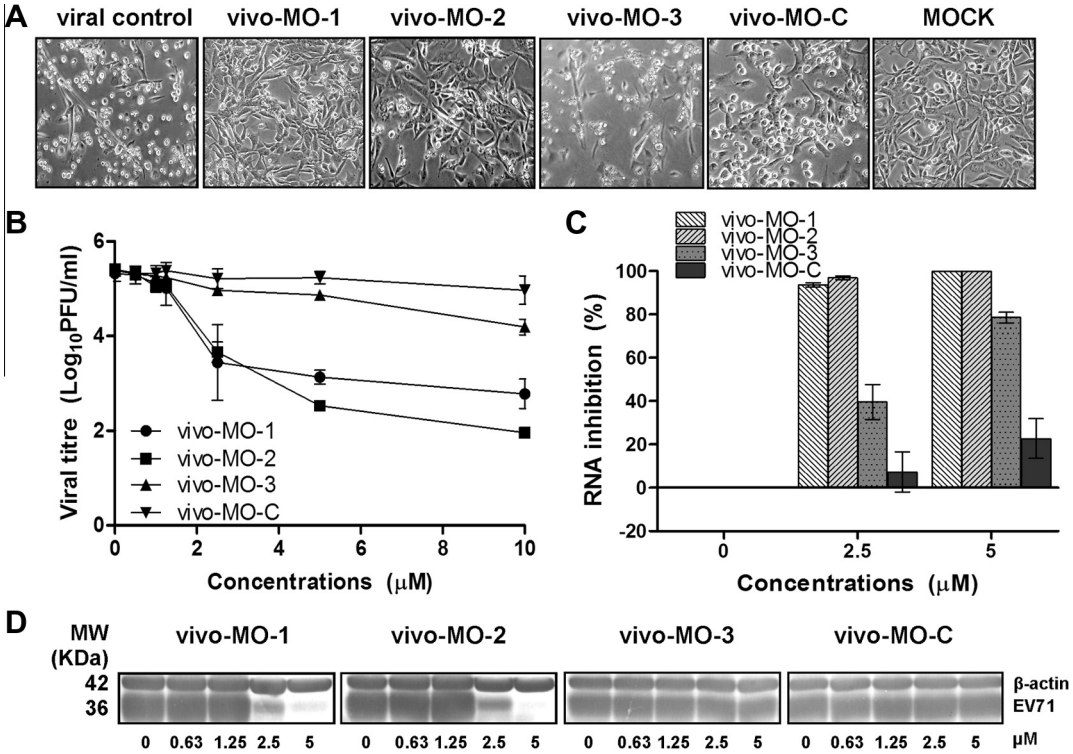

Fig. 2. Inhibitory effect of vivo-MOs in RD cells. Various concentrations of vivo-MOs were applied to RD cells one hour post infection and (A) viral induced CPE (20 × objective) were observed 24 hpi. The total infectious particles or total viral proteins were harvested 24 hpi and evaluated by (B) plaque assay, (C) quantitative TaqMan real-time PCR, and (D) western blot analysis, respectively. EV-71 viral capsid protein was detected by mouse anti-EV-71 monoclonal antibody (Millipore) and cellular β-actin was detected using mouse anti-β-actin monoclonal antibody (Sigma). The data presented were obtained from at least two independent biological replicates.

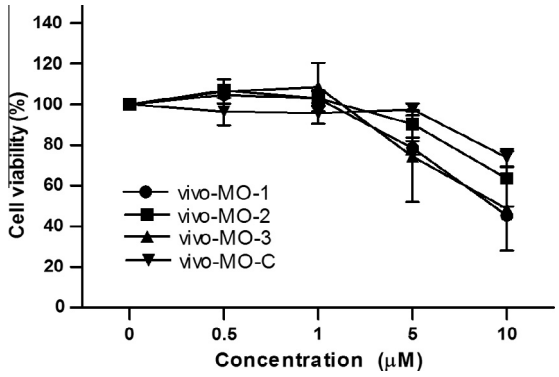

Fig. 3. Cell viability analysis. Various concentrations of vivo-MOs were incubated with RD cells (1.5×10^4 cells) for 24 h in maintenance medium (DMEM supplemented with 2% FBS) followed by MTS assay using Cell Titer 96 AQueous One solution cell proliferation (Promega). The absorbance reading at 490 nm was obtained using a microtiter plate reader after 2 h of incubation at 37 °C. The percentage of cell viability (%) was determined by multiplying the ratio of the absorbance readings obtained from cells treated with vivo-MOs over the non-treated cells with 100%. The data presented were obtained from at least two independent biological replicates.

and UH1/97), PV, CV-A16 and CHIKV as the control virus. The vivo-MO-2 which targets the highly conserved region of the IRES stem-loop structure exhibited significant inhibitory activity against EV-71 strains BrCr and UH1/97, PV and CV-A16 with viral plaque reduction ranging from 1.8 to 3.1 $\log_{10}$PFU/ml (Fig. 4B). However, vivo-MO-1 only exhibited antiviral activities against EV-71 strains BrCr and UH1/97, CV-A16, but not against PV (Fig. 4B). EV-71 strain BrCr which has a single nucleotide mismatch in the middle of the vivo-MO-1 targeted site (Fig. 1) remained sensitive to the vivo-MO-1 treatment. The efficacy of vivo-MO-1 against CV-A16 (0.95 $\log_{10}$PFU/ml reduction) was significantly lower when compared to EV-71(1.86 $\log_{10}$PFU/ml reduction). This could be due to three nucleotide mismatches with the vivo-MO-1. PV with five nucleotide mismatches was completely resistant to the inhibitory effect of vivo-MO-1. All the vivo-MOs did not show any inhibition of CHIKV infection.

3.4. IRES-targeting vivo-MOs blocked EV-71 translation

To investigate the mechanism of action of the antiviral vivo-MOs, cell-free translation analysis was used. As depicted in Fig. 5A, the presence of either vivo-MO-1 or vivo-MO-2 significantly blocked the IRES-dependent translation when compared to the control. Vivo-MO-3 exhibits reduced efficacies as compared to IRES-targeting vivo-MOs. In the EV-71–EGFP inhibition assay, the presence of the vivo-MO-1 or vivo-MO-2 greatly reduced EGFP expression in RD cells 6 hpi with EV-71–EGFP (Fig. 5B).

3.5. Tolerance of vivo-MO-1 to mismatches within the target RNA

We explored whether EV-71 could become resistant to vivo-MO treatments. EV-71 was serially passaged in the presence of increasing concentrations of either vivo-MO-1 or vivo-MO-2. Interestingly, only EV-71 mutants resistant to vivo-MO-1 were isolated after eight passages. We failed to isolate EV-71 mutants that were resistant to vivo-MO-2.

To investigate the determinant(s) of resistance, viral RNA was isolated from the resistant population and was sequenced. A single point mutation from T to C at position 533 was sufficient to confer resistance to vivo-MO-1 (Fig. 6A). To characterize the loss of inhibitory activity by vivo-MO-1, we constructed EV-71 mutants carrying different mismatches at the vivo-MO-1 target site (Table 2), and the inhibitory effects of vivo-MO-1 against each of the mutants

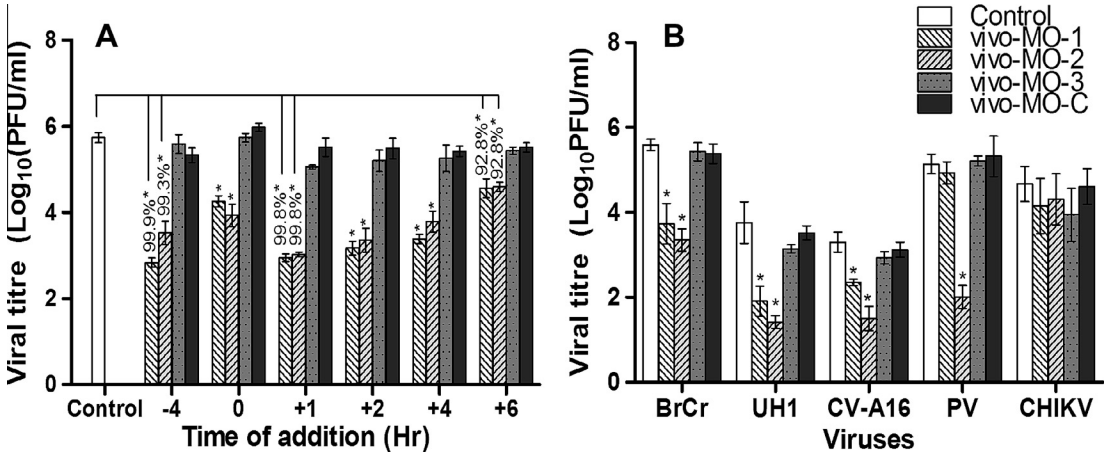

Fig. 4. Time and specificity of vivo-MOs antiviral properties. (A) Vivo-MOs at a final concentration of 5 μM were applied to RD cells at various time points relative to EV-71 inoculation. In brief, vivo-MOs were applied for 4 h before, or 1, 2, 4, or 6 h after EV-71 infection at a MOI of 0.1. (B) RD cells were pre-treated with each of the vivo-MOs at a final concentration of 5 μM for 4 h at 37 °C before infection with other enteroviruses (EV-71 strain BrCr, UH1/97, PV and CV-A16) and CHIKV at a MOI of 0.1. The inhibitory effects of each of the vivo-MOs were evaluated by plaque assay 24 hpi and the percentages of inhibition are shown. Asterisks indicate statistically significant differences compared to the control. The data presented were obtained from at least two independent biological replicates.

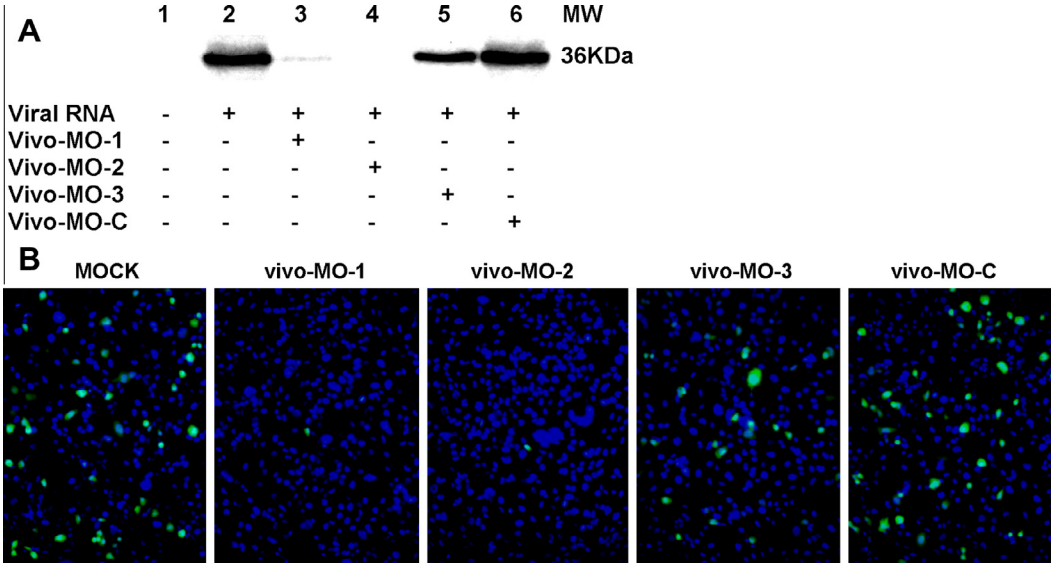

Fig. 5. Translation inhibition assay. (A) *In vitro* translation was performed with 1 μg of RNA using 1-step human coupled IVT kit (Pierce Biotechnology) either in the presence of vivo-MOs at a final concentration of 10 μM. Aliquots of 20 μl of translated product was subjected to SDS–PAGE and western blot analysis. EV-71 viral protein was detected by anti-EV-71 monoclonal antibody through chemiluminescence. (B) EV-71–EGFP inhibition assay. RD cells were first infected with EV-71–EGFP for one hour, followed by addition of maintenance medium containing 2.5 μM of vivo-MOs. The EGFP expression was evaluated 6 hpi using a fluorescence microscope. Nuclei were stained with DAPI. EGFP expression and nuclei are shown in green and blue, respectively. The data presented were obtained from at least two independent biological replicates. (For interpretation of the references to color in this figure legend, the reader is referred to the web version of this article.)

were evaluated. The mismatched RNA target sequences were designed to reflect the most likely natural variations that would arise in the EV-71 sequence. As shown in Fig. 6B, the EV-71 MO-1-mutant-1, which carried a single point mutation at position 533 (T to C substitution), required higher vivo-MO-1 concentrations to achieve a similar inhibitory effect when compared to the wild type. The EV-71 MO-1-mutant-2 with a single point mutation in the middle of the targeted sequence (a T to C substitution at position 523) remained sensitive to vivo-MO-1, but vivo-MO-1 had reduced inhibitory efficacy when compared with the wild type. Increasing the number of mutations on the targeted sequence significantly reduced the inhibitory efficacy of vivo-MO-1. The viral plaque inhibition at 2 μM of vivo-MO-1 against EV-71 MO-1-WT was 98.9% ± 0.1, and reduced to 89.6% ± 3.4 for the MO-1-mutant-1 that carried a point mutation at the 3' end of the target sequence. The viral plaque inhibition by vivo-MO-1 reduced to 78.0% when the number of nucleotide mismatches increased to three.

4. Discussion

To date, there is no FDA approved vaccine available to prevent infection and treatment options remain limited due to a lack of effective antivirals (Chong et al., 2012; Shang et al., 2013b; Tan and Chan, 2013). Highly negatively-charged compounds like suramin or its analog, NF449 that disrupt the virus-host receptor interactions are ineffective when EV-71 mutants acquire Glu98Gln and Lys244Arg substitutions in the VP1 capsid protein (Arita et al., 2008; Tan et al., 2013). A single point mutation, Val192Met in

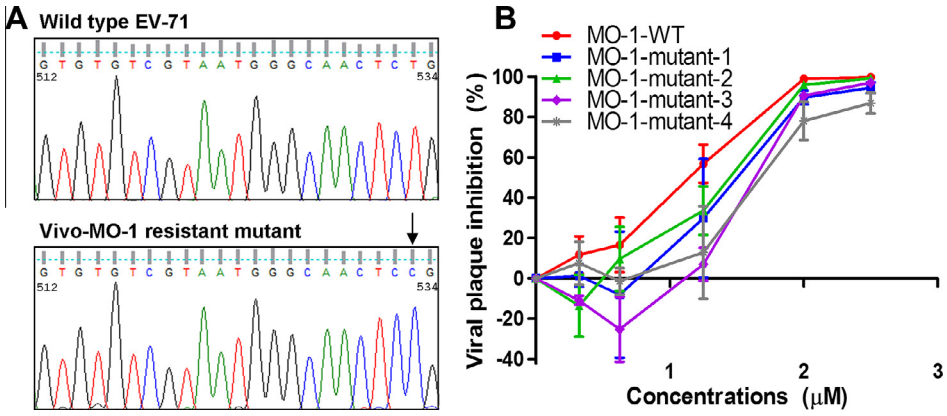

Fig. 6. DNA sequence analysis of vivo-MO-1. (A) EV-71 was serially passaged in the presence of vivo-MO-1 from 1 μM to 5 μM. EV-71 populations that showed resistance to vivo-MO-1 were plaque purified, and subjected to DNA sequencing. Analysis of the vivo-MO-1 resistant mutant showed a T to C substitution at position 533. (B) The effect of sequence mismatches between vivo-MO-1 and target RNA on inhibition assay. Several *in vitro* transcribed RNA, each having a different number of nucleotide mismatches in the target region as described in Section 2 were analyzed. Viral titers were quantitated 24 hpi using standard plaque assay. The data presented were obtained from at least two independent biological replicates.

the VP1, is sufficient to confer resistance to the capsid binder BPROZ-194 (Shih et al., 2004). Therefore, there is an urgent need to develop effective antiviral agents to treat patients with severe EV-71 infection.

The use of antisense mechanisms to inhibit pathogen replication has been under investigation and has shown promising results. Fomivirsen, a 21-mer phosphorothioate oligonucleotide antisense agent used for intravitreal treatment of cytomegalovirus retinitis, is the only antisense agent that has been approved by the FDA to date (de Smet et al., 1999). There are advantages of vivo-MOs over RNA-based antisense oligomers as they are, nuclease-resistant and readily penetrate the cells (Kole et al., 2012; Moulton and Jiang, 2009). These have an advantage over peptide-based cell penetrating molecules, which are susceptible to protease degradation that can impact the effectiveness of PPMOs (Youngblood et al., 2007).

Amongst the three vivo-MOs being examined, the two vivo-MOs targeting the EV-71 IRES stem-loop region exhibited significant antiviral activity. The vivo-MOs blocked EV-71 viral RNA translation in a cell-free inhibition assay, as well as in a cell-based EGFP reporter inhibition assay. Previous studies have also reported that only PMOs targeting the positive strand IRES regions or the AUG start codon sites were effective when compared to PMOs targeting other regions of the viral RNA (Stone et al., 2008; Vagnozzi et al., 2007; Yuan et al., 2006). The PMO may bind with the complementary viral RNA and disrupt the integrity of the IRES stem-loop secondary or tertiary structures, hence arresting IRES-dependent translation (Kole et al., 2012; Warren et al., 2012). The PMOs are likely to block 40S ribosomal subunit binding the viral RNA in the vicinity of the stem-loop V in the picornaviral type I IRES (Belsham, 2009). Furthermore, it has been suggested that the IRES stem-loop V-VI of EV-71 interacts with IRES-specific *trans*-acting factors such as FUSE-binding protein and heterogeneous nuclear ribonucleoprotein Al (Lin et al., 2009a,b; Shih et al., 2011). Unlike synthetic double-stranded siRNA which involve cleavage of mRNA, PMOs are translation-suppressing oligonucleotides which do not lead to RNA degradation (Kole et al., 2012; Warren et al., 2012). This could explain why siRNA targeting the similar viral sequences as vivo-MO-3 was effective, but not acting as a translation suppression oligonucleotide which down-regulates gene expression via steric blockage. IRES-targeting vivo-MO-2 exhibited broad-spectrum activities against multiple enteroviruses, but with different antiviral efficacies. This could have resulted from the IRES stem-loop structure differences between enteroviruses which affect the accessibility of the vivo-MOs to the targeted sites (Dias and Stein, 2002).

In this study, an EV-71 mutant that was resistant to vivo-MO-1 carried a single substitution of T to C at position 533. We failed to isolate any EV-71 resistant to vivo-MO-2 even after eight passages *in vitro*, implying that the vivo-MO-2 targeted region is intolerant to mutation in nature. Our mutagenesis studies further confirm that the position of mutation and the number of mutations affect the antiviral efficacies in RD cells. A single mismatch present in the middle of the targeted sequence (T to C substitution at position 523) was more tolerable than a mutation appearing at the end of the targeted site (T to C substitution at position 533). These findings correlated well with previous findings that PV, FMDV and WNV that showed resistance to PPMO also carry a single point mutation at the end of the PPMO-targeted sequence (Stone et al., 2008; Vagnozzi et al., 2007; Zhang et al., 2008). A similar observation has been made for influenza virus as the degree of inhibition was associated with the number of mismatches (Ge et al., 2006).

5. Conclusion

In summary, we have established two critical locations that are involved in viral translation initiation in the EV-71 genome as targets for vivo-MO antiviral intervention. The vivo-MOs worked well with low micromolar concentrations to inhibit EV-71 infection and showed little cytotoxicity in RD cells. The potent inhibition of several enteroviruses by vivo-MO-2 raises the possibility that it could be developed as a broad-spectrum antiviral agent. Furthermore, the degree of tolerance of mismatches by vivo-MOs suggests a favorable characteristic for their use as a potential antiviral agent.

Acknowledgements

This work was supported by a Ministry of Education E-Science Fund (02-02-16-SF0022) and Sunway University Research Grant (INT-FST-BIOS-0312-02) awarded to CLP, and a University Malaya High Impact Research grant (UM.C/625/1/HIR/MOHE/MED/41), postgraduate research Grant (PV013-2012A) and Exploratory Research Grant Scheme (ER017-2013A) awarded to YFC.

Appendix A. Supplementary data

Supplementary data associated with this article can be found, in the online version, at http://dx.doi.org/10.1016/j.antiviral.2014.04.004.

References

Arita, M., Wakita, T., Shimizu, H., 2008. Characterization of pharmacologically active compounds that inhibit poliovirus and enterovirus 71 infectivity. J. Gen. Virol. 89, 2518–2530.

Belsham, G.J., 2009. Divergent picornavirus IRES elements. Virus Res. 139, 183–192.

Chong, P., Hsieh, S.Y., Liu, C.C., Chou, A.H., Chang, J.Y., Wu, S.C., Liu, S.J., Chow, Y.H., Su, I.J., Klein, M., 2012. Production of EV71 vaccine candidates. Hum. Vaccine Immunother. 8, 1775–1783.

de Smet, M.D., Meenken, C.J., van den Horn, G.J., 1999. Fomivirsen – a phosphorothioate oligonucleotide for the treatment of CMV retinitis. Ocul. Immunol. Inflamm. 7, 189–198.

Deas, T.S., Binduga-Gajewska, I., Tilgner, M., Ren, P., Stein, D.A., Moulton, H.M., Iversen, P.L., Kauffman, E.B., Kramer, L.D., Shi, P.Y., 2005. Inhibition of flavivirus infections by antisense oligomers specifically suppressing viral translation and RNA replication. J. Virol. 79, 4599–4609.

Deng, J.X., Nie, X.J., Lei, Y.F., Ma, C.F., Xu, D.L., Li, B., Xu, Z.K., Zhang, G.C., 2012. The highly conserved 5' untranslated region as an effective target towards the inhibition of enterovirus 71 replication by unmodified and appropriate 2'-modified siRNAs. J. Biomed. Sci. 19, 73.

Dias, N., Stein, C.A., 2002. Antisense oligonucleotides: basic concepts and mechanisms. Mol. Cancer Ther. 1, 347–355.

Ge, Q., Pastey, M., Kobasa, D., Puthavathana, P., Lupfer, C., Bestwick, R.K., Iversen, P.L., Chen, J., Stein, D.A., 2006. Inhibition of multiple subtypes of influenza A virus in cell cultures with morpholino oligomers. Antimicrob. Agents Chemother. 50, 3724–3733.

Kinney, R.M., Huang, C.Y., Rose, B.C., Kroeker, A.D., Dreher, T.W., Iversen, P.L., Stein, D.A., 2005. Inhibition of dengue virus serotypes 1 to 4 in vero cell cultures with morpholino oligomers. J. Virol. 79, 5116–5128.

Kole, R., Krainer, A.R., Altman, S., 2012. RNA therapeutics: beyond RNA interference and antisense oligonucleotides. Nat. Rev. Drug Discov. 11, 125–140.

Lin, J.Y., Li, M.L., Shih, S.R., 2009a. Far upstream element binding protein 2 interacts with enterovirus 71 internal ribosomal entry site and negatively regulates viral translation. Nucleic Acids Res. 37, 47–59.

Lin, J.Y., Shih, S.R., Pan, M., Li, C., Lue, C.F., Stollar, V., Li, M.L., 2009b. HnRNP A1 interacts with the 5' untranslated regions of enterovirus 71 and Sindbis virus RNA and is required for viral replication. J. Virol. 83, 6106–6114.

Moerdyk-Schauwecker, M., Stein, D.A., Eide, K., Blouch, R.E., Bildfell, R., Iversen, P., Jin, L., 2009. Inhibition of herpes simplex virus 1 ocular infection with morpholino oligomers targeting ICP0 and ICP27. Antiviral Res. 84, 131–141.

Moulton, J.D., Jiang, S., 2009. Gene knockdowns in adult animals: PPMOs and vivo-morpholinos. Molecules 14, 1304–1323.

Neuman, B.W., Stein, D.A., Kroeker, A.D., Paulino, A.D., Moulton, H.M., Iversen, P.L., Buchmeier, M.J., 2004. Antisense morpholino-oligomers directed against the 5' end of the genome inhibit coronavirus proliferation and growth. J. Virol. 78, 5891–5899.

Ooi, M.H., Wong, S.C., Lewthwaite, P., Cardosa, M.J., Solomon, T., 2010. Clinical features, diagnosis, and management of enterovirus 71. Lancet Neurol. 9, 1097–1105.

Opriessnig, T., Patel, D., Wang, R., Halbur, P.G., Meng, X.J., Stein, D.A., Zhang, Y.J., 2011. Inhibition of porcine reproductive and respiratory syndrome virus infection in piglets by a peptide-conjugated morpholino oligomer. Antiviral Res. 91, 36–42.

Paessler, S., Rijnbrand, R., Stein, D.A., Ni, H., Yun, N.E., Dziuba, N., Borisevich, V., Seregin, A., Ma, Y., Blouch, R., Iversen, P.L., Zacks, M.A., 2008. Inhibition of alphavirus infection in cell culture and in mice with antisense morpholino oligomers. Virology 376, 357–370.

Patel, D., Opriessnig, T., Stein, D.A., Halbur, P.G., Meng, X.J., Iversen, P.L., Zhang, Y.J., 2008. Peptide-conjugated morpholino oligomers inhibit porcine reproductive and respiratory syndrome virus replication. Antiviral Res. 77, 95–107.

Shang, B., Deng, C., Ye, H., Xu, W., Yuan, Z., Shi, P.Y., Zhang, B., 2013a. Development and characterization of a stable eGFP enterovirus 71 for antiviral screening. Antiviral Res. 97, 198–205.

Shang, L., Xu, M., Yin, Z., 2013b. Antiviral drug discovery for the treatment of enterovirus 71 infections. Antiviral Res. 97, 183–194.

Shih, S.R., Stollar, V., Li, M.L., 2011. Host factors in enterovirus 71 replication. J. Virol. 85, 9658–9666.

Shih, S.R., Tsai, M.C., Tseng, S.N., Won, K.F., Shia, K.S., Li, W.T., Chern, J.H., Chen, G.W., Lee, C.C., Lee, Y.C., Peng, K.C., Chao, Y.S., 2004. Mutation in enterovirus 71 capsid protein VP1 confers resistance to the inhibitory effects of pyridyl imidazolidinone. Antimicrob. Agents Chemother. 48, 3523–3529.

Sim, A.C., Luhur, A., Tan, T.M., Chow, V.T., Poh, C.L., 2005. RNA interference against enterovirus 71 infection. Virology 341, 72–79.

Solomon, T., Lewthwaite, P., Perera, D., Cardosa, M.J., McMinn, P., Ooi, M.H., 2010. Virology, epidemiology, pathogenesis, and control of enterovirus 71. Lancet Infect. Dis. 10, 778–790.

Stone, J.K., Rijnbrand, R., Stein, D.A., Ma, Y., Yang, Y., Iversen, P.L., Andino, R., 2008. A morpholino oligomer targeting highly conserved internal ribosome entry site sequence is able to inhibit multiple species of picornavirus. Antimicrob. Agents Chemother. 52, 1970–1981.

Summerton, J., 1999. Morpholino antisense oligomers: the case for an RNase H-independent structural type. Biochim. Biophys. Acta 1489, 141–158.

Tan, C.W., Chan, Y.F., 2013. Enterovirus 71 receptors: promising drug targets? Expert Rev. Anti Infect. Ther. 11, 547–549.

Tan, C.W., Chan, Y.F., Sim, K.M., Tan, E.L., Poh, C.L., 2012. Inhibition of enterovirus 71 (EV-71) infections by a novel antiviral peptide derived from EV-71 capsid protein VP1. PLoS One 7, e34589.

Tan, C.W., Lai, J.K.F., Sam, I.C., Chan, Y.F., 2014. Recent developments in antiviral agents against enterovirus 71 infection. J. Biomed. Sci. 21, 14.

Tan, C.W., Poh, C.L., Sam, I.C., Chan, Y.F., 2013. Enterovirus 71 uses cell surface heparan sulfate glycosaminoglycan as an attachment receptor. J. Virol. 87, 611–620.

Tan, E.L., Tan, T.M., Chow, V.T., Poh, C.L., 2007a. Enhanced potency and efficacy of 29-mer shRNAs in inhibition of Enterovirus 71. Antiviral Res. 74, 9–15.

Tan, E.L., Tan, T.M., Tak Kwong Chow, V., Poh, C.L., 2007b. Inhibition of enterovirus 71 in virus-infected mice by RNA interference. Mol. Ther. 15, 1931–1938.

Vagnozzi, A., Stein, D.A., Iversen, P.L., Rieder, E., 2007. Inhibition of foot-and-mouth disease virus infections in cell cultures with antisense morpholino oligomers. J. Virol. 81, 11669–11680.

Warfield, K.L., Swenson, D.L., Olinger, G.G., Nichols, D.K., Pratt, W.D., Blouch, R., Stein, D.A., Aman, M.J., Iversen, P.L., Bavari, S., 2006. Gene-specific countermeasures against Ebola virus based on antisense phosphorodiamidate morpholino oligomers. PLoS Pathog. 2, e1.

Warren, T.K., Shurtleff, A.C., Bavari, S., 2012. Advanced morpholino oligomers: a novel approach to antiviral therapy. Antiviral Res. 94, 80–88.

Wu, Z., Yang, F., Zhao, R., Zhao, L., Guo, D., Jin, Q., 2009. Identification of small interfering RNAs which inhibit the replication of several enterovirus 71 strains in China. J. Virol. Methods 159, 233–238.

Yeh, M.T., Wang, S.W., Yu, C.K., Lin, K.H., Lei, H.Y., Su, I.J., Wang, J.R., 2011. A single nucleotide in stem loop II of 5'-untranslated region contributes to virulence of enterovirus 71 in mice. PLoS One 6, e27082.

Youngblood, D.S., Hatlevig, S.A., Hassinger, J.N., Iversen, P.L., Moulton, H.M., 2007. Stability of cell-penetrating peptide-morpholino oligomer conjugates in human serum and in cells. Bioconjug. Chem. 18, 50–60.

Yuan, J., Stein, D.A., Lim, T., Qiu, D., Coughlin, S., Liu, Z., Wang, Y., Blouch, R., Moulton, H.M., Iversen, P.L., Yang, D., 2006. Inhibition of coxsackievirus B3 in cell cultures and in mice by peptide-conjugated morpholino oligomers targeting the internal ribosome entry site. J. Virol. 80, 11510–11519.

Zhang, B., Dong, H., Stein, D.A., Shi, P.Y., 2008. Co-selection of West Nile virus nucleotides that confer resistance to an antisense oligomer while maintaining long-distance RNA/RNA base pairings. Virology 382, 98–106.

Tan et al. Journal of Biomedical Science 2014, 21:14
http://www.jbiomedsci.com/content/21/1/14

NSC
The cost of publication in Journal of Biomedical Science is borne by the National Science Council, Taiwan

JOURNAL OF BIOMEDICAL SCIENCE

REVIEW Open Access

Recent developments in antiviral agents against enterovirus 71 infection

Chee Wah Tan[1†], Jeffrey Kam Fatt Lai[1†], I-Ching Sam[1,2] and Yoke Fun Chan[1,2*]

Abstract

Enterovirus 71 (EV-71) is the main etiological agent of hand, foot and mouth disease (HFMD). Recent EV-71 outbreaks in Asia-Pacific were not limited to mild HFMD, but were associated with severe neurological complications such as aseptic meningitis and brainstem encephalitis, which may lead to cardiopulmonary failure and death. The absence of licensed therapeutics for clinical use has intensified research into anti-EV-71 development. This review highlights the potential antiviral agents targeting EV-71 attachment, entry, uncoating, translation, polyprotein processing, virus-induced formation of membranous RNA replication complexes, and RNA-dependent RNA polymerase. The strategies for antiviral development include target-based synthetic compounds, anti-rhinovirus and poliovirus libraries screening, and natural compound libraries screening. Growing knowledge of the EV-71 life cycle will lead to successful development of antivirals. The continued effort to develop antiviral agents for treatment is crucial in the absence of a vaccine. The coupling of antivirals with an effective vaccine will accelerate eradication of the disease.

Keywords: Enterovirus 71, Enterovirus, Hand, foot and mouth disease, Neurological complications, Antiviral, Virus replication cycle

Introduction

Human enterovirus A71 (EV-71) belongs to the Enterovirus genus within the family of *Picornaviridae*. The EV-71 genome is a single-stranded, positive sense RNA with approximately 7411 nucleotides, and consists of an open reading frame flanked by 5′ and 3′ untranslated regions (UTRs) [1]. Internal ribosome entry site (IRES)-dependent translation initiates synthesis of the viral polyprotein, which is subsequently cleaved into structural proteins (VP1-VP4) and non-structural proteins (2A-2C and 3A-3D). The RNA genome is enclosed in an icosahedral capsid assembled from 60 copies of each of the four structural proteins [2].

EV-71 was first described in 1969, after its isolation from a two-month-old infant with aseptic meningitis in California, USA. Several EV-71 epidemics with high mortality rates occurred in Bulgaria and Hungary in 1975 and 1978 [3-5], respectively. Since then, many EV-71 outbreaks have been reported in Taiwan [6], Australia [7], Singapore [8], Malaysia [9], China [10-14], Vietnam [15] and Cambodia [16].

EV-71 infections usually manifest as mild hand, foot and mouth disease (HFMD), characterized by fever, mouth ulcers, and vesicles on the palms and feet. Unlike other HFMD-related enteroviruses, EV-71 also causes severe neurological manifestations, such as poliomyelitis-like acute flaccid paralysis and brainstem encephalitis in infants and children below 6 years old [17,18]. The fatal brainstem encephalitis is characterized by rapid progression of cardiopulmonary failure. Patients with neurological involvement who survive often have permanent neurological sequelae, with delayed neurodevelopment and reduced cognitive function [19,20].

Similar to the global poliovirus (PV) eradication initiative, an EV-71 vaccine is likely to be the most effective way to control, and hopefully eradicate disease [21,22]. Several promising EV-71 vaccine candidates are currently under clinical trial [23]. Nevertheless, effective antivirals are still needed for treatment of infected patients with severe disease [21,22]. This review will highlight the potential targets for EV-71 antivirals as well as recent

* Correspondence: chanyf@ummc.edu.my
†Equal contributors
[1]Department of Medical Microbiology, Faculty of Medicine, University of Malaya, 50603 Kuala Lumpur, Malaysia
[2]Tropical Infectious Disease Research and Education Center (TIDREC), Faculty of Medicine, University of Malaya, 50603 Kuala Lumpur, Malaysia

developments and future prospects of antivirals against EV-71 infections.

Review

EV-71 virus life cycle

Similar to other viruses, EV-71 infection begins with initial attachment to attachment factors present on the cell surface, followed by interaction with entry receptors. EV-71 enters the cells through clathrin-mediated endocytosis and uncoats in the early endosomes. The viral RNA undergoes IRES-dependent translation, and the polyprotein is cleaved by 2A and 3C proteases into structural and non-structural proteins. Non-structural proteins are mainly involved in negative-sense and positive-sense RNA synthesis. The positive-sense viral RNA is then packed into the procapsid, which finally matures into infectious viral particles. Details of the EV-71 replication steps will be discussed according to their therapeutic targets [18,21,22].

Therapeutics targeting viral attachment and entry

Virus-host receptor interaction is the first essential event during virus infection. The ability to recognize and bind to specific receptors determines the host range and tissue tropism [24]. Cell surface carbohydrates such as heparan sulfate glycosaminoglycan and sialic acid are often targeted by pathogens as attachment factors. EV-71 uses cell surface heparan sulfate [25] and sialylated glycan [26,27] as attachment receptors, which could concentrate the virus on the host cell surface and therefore enhance infectivity. Further interaction with entry receptors is required to initiate infection. Two functionally important entry receptors have been identified, scavenger receptor class B2 (SCARB2) and P-selectin glycoprotein ligand-1 (PSGL-1) [28,29]. SCARB2 is expressed in all cell types and regarded as the major EV-71 entry receptor. At low endosomal pH, SCARB2 is needed to induce viral uncoating [30,31]. Human SCARB2 transgenic mice infected with EV-71 showed lethal neurological manifestations with pathological features similar to humans and monkeys, suggesting that SCARB2 contributes to its pathogenesis [32,33]. PSGL-1 is only present on neutrophils and leukocytes. EV-71 binds to PSGL-1 and enters the cells through the caveolar endocytosis pathway [34]. Transgenic mice expressing human PSGL-1 failed to enhance EV-71 infectivity, suggested that PSGL-1 alone does not contribute to its pathogenesis [35].

Since host-receptor interactions are the first event during infection, inhibitors that block this event could act as potential therapeutics. The soluble form of cellular receptors could act as molecular decoys of cell-associated receptors. Soluble SCARB2, PSGL-1, sialic acid and heparin or heparin mimetics have been demonstrated to exhibit inhibitory effects against EV-71 infection *in vitro* [25,26,28,30,36]. Highly sulfated suramin and its analog, NF449, exhibited antiviral activity against EV-71 infection [25,37]. NF449-resistant mutants consist of two mutations in VP1, E98Q and K244R, implying that NF449 inhibited EV-71 infection by binding to the VP1 protein [37]. Similarly, kappa carrageenan, a sulfated polysaccharide from seaweed, also exhibited significant antiviral activity through targeting EV-71 attachment and entry [38]. The mechanism of these soluble decoys is possibly by disruption of the integrity of the EV-71 capsid structure or steric hindrance of receptor interactions.

Receptor antagonists could also be developed as potential antiviral agents. A peptide derived from EV-71 VP1, designated SP40 peptide (Ac-QMRRKVELFTYMRFD-NH_2), was found to exhibit significant antiviral activity against different strains of EV-71 by blocking viral attachment to the cell surface heparan sulfate [39]. An anti-heparan sulfate peptide (Ac-MPRRRRIRRRQK-NH_2), previously identified by Tiwari *et al.* [40], also inhibited EV-71 infection [25]. Another antimicrobial peptide, lactoferrin, also exhibited anti-EV-71 properties *in vitro* and *in vivo* through blocking viral attachment to the cell surface [41-43].

Therapeutics targeting viral uncoating

The proposed EV-71 uncoating event involves attachment to the entry receptor, triggering a series of conformational changes resulting in A-particle formation that is primed for genome release. A second uncoating event occurs after endocytosis, and an unknown trigger causes RNA expulsion from the A-particles via the 2-fold axis, leaving behind an empty capsid [44]. Formation of the 135S A-particle happens in the presence of SCARB2 receptors and a low pH environment, suggesting that the A-particle is formed in the early endosomes [30,31]. Uncoating inhibitors (pocket binders) have been intensively studied as antiviral agents against many picornaviruses, including rhinovirus [45], PV [45], echovirus [46] and coxsackievirus [47]. The complex of WIN51711 with the EV-71 hydrophobic pocket underneath the canyon depression has recently been resolved by X-ray crystallography [48]. The key success factor of these uncoating inhibitors is their ability to fit into the VP1 hydrophobic pocket, stabilize the capsid structure, and therefore block the receptor-induced uncoating mechanism [48].

A series of modified WIN compounds including BPROZ-194, BPROZ-112, BPROZ-284, BPROZ-103, BPROZ-299, BPROZ-101, BPROZ-033, and BPROZ-074 were effective against EV-71 infection with IC_{50} values ranging from 0.8 nM to 1550 nM [49-54]. However, a single point mutation in VP1 V192M was sufficient to confer resistance to BPROZ-194 [51]. Other than modified WIN compounds, the broad spectrum enterovirus

inhibitor pleconaril also inhibited EV-71 infection *in vitro* and *in vivo* [55,56]. However, pleconaril failed to inhibit the cytopathic effect induced by a Taiwan 1998 EV-71 isolate [49]. Another group of capsid binders, pyridazinyl oxime ethers chemically derived from pirodavir such as BTA39 and BTA188, significantly inhibited EV-71 infection [57]. Crystallographic studies showed the pirodavir predecessor R61837 complexed with rhinovirus 14 by binding to the hydrophobic pocket underneath the canyon floor, similar to the mechanism of WIN compounds [58]. 4′,6-Dichloroflavan (BW683C), previously identified as an anti-rhinovirus compound, was also effective against EV-71 infection [59,60]. Mechanistic studies demonstrated that BW683C binds to and stabilizes rhinovirus to heat or acid inactivation, implying that BW682C acts as viral uncoating inhibitor [61-63].

Therapeutics targeting viral RNA translation

EV-71 protein synthesis commences with translation initiation of the cap-independent IRES element at the 5′UTR of the EV-71 genome [64]. IRES is a *cis*-acting element that forms tertiary RNA structures and requires assistance from IRES-specific *trans*-acting factors (ITAFs) to recruit other cellular translation machinery to the viral RNA. The EV-71 open reading frame (ORF) is translated into a single polyprotein, which is subsequently processed by virus-encoded proteases 2A and 3C into the structural capsid proteins (VP1-VP4) and the nonstructural proteins (2A-2C and 3A-3D) mainly involved in the replication of the viral RNA [65].

The antisense-mediated mechanism consists of oligonucleotides (8-50 nucleotides in length) that bind to RNA through Watson-Crick base pairing and modulate the function of the targeted RNA [66]. RNA interference (RNAi) involves the cleavage of targeted mRNA through the RNA-induced silencing complex. Small interfering RNA (siRNA) targeting highly conserved regions of 5′ UTR [67], VP1, VP2 [68], 2C, 3C, 3D [69,70], and 3′ UTR [69] significantly inhibited EV-71 infection in a dose-dependent manner. In addition, short hairpin RNA (shRNA) was effective against EV-71 infection *in vitro* and *in vivo* [70-72]. The use of siRNA in clinical settings is hampered by its short half-life in plasma. Improved siRNA with 2′O methylation and 2′ fluoro modifications have recently been demonstrated against EV-71 infection [67]. However, siRNA also has poor endosomal uptake which limits the clinical application of these siRNAs. Other translation suppressing nucleotides, for example, peptide conjugated phosphodiamidate morpholino oligomers (PPMO) showed promising results in inhibiting PV and coxsackievirus B3 [73,74]. Unlike siRNA or shRNA, PPMO interacts with targeted RNA, especially the IRES region, and blocks ribosome recruitment and therefore inhibits viral RNA translation [66]. PPMO readily penetrates the cells and is resistant to nuclease degradation. Our unpublished data confirms that PMO are highly effective against EV-71.

Compounds that down-regulate the activity of IRES-dependent translation could potentially be developed into antiviral agents. Quinacrine, which impairs IRES-dependent translation by preventing the interaction between polypyrimidine-tract binding protein (PTB) and IRES, has been demonstrated to act against EV-71 infection [75]. Kaempferol, a flavonoid, was found to inhibit EV-71 IRES activity by altering the composition of ITAFs [76]. Geniposide derived from *Fructus gardeniae* inhibited EV-71 replication via inhibition of viral IRES activity [77]. Amantadine, a tricyclic symmetric amine previously used against influenza A virus infection, was found to suppress EV-71 IRES translation [78-80].

Therapeutics targeting viral polyprotein processing

Maturation cleavage of polyprotein into different viral proteins is a critical step during EV-71 infection. EV-71 2A and 3C protease are the key proteases that cleave the viral precursor polyprotein into each of the component proteins required for viral replication and packaging. Interestingly, EV-71 2A and 3C proteases suppress type I interferon by targeting mitochondrial anti-viral signaling (MAVS) protein and melanoma differentiation associated gene (MDA-5) viral recognition receptor signaling [81,82]. Since EV-71 2A and 3C proteases are involved in multiple roles in EV-71 infection and evasion of host innate immunity, they are important potential targets for development of antiviral therapeutics.

A pseudosubstrate, LVLQTM peptide, could inhibit EV-71 infection through binding to the active site of 2A protease [83]. Rupintrivir (AG7088) is an irreversible peptidomimetic inhibitor of human rhinovirus 3C protease, which reached phase 2 clinical trials with promising outcomes [84-89]. Rupintrivir showed significant inhibition of EV-71 infection *in vitro* and *in vivo* but with reduced efficacy as compared with human rhinoviruses [90-93]. X-ray crystallography of the complex of EV-71 3C protease with rupintrivir revealed that the half-closed S2 sub-site and the size reduced S1′ pocket of EV-71 3C protease limits the access of the rupintrivir's P1′ group which contains a lactam ring [94,95]. A series of 3C protease rupintrivir analogues were designed based on AG7088, with an aldehyde replacement of the α,β-unsaturated ester. Compound 10b significantly inhibited EV-71 infection [96]. An orally bioavailable 3C protease inhibitor, designated as compound 1, also exhibited antiviral activities against multiple rhinovirus serotypes and enteroviruses *in vitro* [89]. Flavonoids such as fisetin and rutin, have also been identified as 3C protease inhibitors [97].

Therapeutics targeting the membranous viral RNA replication complex and other host factors

The genomic replication of enteroviruses has been shown to occur in membranous compartments in the cytoplasm. The membranous vesicles induced during PV infection have been reported to be associated with autophagy signalling [98,99]. These compartments resemble the autophagosomes and consist of viral proteins as well as microtubule-associated protein 1 light chain 3-II (LC3-II). LC3-II is the membrane-bound form of LC3 that serves as the marker of autophagy induction [100]. During PV infection, these double-membrane vesicles consist of viral particles that undergo autophagic maturation typically characterized by LC3-II co-localization with lysosomal-associated membrane protein 1 (LAMP1) [100]. Similarly, EV-71 induces autophagy formation in RD and SK-N-SH cells, and association between autophagosome-like vesicles and EV-71 VP1 in neurons of the cervical spinal cords of mice was observed [101]. The authors concluded that autophagic signalling induced by EV-71 is crucial for EV-71 replication. This provides an alternative antiviral strategy for EV-71 to target host factors related to autophagy that are crucial for viral replication.

The discovery of antiviral drugs is mainly based on virus targets. The high replication and mutation rates of enteroviruses may generate resistance to these direct-acting antivirals. Targeting host factors may establish a higher genetic barrier to resistance and can be used in combination with viral inhibitors. The compound GW5074, a Raf-1 inhibitor, has been shown to influence EV-71 viral yield [37,102]. Activation of the Raf-1/ERK pathway in host cells induces autophagy signalling [103]. The downstream transducer of this pathway, BNIP3 competes with Beclin 1 for binding with Bcl-2 during autophagy induction [104]. GW5074 may impair autophagy activation through the inhibition of the Raf-1/ERK pathway. Thus, the replication of EV-71 that requires autophagosome formation may be inhibited in the presence of the GW5074 compound. Heat shock protein 90 beta (HSP90β), an isomer of HSP90, has been reported to have crucial roles in EV-71 entry and assembly. Geldanamycin (GA) and its analog, 17-allyamino-17-demethoxygeldanamycin (17-AAG), inhibit HSP90β activities and protect hSCARB2 transgenic mice from the challenge with EV-71 [105].

Inhibitors that target host factors such as those involved in cellular autophagy and HSP90β could be used against multiple EV-71 genotypes and enterovirus serotypes, due to their similar pathways of replication [106,107]. The major drawbacks of these inhibitors that target host factors are specificity and cellular toxicity. Therefore, there is an unmet need to develop specific and non-toxic antivirals that impair the cellular autophagy pathway and HSP90β during EV-71 infection.

The amino acid sequences of the non-structural proteins of EV-71 are highly conserved and have more than 60% similarity to PV. Two hydrophobic regions are found in the 2B viral protein of PV and are pivotal for its viroporin functionality [108]. 2B viroporin mediates the integration of viral protein into the ER membrane and this increases the membrane permeability to promote virus release [108]. A study has reported that EV-71 2B protein might mediate a chloride-dependent current in oocytes. A chloride-dependent current inhibitor, 4,4′-diisothiocyano-2,2′-stilbenedisulfonic acid (DIDS) has been reported to inhibit EV-71 infection in RD cells [109]. The 2C viral protein of PV consists of Walker A, B and C motifs that are homologous to the motifs found in NTP-binding proteins or in members of the helicase superfamily III [110]. An amphipathic helix domain is located at the N-terminal of 2C viral protein that has the function of promoting oligomerization [110]. Recently, two antiviral compounds, metrifudil (N-(2-methylphenyl) methyl adenosine) and N^6-benzyladenosine, blocked EV-71 replication via interaction with 2C viral protein or 2BC precursor protein [37]. Mutants resistant to metrifudil had a mutation in the 2C viral protein (E325G), while N^6-benzyladenosine-resistant mutants had double mutations at the 2C viral protein (H118Y and I324M) [37]. However, the mechanism of inhibition is yet to be determined. Both MRL-1237 and TBZE-029, derivatives of benzimidazole, exhibit antiviral activity against various enteroviruses, and have been identified to target the picornaviral 2C viral protein [111,112]. Both of these derivatives may exert potent antiviral activity against EV-71 since EV-71 and PV shared high similarity in all the non-structural proteins. Guanidine hydrochloride is an extensively-studied picornavirus inhibitor [113,114], which inhibits the replication of PV [115,116], coxsackieviruses [117], echoviruses, and foot-and-mouth disease virus [118]. Interestingly, guanidine hydrochloride also inhibits EV-71 infection and a single mutation, M193L at the 2C protein was sufficient to confer resistance [119]. This agent is likely to prevent the association of 2C/2BC with host membrane structures during viral replication [120].

The 3A viral protein of PV contains hydrophobic domains that facilitate its binding with membranous vesicles induced during viral RNA replication [121,122]. A benzimidazole derivative, enviroxime exhibits potent activity against PV and rhinovirus by interacting with 3A viral protein [119]. Strong antiviral effects of enviroxime have been shown against EV-71 [123]. Bifunctional inhibitors AN-12-H5 and AN-23-F6, are enviroxime-like compound that also targets 3A, VP1 and VP3, inhibits EV-71 infection efficiently [124]. However, the precise mechanism of action by enviroxime and AN-12-H5 against EV-71 infection remains unknown. Another

compound, TTP-8307, was identified as a potent 3A inhibitor that significantly inhibited CV-A16 infection, with reduced activity against EV-71 [112].

Therapeutics targeting RNA-dependent RNA polymerase (RdRP) complex

The viral RNA replication of enteroviruses begins with the linkage of genomic RNA with the 3B protein (VPg) at the 5′ end to form the uridylylated state of VPg (VPg-pUpU). Additionally, VPg uridylylation is stimulated by the viral precursor protein 3CD [125]. The positive strand of viral RNA is used as a template to synthesize the negative strand, which in turn serves as the template for the synthesis of new positive strands. The synthesis of both positive and negative strands of viral RNA is primed by VPg-pUpU [126]. Nucleotide site 311 of the RNA-dependent RNA polymerase (RdRP) of EV-71 is pivotal for VPg uridylylation and viral RNA synthesis, as mutations here impair the binding of VPg to RdRP, but did not influence normal RdRP activity [127].

Ribavirin (1-β-D-ribofuranosyl-1,2,4-triazole-3-carboxyamine) is a conventional nucleoside analogue that targets the RdRP of picornaviruses [128]. Ribavirin inhibits EV-71 infection with an IC_{50} of 266 μM, and prevents EV-71

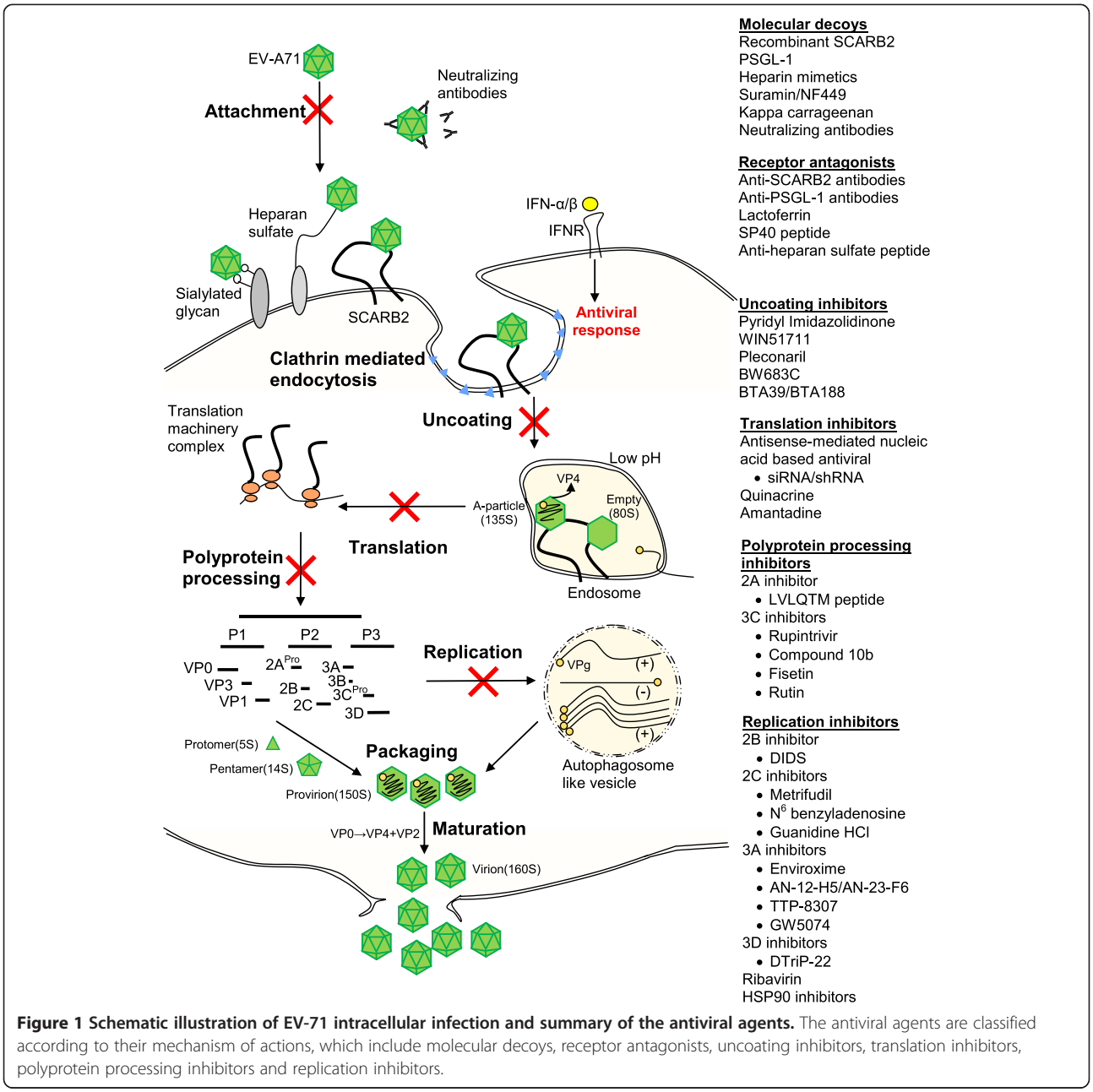

Figure 1 Schematic illustration of EV-71 intracellular infection and summary of the antiviral agents. The antiviral agents are classified according to their mechanism of actions, which include molecular decoys, receptor antagonists, uncoating inhibitors, translation inhibitors, polyprotein processing inhibitors and replication inhibitors.

Table 1 List of antivirals against EV-71 infection tested *in vitro* and *in vivo*

Antivirals	EV-71 genotype tested	IC_{50}/EC_{50}	*In vitro* cell type	Resistant mutants	*In vivo* mouse model	Reference
Therapeutics targeting viral attachment and entry						
Molecular decoys						
Recombinant SCARB2	B3	N/R	RD			[28]
PSGL-1	C2	N/R	L-PSGL-1.1			[29]
Heparin mimetics						
Heparin	C2	205 μg/ml	Vero, RD			[25,36]
Heparan sulfate	C2	290 μg/ml	Vero			[36]
Pentosan polysulfate	C2	238 μg/ml	Vero			[36]
Dextran sulfate	B4	N/R	RD			[25]
Suramin/NF449	B1, B3, B4	6.7 μM	RD	VP1 E98Q, K244R		[25,37]
Kappa carrageenan	B4	N/R	Vero			[38]
Enviroxime-like compounds						
AN-12-H5	B1	0.55 μM	RD	VP1 M119L, VP3 R227K		[124]
AN-23-F6	B1	0.15 μM	RD	VP1 A224T		[124]
Receptor antagonists						
Anti-SCARB2 antibodies	B3	N/R	RD			[28]
Anti-PSGL-1 antibodies	B3, B4, C1, C2, C4	N/R	Jurkat			[29]
Bovine lactoferrin	C2, MP4[a]	10.5 – 24.5 μg/ml	RD, Vero, SK-N-SH		17-days old ICR	[42,43]
Human lactoferrin	N/R	103.3 – 185.0 μg/ml	RD, Vero			[42]
SP40 peptide	A, B4, C2	6 – 9.3 μM	RD, HeLa, HT-29, Vero			[39]
Anti-heparan sulfate peptide	B4	N/R	RD			[25,40]
Therapeutics targeting viral uncoating						
Pyridyl imidazolidinone						
BPROZ-299	C2	0.02 μM	RD	VP1 V192M		[52]
BPROZ-284	A, B1, C2	0.04 μM	RD			[49]
BPROZ-194	C2	1.552 μM	RD	VP1 V192M		[51,52]
BPROZ-160	C2	0.011 μM	RD	VP1 V192M		[52]
BPROZ-112	A, B1, C2	0.04 μM	RD			[49]
BPROZ-103	C2	0.13 μM	RD	VP1 V192M		[52]
BPROZ-101	A, B1, C2	0.0012 μM	RD			[52,53]
BPROZ-074	A, B1, C2	0.0008 – 0.018 μM	RD	VP1 V192M		[52,54]
BPROZ-033	A, B1, C2	0.0088 – 0.069 μM	RD			[52,54]
WIN51711	B3	N/R	RD			[48]
Pleconaril	A	0.13-0.54 μg/ml	RD		1-day old ICR	[56]
BW683C	A	> 10 μM	HEp-2			[59]
Compound 3 g	A	0.45 μM	HEp-2			[59]
BTA39	A	0.001 μM	Vero			[57]

Table 1 List of antivirals against EV-71 infection tested *in vitro* and *in vivo* (Continued)

BTA188	A	0.082 μM	Vero			[57]
Therapeutics targeting viral translation						
RNA-based therapeutics						
siRNA	B4	< 1 nM	RD		1-day old Balb/c	[67-72]
shRNA	B4	< 1 nM	RD		1-day old Balb/c	[67-72]
Quinacrine	C4	9.71 μM	RD			[75]
Amantadine	Pseudo-EV-71	N/R	COS-1			[78]
Therapeutics targeting viral polyprotein processing						
2A inhibitor						
LVLQTM peptide	C4	9.6 μM	HeLa			[83]
3C inhibitors						
Rupintrivir	C4	0.014 μM	RD		2-days old ICR	[93]
Compound 10b	C2	0.018 μM	RD			[96]
Fisetin	CMUH01*	85 μM	RD			[97]
Rutin	CMUH01*	110 μM	RD			[97]
Therapeutics targeting viral replication						
2B inhibitor						
DIDS	C4	N/R	RD			[109]
2C inhibitors						
Metrifudil	B1	1.3 μM	RD	2C E325G		[37]
N^6 benzyladenosine	B1	0.1 μM	RD	2C H118Y, I324M		[37]
Guanidine-HCl	B3	N/R	RD	2C M193L		[119]
3A inhibitors						
Enviroxime	A	0.15 μM	Vero			[112]
AN-12-H5	B1	0.55 μM	RD	3A E39G		[124]
AN-23-F6	B1	0.15 μM	RD			[124]
TTP-8307	A	> 60 μM	Vero			[112]
GW5074	B1	6.4 μM	RD			[124]
3D inhibitors						
DTriP-22	A, B2, C2	0.3 μM	RD	3D R163K		[130]
Ribavirin	C2, M2[b]	266 μM	RD, SK-N-SH, N18	3D G64R, S264L	12-days old ICR	[129]
Heat-shock protein 90 inhibitor						
Geldanamycin	B4, C2	N/R	RD			[105]
17-AAG	C2, C4	N/R	N/R		7-days old hSCARB-Tg C57BL/6 mice	[105]

[a]Mouse-adapted EV-71 strain Tainan/4643/98 (C2); [b]Mouse-adapted EV-71 strain derived from MP4 with additional two passages in mice; *EV-71 strain with unidentified genotype; and N/R means not reported.
RD: rhabdomyosarcoma cells; Vero: African green monkey kidney cells; SK-N-SH: human neuroblastoma cells; N18: mouse neuroblastoma cells; HeLa: human cervical adenocarcinoma epithelial cells; HT-29: human colon adenocarcinoma cells; HEp-2: HeLa contaminant cells; Jurkat: human T lymphocytes cells; and COS-1: monkey kidney fibroblast cells.

induced paralysis and death in mice [129]. Recently, a piperazine-containing pyrazolo [3,4-*d*] pyrimidine derivative, DTriP-22, was shown to effectively target the RdRP of EV-71 with IC_{50} values of 0.15 – 0.98 μM, and suppress the accumulation of both positive and negative strands of viral RNA during EV-71 infection. DTriP-22-resistant

mutants had mutations in the RdRP, implying that DTriP-22 interacts with RdRP and inhibits poly (U) elongation activity, but not VPg uridylylation [130].

Conclusion

Figure 1 and Table 1 summarizes all the potential targets of antivirals and lists the recent antiviral agents with significant antiviral activities against EV-71 infection as discussed above. Amongst these drugs, modified WIN compounds are antivirals with the lowest IC_{50}. Only bovine lactoferrin, pleconaril, shRNA, siRNA, rupintrivir, ribavirin and 17-AAG have been tested *in vivo*. Ribavirin and amantadine are already in clinical use for other viruses, and rupintrivir and pleconaril are in clinical development.

The availability of a suitable animal model carrying all the required receptors and attachment factors for testing of the antivirals will accelerate the development of antivirals. The clinical use of other antiviral agents has been hampered by the potential adverse effects to the host and emergence of drug resistance mutants. Combination therapy targeting different replication steps of EV-71 infection cycle has shown synergistic activity [131] and could minimize the emergence of antiviral resistance. A new antiviral strategy to screen all licensed drugs against EV-71 infection would be more promising for clinical use. Other newer antivirals that act as immunomodulators and lethal mutagens offer a new strategy for development of antivirals. With the endemic and epidemic nature of EV-71, the continued efforts to develop antiviral agents for prophylaxis or treatment are crucial in the absence of a vaccine. Together with an effective vaccine, eradication of EV-71 is anticipated.

Abbreviations

EV-71: Enterovirus 71; HFMD: Hand, foot and mouth disease; IRES: Internal ribosome entry site; ITAF: IRES-specific *trans*-acting factor; MAVS: Mitochondrial anti-viral signaling; MDA-5: Melanoma differentiation associated gene; ORF: Open reading frame; PV: Poliovirus; RdRP: RNA-dependent RNA polymerase; VPg: Viral protein genome-linked.

Competing interests

CWT and YFC have a pending patent on SP40 peptide.

Authors' contributions

CWT, JKFL, ICS and YFC drafted the manuscript. All authors read and approved the final manuscript.

Acknowledgement

This work was supported by the High Impact Research grant (UM.C/625/1/HIR/MOHE/MED/41), postgraduate research grants (PV013-2012A and PG114-2012B), and University Malaya Research Grant Scheme (RG522-13HTM) from University Malaya; and the Fundamental Research Grant Scheme (FP015-2012A) and Exploratory Research Grant Scheme (ER017-2013A) from the Ministry of Education, Malaysia.

Received: 29 November 2013 Accepted: 9 February 2014
Published: 12 February 2014

References

1. Brown BA, Pallansch MA: **Complete nucleotide sequence of enterovirus 71 is distinct from poliovirus.** *Virus Res* 1995, **39:**195–205.
2. Plevka P, Perera R, Cardosa J, Kuhn RJ, Rossmann MG: **Crystal structure of human enterovirus 71.** *Science* 2012, **336:**1274.
3. Chumakov M, Voroshilova M, Shindarov L, Lavrova I, Gracheva L, Koroleva G, Vasilenko S, Brodvarova I, Nikolova M, Gyurova S, *et al*: **Enterovirus 71 isolated from cases of epidemic poliomyelitis-like disease in Bulgaria.** *Arch Virol* 1979, **60:**329–340.
4. Shindarov LM, Chumakov MP, Voroshilova MK, Bojinov S, Vasilenko SM, Iordanov I, Kirov ID, Kamenov E, Leshchinskaya EV, Mitov G, *et al*: **Epidemiological, clinical, and pathomorphological characteristics of epidemic poliomyelitis-like disease caused by enterovirus 71.** *J Hyg Epidemiol Microbiol Immunol* 1979, **23:**284–295.
5. Nagy G, Takatsy S, Kukan E, Mihaly I, Domok I: **Virological diagnosis of enterovirus type 71 infections: experiences gained during an epidemic of acute CNS diseases in Hungary in 1978.** *Arch Virol* 1982, **71:**217–227.
6. Huang KY, Zhang X, Chung PH, Tsao KC, Lin TY, Su LH, Chiu CH: **Enterovirus 71 in Taiwan, 2004-2006: epidemiological and virological features.** *Scand J Infect Dis* 2008, **40:**571–574.
7. Brown BA, Oberste MS, Alexander JP Jr, Kennett ML, Pallansch MA: **Molecular epidemiology and evolution of enterovirus 71 strains isolated from 1970 to 1998.** *J Virol* 1999, **73:**9969–9975.
8. Chan KP, Goh KT, Chong CY, Teo ES, Lau G, Ling AE: **Epidemic hand, foot and mouth disease caused by human enterovirus 71, Singapore.** *Emerg Infect Dis* 2003, **9:**78–85.
9. AbuBakar S, Chee HY, Al-Kobaisi MF, Xiaoshan J, Chua KB, Lam SK: **Identification of enterovirus 71 isolates from an outbreak of hand, foot and mouth disease (HFMD) with fatal cases of encephalomyelitis in Malaysia.** *Virus Res* 1999, **61:**1–9.
10. Tan X, Huang X, Zhu S, Chen H, Yu Q, Wang H, Huo X, Zhou J, Wu Y, Yan D, *et al*: **The persistent circulation of enterovirus 71 in People's Republic of China: causing emerging nationwide epidemics since 2008.** *PLoS One* 2011, **6:**e25662.
11. Zhang Y, Tan XJ, Wang HY, Yan DM, Zhu SL, Wang DY, Ji F, Wang XJ, Gao YJ, Chen L, *et al*: **An outbreak of hand, foot, and mouth disease associated with subgenotype C4 of human enterovirus 71 in Shandong, China.** *J Clin Virol* 2009, **44:**262–267.
12. Zhang Y, Wang J, Guo W, Wang H, Zhu S, Wang D, Bai R, Li X, Yan D, Zhu Z, *et al*: **Emergence and transmission pathways of rapidly evolving evolutionary branch C4a strains of human enterovirus 71 in the Central Plain of China.** *PLoS One* 2011, **6:**e27895.
13. Zhang Y, Zhu Z, Yang W, Ren J, Tan X, Wang Y, Mao N, Xu S, Zhu S, Cui A, *et al*: **An emerging recombinant human enterovirus 71 responsible for the 2008 outbreak of hand foot and mouth disease in Fuyang city of China.** *Virol J* 2010, **7:**94.
14. Zhu RN, Qian Y, Deng J, Xing JF, Zhao LQ, Wang F, Liao B, Ren XX, Li Y, Zhang Q, Li J: **Study on the association of hand, foot and mouth disease and enterovirus 71/CA16 among children in Beijing, 2007.** *Zhonghua Liu Xing Bing Xue Za Zhi* 2007, **28:**1004–1008.
15. le Thoa PK, Chiang PS, Khanh TH, Luo ST, Dan TN, Wang YF, Thuong TC, Chung WY, Hung NT, Wang JR, *et al*: **Genetic and antigenic characterization of enterovirus 71 in Ho Chi Minh city, Vietnam, 2011.** *PLoS One* 2013, **8:**e69895.
16. Biswas T: **Enterovirus 71 causes hand, foot and mouth disease outbreak in Cambodia.** *Natl Med J India* 2012, **25:**316.
17. Ooi MH, Wong SC, Lewthwaite P, Cardosa MJ, Solomon T: **Clinical features, diagnosis, and management of enterovirus 71.** *Lancet Neurol* 2010, **9:**1097–1105.
18. Solomon T, Lewthwaite P, Perera D, Cardosa MJ, McMinn P, Ooi MH: **Virology, epidemiology, pathogenesis, and control of enterovirus 71.** *Lancet Infect Dis* 2010, **10:**778–790.
19. Chang LY, Lin TY, Hsu KH, Huang YC, Lin KL, Hsueh C, Shih SR, Ning HC, Hwang MS, Wang HS, Lee CY: **Clinical features and risk factors of pulmonary oedema after enterovirus-71-related hand, foot, and mouth disease.** *Lancet* 1999, **354:**1682–1686.
20. Chang LY, Huang LM, Gau SS, Wu YY, Hsia SH, Fan TY, Lin KL, Huang YC, Lu CY, Lin TY: **Neurodevelopment and cognition in children after enterovirus 71 infection.** *N Engl J Med* 2007, **356:**1226–1234.
21. Shang LQ, Xu MY, Yin Z: **Antiviral drug discovery for the treatment of enterovirus 71 infections.** *Antiviral Res* 2013, **97:**183–194.

22. Kuo RL, Shih SR: **Strategies to develop antivirals against enterovirus 71.** *Virol J* 2013, **10:**28.
23. Chong P, Hsieh SY, Liu CC, Chou AH, Chang JY, Wu SC, Liu SJ, Chow YH, Su IJ, Klein M: **Production of EV71 vaccine candidates.** *Hum Vaccin Immunother* 2012, **8:**1775–1783.
24. Haywood AM: **Virus receptors: binding, adhesion strengthening, and changes in viral structure.** *J Virol* 1994, **68:**1–5.
25. Tan CW, Poh CL, Sam IC, Chan YF: **Enterovirus 71 uses cell surface heparan sulfate glycosaminoglycan as an attachment receptor.** *J Virol* 2013, **87:**611–620.
26. Yang B, Chuang H, Yang KD: **Sialylated glycans as receptor and inhibitor of enterovirus 71 infection to DLD-1 intestinal cells.** *Virol J* 2009, **6:**141.
27. Su PY, Liu YT, Chang HY, Huang SW, Wang YF, Yu CK, Wang JR, Chang CF: **Cell surface sialylation affects binding of enterovirus 71 to rhabdomyosarcoma and neuroblastoma cells.** *BMC Microbiol* 2012, **12:**162.
28. Yamayoshi S, Yamashita Y, Li J, Hanagata N, Minowa T, Takemura T, Koike S: **Scavenger receptor B2 is a cellular receptor for enterovirus 71.** *Nat Med* 2009, **15:**798–801.
29. Nishimura Y, Shimojima M, Tano Y, Miyamura T, Wakita T, Shimizu H: **Human P-selectin glycoprotein ligand-1 is a functional receptor for enterovirus 71.** *Nat Med* 2009, **15:**794–797.
30. Yamayoshi S, Ohka S, Fujii K, Koike S: **Functional comparison of SCARB2 and PSGL1 as receptors for enterovirus 71.** *J Virol* 2013, **87:**3335–3347.
31. Chen P, Song Z, Qi Y, Feng X, Xu N, Sun Y, Wu X, Yao X, Mao Q, Li X, *et al*: **Molecular determinants of enterovirus 71 viral entry: cleft around GLN-172 on VP1 protein interacts with variable region on scavenge receptor B 2.** *J Biol Chem* 2012, **287:**6406–6420.
32. Lin YW, Yu SL, Shao HY, Lin HY, Liu CC, Hsiao KN, Chitra E, Tsou YL, Chang HW, Sia C, *et al*: **Human SCARB2 transgenic mice as an infectious animal model for enterovirus 71.** *PLoS One* 2013, **8:**e57591.
33. Fujii K, Nagata N, Sato Y, Ong KC, Wong KT, Yamayoshi S, Shimanuki M, Shitara H, Taya C, Koike S: **Transgenic mouse model for the study of enterovirus 71 neuropathogenesis.** *Proc Natl Acad Sci U S A* 2013, **110:**14753–14758.
34. Lin HY, Yang YT, Yu SL, Hsiao KN, Liu CC, Sia C, Chow YH: **Caveolar endocytosis is required for human PSGL-1-mediated enterovirus 71 infection.** *J Virol* 2013, **87:**9064–9076.
35. Liu J, Dong W, Quan X, Ma C, Qin C, Zhang L: **Transgenic expression of human P-selectin glycoprotein ligand-1 is not sufficient for enterovirus 71 infection in mice.** *Arch Virol* 2012, **157:**539–543.
36. Pourianfar HR, Poh CL, Fecondo J, Grollo L: **In vitro evaluation of the antiviral activity of heparan sulphate mimetic compounds against enterovirus 71.** *Virus Res* 2012, **169:**22–29.
37. Arita M, Wakita T, Shimizu H: **Characterization of pharmacologically active compounds that inhibit poliovirus and enterovirus 71 infectivity.** *J Gen Virol* 2008, **89:**2518–2530.
38. Chiu YH, Chan YL, Tsai LW, Li TL, Wu CJ: **Prevention of human enterovirus 71 infection by kappa carrageenan.** *Antiviral Res* 2012, **95:**128–134.
39. Tan CW, Chan YF, Sim KM, Tan EL, Poh CL: **Inhibition of enterovirus 71 (EV-71) infections by a novel antiviral peptide derived from EV-71 capsid protein VP1.** *PLoS One* 2012, **7:**e34589.
40. Tiwari V, Liu J, Valyi-Nagy T, Shukla D: **Anti-heparan sulfate peptides that block herpes simplex virus infection in vivo.** *J Biol Chem* 2011, **286:**25406–25415.
41. Chen HL, Wang LC, Chang CH, Yen CC, Cheng WT, Wu SC, Hung CM, Kuo MF, Chen CM: **Recombinant porcine lactoferrin expressed in the milk of transgenic mice protects neonatal mice from a lethal challenge with enterovirus type 71.** *Vaccine* 2008, **26:**891–898.
42. Lin TY, Chu C, Chiu CH: **Lactoferrin inhibits enterovirus 71 infection of human embryonal rhabdomyosarcoma cells in vitro.** *J Infect Dis* 2002, **186:**1161–1164.
43. Weng TY, Chen LC, Shyu HW, Chen SH, Wang JR, Yu CK, Lei HY, Yeh TM: **Lactoferrin inhibits enterovirus 71 infection by binding to VP1 protein and host cells.** *Antiviral Res* 2005, **67:**31–37.
44. Shingler KL, Yoder JL, Carnegie MS, Ashley RE, Makhov AM, Conway JF, Hafenstein S: **The enterovirus 71 A-particle forms a gateway to allow genome release: a cryoEM study of picornavirus uncoating.** *PLoS Pathog* 2013, **9:**e1003240.
45. Fox MP, Otto MJ, McKinlay MA: **Prevention of rhinovirus and poliovirus uncoating by WIN 51711, a new antiviral drug.** *Antimicrob Agents Chemother* 1986, **30:**110–116.
46. McKinlay MA, Frank JA Jr, Benziger DP, Steinberg BA: **Use of WIN 51711 to prevent echovirus type 9-induced paralysis in suckling mice.** *J Infect Dis* 1986, **154:**676–681.
47. See DM, Tilles JG: **Treatment of coxsackievirus A9 myocarditis in mice with WIN 54954.** *Antimicrob Agents Chemother* 1992, **36:**425–428.
48. Plevka P, Perera R, Yap ML, Cardosa J, Kuhn RJ, Rossmann MG: **Structure of human enterovirus 71 in complex with a capsid-binding inhibitor.** *Proc Natl Acad Sci U S A* 2013, **110:**5463–5467.
49. Shia KS, Li WT, Chang CM, Hsu MC, Chern JH, Leong MK, Tseng SN, Lee CC, Lee YC, Chen SJ, *et al*: **Design, synthesis, and structure-activity relationship of pyridyl imidazolidinones: a novel class of potent and selective human enterovirus 71 inhibitors.** *J Med Chem* 2002, **45:**1644–1655.
50. Shih SR, Chen SJ, Hakimelahi GH, Liu HJ, Tseng CT, Shia KS: **Selective human enterovirus and rhinovirus inhibitors: an overview of capsid-binding and protease-inhibiting molecules.** *Med Res Rev* 2004, **24:**449–474.
51. Shih SR, Tsai MC, Tseng SN, Won KF, Shia KS, Li WT, Chern JH, Chen GW, Lee CC, Lee YC, *et al*: **Mutation in enterovirus 71 capsid protein VP1 confers resistance to the inhibitory effects of pyridyl imidazolidinone.** *Antimicrob Agents Chemother* 2004, **48:**3523–3529.
52. Chen TC, Liu SC, Huang PN, Chang HY, Chern JH, Shih SR: **Antiviral activity of pyridyl imidazolidinones against enterovirus 71 variants.** *J Biomed Sci* 2008, **15:**291–300.
53. Chern JH, Shia KS, Hsu TA, Tai CL, Lee CC, Lee YC, Chang CS, Tseng SN, Shih SR: **Design, synthesis, and structure-activity relationships of pyrazolo [3,4-d]pyrimidines: a novel class of potent enterovirus inhibitors.** *Bioorg Med Chem Lett* 2004, **14:**2519–2525.
54. Chang CS, Lin YT, Shih SR, Lee CC, Lee YC, Tai CL, Tseng SN, Chern JH: **Design, synthesis, and antipicornavirus activity of 1-[5-(4-arylphenoxy) alkyl]-3-pyridin-4-ylimidazolidin-2-one derivatives.** *J Med Chem* 2005, **48:**3522–3535.
55. Pevear DC, Tull TM, Seipel ME, Groarke JM: **Activity of pleconaril against enteroviruses.** *Antimicrob Agents Chemother* 1999, **43:**2109–2115.
56. Zhang G, Zhou F, Gu B, Ding C, Feng D, Xie F, Wang J, Zhang C, Cao Q, Deng Y, *et al*: **In vitro and in vivo evaluation of ribavirin and pleconaril antiviral activity against enterovirus 71 infection.** *Arch Virol* 2012, **157:**669–679.
57. Barnard DL, Hubbard VD, Smee DF, Sidwell RW, Watson KG, Tucker SP, Reece PA: **In vitro activity of expanded-spectrum pyridazinyl oxime ethers related to pirodavir: novel capsid-binding inhibitors with potent antipicornavirus activity.** *Antimicrob Agents Chemother* 2004, **48:**1766–1772.
58. Chapman MS, Minor I, Rossmann MG, Diana GD, Andries K: **Human rhinovirus 14 complexed with antiviral compound R 61837.** *J Mol Biol* 1991, **217:**455–463.
59. Genovese D, Conti C, Tomao P, Desideri N, Stein ML, Catone S, Fiore L: **Effect of chloro-, cyano-, and amidino-substituted flavanoids on enterovirus infection in vitro.** *Antiviral Res* 1995, **27:**123–136.
60. Conti C, Mastromarino P, Sgro R, Desideri N: **Anti-picornavirus activity of synthetic flavon-3-yl esters.** *Antivir Chem Chemother* 1998, **9:**511–515.
61. Bauer DJ, Selway JW, Batchelor JF, Tisdale M, Caldwell IC, Young DA: **4′,6-Dichloroflavan (BW683C), a new anti-rhinovirus compound.** *Nature* 1981, **292:**369–370.
62. Tisdale M, Selway JW: **Inhibition of an early stage of rhinovirus replication by dichloroflavan (BW683C).** *J Gen Virol* 1983, **64:**795–803.
63. Tisdale M, Selway JW: **Effect of dichloroflavan (BW683C) on the stability and uncoating of rhinovirus type 1B.** *J Antimicrob Chemother* 1984, **14**(Suppl A):97–105.
64. Thompson SR, Sarnow P: **Enterovirus 71 contains a type I IRES element that functions when eukaryotic initiation factor eIF4G is cleaved.** *Virology* 2003, **315:**259–266.
65. Lin JY, Chen TC, Weng KF, Chang SC, Chen LL, Shih SR: **Viral and host proteins involved in picornavirus life cycle.** *J Biomed Sci* 2009, **16:**103.
66. Kole R, Krainer AR, Altman S: **RNA therapeutics: beyond RNA interference and antisense oligonucleotides.** *Nat Rev Drug Discov* 2012, **11:**125–140.
67. Deng JX, Nie XJ, Lei YF, Ma CF, Xu DL, Li B, Xu ZK, Zhang GC: **The highly conserved 5′ untranslated region as an effective target towards the inhibition of enterovirus 71 replication by unmodified and appropriate 2′- modified siRNAs.** *J Biomed Sci* 2012, **19:**73.
68. Wu Z, Yang F, Zhao R, Zhao L, Guo D, Jin Q: **Identification of small interfering RNAs which inhibit the replication of several enterovirus 71 strains in China.** *J Virol Methods* 2009, **159:**233–238.

69. Sim AC, Luhur A, Tan TM, Chow VT, Poh CL: **RNA interference against enterovirus 71 infection.** *Virology* 2005, **341:**72–79.
70. Tan EL, Tan TM, Tak Kwong Chow V, Poh CL: **Inhibition of enterovirus 71 in virus-infected mice by RNA interference.** *Mol Ther* 2007, **15:**1931–1938.
71. Tan EL, Tan TM, Chow VT, Poh CL: **Enhanced potency and efficacy of 29-mer shRNAs in inhibition of enterovirus 71.** *Antiviral Res* 2007, **74:**9–15.
72. Lu WW, Hsu YY, Yang JY, Kung SH: **Selective inhibition of enterovirus 71 replication by short hairpin RNAs.** *Biochem Biophys Res Commun* 2004, **325:**494–499.
73. Stone JK, Rijnbrand R, Stein DA, Ma Y, Yang Y, Iversen PL, Andino R: **A morpholino oligomer targeting highly conserved internal ribosome entry site sequence is able to inhibit multiple species of picornavirus.** *Antimicrob Agents Chemother* 2008, **52:**1970–1981.
74. Yuan J, Stein DA, Lim T, Qiu D, Coughlin S, Liu Z, Wang Y, Blouch R, Moulton HM, Iversen PL, Yang D: **Inhibition of coxsackievirus B3 in cell cultures and in mice by peptide-conjugated morpholino oligomers targeting the internal ribosome entry site.** *J Virol* 2006, **80:**11510–11519.
75. Wang J, Du J, Wu Z, Jin Q: **Quinacrine impairs enterovirus 71 RNA replication by preventing binding of polypyrimidine-tract binding protein with internal ribosome entry sites.** *PLoS One* 2013, **8:**e52954.
76. Tsai FJ, Lin CW, Lai CC, Lan YC, Lai CH, Hung CH, Hsueh KC, Lin TH, Chang HC, Wan L, *et al*: **Kaempferol inhibits enterovirus 71 replication and internal ribosome entry site (IRES) activity through FUBP and HNRP proteins.** *Food Chem* 2011, **128:**312–322.
77. Lin YJ, Lai CC, Lai CH, Sue SC, Lin CW, Hung CH, Lin TH, Hsu WY, Huang SM, Hung YL, *et al*: **Inhibition of enterovirus 71 infections and viral IRES activity by Fructus gardeniae and geniposide.** *Eur J Med Chem* 2013, **62:**206–213.
78. Chen YJ, Zeng SJ, Hsu JT, Horng JT, Yang HM, Shih SR, Chu YT, Wu TY: **Amantadine as a regulator of internal ribosome entry site.** *Acta Pharmacol Sin* 2008, **29:**1327–1333.
79. Davies WL, Grunert RR, Hoffmann CE: **Influenza virus growth and antibody response in amantadine-treated mice.** *J Immunol* 1965, **95:**1090–1094.
80. Hoffmann CE, Neumayer EM, Haff RF, Goldsby RA: **Mode of action of the antiviral activity of amantadine in tissue culture.** *J Bacteriol* 1965, **90:**623–628.
81. Wang B, Xi X, Lei X, Zhang X, Cui S, Wang J, Jin Q, Zhao Z: **Enterovirus 71 protease 2Apro targets MAVS to inhibit anti-viral type I interferon responses.** *PLoS Pathog* 2013, **9:**e1003231.
82. Lei X, Xiao X, Xue Q, Jin Q, He B, Wang J: **Cleavage of interferon regulatory factor 7 by enterovirus 71 3C suppresses cellular responses.** *J Virol* 2013, **87:**1690–1698.
83. Falah N, Montserret R, Lelogeais V, Schuffenecker I, Lina B, Cortay JC, Violot S: **Blocking human enterovirus 71 replication by targeting viral 2A protease.** *J Antimicrob Chemother* 2012, **67:**2865–2869.
84. Witherell G: **AG-7088 Pfizer.** *Curr Opin Investig Drugs* 2000, **1:**297–302.
85. Binford SL, Maldonado F, Brothers MA, Weady PT, Zalman LS, Meador JW 3rd, Matthews DA, Patick AK: **Conservation of amino acids in human rhinovirus 3C protease correlates with broad-spectrum antiviral activity of rupintrivir, a novel human rhinovirus 3C protease inhibitor.** *Antimicrob Agents Chemother* 2005, **49:**619–626.
86. Binford SL, Weady PT, Maldonado F, Brothers MA, Matthews DA, Patick AK: **In vitro resistance study of rupintrivir, a novel inhibitor of human rhinovirus 3C protease.** *Antimicrob Agents Chemother* 2007, **51:**4366–4373.
87. Patick AK: **Rhinovirus chemotherapy.** *Antiviral Res* 2006, **71:**391–396.
88. Patick AK, Binford SL, Brothers MA, Jackson RL, Ford CE, Diem MD, Maldonado F, Dragovich PS, Zhou R, Prins TJ, *et al*: **In vitro antiviral activity of AG7088, a potent inhibitor of human rhinovirus 3C protease.** *Antimicrob Agents Chemother* 1999, **43:**2444–2450.
89. Patick AK, Brothers MA, Maldonado F, Binford S, Maldonado O, Fuhrman S, Petersen A, Smith GJ 3rd, Zalman LS, Burns-Naas LA, Tran JQ: **In vitro antiviral activity and single-dose pharmacokinetics in humans of a novel, orally bioavailable inhibitor of human rhinovirus 3C protease.** *Antimicrob Agents Chemother* 2005, **49:**2267–2275.
90. Zhang XN, Song ZG, Jiang T, Shi BS, Hu YW, Yuan ZH: **Rupintrivir is a promising candidate for treating severe cases of Enterovirus-71 infection.** *World J Gastroenterol* 2010, **16:**201–209.
91. Hung HC, Wang HC, Shih SR, Teng IF, Tseng CP, Hsu JT: **Synergistic inhibition of enterovirus 71 replication by interferon and rupintrivir.** *J Infect Dis* 2011, **203:**1784–1790.
92. Lu G, Qi J, Chen Z, Xu X, Gao F, Lin D, Qian W, Liu H, Jiang H, Yan J, Gao GF: **Enterovirus 71 and coxsackievirus A16 3C proteases: binding to rupintrivir and their substrates and anti-hand, foot, and mouth disease virus drug design.** *J Virol* 2011, **85:**10319–10331.
93. Zhang X, Song Z, Qin B, Chen L, Hu Y, Yuan Z: **Rupintrivir is a promising candidate for treating severe cases of enterovirus-71 infection: evaluation of antiviral efficacy in a murine infection model.** *Antiviral Res* 2013, **97:**264–269.
94. Wang J, Fan T, Yao X, Wu Z, Guo L, Lei X, Wang M, Jin Q, Cui S: **Crystal structures of enterovirus 71 3C protease complexed with rupintrivir reveal the roles of catalytically important residues.** *J Virol* 2011, **85:**10021–10030.
95. Wu C, Cai Q, Chen C, Li N, Peng X, Cai Y, Yin K, Chen X, Wang X, Zhang R, *et al*: **Structures of enterovirus 71 3C proteinase (strain E2004104-TW-CDC) and its complex with rupintrivir.** *Acta Crystallogr D Biol Crystallogr* 2013, **69:**866–871.
96. Kuo CJ, Shie JJ, Fang JM, Yen GR, Hsu JT, Liu HG, Tseng SN, Chang SC, Lee CY, Shih SR, Liang PH: **Design, synthesis, and evaluation of 3C protease inhibitors as anti-enterovirus 71 agents.** *Bioorg Med Chem* 2008, **16:**7388–7398.
97. Lin YJ, Chang YC, Hsiao NW, Hsieh JL, Wang CY, Kung SH, Tsai FJ, Lan YC, Lin CW: **Fisetin and rutin as 3C protease inhibitors of enterovirus A71.** *J Virol Methods* 2012, **182:**93–98.
98. Rust RC, Landmann L, Gosert R, Tang BL, Hong W, Hauri HP, Egger D, Bienz K: **Cellular COPII proteins are involved in production of the vesicles that form the poliovirus replication complex.** *J Virol* 2001, **75:**9808–9818.
99. Egger D, Teterina N, Ehrenfeld E, Bienz K: **Formation of the poliovirus replication complex requires coupled viral translation, vesicle production, and viral RNA synthesis.** *J Virol* 2000, **74:**6570–6580.
100. Jackson WT, Giddings TH Jr, Taylor MP, Mulinyawe S, Rabinovitch M, Kopito RR, Kirkegaard K: **Subversion of cellular autophagosomal machinery by RNA viruses.** *PLoS Biol* 2005, **3:**e156.
101. Huang SC, Chang CL, Wang PS, Tsai Y, Liu HS: **Enterovirus 71-induced autophagy detected in vitro and in vivo promotes viral replication.** *J Med Virol* 2009, **81:**1241–1252.
102. Arita M, Wakita T, Shimizu H: **Cellular kinase inhibitors that suppress enterovirus replication have a conserved target in viral protein 3A similar to that of enviroxime.** *J Gen Virol* 2009, **90:**1869–1879.
103. Shima Y, Okamoto T, Aoyama T, Yasura K, Ishibe T, Nishijo K, Shibata KR, Kohno Y, Fukiage K, Otsuka S, *et al*: **In vitro transformation of mesenchymal stem cells by oncogenic H-rasVal12.** *Biochem Biophys Res Commun* 2007, **353:**60–66.
104. Bellot G, Garcia-Medina R, Gounon P, Chiche J, Roux D, Pouyssegur J, Mazure NM: **Hypoxia-induced autophagy is mediated through hypoxia-inducible factor induction of BNIP3 and BNIP3L via their BH3 domains.** *Mol Cell Biol* 2009, **29:**2570–2581.
105. Tsou YL, Lin YW, Chang HW, Lin HY, Shao HY, Yu SL, Liu CC, Chitra E, Sia C, Chow YH: **Heat shock protein 90: role in enterovirus 71 entry and assembly and potential target for therapy.** *PLoS One* 2013, **8:**e77133.
106. Pfefferle S, Schopf J, Kogl M, Friedel CC, Muller MA, Carbajo-Lozoya J, Stellberger T, von Dall'Armi E, Herzog P, Kallies S, *et al*: **The SARS-coronavirus-host interactome: identification of cyclophilins as target for pan-coronavirus inhibitors.** *PLoS Pathog* 2011, **7:**e1002331.
107. Marcellin P, Horsmans Y, Nevens F, Grange JD, Bronowicki JP, Vetter D, Purdy S, Garg V, Bengtsson L, McNair L, Alam J: **Phase 2 study of the combination of merimepodib with peginterferon-alpha2b, and ribavirin in nonresponders to previous therapy for chronic hepatitis C.** *J Hepatol* 2007, **47:**476–483.
108. Martinez-Gil L, Bano-Polo M, Redondo N, Sanchez-Martinez S, Nieva JL, Carrasco L, Mingarro I: **Membrane integration of poliovirus 2B viroporin.** *J Virol* 2011, **85:**11315–11324.
109. Xie S, Wang K, Yu W, Lu W, Xu K, Wang J, Ye B, Schwarz W, Jin Q, Sun B: **DIDS blocks a chloride-dependent current that is mediated by the 2B protein of enterovirus 71.** *Cell Res* 2011, **21:**1271–1275.
110. Adams P, Kandiah E, Effantin G, Steven AC, Ehrenfeld E: **Poliovirus 2C protein forms homo-oligomeric structures required for ATPase activity.** *J Biol Chem* 2009, **284:**22012–22021.
111. Shimizu H, Agoh M, Agoh Y, Yoshida H, Yoshii K, Yoneyama T, Hagiwara A, Miyamura T: **Mutations in the 2C region of poliovirus responsible for altered sensitivity to benzimidazole derivatives.** *J Virol* 2000, **74:**4146–4154.

112. De Palma AM, Thibaut HJ, van der Linden L, Lanke K, Heggermont W, Ireland S, Andrews R, Arimilli M, Al-Tel TH, De Clercq E, *et al*: **Mutations in the nonstructural protein 3A confer resistance to the novel enterovirus replication inhibitor TTP-8307.** *Antimicrob Agents Chemother* 2009, **53:**1850–1857.
113. Caliguiri LA, Tamm I: **Distribution and translation of poliovirus RNA in guanidine-treated cells.** *Virology* 1968, **36:**223–231.
114. Caliguiri LA, Tamm I: **Action of guanidine on the replication of poliovirus RNA.** *Virology* 1968, **35:**408–417.
115. Loddo B, Ferrari W, Brotzu G, Spanedda A: **In vitro inhibition of infectivity of polio viruses by guanidine.** *Nature* 1962, **193:**97–98.
116. Rightsel WA, Dice JR, Mc AR, Timm EA, Mc LI Jr, Dixon GJ, Schabel FM Jr: **Antiviral effect of guanidine.** *Science* 1961, **134:**558–559.
117. Herrmann EC Jr, Herrmann JA, Delong DC: **Prevention of death in mice infected with coxsackievirus A16 using guanidine HCl mixed with substituted benzimidazoles.** *Antiviral Res* 1982, **2:**339–346.
118. Saunders K, King AM, McCahon D, Newman JW, Slade WR, Forss S: **Recombination and oligonucleotide analysis of guanidine-resistant foot-and-mouth disease virus mutants.** *J Virol* 1985, **56:**921–929.
119. Sadeghipour S, Bek EJ, McMinn PC: **Selection and characterisation of guanidine-resistant mutants of human enterovirus 71.** *Virus Res* 2012, **169:**72–79.
120. Bienz K, Egger D, Troxler M, Pasamontes L: **Structural organization of poliovirus RNA replication is mediated by viral proteins of the P2 genomic region.** *J Virol* 1990, **64:**1156–1163.
121. Taylor MP, Burgon TB, Kirkegaard K, Jackson WT: **Role of microtubules in extracellular release of poliovirus.** *J Virol* 2009, **83:**6599–6609.
122. Wessels E, Duijsings D, Notebaart RA, Melchers WJ, van Kuppeveld FJ: **A proline-rich region in the coxsackievirus 3A protein is required for the protein to inhibit endoplasmic reticulum-to-golgi transport.** *J Virol* 2005, **79:**5163–5173.
123. De Palma AM, Vliegen I, De Clercq E, Neyts J: **Selective inhibitors of picornavirus replication.** *Med Res Rev* 2008, **28:**823–884.
124. Arita M, Takebe Y, Wakita T, Shimizu H: **A bifunctional anti-enterovirus compound that inhibits replication and the early stage of enterovirus 71 infection.** *J Gen Virol* 2010, **91:**2734–2744.
125. Pathak HB, Arnold JJ, Wiegand PN, Hargittai MR, Cameron CE: **Picornavirus genome replication: assembly and organization of the VPg uridylylation ribonucleoprotein (initiation) complex.** *J Biol Chem* 2007, **282:**16202–16213.
126. Paul AV, Rieder E, Kim DW, van Boom JH, Wimmer E: **Identification of an RNA hairpin in poliovirus RNA that serves as the primary template in the in vitro uridylylation of VPg.** *J Virol* 2000, **74:**10359–10370.
127. Sun Y, Wang Y, Shan C, Chen C, Xu P, Song M, Zhou H, Yang C, Xu W, Shi PY, *et al*: **Enterovirus-71 VPg uridylylation uses a two-molecular mechanism of 3Dpol.** *J Virol* 2012, **86:**13662–13671.
128. Graci JD, Too K, Smidansky ED, Edathil JP, Barr EW, Harki DA, Galarraga JE, Bollinger JM Jr, Peterson BR, Loakes D, *et al*: **Lethal mutagenesis of picornaviruses with N-6-modified purine nucleoside analogues.** *Antimicrob Agents Chemother* 2008, **52:**971–979.
129. Li ZH, Li CM, Ling P, Shen FH, Chen SH, Liu CC, Yu CK: **Ribavirin reduces mortality in enterovirus 71-infected mice by decreasing viral replication.** *J Infect Dis* 2008, **197:**854–857.
130. Chen TC, Chang HY, Lin PF, Chern JH, Hsu JT, Chang CY, Shih SR: **Novel antiviral agent DTriP-22 targets RNA-dependent RNA polymerase of enterovirus 71.** *Antimicrob Agents Chemother* 2009, **53:**2740–2747.
131. Thibaut HJ, Leyssen P, Puerstinger G, Muigg A, Neyts J, De Palma AM: **Towards the design of combination therapy for the treatment of enterovirus infections.** *Antiviral Res* 2011, **90:**213–217.

doi:10.1186/1423-0127-21-14
Cite this article as: Tan *et al.*: Recent developments in antiviral agents against enterovirus 71 infection. *Journal of Biomedical Science* 2014 **21**:14.

Enterovirus 71 receptors: promising drug targets?

Expert Rev. Anti Infect. Ther. 11(6), 547–549 (2013)

Chee Wah Tan

Department of Medical Microbiology, Faculty of Medicine, Tropical Infectious Diseases Research & Education Centre, University Malaya, 50603, Kuala Lumpur, Malaysia

Yoke-Fun Chan

Author for correspondence: Department of Medical Microbiology, Faculty of Medicine, Tropical Infectious Diseases Research & Education Centre, University Malaya, 50603, Kuala Lumpur, Malaysia
chanyf@um.edu.my

"The key factor that determines drug efficacy is its ability to fit into the hydrophobic pocket of the VP1 capsid protein and stabilize the virus."

Human enterovirus 71 (EV-A71) is the main etiological agent of hand, foot and mouth disease (HFMD). Typical clinical symptoms of HFMD are fever, rashes on the palms and soles and oral ulcers. Unlike other enteroviruses that cause HFMD, EV-A71 is more frequently associated with severe neurological complications, such as brainstem encephalitis and aseptic meningitis in children below 6 years of age. The first outbreak was reported in 1969 and subsequently many large outbreaks have been reported in Japan, Hungary, Bulgaria, Malaysia, Taiwan, Singapore, Australia, Vietnam, China and Cambodia [1]. The recent outbreak in China affected half a million people with more than 500 deaths. Fatalities are predominantly seen in Asian outbreaks, but neither a vaccine nor an antiviral is presently available for clinical use.

"...further chemical modifications to improve the potency, efficacy, oral administration, safety and cost will be needed for enterovirus 71 antivirals..."

EV-A71 could emerge as the next significant enteroviral health threat after eradication of polioviruses. Owing to the potential severe neurological complications in EV-A71 infection, there is a pressing need to develop effective antiviral therapeutics. Our growing knowledge in EV-A71 viral–host receptor interactions provides opportunities to identify new targets for rational design of attachment or entry inhibitors.

Discovery of EV-A71 viral–host receptors interactions: insights into therapeutics development

EV-A71 belongs to the Picornaviridae family and the genome is enclosed within a non-enveloped, icosahedral capsid, assembled from four capsid proteins, VP1–VP4, of which VP1–VP3 are located on the exterior surface while VP4 is located on the inner surface. The EV-A71 capsid will initially attach to the cell surface, then bind to the entry receptor and finally enter the cell by endocytosis. Virus–host receptor interaction is the first essential event during virus infection. In the absence of susceptible host receptors, the virus will not enter the cells to initiate an infection. Receptor availability is therefore one of the factors that determine host range and tissue tropism.

Carbohydrates are expressed abundantly on the human cell surface and are often initial attachment targets of most pathogens. The function of these carbohydrate attachment factors could be to concentrate the virus on the host cell surface and, hence, enhance infectivity. EV-A71 attaches to the cell surface carbohydrate, heparan sulfate, possibly by electrostatic interactions, before binding to entry receptors. The symmetrical arrangement of positively-charged amino acids at the fivefold axis of the EV-A71 pentamer could be the major site where heparan sulfate interacts [2]. In addition, EV-A71 also interacts with sialylated glycans [3].

Most picornavirus receptors belong to the immunoglobulin superfamily, such as ICAM-1 for the major group rhinoviruses

Keywords: attachment • drug target • enterovirus 71 • entry • inhibitor • receptor

 10.1586/ERI.13.47 ISSN 1478-7210

and CD155 for the polioviruses. Cryo-electron microscopy reveals that these receptors interact with viral capsids through penetration into the canyon, a depression that encircles the fivefold axis, and trigger capsid structural transition to allow virus entry [4]. The two EV-A71 entry receptors, scavenger receptor class B2 (SCARB2) and P-selectin glycoprotein ligand-1 (PSGL-1) are different from the known enterovirus receptors. SCARB2 is a type III double transmembrane protein that is widely expressed in different cell types. In most cell types, EV-A71 binds to the SCARB2 receptor and is then internalized via clathrin-mediated endocytosis [5,6]. The canyon around the EV-A71 VP1 Gln172 has been showed to interact with the amino acids between 144 and 151 of SCARB2 [7]. Interestingly, desialylation of SCARB2 abolished the EV-A71–SCARB2 interactions, implying that the sialic acids present on the SCARB2 are critical [3]. Involvement of PSGL-1 as an EV-A71 receptor has also been demonstrated, but this receptor is only expressed in neutrophils and lymphocytes [8]. Recent studies have demonstrated that SCARB2 is functionally more important than PSGL-1 as a receptor. At pH <6.0, EV-A71 uncoating was observed when SCARB2 was present, but not PSGL-1 [9].

> "The major obstacle is delivering a sufficient amount of the inhibitor to the targeted site early enough to delay disease progression to neurological involvement or to prevent the spread of infection to others."

Recent developments of receptor inhibitors for EV-A71 involve targeting the virus capsid proteins (such as hydrophobic pocket binders) or host-receptor binding sites (host-receptor inhibitors). Small synthetic capsid hydrophobic pocket binders are known to be effective inhibitors against picornaviruses through stabilizing the capsid against receptor-induced conformational changes and thereby preventing uncoating. The mechanism of the capsid-binding drug WIN51711 (5-[7-[4-(4,5-dihydro-2-oxazolyl)phenoxy]heptyl]-3-methylisoxazole) against EV-A71 uncoating was recently resolved by x-ray crystallography [10]. BPROZ-194, a pyridyl imidazolidinone, is a novel class capsid binder that exhibited antiviral activity against EV-A71 with EC_{50} between 2.13 and 4.67 µM [11]. The key factor that determines drug efficacy is its ability to fit into the hydrophobic pocket of the VP1 capsid protein and stabilize the virus. Inhibitors of host attachment factors include SP40, a VP1-derived synthetic peptide that blocks viral attachment to cell surface heparan sulfate with IC_{50} between 6 and 9 µM [12]. Similarly, bovine lactoferrin that binds to heparan sulfate and VP1 also inhibits EV-A71 infection *in vivo* [13]. Pre-incubation of cells with anti-SCARB2 antibodies or monoclonal antibody targeting the N-terminal of PSGL-1 inhibits EV-A71 infection in a dose-dependent manner, but does not completely protect the cells from infection [5,8,9]. The soluble form of cellular receptors could act as molecular decoys of cell-associated receptors. Soluble forms of highly negatively charged heparin, dextran sulfate and suramin reduces viral infectivity, possibly due to disruption of the integrity of the EV71 capsid structure or steric hindrance of receptor interactions [2].

Virus receptors for therapeutics: the success stories of HIV entry inhibitors

A successful example of entry inhibitors is the HIV fusion inhibitor enfuvirtide, which obtained US FDA approval in March 2003. Enfurvitide is used in combination with other antiretroviral agents in the treatment of experienced patients with resistance to other antiretroviral drugs. Enfuvirtide is a 36-amino acid peptide derived from the heptad repeat region-2 sequence of the HIV transmembrane protein GP41. Enfuvirtide interacts with the $CD4^+$ T-cell receptor and prevents the critical fusion step of the viral entry process. As a result of low bioavailability and short half-life, second- and third-generation peptide-based fusion inhibitors with improved stability and potency have been developed [14]. These include sifuvirtide, which has a more stable secondary structure of the α-helix structure and prolonged plasma stability of up to 22 h [15]. This will result in lower dosage and frequency of administration. Another successful entry inhibitor has been maraviroc, which was approved by the FDA in 2007. Maraviroc binds to the chemokine co-receptor CCR5, blocking the binding of HIV-1 virus envelope glycoprotein GP120, hence preventing HIV-1 from entering and infecting immune cells [16].

Challenges of developing EV-A71 entry inhibitors

Cost, efficacy, route of administration and safety will continue to be the barriers to the success of taking antivirals targeting receptors from benchside to bedside. A possible use for attachment and entry inhibitors is for prophylaxis; for example, during an outbreak of HFMD associated with severe neurological disease in a kindergarden. However, this approach is unlikely to be cost-effective for resource-limited countries in Asia where large outbreaks frequently occur. The effectiveness of the attachment or entry inhibitor would be highly dependent on the timing of the treatment provided. The major obstacle is delivering a sufficient amount of the inhibitor to the targeted site early enough to delay disease progression to neurological involvement or to prevent the spread of infection to others. Bioavailability is often a determinant of drug efficacy. Although WIN compounds exhibit significant *in vitro* activity against rhinovirus, it has been unsuccessful due to their poor bioavailability. Similarly, clinical trials of intranasal anti-ICAM-1 antibodies targeting the rhinovirus receptor only delays onset of infection, but does not eliminate it [17]. EV-A71 peptide-based inhibitors such as the SP40 peptide currently have limited bioavailability and stability in plasma. Further chemical modifications, such as addition of N-terminal pyroglutamate and C-terminal homoserine lactone to the peptide, could improve the resistance to peptidase [18].

An additional challenge of small synthetic inhibitors such as the WIN compounds and peptides is the development of resistant mutants. RNA viruses exist as quasispecies, a cloud of virus variants carrying different mutations within a virus population. This can eventually lead to selection of mutant viruses resistant to the inhibitors. A single Val192Met mutation in *VP1* is sufficient to confer resistance to BPROZ-194, the capsid binder [19]. EV-A71 mutants with VP1 Glu98Gln and Lys244Arg mutations conferred resistance to the suramin analog, NF449 [20]. Based on

lessons from HIV combination therapy, targeting multiple stages in viral replication can significantly reduce the emergence of resistant mutants. Understanding the molecular mechanisms of resistance may lead to design of improved inhibitors.

Outlook for the future

Limited antivirals targeting HIV, influenza, herpesviruses and hepatitis viruses are available on the market. Emerging infections with epidemic potential such as EV-A71 warrant greater attention. Development of antivirals based on understanding of virus–host receptor interactions show promise, exemplified by the success of enfuvirtide. However, further chemical modifications to improve the potency, efficacy, oral administration, safety and cost will be needed for EV-A71 antivirals, such as SP40 peptide, BPROZ-194 and WIN51711. Combination therapy with more than one inhibitor may yield more promising results. There should be more concerted efforts to screen other targets involved in the virus life cycle (e.g., polyprotein processing, capsid assembly and virus release) and host cellular pathways (e.g., apoptosis and autophagy). Additionally, several EV-A71 inactivated vaccines are currently in clinical trials and showing promising results.

While waiting for a new antiviral or vaccine, preventive measures, such as early detection of infection, social distancing. hand hygiene and effective supportive clinical treatment remain the cornerstones to combating EV-A71 infection.

Acknowledgement

The authors would like to thank IC Sam for helpful discussions and critical review of the manuscript.

Financial & competing interests disclosure

The authors received research funding from University Malaya High Impact Research Grants (E000013-20001 and UM.C/625/1/HIR/014). The authors have a pending patent on the SP40 peptide. The authors have no other relevant affiliations or financial involvement with any organization or entity with a financial interest in or financial conflict with the subject matter or materials discussed in the manuscript apart from those disclosed.

No writing assistance was utilized in the production of this manuscript.

References

1 Chan YF, Sam IC, Wee KL, Abubakar S. Enterovirus 71 in Malaysia: a decade later. *Neurol. Asia* 16(1), 1–15 (2011).

2 Tan CW, Poh CL, Sam IC, Chan YF. Enterovirus 71 uses cell surface heparan sulfate glycosaminoglycan as an attachment receptor. *J. Virol.* 87(1), 611–620 (2013).

3 Su PY, Liu YT, Chang HY *et al.* Cell surface sialylation affects binding of enterovirus 71 to rhabdomyosarcoma and neuroblastoma cells. *BMC Microbiol.* 12, 162 (2012).

4 Rossmann MG, He Y, Kuhn RJ. Picornavirus–receptor interactions. *Trends Microbiol.* 10(7), 324–331 (2002).

5 Yamayoshi S, Yamashita Y, Li J *et al.* Scavenger receptor B2 is a cellular receptor for enterovirus 71. *Nat. Med.* 15(7), 798–801 (2009).

6 Hussain KM, Leong KL, Ng MM, Chu JJ. The essential role of clathrin-mediated endocytosis in the infectious entry of human enterovirus 71. *J. Biol. Chem.* 286(1), 309–321 (2011).

7 Chen P, Song Z, Qi Y *et al.* Molecular determinants of enterovirus 71 viral entry: cleft around GLN-172 on VP1 protein interacts with variable region on scavenge receptor B 2. *J. Biol. Chem.* 287(9), 6406–6420 (2012).

8 Nishimura Y, Shimojima M, Tano Y, Miyamura T, Wakita T, Shimizu H. Human P-selectin glycoprotein ligand-1 is a functional receptor for enterovirus 71. *Nat. Med.* 15(7), 794–797 (2009).

9 Yamayoshi S, Ohka S, Fujii K, Koike S. Functional comparison of SCARB2 and PSGL1 as receptors for enterovirus 71. *J. Virol.* 87(6), 3335–3347 (2013).

10 Plevka P, Perera R, Yap ML, Cardosa J, Kuhn RJ, Rossmann MG. Structure of human enterovirus 71 in complex with a capsid-binding inhibitor. *Proc. Natl Acad. Sci. USA* 110(14), 5463–5467 (2013).

11 Shia KS, Li WT, Chang CM *et al.* Design, synthesis, and structure–activity relationship of pyridyl imidazolidinones: a novel class of potent and selective human enterovirus 71 inhibitors. *J. Med. Chem.* 45(8), 1644–1655 (2002).

12 Tan CW, Chan YF, Sim KM, Tan EL, Poh CL. Inhibition of enterovirus 71 (EV-71) infections by a novel antiviral peptide derived from EV-71 capsid protein VP1. *PLoS ONE* 7(5), e34589 (2012).

13 Weng TY, Chen LC, Shyu HW *et al.* Lactoferrin inhibits enterovirus 71 infection by binding to VP1 protein and host cells. *Antiviral Res.* 67(1), 31–37 (2005).

14 Berkhout B, Eggink D, Sanders RW. Is there a future for antiviral fusion inhibitors? *Curr. Opin. Virol.* 2(1), 50–59 (2012).

15 He Y, Xiao Y, Song H *et al.* Design and evaluation of sifuvirtide, a novel HIV-1 fusion inhibitor. *J. Biol. Chem.* 283(17), 11126–11134 (2008).

16 Dorr P, Westby M, Dobbs S *et al.* Maraviroc (UK-427,857), a potent, orally bioavailable, and selective small-molecule inhibitor of chemokine receptor CCR5 with broad-spectrum anti-human immunodeficiency virus type 1 activity. *Antimicrob. Agents Chemother.* 49(11), 4721–4732 (2005).

17 Norkin LC. Virus receptors: implications for pathogenesis and the design of antiviral agents. *Clin. Microbiol. Rev.* 8(2), 293–315 (1995).

18 Kajiwara K, Watanabe K, Tokiwa R *et al.* Bioorganic synthesis of a recombinant HIV-1 fusion inhibitor, SC35EK, with an N-terminal pyroglutamate capping group. *Bioorg. Med. Chem.* 17(23), 7964–7970 (2009).

19 Shih SR, Tsai MC, Tseng SN *et al.* Mutation in enterovirus 71 capsid protein VP1 confers resistance to the inhibitory effects of pyridyl imidazolidinone. *Antimicrob. Agents Chemother.* 48(9), 3523–3529 (2004).

20 Arita M, Wakita T, Shimizu H. Characterization of pharmacologically active compounds that inhibit poliovirus and enterovirus 71 infectivity. *J. Gen. Virol.* 89(Pt 10), 2518–2530 (2008).